LIBRARY
Michigan State
University

PLACE IN RETURN BOX to remove this checkout from your record.
TO AVOID FINES return on or before date due.

DATE DUE	DATE DUE	DATE DUE

MSU is An Affirmative Action/Equal Opportunity Institution
c:\circ\datedue.pm3-p.1

NEW APPROACHES TO THE MONONUCLEAR AND HETEROPOLYNUCLEAR CHEMISTRY OF 3d METALS WITH A HIGHLY BASIC FUNCTIONALIZED LIGAND

By

Anne Quillevéré

A DISSERTATION

Submitted to
Michigan State University
in partial fulfillment of the requirements
for the degree of

DOCTOR OF PHILOSOPHY

Department of Chemistry

1992

7149-449

ABSTRACT

NEW APPROACHES TO THE MONONUCLEAR AND HETEROPOLYNUCLEAR CHEMISTRY OF 3d METALS WITH A HIGHLY BASIC FUNCTIONALIZED LIGAND

By

Anne Quillevéré

In the past thirty years the chemistry of transition metals with phosphines has been heavily investigated due, in part, to the demonstrated ability of such ligands to play a pivotal role in homogeneous catalytic processes and to stabilize metal centers in low oxidation states. The synergistic σ-donor and π-acceptor properties, as well as the steric effects of such ligands, affect the coordination of tertiary aryl-phosphines to 3d elements in which there has been a considerable interest because the complexes that they form exhibit an enhanced reactivity toward small molecules such as N_2, O_2, or CO. A recent approach to transition metal phosphine chemistry involves the use of ether-functionalized phosphines in which the presence of oxygen donor substituents provides a unique combination of soft (P) and hard (O) donor atoms, as well as opens up the possibility to form weak metal-ether interactions that are sufficiently labile in solution so as to promote chemistry at the metal center.

Tris(2,4,6-trimethoxyphenyl)phosphine (TMPP) is an ether-functionalized derivative of triphenylphosphine that combines some of the aforementioned properties, along with steric bulk and high basicity.

Because of its unique combination of properties and the fact that the transition metal chemistry of the ligand is virtually nonexistent, our group has been investigating its chemistry with a variety of transition metals. The unusual properties of TMPP have allowed for the isolation of unprecedented complexes such as the di-ferrous, ferromagnetic salt [H-TMPP]$_2$[Fe_2Cl_6] (**2**) (H-TMPP = [H-P{$C_6H_2(OMe)_3$}$_3$]$^+$) from the equimolar reaction of $FeCl_3$ with TMPP. The reaction of **2** with molecular oxygen involves a series of reactions which eventually lead to the formation of the neutral, mono-phosphine oxide adduct $FeCl_3$(O=TMPP) (**6**). Compounds **2** and **6**, along with two other intermediates, [H-TMPP]$_2$[$Fe^{II}Cl_4$] (**4**) and [H-TMPP][$Fe^{III}Cl_4$] (**5**), were characterized by a variety of techniques including single crystal X-ray crystallography, magnetic susceptibility, as well as epr and Mössbauer spectroscopies. These studies lend new insight on the mechanism of the $FeCl_3$-catalyzed oxidation of phosphine to phosphine oxide.

The chemistry of TMPP with Co(II) and Ni(II) has also proven to be very rich. Demethylation of the ligand resulted in the formation of phosphino-phenoxide complexes of general formula M(TMPP-*O*)$_2$ (M = Co (**12**), Ni (**18**); TMPP-*O* = [P{$C_6H_2(OMe)_3$}$_2${$C_6H_2(OMe)_2O$}]$^-$). Compound **12**, in which the two phosphine ligands are mutually *cis*, reacts with MCl_2 (M = Co, Mn) to form the homo- and heterobimetallic species $Cl_2MCo\{\mu\text{-}\eta^2\text{-}(TMPP\text{-}O)_2\}$. Oxidation of complex **18** yields [Ni^{III}(TMPP-*O*)$_2$]$^+$ (**19**), whose identity as a S = 1/2 spin system was confirmed by epr spectroscopy and magnetic susceptibility measurements. The stabilization of compounds **18**, Ni^{II}, and **19**, Ni^{III}, with the identical ligand set provides an excellent example of how careful tailoring of a ligand can allow access to unusual oxidation states.

To the Memory of my Grand-Parents,

Louise Vala and Germain Quillevéré.

ACKNOWLEDGEMENTS

This work would not have been possible without my research director, Professor Kim R. Dunbar, whose constant support and friendship accompanied me through these four years. Her enthusiasm, knowledge and advice were invaluable to me, and most importantly she taught me to always be critical of myself. I also greatly appreciate all the opportunities I was given to meet people and go to scientific meetings, which resulted in fruitful interactions with numerous chemists. Past and present members of the Dunbar Group will be remembered, in particular (Dr.) Sue-Jane Chen and John Matonic, Sue-Jane for supplying us with so many "Sue-Jane stories" that, after she graduated, we rarely had a day without asking each other "Remember the time Sue-Jane....?" and John for his incredible patience and dedication in teaching me over, and over again, the most simple things that seemed so complicated to me, and because Sundays spent struggling with the diffractometer would not have been the same without him around. Special thanks go to Laura Pence for sharing the "throes of thesis writing" with me and to Dr. Vijay Saharan for bringing a much needed new approach to life and science, and above all, for being such a "nice chap". As my (tor)mentor, Steve Haefner, will always keep a special place in my memory, for teaching me much about chemistry, but also about friendship, moral support, abuse, alternative music and colorful

English. It is rather rare to meet somebody as dedicated as Steve, dedicated to the point of putting my crystal on the diffractometer at 2:00 am on a Saturday night... His encouragements and constant interest for my work are a big part of what kept me going. "What a long, strange trip it's been", indeed. Sharing it with these special people made it all the more worthwhile. Finally, of all my friends here at Michigan State University, I would like to especially mention the 1988 Owen Hall crew: Edwin, Paul, Nadine, Jan, Amitabh. Being part of the Owen International Committee was a lot of fun. And also, all my fellow country(wo)men in the Chemistry Department, Pascal Rigollier, for showing me that it was possible to make it here (even in 3 1/2 years), Laurent Michot for his advice, and the French flavor his occasional outbursts would bring to the otherwise quiet fourth floor, Jean-Rémi Butruille and Astrid Bavière for a lot of fun and all the times I had to answer questions like "Don't you have enough crystals yet ?" or "Why do you have to be on the diffractometer tonight?".

My last thanks go to my family and friends from home who supported me all along even though they did not quite always understand what it was I was actually doing here, and particularly to my parents and grand-parents, for whom the fact that I was going to be studying for so long, and abroad, was never questioned but just the way things were supposed to be.

Finally, this thesis is an answer to the question my father has been asking me for the last ten years or so: "A quoi ça sert donc que je te paie des études depuis si longtemps ?"

TABLE OF CONTENTS

LIST OF TABLES

Page

Page

LIST OF FIGURES

Page

Page

Page

LIST OF SYMBOLS AND ABBREVIATIONS

Å	Ångström
Ag/AgCl	silver-silver chloride reference electrode
br	broad
ca.	circa, about
CH_3-TMPP	tris(2,4,6-trimethoxyphenyl)methyl phosphonium
$ClCH_2$-TMPP	tris(2,4,6-trimethoxyphenyl)chloromethyl phosphonium
cm	centimeter
COD	1,5-cyclooctadiene
CV	cyclic voltammetry
℃	degree centigrade
d	doublet (NMR), day, deuterated
δ	parts per million (ppm)
dippe	bis(diisopropylphosphino)ethane
dmpe	bis(dimethylphosphino)ethane
$E_{p,a}$	anodic peak potential
$E_{p,c}$	cathodic peak potential
EPR	electron paramagnetic resonance
emu	electromagnetic unit
esd	estimated standard deviation
EtOH	ethanol
ε	molar extinction coefficient
FAB	Fast Atom Bombardment
g	epr g-value
G	Gauss
h	hour
H-TMPP	tris(2,4,6-trimethoxyphenyl)phosphonium
(M)Hz	(Mega)Hertz
IR	infrared
^{i}Pr	isopropyl

K	Kelvin
m	medium
M	moles per liter
Me	methyl
MeCN	acetonitrile
MeOH	methanol
mg	milligram
min.	minute
mL	milliliter
mmol	millimole
μ	bridging ligand
μ_B or B. M.	Bohr magneton
nm	nanometer
ν	frequency
NMR	nuclear magnetic resonance
ox	oxidation
PCy_3	tricyclohexylphosphine
PPh_3	triphenylphosphine
ppm	parts per million
red	reduction
r.t.	room temperature
s	singlet (NMR), strong (IR)
sh	shoulder
SQUID	Super Quantum Interference Device
$TBABF_4$	tetra-*n*-butylammonium tetrafluoroborate
^{t}Bu	tert-butyl
THF	tetrahydrofuran
TMPP	tris(2,4,6-trimethoxyphenyl)phosphine
TMPP-*O*	$P[\{C_6H_2(CH_3O)_3\}_2\{C_6H_2(CH_3O)_2O\}]^-$
TMS	tetramethylsilane
UV	ultraviolet
V	Volt
vs	versus, very strong
w	weak
X	halide ligand

LIST OF COMPOUNDS

(1) $[CH_3\text{-TMPP}]_2[FeCl_4]$

(2) $[H\text{-TMPP}]_2[Fe_2Cl_6]$

(3) $[Cl\text{-TMPP}][FeCl_4]$

(4) $[H\text{-TMPP}]_2[FeCl_4]$

(5) $[H\text{-TMPP}][FeCl_4]$

(6) $FeCl_3(O{=}TMPP)$

(7) $[ClCH_2\text{-TMPP}][FeCl_4]$

(8) $[CH_3\text{-TMPP}]_2[Co_2Cl_6]$

(9) $[H\text{-TMPP}]_2[CoCl_4]$

(10) $[CH_3\text{-TMPP}]_2[CoCl_4]$

(11) $[ClCH_2\text{-TMPP}]_2[CoCl_4]$

(12) $Co(TMPP\text{-}O)_2$

(13) $[Co(TMPP)_2][BF_4]_2$

(14) $Cl_2Co_2\{\mu\text{-}\eta^2\text{-}(TMPP\text{-}O)_2\}$

(15) $Cl_2MnCo\{\mu\text{-}\eta^2\text{-}(TMPP\text{-}O)_2\}$

(16) $[Cp_2TiCo(TMPP\text{-}O)_2][CoCl_4]$

(17) $[(COD)Rh\text{-}Co(TMPP\text{-}O)_2][BF_4]_2$

(18) $Ni(TMPP\text{-}O)_2$

(19) $[Ni(TMPP\text{-}O)_2][BF_4]$

(20) $[Re_2(NCCH_3)_{10}][BF_4]_4$

CHAPTER I

INTRODUCTION

Phosphines have been used by coordination chemists for more than forty years, not only because of their synthetic availability, but also because of their fascinating chemistry with transition elements [1]. The discovery in the early 1960's that metal phosphine complexes catalyze numerous chemical reactions, such as hydroformylation or olefin hydrogenation, to cite a few, spurred a considerable amount of research [2]. The first report by Wilkinson that $RhCl(PPh_3)_3$, which became known as "Wilkinson's catalyst", played a pivotal role in the catalysis of hydrogenation [3] spawned a whole field of investigation involving the coordination chemistry of triphenylphosphine with a variety of transition metals [2]. The electronic "ambivalence" of phosphines, which can act as σ-donors as well as π-acceptors [4], combined with steric effects, allows for the stabilization of metal centers in a variety of oxidation states, from low-valent Ni(0) in $Ni(PPh_3)_4$ [5] to high-valent W(IV) in $WCl_4(PMe_3)_2$ [6].

The commercial availability of first-row transition metal halides has historically placed them in the category of starting materials most used in the coordination chemistry of a variety of ligands, among which are phosphines [7]. As early as the late 1950's, Issleib initiated a systematic investigation of the reactivity of tertiary phosphines PR_3 (R = Ph, Cy, Et, ^{n}Bu), as well as secondary phosphines PHR_2, with 3d metal di- and trihalides [8]. The results reported in this series of papers constitute the first data base for $MX_n(L)_m$ (L = phosphine) compounds. Unfortunately, no structural information was obtained for these compounds, and it was not until the advent of X-ray crystallography in the mid-1960's that this area of inorganic chemistry began to flourish. It was discovered that much of the earlier work reported in the literature did not take into account the inherent incompatibility of soft, basic tertiary phosphines with hard, acidic

3d metal halides. In fact, most of the complexes turned out to be of general formulae $[MX_4][MX_2(L)_2]$ or $[MX_4][H\text{-}L]_n$ (L = phosphine) [9]; the paucity of neutral complexes of the type $MX_n(L)_m$ from the early chemistry was an indication that a new approach was needed, be it using different starting materials, or tailoring of the phosphine ligands to render them more compatible with 3d metals. Several years ago, Girolami and coworkers developed a very successful synthetic route to low-valent, coordinatively unsaturated metal-phosphine complexes [10]. These complexes provide an excellent entry in the organometallic chemistry of chromium, titanium and vanadium because they exhibit enhanced reactivity toward small molecules such as O_2, CO, N_2 or C_2H_4 [11]. In the case of titanium, some interesting catalytic properties in the polymerization of ethylene were discovered [10c]. This approach takes advantage of the chelating ability of diphosphines such as dmpe (bis(dimethylphosphino)ethane) or dippe (bis(diisopropylphosphino)ethane) to stabilize metal dihalides and form complexes of general formula $MX_2(P\sim P)_n$ (X = Cl, Br; n = 1, 2). Diphosphines are not easily protonated and their bidentate coordination mode renders the complexes thus formed very stable. Several of the complexes reported by Girolami *et al.* were structurally characterized and constitute, to date, the sole examples of authentic *mononuclear* phosphine adducts of divalent first-row transition elements.

The chemistry of *monodentate* tertiary phosphines with metal halides was recently revived by Poli and coworkers, who studied the interaction of both triaryl- and trialkylphosphines with the hard Lewis acid, $FeCl_3$ [12]. They were able to demonstrate in their work that bulky monodentate phosphine lead to *mono*-adducts of the type $FeCl_3(PR_3)$ (R = Cy, ^{t}Bu),

whereas less sterically encumbered phosphines favor the *bis*-adducts $FeCl_3(PR_3)_2$ (R = Me, Ph). These results were in contrast to that reported in the literature for the same phosphines, namely, the complexes $FeCl_3(PCy_3)$ [8a] and $FeCl_3(PPh_3)$ [13a], the latter formulation being subsequently confirmed by Mössbauer spectroscopy [13b]. In addition to characterization by infrared spectroscopy and elemental analysis, the earlier reports described the compounds as yellow solids, whereas the recent work by Poli mentions their color as being dark red. None of the mono-phosphine adducts were structurally characterized and it appears that the complexes were not stable in solution. The synthetic difficulties and the lack of reproducibility encountered in the use of traditional triaryl- and trialkylphosphines necessitated that the electronic and steric properties of the ligands be modified; this may be achieved by the functionalization of the substituents on the phosphorus atom. The past twenty years have witnessed a development of this approach, in that inorganic and organometallic chemists have started employing phosphines with nitrogen [14] and oxygen [15] substituents. Among the most frequently studied in the latter category are ether groups. The properties, coordination chemistry and applications to homogeneous catalysis of ether-phosphine ligands, hereafter referred to as (P,O) ligands, have been extensively reviewed in the recent literature [15]. The use of (P,O) ligands for homogeneous catalysis has been extensively explored by Lindner and coworkers [16], but the earlier work of Anderson [17], Rauchfuss [18] and Shaw [19] had shown the usefulness of ether-phosphines, in particular ortho-substituted arylphosphines, for the stabilization of elusive species such as mononuclear Rh^{2+} and Ir^{2+}, through the formation of five-membered metallacycles, as illustrated in the scheme below.

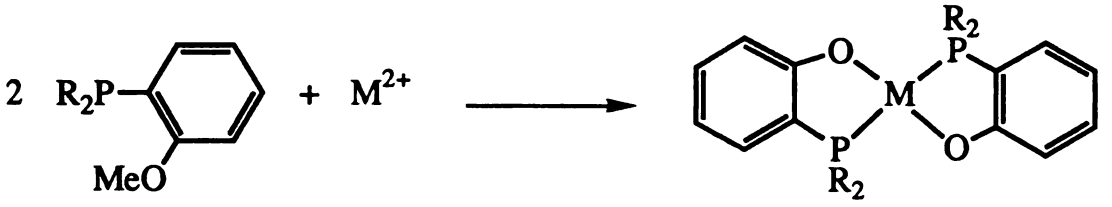

R = Me, ^{t}Bu

M = Rh, Ir

Some of the most interesting properties of (P,O) ligands are a direct consequence of the presence of ether substituents that can act as "built-in" solvent molecules by forming weak interactions with the metal center. These are quite labile in solution, thereby providing vacant coordination sites available for substitution or reversible addition chemistry. These ligands have been referred to as "hemi-labile" [18], since they engage in an "arm on/arm off" mechanism to accommodate the coordination sphere of the metal, by coordinating either in an η^1 mode through the phosphorus atom, or in a polydentate mode through the phosphorus and several oxygen atoms. Moreover, the presence of both soft and hard donor atoms in the same ligands has allowed for the stabilization of different metals in a variety of oxidation states (from Group VII to Group X) [15], and the increased electron density at the metal center facilitates the oxidative addition of an incoming substrate, as well as the reductive elimination of the product. The recent work of Lindner with ruthenium and rhodium ether-phosphine complexes has demonstrated the pivotal role of the ether groups in catalytic processes such as methanol carbonylation and hydrocarbonylation to produce ethanol, acetaldehyde or acetic acid, in addition to selective hydroformylation, hydrosilylation and hydrogenation [16]. Lindner has recently extended his explorations to include cobalt and nickel compounds [16v,w], as previous work by Braunstein *et al.* had

already demonstrated promising results with nickel [20]. These observations, combined with the demonstrated lack of compatibility of traditional monophosphines with 3d metals, certainly render the concept of using ether-functionalized phosphines very attractive, since the added (hard) ether groups should increase the compatibility of the ligands with the typically hard first-row metal cations.

Our approach is to use an ether-functionalized derivative of triphenylphosphine, tris(2,4,6-trimethoxyphenyl)phosphine, referred to as TMPP throughout this dissertation.

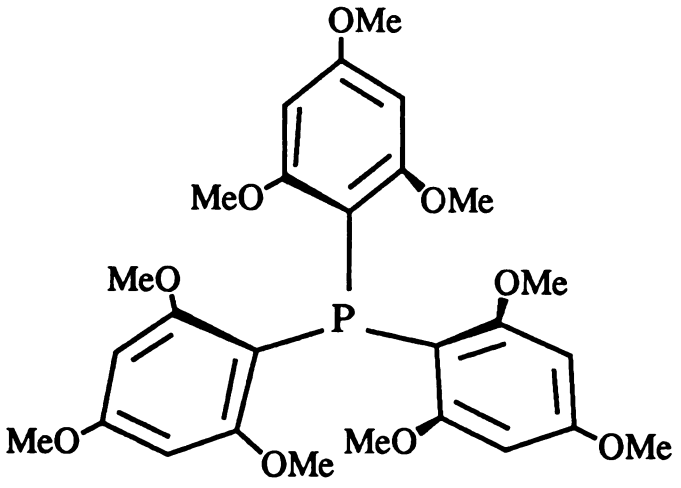

The synthesis of TMPP was initially reported in the Soviet literature in 1963, by Protopopov *et al.*, by a route that involved the coupling of (1,3,5-trimethoxy)benzene by PCl_3 in the presence of $ZnCl_2$ [21]. More recently, Wada and coworkers reported an alternate synthesis, which involves lithiation of (1,3,5-trimethoxy)benzene by *n*-butyllithium followed by coupling with triphenylphosphite [22]. A modification of this literature procedure is currently used in our laboratories as shown in equation 1 [23].

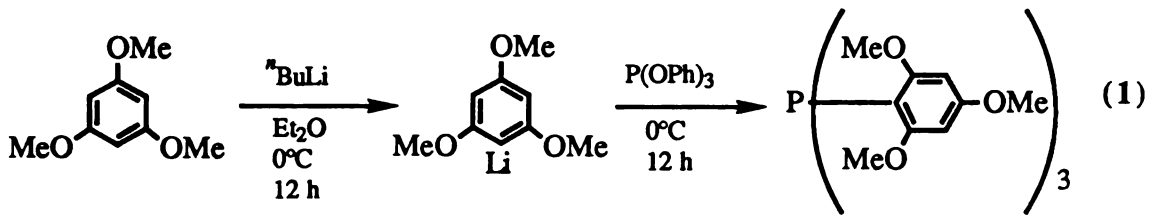

(1)

Wada has explored the use of TMPP in organic reactions such as epoxidations or Michael additions, as well as for the extraction of metal ions such as Fe^{3+} and Ga^{3+} [24]. These applications are certainly a direct result of the unusual chemical and physical properties of this phosphine. One of the most striking features of TMPP is its extreme basicity, which arises from the presence of *three* methoxy groups on the phenyl ring. In fact, the ortho *di*substituted phosphine, namely tris(2,6-dimethoxyphenyl)phosphine, is less basic, and the basicity of the phosphine increases with the level of methoxy substitution. The pK_a of the conjugate acid of TMPP is 11.0; a comparison with other substituted phosphines and known bases is shown below [22]:

$P\{2,4,6\text{-}(MeO)_3C_6H_2\}_3$ (TMPP) ≥ piperidine, Et_2NH, Et_3N ≥ $P\{2,6\text{-}(MeO)_2C_6H_3\}_3$ > $PPh_2\{2,4,6\text{-}(MeO)_3C_6H_2\}$ > $PPh\{2,6\text{-}(MeO)_2C_6H_3\}_2$ > pyridine > $PPh_2\{2,4,6\text{-}(MeO)_3C_6H_2\}$ > $PPh_2\{2,6\text{-}(MeO)_2C_6H_3\}$ ≥ $P\{4\text{-}(MeO)C_6H_4\}_3$, PPh_3.

Figure 1 shows the shift of the C≡O stretching frequency for $Ni(CO)_3L$ complexes, in which L is a tertiary phosphine; this shift is a measure of the donating ability of the phosphine since it bears a direct relationship to the π-backbonding from the filled d-orbitals into the empty C≡O π* orbitals, thereby indicating the strength of the C≡O bond, as shown in the study

Figure 1. A plot of the cone angles versus the $\nu(CO)_{A1}$ stretch for various $Ni(CO)_3L$ complexes (L = phosphine).

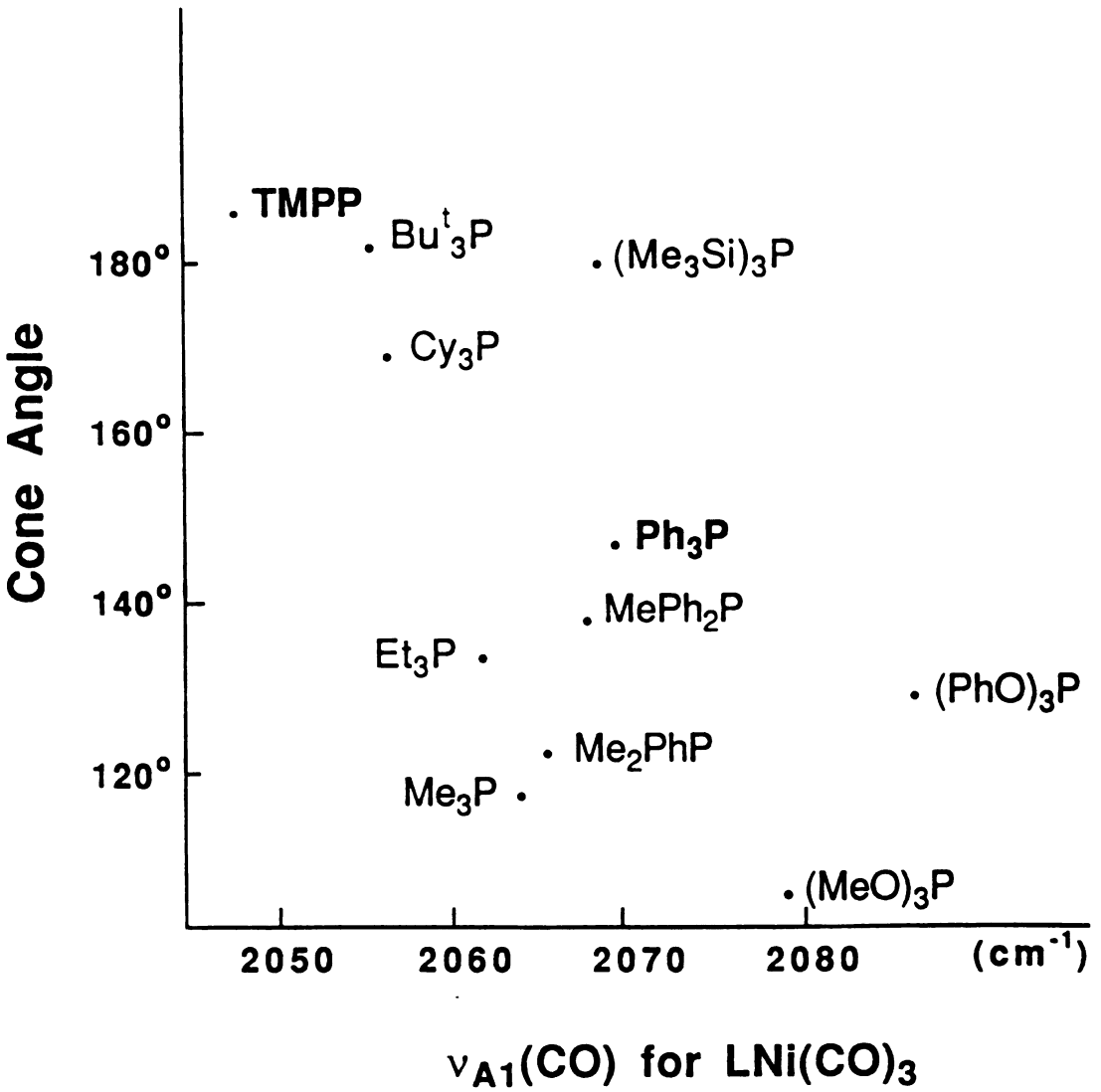
Cone Angle
180°
160°
140°
120°
TMPP
Bu$^t_3$P
(Me$_3$Si)$_3$P
Cy$_3$P
Ph$_3$P
MePh$_2$P
Et$_3$P
(PhO)$_3$P
Me$_2$PhP
Me$_3$P
(MeO)$_3$P
2050
2060
2070
2080
(cm^{-1})
ν_{A1}(CO) for LNi(CO)$_3$

Figure 1.

Figure 2. ORTEP diagram for TMPP showing the atom labeling scheme [23].

abeling

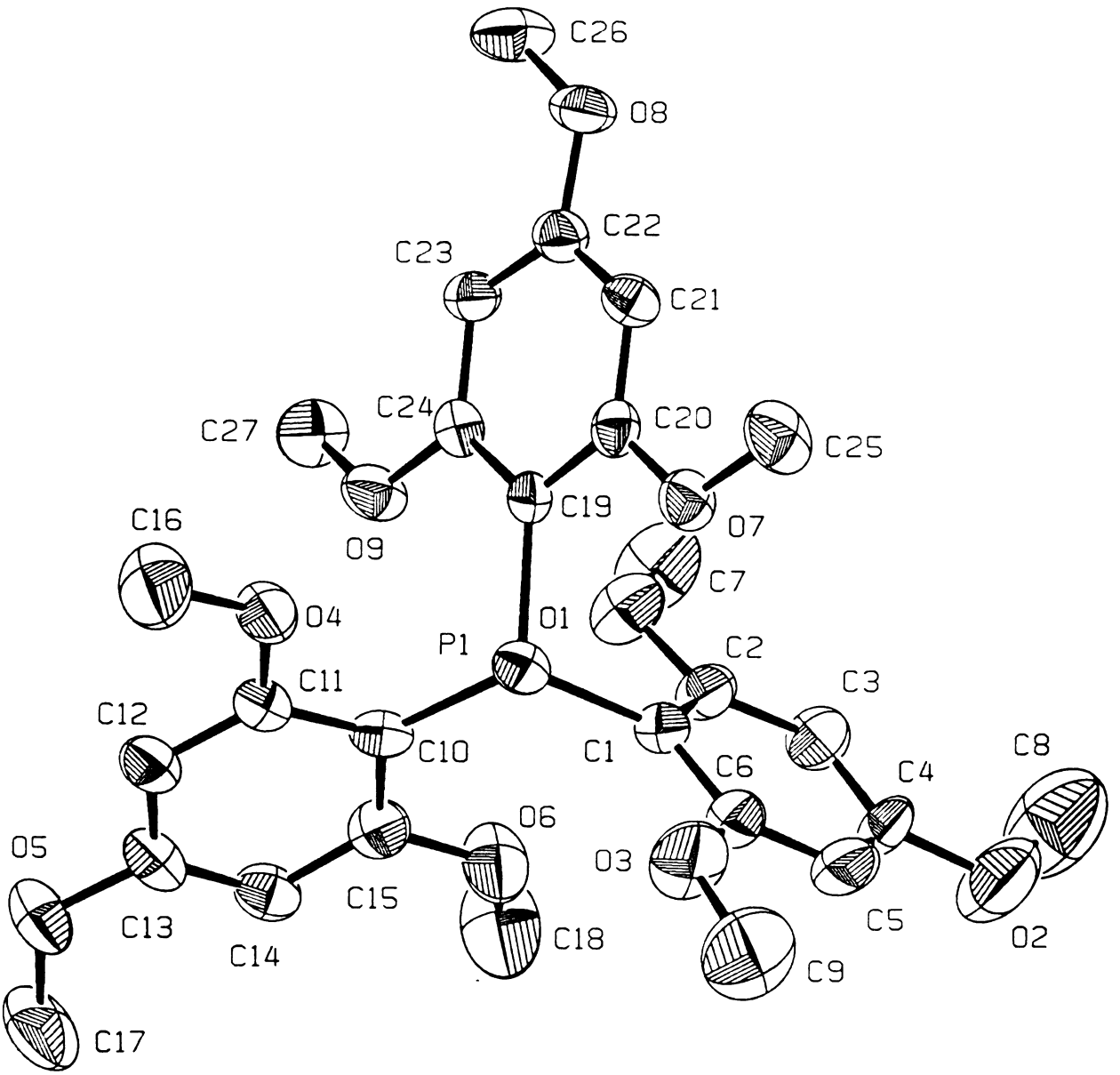

Figure 2.

carried out by Tolman [25]. This figure clearly illustrates the fact that TMPP is the most basic phosphine known to date. Another interesting feature of this ligand is its steric bulk, which arises from the presence of the ortho methoxy substituents. An ORTEP diagram of the molecule, presented in Figure 2 [23], clearly shows the typical propeller arrangement of the phenyl rings adopted by triarylphosphines. The cone angle value of 184° that was reported by Wada has since been confirmed in our laboratories, using the Tolman cone angle method [25]. This method requires the construction of a CPK model with the assumption that the M-P bond is 2.28 Å as illustrated in Figure 3. This experiment confirmed that TMPP was the third largest phosphine after $P(mes)_3$ (mes = $C_6H_2(CH_3)_3$) and $P(o\text{-tol})_3$ (tol = $C_6H_4(CH_3)$), and far more bulky than PPh_3, which has a cone angle of about 145°.

Some of the most useful characterization tools in this chemistry are NMR and infrared spectroscopies; representative data for TMPP and various phosphonium salts of TMPP are listed in Table 1 and Table 2. Figure 4 depicts the infrared spectra of various TMPP derivatives in the 1000-800 cm^{-1} region; these patterns are indeed "fingerprints" of the different types of TMPP derivatives, such as protic phosphonium $[H\text{-TMPP}]^+$, methylphosphonium $[CH_3\text{-TMPP}]^+$ or chloromethylphosphonium $[ClCH_2\text{-TMPP}]^+$, which are often encountered as by-products in the chemistry of TMPP. The ^1H NMR spectrum of free TMPP (in CD_3CN) consists of three resonances at δ = + 3.43 (singlet, 18 H) and δ = + 3.75 (singlet, 9 H) ppm, corresponding to the ortho and para methoxy groups, respectively, and at δ = + 6.05 (doublet, 6 H, $^{H,P}J$ = 3 Hz) ppm corresponding to the meta protons. Coordination of TMPP to a diamagnetic metal center is easily detected by ^1H or ^{31}P NMR, as it renders

Figure 3. Tolman cone angle for various tertiary phosphines.

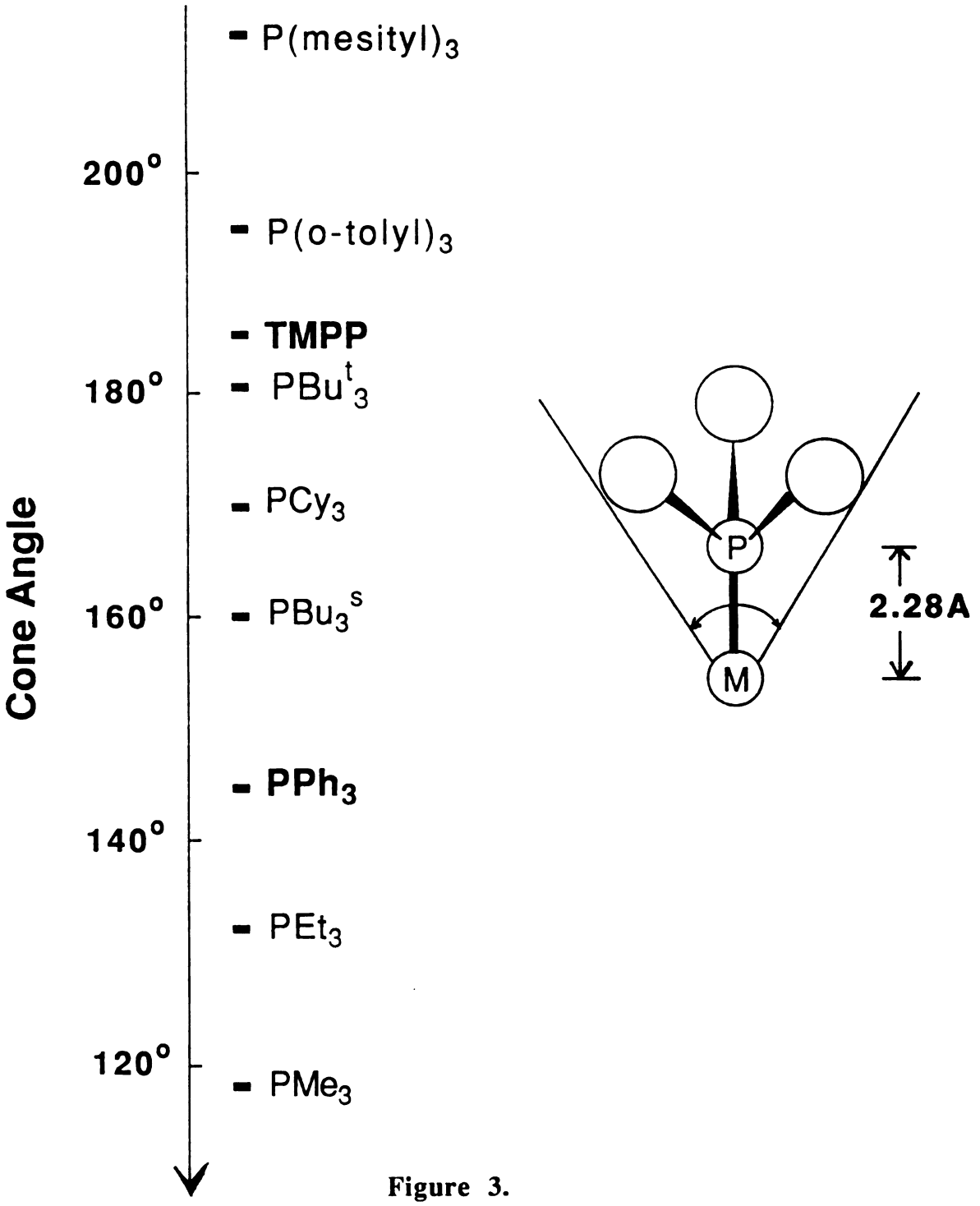
Cone Angle
200°
180°
160°
140°
120°
P(mesityl)3
P(o-tolyl)3
TMPP
PBu^t_3
PCy3
PBu^s_3
PPh3
PEt3
PMe3
P
M
2.28A

Figure 3.

the rings magnetically inequivalent according to the type of bonding mode it adopts.

Our initial venture into the chemistry of TMPP with transition metals was the reaction of the fully solvated dirhodium cation $[Rh_2(NCCH_3)_{10}]^{4+}$ [26] with four equivalents of TMPP to produce the first structurally characterized mononuclear Rh(II) species, *ie*, $[Rh(\eta^3\text{-}TMPP)_2]^{2+}$ [27]. This unusual d^7 metalloradical possesses an axially elongated octahedral geometry, in which two mutually *cis* phosphine ligands are coordinated to the metal center in a tridentate fashion. Furthermore, this complex has four metal-ether interactions that are labile in solution and allow for some fascinating substitution chemistry with isocyanides CNR (R = ^{t}Bu, ^{i}Pr) [28] and reversible addition of CO [29]. Our group has also isolated compounds of TMPP with a variety of other transition metals [30], both early, as in the case of $Mo(CO)_3(\eta^3\text{-}TMPP)$ [31] and late as in $Ir(CO)_2(TMPP)_2$ [32], but also with polynuclear systems such as trinuclear carbonyl clusters of Group VIII [33] or dinuclear species such as $Rh_2(OAc)_4$ [34]. Our main goal, however, was to access other mononuclear d^7 radical systems to compare their reactivity to the Rh(II) species. Wayland and coworkers have recently reported facile C-H bond activation of methane by using a porphyrin-based Rh(II) radical [35], and in view of these results and our prior experience in Rh(II) chemistry we set out to investigate the chemistry of d^7 systems for 3d metals, namely Co(II) and Ni(III). The successful use of a fully solvated cation as a starting material in the Rh(II) chemistry prompted us to begin our study with solvated cations of Co(II) and Ni(II).

The second, third and sixth chapters of this dissertation describe our findings in our attempts to prepare monophosphine adducts of Fe, V, Cr,

Table 1. ^{1}H NMR data for TMPP and various phosphonium salts.

Compound	*o*-OCH_3	*p*-OCH_3	*m*-H	P-H	P-CH_3	P-CH_2Cl	[ref]
			in d_3-acetonitrile				
TMPP	3.43(s)	3.75(s)	6.05(d) J = 3 Hz				23
[H-TMPP]$^+$	3.68(s)	3.86(s)	6.26(d) 6 Hz	8.38(d) 541 Hz			23
[CH_3-TMPP]$^+$	3.54(s)	3.85(s)	6.22(d) 6 Hz		2.47(d) 15 Hz		23
[$ClCH_2$-TMPP]$^+$	3.50(s)	3.80(s)	6.22(d) 6 Hz			4.88(d) 9 Hz	this work
			in d-chloroform				
TMPP	3.47(s)	3.76(s)	6.03(d) $^{P,H}J$ = 3 Hz				22b
[H-TMPP]$^+$	3.69(s)	3.89(s)	6.17 (d) 5 Hz	8.35(d) 541 Hz			22b
[CH_3-TMPP]$^+$	3.58(s)	3.89(s)	6.13(d) 5 Hz		2.45(d) 15 Hz		22b
[$ClCH_2$-TMPP]$^+$	3.63(s)	3.88(s)	6.14(d) 5 Hz			4.25(d) 7.5 Hz	22b

Table 2. Infrared data for TMPP and various phosphonium salts in the 1000 - 800 cm^{-1} region.

compound	mid-infrared bands
TMPP	950 (s) 920 (w)
[H-TMPP]+ *	951 (s) 936 (s) 917 (s) 899 (m)
[H-TMPP]+ **	949 (m) 928 (s) 916 (s) 907 (m) 884(m)
[CH_3-TMPP]+	950 (s) 918 (s, br)
[$ClCH_2$-TMPP]+	949 (s) 916 (s)

* in a 1:1 salt

** in a 1:2 salt

Figure 4. Infrared spectra of TMPP (a), $[H\text{-}TMPP]^+$ in a 1:1 salt (b), $[H\text{-}TMPP]^+$ in a 1:2 salt (c), $[CH_3\text{-}TMPP]^+$ (d), and $[ClCH_2\text{-}TMPP]^+$ (e) in the 1000 - 800 cm^{-1} region.

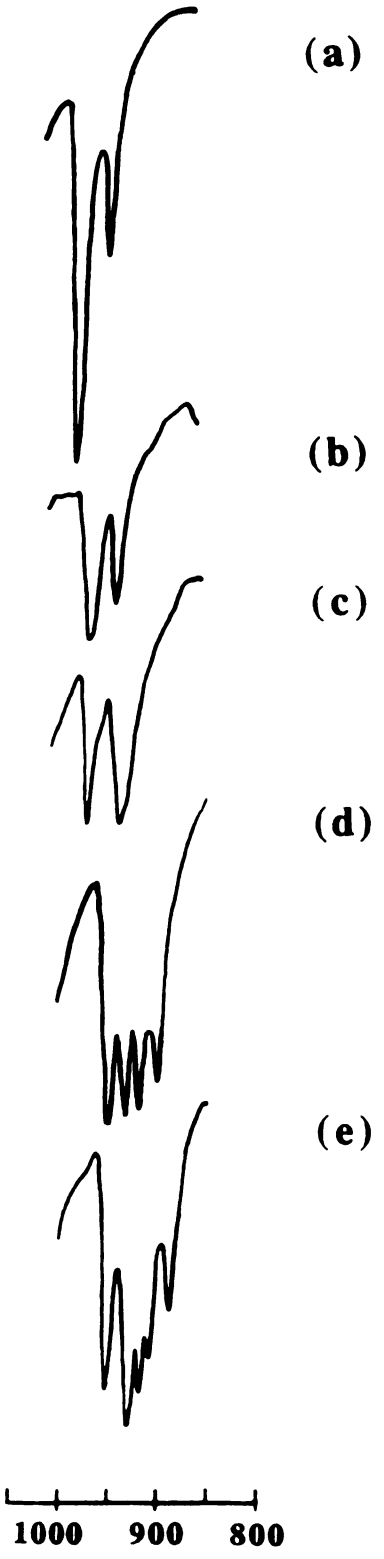

Figure 4.

lt (b),
$ClCH_2$-

and Mn halides. Chapters IV and V are an account of the chemistry of the solvated cations $[M(NCCH_3)_6]^{2+}$ (M = Co, Ni) with TMPP. Finally, Chapter VII summarizes our findings and projects future directions for this research.

LIST OF REFERENCES

1. McAuliffe, C. A.; Levason, W. *Phosphine, Arsine and Stibine Complexes of the Transition Elements*; Elsevier: New York, **1979.**

2. (a) Alyea, E. C.; Meek, D. W. *Catalytic Aspects of Metal Phosphine Complexes.*; Adv. in Chemistry Series 196; American Chemical Society: Washington, DC, **1982.** (b) Pignolet, L. H. *Homogeneous Catalysis with Metal Phosphine Complexes*; Plenum: New York, **1983.** (c) Kagan, H. B. *Comprehensive Organometallic Chemistry*; Pergamon Press: Oxford, **1982**, vol. 8, p. 464. (d) Parshall, G. W. *Homogeneous Catalysis: Applications and Chemistry of Catalysis by Soluble Transition Metal Complexes*; Wiley: New York, **1980.** (e) Stelzer, O. *Top. Phosphorus Chem.* **1977**, *9*, 1. (f) McAuliffe, C. A. *Comprehensive Coordination Chemistry*; Pergamon Press: Oxford, **1987**, Vol. 2, Ch. 14, p. 989. (g) Lukehart, C. M. *Fundamental Transition Metal Organometallic Chemistry*; Brooks/Cole Publishing Company: Monterey, CA, **1985**, Ch. 13, p. 389.

3. Evans, D.; Osborn, J. A.; Wilkinson, G. *J. Chem. Soc.(A)* **1968**, 3133.

4. Rahman, M. M.; Liu, H. - Y.; Eriks, K.; Prock, A.; Giering, W. P. *Organometallics*, **1989**, *8*, 1.

5. Behrens, H.; Muller, A. *Z. Anorg. Allg. Chem.* **1965**, *341*, 124.

6. Carmona, E.; Sanchez, L.; Poveda, M. L.; Jones, R. A.; Hefner, J. G. *Polyhedron* **1983**, *2*, 797.

7. Bailar, J. C., Jr. *The Chemistry of the Coordination Compounds*; Reinhold Publishing Corporation: New York, **1956.**

8. (a) Issleib, K.; Brack, A. *Z. Anorg. Allg. Chem.* **1954**, *277*, 258. (b) Issleib, K.; Tzschach, A. *Z. Anorg. Allg. Chem.* **1958**, *297*, 121. (c) Issleib, K.; Fröhlich, H. O. *Z. Anorg. Allg. Chem.* **1959**, *298*, 84. (d) Issleib, K.; Tzschach, A.; Fröhlich, H. O. *Z. Anorg. Allg. Chem.* **1959**, *298*, 164. (e) Issleib, K.; Bohn, G. *Z. Anorg. Allg. Chem.* **1959**, *301*, 188. (f) Issleib, K.; Döll, G. *Z. Anorg. Allg.*

Chem. **1960**, *305*, 1. (g) Issleib, K.; Wenschuh, E. *Z. Anorg. Allg. Chem.* **1960**, *305*, 15.

9. Cotton, F. A.; Wilkinson, G. *Advanced Inorganic Chemistry*; 5th Edition; John Wiley: New York, **1988**.

10. (a) Hermes, A. R.; Girolami, G. S. *Organometallics* **1987**, *6*, 763. (b) Hermes, A. R.; Girolami, G. S. *Organometallics* **1988**, 7, 394. (c) Hermes, A. R.; Moris, R. J.; Girolami, G. S. *Organometallics* **1988**, 7, 2372.

11. (a) Girolami, G. S.; Wilkinson, G.; Galas, A. M. R.; Thornton-Pett, M.; Hursthouse, M. B. *J. Chem. Soc., Dalton Trans.* **1985**, 1339. (b) Hermes, A. R.; Girolami, G. S. *Inorg. Chem.* **1988**, *27*, 1775. (c) Hermes, A. R.; Girolami, G. S. *Inorg. Chem.* **1990**, *29*, 313.

12. (a) Walker, J. D.; Poli, R. *Inorg. Chem.* **1989**, *28*, 1793. (b) Walker, J. D.; Poli, R. *Polyhedron* **1989**, *8*, 1293. (c) Walker, J. D.; Poli, R. *Inorg. Chem.* **1990**, *29*, 756.

13. (a) Singh, P. P.; Rivest, R. *Can. J. Chem.* **1968**, *46*, 1733. (b) Birchall, T. *Can. J. Chem.* **1969**, *47*, 1351.

14. (a) Katti, K. V.; Cavell, R. G. *Comments Inorg. Chem.* **1990**, *10*, 53. (b) Cooper. M. K.; Organ, G. J. *J. Chem. Soc., Dalton Trans.* **1988**, 2287. (c) Organ, G. J.; Cooper, M. K.; Hendrick, K.; McPartlin, M. *J. Chem. Soc., Dalton Trans.* **1984**, 2377.

15. (a) Popov, L. D.; Shevts, A. A.; Kogan, V. A. *Koord. Khim.* **1989**, *15*, 1299. (b) Bader, A.; Lindner, E. *Coord. Chem. Rev.* **1991**, *108*, 27.

16. (a) Lindner, E.; Reber, J. P.; Wegner, P. *Z. Naturforsch.* **1988**, *43b*, 1268. (b) Lindner, E.; Sickinger, A.; Wegner, P. *J. Organomet. Chem.* **1988**, *349*, 75. (c) Lindner, E.; Schrober, U.; Glaser, E.; Norz, H.; Wegner, P. *Z. Naturforsch.* **1987**, *42b*, 1527. (d) Lindner, E.; Mayer, H. A.; Wegner, P. *Chem. Ber.***1986**, *119*, 2616. (e) Lindner, E.; Sickinger, A.; Wegner, P. *J. Organomet. Chem.* **1986**, *312*, C37. (f) Lindner, E.; Raudeler, H ; Scheytt, C.; Mayer, H. A.; Hiller, W.; Fawzi, R.; Wegner, P. *Z. Naturforsch.* **1984**, *39b*, 632. (g) Lindner, E.; Scheytt, C. *Z. Naturforsch.* **1986**, *41b*, 10. (h) Lindner, E.; Scheytt, C.; Wegner, P. *J. Organomet. Chem.* **1986**, *308*, 311. (i) Lindner, E.; Fawzi, R.; Mayer, H. A.;

Eichele, K.; Pohmer, K. *J. Organomet. Chem.* **1990**, *386*, 63. (j) Lindner, E.; Schober, U.; Fawzi, R.; Hiller, W.; Englert, U.; Wegner, P. *Chem. Ber.* **1987**, *120*, 1621. (k) Lindner, E.; Karle, B. *Chem. Ber.* **1990**,*123*, 1464. (l) Lindner, E.; Karle, B. *Z. Naturforsch.* **1990**, *45b*, 1108. (m) Lindner, E.; Schober, U. *Inorg. Chem.* **1988**, *27*, 212. (n) Lindner, E.; Andres, B. *Chem. Ber.* **1987**, *120*, 761. (o) Lindner, E.; Andres, B. *Chem. Ber.* **1988**, *121*, 829. (p) Lindner, E.; Norz, H. *Chem. Ber.* **1990**, *123*, 459. (q) Lindner, E.; Norz, H. *Z. Naturforsch.* **1989**, *44b*, 1493. (r) Lindner, E.; Meyer, S. *J. Organomet. Chem.* **1988**, *339*, 193. (s) Lindner, E.; Andres, B. *Z. Naturforsch.* **1988**, *43b*, 369. (t) Lindner, E.; Speidel, R. *Z. Naturforsch.* **1989**, *44b*, 437. (u) Lindner, E.; Rothfuß, H.; Fawzi, R.; Hiller, W. *Chem. Ber.* **1992**, *125*, 541. (v) Lindner, E.; Bader, A.; Mayer, H. A. *Z. Anorg. Allg. Chem.* **1991**, *598/599*, 235. (w) Lindner, E.; Dettinger, J.; Möckel, A. *Z. Naturforsch.* **1991**, *46b*, 1519.

17. (a) Anderson, G. K.; Kumar, R. *Inorg. Chem.* **1984**, *23*, 4064. (b) Anderson, G. K.; Corey, E. R.; Kumar, R. *Inorg. Chem.* **1987**, *26*, 97. (c) Anderson, G. K.; Kumar, R. *Inorg. Chim. Acta* **1988**, *146*, 89.

18. (a) Rauchfuss, T. B.; Patino, F. T.; Roundhill, D. M. *Inorg. Chem.* **1975**, *14*, 652. (b) Jeffrey, J. C; Rauchfuss, T. B. *Inorg. Chem.* **1979**, *18*, 2658.

19. (a) Mason, R.; Thomas, K. M.; Empsall, H. D.; Fletcher, S. R.; Heys, P. N.; Hyde, E. M.; Jones, C. E.; Shaw, B. L. *J. Chem. Soc., Chem. Commun.* **1974**, 612. (b) Jones, C. E.; Shaw, B. L.; Turtle, B. L. *J. Chem. Soc., Dalton Trans.* **1974**, 992. (c) Empsall, H. D.; Heys, P. N.; Shaw, B. L. *J. Chem. Soc., Dalton Trans.* **1978**, 257.

20. Braunstein, P.; Matt, D.; Nobel, D.; Balegroune, F.; Bouaoud, S.-E.; Grandjean, D.; Fischer, J. *J. Chem. Soc., Dalton Trans.* **1988**, 353.

21. (a) Protopopov, I. S.; Kraft, M. Ya. *Zhurnal Obshchei Khimii* **1963**, *33*, 3050. (b) Protopopov, I. S.; Kraft, M. Ya. *Med. Prom. SSSR* **1959**, *13*, 5.

22. (a) Wada, M.; Higashizaki, S. *J. Chem. Soc.; Chem. Commun.* **1984**, 482. (b) Wada, M. *J. Chem. Res.* **1985**, (S), 38; (M), 0467.

23. Dunbar, K. R.; Haefner, S. C. manuscript in preparation.

24. (a) Wada, M. *Seisan to Gijutsu* **1989**, *41*, 9. (b) Wada, M. *Yuki Gosei Kagaku Kyokaishi* **1986**, *44*, 957. (c) Wada, M.; Tsuboi, A. *J. Chem. Soc., Perkin Trans. I* **1987**, 151. (d) Yamashoji, Y.; Matshshita, T.; Wada, M.; Shono, T. *Chem. Lett.* **1988**, 43. (e) Wada, M.; Tsuboi, A.; Nishimura, K.; Erabi, T. *Nippon Kagaku Kaishi* **1987**, *7*, 1284. (f) Wada, M.; Ohta, H.; Hashizume, N.; Kanzaki, M.; Hiratu, K.; Erabi, T. *Chem. Express* **1988**, *3*, 471. (g) Wada, M. *Polyhedron* **1989**, *8*, 1053.

25. (a) Tolman, C. A. *Chem. Rev.* **1977**, *77*, 313. (b) Ferguson, G.; Roberts, P. J.; Alyea, E. C.; Khan, M. *Inorg. Chem.* **1978**, *17*, 2965.

26. Dunbar, K. R. *J. Am. Chem. Soc.* **1988**, *110*, 8247.

27. Dunbar, K. R.; Haefner, S. C.; Pence, L. E. *J. Am. Chem. Soc.* **1989**, *111*, 5504.

28. Dunbar, K. R.; Haefner, S. C. *Organometallics* **1992**, *11*, 1431.

29. (a) Dunbar, K, R.; Haefner, S. C.; Swepston, P. N. *J. Chem. Soc., Chem. Commun.* **1991**, 460. (b) Haefner, S. C.; Dunbar, K. R.; Bender, C. *J. Am. Chem. Soc.* **1991**, *112*, 9540. (c) Dulebohn, J. I.; Haefner, S. C.; Berglund, K. A.; Dunbar, K. R. *Chem. Mater.* **1992**, *4*, 506.

30. Dunbar, K. R. *Comments Inorg. Chem.* **1992**, *13*, 0000.

31. Dunbar, K. R.; Haefner, S. C.; Burzynski, D. J. *Organometallics* **1990**, *9*, 1347.

32. Haefner, S. C. Ph. D. dissertation, Michigan State University, **1992**.

33. Chen, S. - J. Ph. D. dissertation, Michigan State University, **1991**.

34. (a) Chen, S. - J.; Dunbar, K. R. *Inorg. Chem.* **1990**, *29*, 588. (b) Chen, S. - J.; Dunbar, K. R. *Inorg. Chem.* **1991**, *30*, 2018.

35. (a) Sherry, A. E.; Wayland, B. B. *J. Am. Chem. Soc.* **1989**, *111*, 5010. (b) Sherry, A. E.; Wayland, B. B. *J. Am. Chem. Soc.* **1990**, *112*, 1259. (c) Wayland, B. B.; Ba, S.; Sherry, A. E. *J. Am. Chem.*

Soc. **1991**, *113*, 5305. (d) Wayland, B. B.; Sherry, A. E.; Poszmik, G.; Bunn, A. G. *J. Am. Chem. Soc.* **1992**, *114*, 1673.

CHAPTER II

CHEMISTRY OF TRIS(2,4,6-TRIMETHOXYPHENYL)PHOSPHINE WITH IRON(II) AND IRON(III)

1. Introduction

Despite the considerable amount of research that has been carried out on iron(II) and iron(III) chemistry, only the former oxidation state has been subjected to a broad investigation of its reactivity with phosphine ligands [1]. Indeed, there are few documented examples of neutral adducts of $FeCl_3$ with any ligand type [2] including phosphines [3-6]. In view of the demonstrated catalytic role of $FeCl_3$ in the oxidation of triphenylphosphine to triphenylphosphine oxide, especially the recent work of Ondrejovic *et al.* [7], we were interested to see if we could stabilize a mono-TMPP adduct of $FeCl_3$, and study its reactivity with dioxygen.

This chapter reports our investigations of the chemistry of TMPP with $FeCl_2$ and $FeCl_3$, and the reactivity of some of the products with molecular oxygen.

2. Experimental

A. Synthesis

(1) Reaction of $FeCl_2$ with TMPP

(i) with one equivalent of TMPP

In a typical reaction, a sample of anhydrous ferrous chloride (0.127 g, 1.002 mol) was reacted with one equivalent of TMPP (0.534 g, 1.003 mmol) in *ca.* 20 mL of carefully deoxygenated benzene to produce a pale brown solution. The solution was stirred at room temperature for about 24 hours, after which time it was reduced to a residue. The resulting brown solid was washed with copious amounts of benzene (3 x 10 mL) and dried under vacuum; yield of $[CH_3\text{-TMPP}]_2[FeCl_4]$ (**1**): 0. 210 g (16% relative to $FeCl_2$).

After evaporation in air, the washings produced a large crop of white crystals after 5 days, which was washed with diethyl ether, acetone

and ethanol and characterized as free TMPP by ^1H NMR (CD_3CN, δppm: 3.50(s), 3.73(s), 6.02(d)) and infrared (949(s) and 918(w) cm^{-1}) spectroscopies.

The brown solid was identified by ^1H NMR (CD_3CN, δppm: 2.48 (d), 3.55(s), 3.86(s) and 6.21(d)) and infrared (949(s) and 916(s, br) cm^{-1}) spectroscopies as containing the cation $[CH_3\text{-TMPP}]^+$ and $[FeCl_4]^{2-}$ ($\nu_{Fe\text{-}Cl}$ = 283 cm^{-1}); UV-visible spectrum (CH_3CN, λ_{max}, nm) : 310, 360.

(ii) with two equivalents of TMPP

An amount of $FeCl_2$ was reacted with two equivalents of TMPP following the procedure described in A(1)(i), and a similar work-up was employed. An attempted characterization of the pale yellow-brown product revealed only the presence of free TMPP and $[H\text{-TMPP}]^+$. No evidence for a Fe-Cl stretch was observed in the infrared spectrum.

(2) Reactions of $[Fe(NCCH_3)_6][BF_4]_2$ with TMPP

The salt $[Fe(NCCH_3)_6][BF_4]_2$ was prepared as reported in the literature [8]. The reaction of $[Fe(NCCH_3)_6][BF_4]_2$ with two equivalents of TMPP was performed in a variety of solvents (MeOH, CH_3CN, benzene, acetone). A typical experiment was carried out as follows. A quantity of $[Fe(NCCH_3)_6][BF_4]_2$ (0.133 g, 0.280 mmol) was added to 2 equivalents of TMPP (0.298 g, 0.559 mmol) in *ca.* 20 mL of solvent and the resulting pale brown-yellow solution was stirred at room temperature for *ca.* 1 hour. A pale solid precipitated from the solution after slow addition of diethyl ether and was dried *in vacuo*. ^1H NMR and infrared spectroscopies of this residue established its identity as $[H\text{-TMPP}][BF_4]$; yield: 0.173 g (48% relative to TMPP).

(3) Reactions of $FeCl_3$ with TMPP

(i) Reaction of $FeCl_3$ with TMPP in ethanol

A Schlenk flask was charged with equimolar amounts of anhydrous ferric chloride (0.167 g, 1.030 mmol) and TMPP (0.549 g, 1.030 mmol). Upon addition of ethanol (20 mL), a bright orange microcrystalline solid formed which was filtered through a medium frit, washed with ethanol and dried; yield: 0.447 g. ^1H NMR (CD_3CN, δppm): 3.69 (s, *o*-O<u>CH_3</u>), 3.88 (s, *p*-O<u>CH_3</u>), 6.26 (d, *m*-<u>H</u>), 8.40 (d, P-<u>H</u>), IR (CsI, Nujol, cm^{-1}): ν(Fe-Cl) = 366(s) and 320(m); UV-visible (CH_3CN, λ_{max} (nm)): 381, 320, 286, 260 and 219; electrochemistry: $(E_{1/2})_{red}$ = - 0.44 V (vs. Ag/AgCl). In the absence of a structure, the identity of the iron-containing anion is postulated as $[Fe_2Cl_6(\mu\text{-}OH)_2]^{2-}$. Anal. Calc'd for $Fe_2Cl_6P_2O_{20}C_{54}H_{70}$: C: 45.51; H: 4.95; Found: C: 45.10; H: 4.77.

(ii) Reaction of $FeCl_3$ with TMPP in $CHCl_3$

A sample of $FeCl_3$ (0.151 g, 0.931 mmol) was stirred with one equivalent of TMPP (0.495 g, 0.929 mmol) in 20 mL of $CHCl_3$ at r.t. for *ca.* 36 hours after which time the solvent was removed under reduced pressure to produce a dark yellow residue. This solid was washed with several aliquots of freshly distilled benzene (3 x 10 mL) and dried *in vacuo*; yield of $[FeCl_4]$[H-TMPP] (**5**): 0.358 g (53% relative to $FeCl_3$). The far-infrared spectrum exhibited the typical ν(Fe-Cl) stretch for $[FeCl_4]^-$ at 375 cm^{-1} whereas the mid-infrared region was indicative of the presence of $[H\text{-}TMPP]^+$ as the cation.

(iii) Reaction of $FeCl_3$ with TMPP in CH_3CN

Equimolar amounts of $FeCl_3$ (0.144 g, 0.888 mmol) and TMPP (0.471 g, 0.884 mmol) were dissolved in 20 mL of CH_3CN to yield a homogeneous brown-green solution which was stirred at room temperature

for *ca.* 4 days. The volume of the reaction solution was reduced to about 5 mL and layered with hexanes followed by diethyl ether. Within 3 days, a mixture of red crystals (identified as $FeCl_3(O{=}PR_3)$ (**6**), *vide infra*) and yellow crystals were present. The latter were characterized as [H-TMPP]$_2$[Fe_2Cl_6] (**2**) (*vide infra*) on the basis of infrared and ^{1}H NMR spectroscopies.

(iv) Preparation of [H-TMPP]$_2$[$Fe_2^{II,II}Cl_6$] (2) in benzene

A quantity of anhydrous $FeCl_3$ (0.162 g, 0.999 mmol) was added to one equivalent of TMPP (0.532 g, 0.999 mmol) in 30 mL of deoxygenated benzene. The resulting suspension was stirred at room temperature for 24 hours, after which time the solvent was decanted from a yellow solid. The product was washed with several aliquots of benzene (3 x 10 mL) and THF (3 x 10 mL) until the supernatant was colorless. The resulting pale yellow product was dried *in vacuo*; yield: 0.456 g (65% relative to $FeCl_3$). Anal. Calc'd for $Fe_2Cl_6PC_{54}O_{18}H_{68}$: Cl: 15.28; C: 46.61; H: 4.92; Found: Cl: 15.27; C: 45.98; H: 4.90. Slow diffusion of hexanes into an acetone solution of **2** resulted in the formation of X-ray quality yellow crystals. Four ν(Fe-Cl) stretches were observed in the far-infrared spectrum at 360(s), 300(m), 280(m) and 230(w) cm^{-1}, and the ^{1}H NMR spectrum exhibited characteristic resonances attributed to the protonated phosphine (CD_3CN, δppm): 3.67 (s, *o*-O<u>CH$_3$</u>), 3.85 (s, *p*-O<u>CH$_3$</u>), 6.24 (d, *m*-<u>H</u>), 8.37 (d, P-<u>H</u>). The electronic spectrum consists of three features ($CHCl_3$, λ_{max} (nm); ε, M^{-1} cm^{-1}): 377(1.80 x 10^3), 287(sh) and 260(6.80 x 10^4).

The dark red-brown filtrate was evaporated to a residue; yield of [TMPP-Cl][$FeCl_4$] (**3**): 0.078 g (11% relative to $FeCl_3$). ^{1}H NMR (CD_3CN, δppm): 3.35 (s, 18 H), 3.64 (s, 9 H), 5.95 (d, 6 H); ^{31}P NMR

(CD_3CN, δppm): - 1.56; IR (CsI, Nujol): ν(Fe-Cl) = 380 cm^{-1}, FAB-mass spectrum: m/z = 567 (corresponding to $[TMPP-Cl]^+$).

(v) Preparation of $[H\text{-}TMPP]_2[Fe_2^{II,II}Cl_6]$ (2) in diethyl ether

A quantity of $FeCl_3$ (0.062 g, 0.380 mmol) was dissolved in 15 mL of diethyl ether and filtered into a 25 mL diethyl ether solution of TMPP (0.203 g, 0.380 mmol). The resulting yellow suspension was stirred at room temperature for 24 hours. The reaction was treated in a manner identical to that described in A(3)(iv) above; yield: 0.148 g (56 %).

(4) Preparation of $[H\text{-}TMPP]_2[Fe^{II}Cl_4]$ (4):

(i) Decomposition of $[H\text{-}TMPP]_2[Fe_2Cl_6]$ (2) in ethanol

An amount of **2** (0.050 g, 0.072 mmol) was dissolved in 40 mL of ethanol. The resulting yellow solution slowly became colorless over the period of one week under an argon atmosphere. Careful evaporation of the solvent by purging the solution with a strong flow of argon yielded a crop of pale yellow crystals of a quality suitable for a single crystal X-ray study.

(ii) Reaction of $[Fe^{II}(NCCH_3)_6][AlCl_4]_2$ with TMPP

An amount of $[Fe(NCCH_3)_6][AlCl_4]_2$ [9] (0.303 g, 0.474 mmol) was reacted with two equivalents of TMPP (0.505 g, 0.949 mmol) in 20 mL of methanol. The bright yellow solution was stirred at room temperature for 0.5 h. A pale yellow solid, isolated after reduction of the volume, was dried under a dynamic vacuum and recrystallized from an acetone/hexanes mixture (v/v 1:1); yield: 0.240 g (40%). Anal. Calc'd for $FeCl_4P_2C_{54}O_{18}H_{68}$: C: 51.29; H: 5.42; Found: C: 49.0; H: 5.89. Pale yellow microcrystals were grown by slow diffusion of diethyl ether into a THF solution of **4**, or by diffusion of toluene into a CH_2Cl_2 solution.

Infrared (CsI, Nujol, cm^{-1}): 280(s) (ν(Fe-Cl)); UV-visible ($CHCl_3$, λ_{max} (nm); ε, $M^{-1}cm^{-1}$): 361(4.6 x 10^3), 309(4.9 x 10^3), 287(sh), 261(7.2 x 10^4); ^1H NMR (CD_3CN, δppm): 3.68(s), 3.88(s), 6.25(d), 8.40(d); cyclic voltammetry: $(E_{1/2})_{ox}$ = + 0.04 V, μ_{eff} = 5.29 μ_B.

(5) Preparation of [H-TMPP][$Fe^{III}Cl_4$] (5):

(i) Oxidation of [H-TMPP]$_2$[$Fe^{II}Cl_4$] (4) with molecular oxygen

An amount of **4** (0.050 g, 0.039 mmol) was dissolved in methanol. Upon bubbling dry oxygen into the solution, the color changed from yellow to orange. Rapid evaporation of the solution produced long orange needles that were of a quality suitable for an X-ray study. Anal. Calc'd for $FeCl_4PC_{27}O_9H_{34}$: C: 44.31; H: 4.65; Found: C: 44.26; H: 4.71. IR (CsI, Nujol, cm^{-1}): ν(Fe-Cl) = 380(s); ^1H NMR (CD_3CN, δppm): 3.70(s), 3.88(s), 6.26(d), 8.38(d); UV-visible ($CHCl_3$, λ_{max} (nm); ε, M^{-1} cm^{-1}): 365(5.05 x 10^3), 315(4.9 x 10^3), 289(sh) and 261(7.54 x 10^4); cyclic voltammetry: $(E_{1/2})_{red}$ = + 0.03 V; μ_{eff} = 6.11 μ_B.

(ii) Reaction of [$Fe^{II}(NCCH_3)_6$][$SbCl_6$]$_2$ with TMPP

A quantity of [$Fe(NCCH_3)_6$][$SbCl_6$]$_2$ [10] (0.173 g, 0.179 mmol) was added to two equivalents of TMPP (0.190 g, 0.357 mmol) in 10 mL of methanol. Upon addition of the solvent, a bright yellow solid rapidly precipitated from an orange solution. The orange filtrate was decanted from the solid and subjected to a dynamic vacuum to yield a residue which was washed with diethyl ether (2 x 10 mL) and dried *in vacuo*; yield: 0.064 g (51% relative to Fe^{2+}). The yellow solid was characterized as [H-TMPP][$SbCl_6$]; yield: 0.089 g (40% relative to TMPP). Anal. Calc'd for $SbCl_6PC_{27}O_9H_{34}$: Cl: 24.09; C: 36.69; H: 3.93; Found: Cl: 24.51; C: 37.33; H: 3.92. Infrared (CsI, Nujol): ν(Sb-Cl) = 345 cm^{-1}; ^1H NMR

($CDCl_3$, δppm): 3.69(s), 3.87(s), 6.11(d) and 8.33(d). The identical compound was independently prepared from the reaction of $Na^+SbCl_6^-$ with one equivalent of TMPP in MeOH.

(6) Preparation of $Fe^{III}Cl_3$(O=TMPP) (6):

(i) Reaction of $[H\text{-}TMPP]_2[Fe_2Cl_6]$ (2) with molecular oxygen

An amount of **2** (0.050 g, 0.072 mmol) was dissolved in 30 mL of ethanol. The resulting yellow solution was bubbled with dry oxygen for 10 minutes, during which time it turned to a dark orange color. The reaction solution was then left to evaporate under a purge of O_2 gas which produced red-orange crystals of **6**; yield: 0.041 g (80% relative to **2**). Anal. Calc'd for $FeCl_3PO_{10}C_{27}H_{33}$: C: 45.59; H: 4.64; Found: C: 45.88; H: 4.73. IR (CsI, Nujol, cm^{-1}): ν(Fe-Cl) = 380(s) and 320(w); electronic spectrum ($CHCl_3$, λ_{max} (nm); ε, $M^{-1}\ cm^{-1}$): 342(4.3×10^3), 287(sh), 258(4.0×10^4); FAB-mass spectrum: m/z = 548 (corresponding to TMPP=O); ^1H NMR (CD_3CN): very broad; CV: $(E_{1/2})_{red}$ = - 0.02 V; μ_{eff} = 6.31 μ_B.

An anaerobic EtOH solution of **2** as described above became colorless during the period of 1 week. After bubbling O_2 through this solution for 5 minutes, a yellow color ensued which converted to dark orange within 10 minutes. Red-orange crystals of **6** formed under an oxygen atmosphere after several days.

An amount of **2** (0.050 g, 0.036 mmol) was dissolved in 50 mL of acetone and a stream of O_2 gas was passed through the solution for *ca.* 1 hour. The resulting orange solution was layered with hexanes and diethyl ether. Crystals of **6** were isolated from this solvent mixture; yield: 0.040 g (78% relative to **2**).

(ii) Reaction of $[H\text{-}TMPP]_2[Fe^{II}Cl_4]$ (4) with molecular oxygen

An amount of **4** (0.100 g, 0.079 mmol) was dissolved in 20 mL of methanol, treated with O_2 for 4 hours, and layered with hexanes and diethyl ether to produce red-orange crystals of **6**; yield: 0.030 g (53% relative to **4**).

(iii) Reaction of $[H\text{-}TMPP][Fe^{III}Cl_4]$ (5) with molecular oxygen

A quantity of **5** (0.100 g, 0.137 mmol) was dissolved in 30 mL of methanol whereupon the solution was bubbled with O_2 for 3-4 days. During this time, the solvent was replenished regularly to avoid complete evaporation. Red-orange crystals of **6** were eventually deposited at the bottom of the flask; yield: 0.058 g (60% relative to **5**).

(iv) Reaction of $FeCl_3$ with TMPP in the presence of oxygen

An amount of $FeCl_3$ (0.142 g, 0.874 mmol) was treated with one equivalent of TMPP (0.465 g, 0.874 mmol) in 20 mL of ethanol under a slow stream of O_2 for 3 hours. The resulting orange solution was evaporated under reduced pressure to yield a dark orange solid, which was then recrystallized from ethanol and diethyl ether.

(v) Reaction of $FeCl_3$ with TMPP=O

A quantity of TMPP oxide (0.404 g, 0.736 mmol), which was prepared as reported in the literature [46], was added to a suspension of $FeCl_3$ (0.119 g, 0.736 mmol) in 12 mL of ethanol. The resulting orange reaction solution was stirred at room temperature for *ca.* 1 hour until all of the $FeCl_3$ had dissolved. The suspension was then filtered in air and

washed with ethanol (3 x 10 mL) followed by diethyl ether (1 x 10 mL) and finally dried *in vacuo*; yield: 0.423 g (81% relative to $FeCl_3$).

Note: it is worth mentioning that all the aforementioned reactions will eventually yield $FeCl_3$(O=TMPP) as the major product if O_2 or air is introduced into the system.

(7) Preparation of TMPP=O

A quantity of $FeCl_3$(O=TMPP) (**6**) (0.067 g, 0.094 mmol) was reacted with a 10-fold excess of TMPP (0.500 g, 0.939 mmol) in 20 mL of acetone under a stream of dry O_2. The solution was stirred at room temperature for 1-2 hours during which time a significant amount of white solid precipitated from the solution. The orange solution was decanted from the solid, which was washed with ether (3 x 10 mL) and dried *in vacuo*. Chilling of the orange filtrate produced an additional amount of of white product, characterized as TMPP=O; yield: 0.325 g (63% relative to TMPP). Work-up of the remaining orange solution consisted of successive extractions by CH_2Cl_2 and EtOH which yielded crystals of $FeCl_3$(O=TMPP); total recovered yield: 0.062 g (93% of the initial mass). IR (CsI, Nujol, cm^{-1}): 951(s), 920(s); ^1H NMR (CD_3CN, δppm): 3.48(s), 3.79(s), 6.10(d).

The reaction can also be performed in acetonitrile but the separation of TMPP=O and $FeCl_3$(O=TMPP) is much less straightforward.

(8) Reaction of $FeCl_3$ with PPh_3 in benzene

Anhydrous $FeCl_3$ (0.193 g, 1.187 mmol) and PPh_3 (0.312 g, 1.190 mmol) were dissolved in 30 mL of benzene to produce a deep-red solution, which was stirred at room temperature for 1 day. During this time the solution had turned dark yellow and produced an amount of yellow solid. The solvent was removed under reduced pressure and the resulting residue

was washed with diethyl ether (1 x 10 mL) and hexanes (1 x 20 mL) and dried *in vacuo*. The residue was dissolved in acetone and layered with hexanes to produce a crop of yellow crystals within 2-3 hours, yield: 0.123 g. The far-infrared spectrum exhibited an identical pattern as the corresponding spectrum of $[H\text{-}TMPP]_2[Fe_2Cl_6]$, *i.e.*, four Fe-Cl stretching bands at 380(s), 330(m), 320(m) and 300(w) cm^{-1}, and the highest peak in the FAB-mass spectrum was at m/z = 263, corresponding to $[H\text{-}PPh_3]^+$. The UV-visible spectrum exhibits one feature at 369 nm, and the cyclic voltammogram consists of one irreversible oxidation at $E_{p,a}$ = + 0.64 V (vs. Ag/AgCl).

(9) Reaction of $FeCl_3$ with PCy_3 in benzene

Equimolar amounts of $FeCl_3$ (0.100 g, 0.617 mmol) and tricyclohexylphosphine (0.173 g, 0.617 mmol) were added to a flask containing 15 mL of benzene to form a deep-red solution, which was stirred under ambient conditions for 1 day. A dark yellow solid was separated from the solution, washed with diethyl ether (10 mL) and dried under vacuum; yield: 0.110 g. The infrared spectrum exhibited four ν(Fe-Cl) stretches at 380(s), 360(m), 315(m) and 300(w) cm^{-1}; the highest peak in the FAB-mass spectrum was at m/z = 281, in agreement with $[H\text{-}PCy_3]^+$. In addition, the characteristic P-H stretch at 2400 cm^{-1} was observed in the mid-IR region.

(10) Preparation of $[Cl\text{-}TMPP][FeCl_4]$

(i) Preparation of [TMPP-X]X (X = Cl, I)

Preparation of TMPP-I_2: Equimolar amounts of TMPP (0.500 g, 0.939 mmol) and iodine (0.238 g, 0.939 mmol) were dissolved in 20 mL of benzene to produce a bright yellow solution along with a small amount of undissolved I_2. After *ca.* 1 hour all the I_2 had dissolved and a yellow

precipitate was present in an orange solution. The solution was decanted from this solid, which was washed with 10 mL of benzene and dried *in vacuo*; yield of TMPP-I_2: 0.667 g (90% relative to TMPP). ^1H NMR ($CDCl_3$, δppm): 3.61(s), 3.80(s), 6.02(d); IR (CsI, Nujol, cm^{-1}): 955(s), 919(s); FAB-mass spectrum: m/z = 659.4 (corresponding to $[TMPP\text{-}I]^+$)

Preparation of [TMPP-Cl]Cl: A solution of TMPP (0.461 g, 0.867 mmol) in 20 mL of benzene was bubbled with chlorine gas for 1-2 minutes until it had turned bright yellow. It was then pumped down to a sticky residue which was used as such in the reaction described below.

(ii) Reaction of [TMPP-Cl]Cl with $FeCl_3$

The aforementioned residue of [TMPP-Cl]Cl was redissolved in 20 mL of benzene and an amount of $FeCl_3$ (0.141 g, 0.867 mmol) was added to this solution. A color change from yellow to dark red-brown immediately ensued. The solvent was removed under dynamic vacuum to produce a brown residue that was recrystallized from an acetone/hexanes mixture (v/v 1:1); yield: 0.020 g. The properties of this solid were identical to those described for [TMPP-Cl][$FeCl_4$] (*vide supra*).

(11) Reactivity of $[H\text{-}TMPP]_2[Fe_2Cl_6]$ (2) in CH_2Cl_2

(i) Thermal reaction of (2) in CH_2Cl_2

A CH_2Cl_2 solution of **1** was refluxed for one week, during which time the initially yellow solution had turned green-brown. Evaporation of the solvent under reduced pressure yielded a brown solid which infrared spectroscopy clearly established as [$ClCH_2$-TMPP][$FeCl_4$] (**7**), with a ν(Fe-Cl) stretch at 379 cm^{-1} and the typical pattern for chloromethylphosphonium (950(s) and 918(s) cm^{-1}).

(ii) Reaction with O_2 at room temperature

A stream of dry O_2 was passed through a solution of **1** (0.106 g, 0.077 mmol) in 40 mL of CH_2Cl_2, which resulted in an instantaneous color change from yellow to dark green. This reaction was carried out at room temperature for 1 hour, after which time the solution was pumped down to a residue; yield: 0.077 g. Infrared (CsI, Nujol): 365(vs) and 320(s) cm^{-1}; the mid-IR region showed a mixture of $[H\text{-}TMPP]^+$ and $[ClCH_2\text{-}TMPP]^+$; FAB-mass spectrum: m/z = 533 and 582.

(iii) Reaction with O_2 at high temperature

A typical reaction was performed following the procedure described in A(11)(ii) above but under a reflux conditions (0.061 g of **1**, 0.044 mmol). The resulting solution, which was much darker than in the analogous room temperature reaction, was pumped to a residue after 1 hour; yield: 0.064 g. Infrared (CsI, Nujol): ν(Fe-Cl) = 385(vs) cm^{-1} ($[FeCl_4]^-$), 950(s, sharp) and 920(s, sharp) cm^{-1} ($[ClCH_2\text{-}TMPP]^+$).

(iv) Reaction with O_2 at low temperature

A solution of **1** (0.130 g, 0.093 mmol) in 40 mL of CH_2Cl_2 was placed in an acetone/dry-ice low temperature bath, and O_2 was bubbled through the solution for 3 hours resulting in an orange solution. The solvent was removed under reduced pressure, and an orange solid was obtained; yield: 0.107 g. Infrared (CsI, nujol): ν(Fe-Cl) = 385(vs) cm^{-1} (for $[FeCl_4]^-$), the 1000-800 cm^{-1} region showed that $[ClCH_2\text{-}TMPP]^+$ was the major TMPP species but traces of $[H\text{-}TMPP]^+$ could also be detected.

B. X-ray Crystal Structures

The structures of complexes **2**, **4**, **5** and **6** were determined by applications of general procedures described elsewhere [11]. Geometric

and intensity data were collected on a Nicolet P3/F diffractometer for **4** and **6** and on a Rigaku AFC6S diffractometer for **2** and **5**; both instruments were equipped with graphite monochromated MoK_α (λ_α = 0.71073 Å and 0.71069 Å, respectively) radiation. The data were corrected for Lorentz and polarization effects. Calculations for **2** and **4-6** were performed on a VAXSTATION 2000 computer using programs from the TEXSAN Crystallographic Package of the Molecular Structure Corporation (**2, 4, 5**) [12] and from the Structure Determination Package (SDP) of Enraf-Nonius (**6**) [13].

(1) $[H\text{-}TMPP]_2[Fe_2Cl_6]$ (2)

A yellow parallelepiped of approximate dimensions 0.31 x 0.47 x 0.52 mm^3 was mounted at the end of a glass fiber with Dow Corning silicone grease and placed in a N_2 cold stream at -100 ± 2° C. A preliminary monoclinic cell was determined by centering and indexing 20 reflections. The cell was then refined by least-squares determinations of 21 reflections with $23 \leq 2\theta \leq 30$. Intensity data were collected over the range 4 - 47° in 2θ, by using the θ - 2θ scan mode. Three standard reflections were measured at regular intervals during data collection and showed no significant decay in crystal quality. After averaging equivalent reflections, 4952 unique data remained, of which 3440 were observed with $F_o^2 \geq 3\sigma(F_o)^2$.

The position of the metal atom was determined from a solution provided by the direct method program SHELXS-86 [14]. The positions of the remaining non-hydrogen atoms and of H(1) bound to the phosphorus atom were located by use of the program DIRDIF [15]. An empirical absorption correction was applied by application of the program DIFABS [16] after isotropic convergence. The positions of the hydrogen atoms that

Table 3. Crystallographic data for $[H\text{-}TMPP]_2[Fe_2Cl_6]$ (2)

Formula	$Fe_2Cl_6P_2C_{54}O_{18}H_{68}$
Formula weight	1391.48
Space group	$P2_1/n$
a, Å	14.294(8)
b, Å	10.140(9)
c, Å	22.543(8)
α, deg	90.0
β, deg	105.76(4)
γ, deg	90.0
V, $Å^3$	3144(3)
Z	2
d_{calc}, g/cm^3	1.469
μ (MoK_α), cm^{-1}	8.32
Data collection range, 2θ, deg	4 - 47
No. unique data	4952
total with $F_o^2 \geq 3\sigma(F_o)^2$	3440
Number of parameters refined	370
Trans. factors, max., min.	1.26 - 0.82
R	0.046
R_w	0.079
Quality-of-fit	2.84
Largest shift/esd, final cycle	0.00
Largest peak, $e^-/Å^3$	0.96

were not directly located were generated by a program in the TEXSAN package. These were included in the structure factor calculations but not refined. The final full-matrix refinement involved 3440 data and 370 parameters and converged with residuals $R(R_w) = 0.046(0.079)$ and a quality-of-fit of 2.84. The final difference Fourier map showed a highest peak of 0.96 $e^-/Å^3$. Table 3 contains a summary of important crystallographic data.

(2) $[H\text{-}TMPP]_2[Fe^{II}Cl_4]$ (4)

Crystallographic data are summarized in Table 4. A pale yellow crystal of approximate dimensions 0.12 x 0.22 x 0.32 mm^3 was mounted at the end of a glass fiber and placed in a N_2 cold stream at -160° C. A preliminary triclinic unit cell was determined by centering and indexing 16 reflections chosen from a rotational photograph. The cell was then refined by least-squares determination of 25 reflections with $15 \leq 2\theta \leq 22$. Intensity data were collected over the range 5 - 35° in 2θ, using the θ - 2θ scan mode. Three standard reflections were measured at regular intervals during data collection and showed no significant decay in crystal quality. After averaging equivalent reflections, 3291 unique data remained, of which 2274 were observed with $F_o^2 \geq 3\sigma(F_o)^2$.

Failure to solve the structure in a triclinic space group prompted us to re-examine the data. The program CLEGG [17] gave a monoclinic cell. Transformation of the initial cell was performed using the following matrices:

$$\begin{matrix} -1 & 2 & 0 \\ -1 & 0 & 0 \\ 0 & -1 & 1 \end{matrix} \quad \text{and} \quad \begin{matrix} 0 & 0 & -1 \\ 0 & 1 & 0 \\ 1 & 0 & 1 \end{matrix} \quad ,$$

which gave the final monoclinic cell used in the solution and the refinement. The position of the metal atom was obtained from a solution

Table 4. Crystallographic data for [H-TMPP]$_2$[FeCl$_4$] (4) and [H-TMPP][FeCl$_4$](5)

Formula	$FeCl_4P_2C_{54}O_{18}H_{68}$	$FeCl_4PC_{27}O_9H_{34}$
Formula weight	1264.7	731.19
Space group	I2/a	Pbca
a, Å	23.27(2)	19.952(5)
b, Å	10.06(1)	19.352(7)
c, Å	28.07(3)	17.821(4)
α, deg	90.0	90.0
β, deg	108.9(1)	90.0
γ, deg	90.0	90.0
V, Å^3	6211(12)	6881(6)
Z	2	8
d_{calc}, g/cm^3	1.352	1.411
μ (MoK_α), cm^{-1}	5.29	8.40
Data collection range, 2θ, deg	5 - 35	4 - 45
No. unique data	3291	3612
total with $F_o^2 \geq 3\sigma(F_o)^2$	2274	1472
Number of parameters refined	177	379
Trans. factors, max., min.	1.13 - 0.83	1.00 - 0.79
R	0.105	0.051
R_w	0.143	0.066
Quality-of-fit	3.67	1.457
Largest shift/esd, final cycle	0.01	0.07
Largest peak, e$^-$/Å^3	2.22	0.49

provided by the direct method program SHELXS-86. The positions of the remaining non-hydrogen atoms and of H(1) bound to the phosphorus atom were located by use of the program DIRDIF. A sequence of successive difference Fourier maps and least-squares cycles was then carried out. An empirical absorption correction was applied by application of the program DIFABS. The positions of the hydrogen atoms that were not directly located were generated by a program in the TEXSAN package. These were included in the structure factor calculations but not refined. Only the iron, chlorine and phosphorus atoms were refined anisotropically. Lack of data and problems with refining the solvent molecule precluded a full isotropic refinement of the structure; the final refinement converged with residuals of $R = 0.105$ and $R_w = 0.143$, and included 2274 data and 177 parameters.

(3) [H-TMPP][$Fe^{III}Cl_4$] (5)

A summary of crystallographic data can be found in Table 4. An orange platelet of approximate dimensions 0.10 x 0.21 x 0.52 mm^3 was selected and mounted on the end of a glass fiber with epoxy cement. Intensity and geometric data were collected at room temperature. A preliminary orthorhombic unit cell was determined by centering and indexing on 20 reflections. The cell was then refined by a least-squares determination of 24 reflections with $9 \leq 2\theta \leq 23$. Intensity data were collected over the range 4 - 45° in 2θ, by the θ - 2θ scan mode. Three standard reflections were measured at regular intervals during data collection and showed no decay over time. After averaging equivalent reflections, 3612 unique data remained, of which 1472 were observed with $F_o^2 \geq 3\sigma(F_o)^2$. The position of the metal atom was determined from a solution provided by the direct method program MITHRIL [18]. The positions of the remaining non-hydrogen atoms and of H(1) were located

by the program DIRDIF. An empirical absorption correction coefficient of 8.404 was applied using the PSI-Scan program within the TEXSAN package. All of the non-hydrogen atoms were refined anisotropically. The position of the hydrogen atoms were calculated by programs located in the solution package; they were included in the structure factor calculations but not refined. The final full-matrix refinement involved 1472 data and 379 parameters. The refinement converged with residuals, R and R_w of 0.051 and 0.066, respectively, and a quality-of-fit indicator of 1.457. The final difference Fourier map showed a highest peak of 0.49 $e^-/Å^3$.

(4) $Fe^{III}Cl_3$(O=TMPP) (6)

A red-orange parallelepiped of approximate dimensions 0.28 x 0.20 x 0.13 mm^3 was mounted at the end of a glass fiber with epoxy cement. Intensity and geometric data were collected at room temperature. A preliminary triclinic unit cell was determined by centering and indexing on 14 reflections chosen from a rotational photograph. The cell was further refined by a least-squares determination of 12 reflections with $15 \leq 2\theta \leq 20$. Axial photographs and intensity data confirmed the choice of the triclinic cell. Intensity data were collected at room temperature over the range 4 - 40° in 2θ, using the θ - 2θ scan mode. In addition, three check reflections were measured at regular intervals during intensity data collection. A plot of the intensity of these reflections versus time showed that no decay in crystal quality had occurred. After averaging equivalent reflections, 2886 unique data remained of which 1606 were observed with $F_o^2 \geq 3\sigma(F_o)^2$. The position of the metal atom was obtained from a solution provided by the direct methods program in SHELXS-86. The positions of the remaining non-hydrogen atoms were located through a sequence of successive difference Fourier maps and least-squares cycles.

Table 5. Crystallographic data for $FeCl_3(O=TMPP)$ (6)

Formula	$FeCl_3PC_{54}O_{10}H_{33}$
Formula weight	710.74
Space group	P-1
a, Å	12.23(1)
b, Å	14.06(1)
c, Å	13.13(1)
α, deg	110.78(7)
β, deg	109.88(8)
γ, deg	72.58(8)
V, $Å^3$	1648(3)
Z	2
d_{calc}, g/cm^3	1.432
μ (MoK_α), cm^{-1}	7.976
Data collection range, 2θ, deg	4 - 40
No. unique data	2886
total with $F_o^2 \geq 3\sigma(F_o)^2$	1606
Number of parameters refined	374
R[a]	0.068
R_w[b]	0.078
Quality-of-fit[c]	1.919
Largest shift/esd, final cycle	0.01
Largest peak, $e^-/Å^3$	0.454

[a] $R = \Sigma||F_o|-|F_c||/\Sigma|F_o|$; [b] $R = |\Sigma(w|F_o|-|F_c|)^2/\Sigma w|F_o|^2]^{1/2}$; $w = 1/\sigma^2(|F_o|)$

[c] Quality-of-fit = $[\Sigma(w|F_o|-|F_c|)^2/(N_{obs}-N_{parameters})]^{1/2}$

All of the non-hydrogen atoms, except one carbon in the *meta*-position of a phenyl ring, were refined anisotropically. The final full-matrix refinement involved 374 parameters and 1606 data. The refinement converged with residuals, R and R_w of 0.068 and 0.078, respectively, and a quality-of-fit of 1.919. The final difference Fourier map showed a highest peak of 0.45 $e^-/Å^3$. A summary of crystallographic parameters is found in Table 5.

3. Results and Discussion

A. Synthesis

The reaction of $FeCl_2$ with TMPP produces the tetrachloroferrate(II) salt containing the methylphosphonium form of the TMPP ligand, $[CH_3\text{-TMPP}]_2[FeCl_4]$ (**1**). These results are similar to those obtained in the chemistry with other metal di-halides as described in the Chapter VI of this dissertation. Reactions carried out in the presence of an excess of the ligand did not affect the outcome, since the only isolable product was free TMPP.

The chemistry of TMPP with $FeCl_3$ was, however, much more promising and produced one very unusual compound. Although hard first-row transition metals are not particularly compatible with a soft donor atom such as phosphorus, as evidenced by the paucity of homoleptic first-row metal phosphine complexes in the +2 or +3 oxidation state [6], it was our rationale that a soft and basic phosphine would be rendered more compatible with a hard Lewis acid such as $FeCl_3$ by the presence of the harder oxygen donors, and that it would then be possible to form a mono-TMPP adduct, namely $FeCl_3(\eta^3\text{-TMPP})$. Indeed, the equimolar reaction between $FeCl_3$ and TMPP in benzene yielded a pale yellow, air-sensitive solid, which analyzed as "$FeCl_3$(TMPP)". In the absence of an X-ray

determination, its molecular structure was proposed to be octahedral on the basis of the number of ν(Fe-Cl) modes in the infrared spectrum. Three stretches at 360, 300 and 230 cm^{-1} were observed, in agreement with an overall C_s symmetry. Such a tridentate mode for TMPP had previously been observed in $Mo(CO)_3(\eta^3\text{-TMPP})$ [47] and $[Rh(\eta^3\text{-TMPP})_2][BF_4]_n$ (n = 2, 3) [48], wherein the ligand is coordinated to the metal center through the phosphorus atom and two oxygen atoms from the pendent methoxy groups on the phenyl rings. Initial studies on the magnetism of this compound revealed that it followed a non-Curie-Weiss behavior, with a μ_{eff} corresponding to an iron(II) center at room temperature [19]. In order to probe the validity of our structural assignment (tetrahedral vs. octahedral) and to determine the oxidation state of the metal center in this complex, Mössbauer and epr studies were carried out and are discussed in Chapter III of this dissertation. These results also did not agree with the aforementioned mononuclear formulation of an Fe(III) complex. We were finally able to crystallize compound **2** from the aprotic, non coordinating solvent acetone, and the single crystal X-ray study revealed that the complex is actually $[H\text{-TMPP}]_2[Fe_2Cl_6]$, which results from a reduction of Fe^{III} to Fe^{II} and protonation of the phosphine. Facile reduction of $FeCl_3$ is common in solvents such as ethanol, as in the synthesis of $Fe^{II}Cl_2(HPyS)_2$ from the reaction of $FeCl_3$ and HPyS (HPyS = 2-mercaptopyridine) [20]. However, TMPP is sensitive to quaternarization in the presence of metal halides, as discussed in Chapter VI, with similar chemistry also occurring in the reaction of $CoCl_2$ with TMPP in benzene to form $[CH_3\text{-TMPP}]_2[Co_2Cl_6]$ [21]. To our knowledge, there is no documented literature regarding the existence of the $[Fe_2Cl_6]^{2-}$ di-anion although the Co(II) and the Cu(II) analogues are known [21]. When the reaction is

carried out in acetonitrile, small amounts of **2** can also be isolated, but if other solvents such as chloroform or ethanol are used, [H-TMPP][$Fe^{III}Cl_4$] (**5**) is obtained, indicating that no reduction of the metal center is taking place in these solvents.

Upon slow dissolution of [H-TMPP]$_2$[Fe_2Cl_6] in ethanol under anaerobic conditions, the phosphonium salt **4**, [H-TMPP]$_2$[$Fe^{II}Cl_4$], is observed to form. This salt was prepared independently by the reaction of [$Fe^{II}(NCCH_3)_6$][$AlCl_4$]$_2$ with two equivalents of TMPP in methanol. Redissolution of **2** in methanol, followed by rapid evaporation in air, or by treatment with a stream of O_2 gas yielded the oxidized form [H-TMPP][$Fe^{III}Cl_4$] (**5**). The conversion of Fe^{II} to Fe^{III} was monitored by infrared spectroscopy in the far-IR region, according to the Fe-Cl stretching frequency which occurs at 280 cm^{-1} for $\nu(Fe^{II}$-Cl) and 380 cm^{-1} for $\nu(Fe^{III}$-Cl). Compound **5** was, in turn, independently prepared by the reaction of [$Fe^{II}(NCCH_3)_6$][$SbCl_6$]$_2$ with two equivalents of TMPP in methanol. Approximately fifty percent of the original phosphine is consumed to form [H-TMPP][$SbCl_6$], as determined by NMR and IR spectroscopies as well as elemental analysis. Antimony (VI) is a very strong oxidizing agent [22], and therefore it is not surprising to observe an oxidation from Fe^{II} to Fe^{III} in this reaction. In a similar fashion to **4**, protonation of the phosphine occurs with the formation of the very stable [$FeCl_4$]$^-$ anion, which is quite a common phenomenon observed by others [4b]. The spectroscopic and electrochemical properties of **4** and **5** are in excellent agreement with the reported literature on various salts of [$Fe^{II}Cl_4$]$^{2-}$ and [$Fe^{III}Cl_4$]$^-$ [23].

Lastly, $FeCl_3$(O=TMPP) (**6**) can be obtained, *inter alia*, from the reaction of **5** with O_2 in methanol over the period of 1-2 days. The

Figure 5. Synthetic routes to $FeCl_3$(O=TMPP) (**6**).

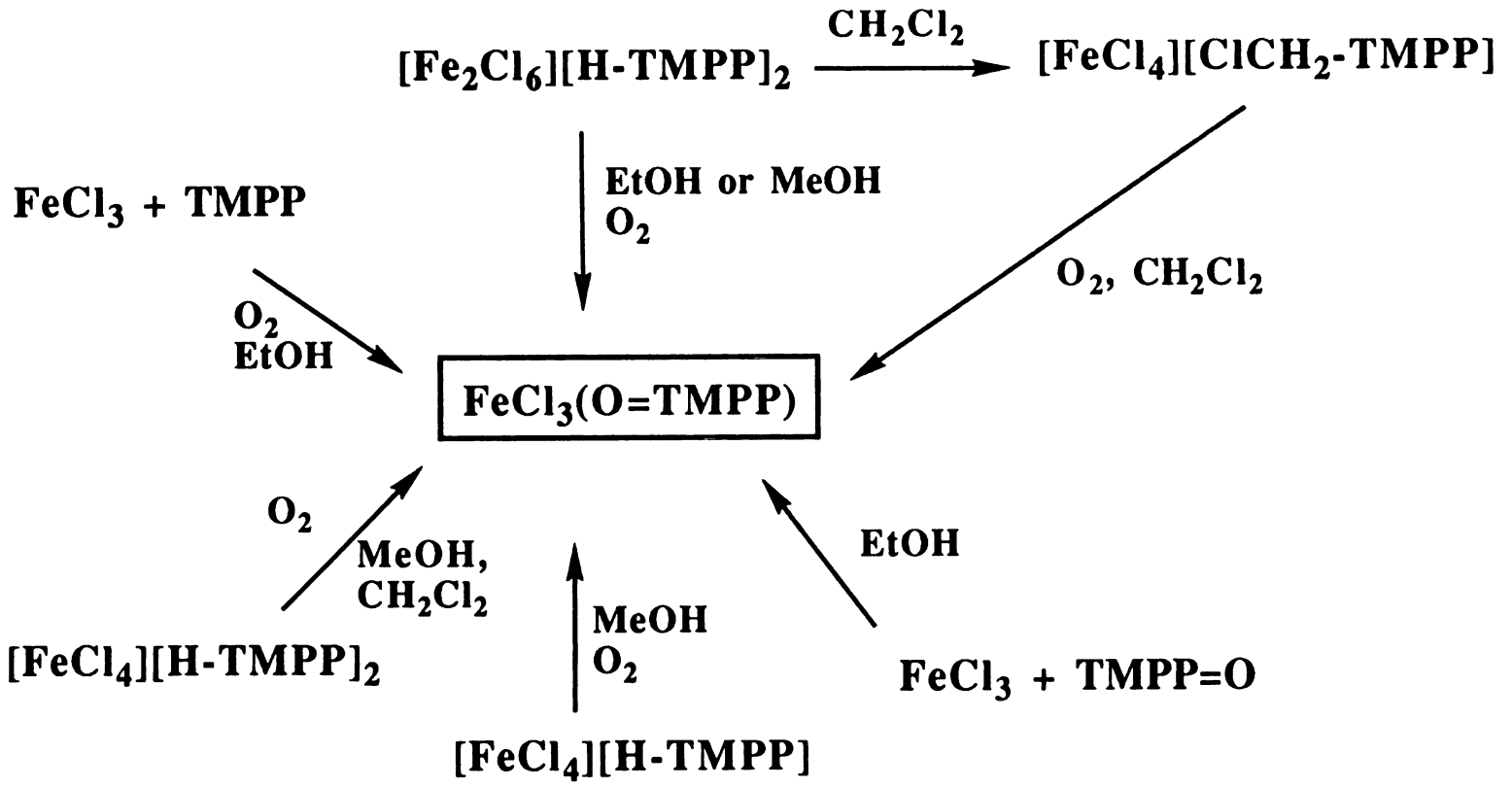
[Fe2Cl6][H-TMPP]2
CH2Cl2
[FeCl4][ClCH2-TMPP]
FeCl3 + TMPP
EtOH or MeOH
O2
O2, CH2Cl2
O2
EtOH
FeCl3(O=TMPP)
O2
MeOH,
CH2Cl2
EtOH
[FeCl4][H-TMPP]2
MeOH
O2
FeCl3 + TMPP=O
[FeCl4][H-TMPP]

Figure 5.

stability of $FeCl_3$(O=TMPP) is evidenced by the extreme facility with which this compound is formed directly or indirectly from **2**, **4** or **5**. Figure 5 summarizes the different synthetic routes to **6**.

B. Molecular Structures

(1) [H-TMPP]$_2$[Fe_2Cl_6] (2)

The X-ray structure unequivocally established the identity of **1** as a $[Fe_2Cl_6]^{2-}$ salt for which two protonated phosphines serve as counterions. Important bond distances and angles are summarized in Table 6. An ORTEP representation of the [H-TMPP]$_2$[Fe_2Cl_6] salt is presented in Figure 6, and Figure 7 shows the structure of the $[Fe_2Cl_6]^{2-}$ di-anion. It consists of two edge-sharing tetrahedra with two terminal and two bridging chlorides per metal atom, with an inversion center at the midpoint of the Fe(1)···Fe(1)' axis, as had been previously observed in the isomorphous structure of [CH_3-TMPP]$_2$[Co_2Cl_6] [21]. The long Fe(1)···Fe(1)' separation of 3.350(4) Å, much larger than the sum of the covalent radii, precludes the assignment of a direct bond, and is comparable to the distances of 3.32 Å found [Fe_2(μ–OH)(OAc)$_2$(Me_3TACN)$_2$](ClO_4) [24] and 3.35 Å in [Fe_2(BPMP)(OPr)$_2$](BPh_4) [25], but shorter than the corresponding value reported for [Fe_2(BIPhMe)$_2$(O_2CCH)$_4$] (3.585 Å) [26]. The Fe···Fe distances reported for the two closely related structures $[Fe_2(SEt)_6]^{2-}$ and $[Fe_2Cl_4(OPh)_2]^{2-}$ are considerably shorter, being 2.978(1) and 3.177(3) Å, respectively [27,28]. The average Fe^{II}-Cl bond distance for the terminal chloride (2.231[2] Å) is somewhat intermediate between the reported range for Fe^{II}-Cl (2.35-2.35 Å) [29] and Fe^{III}-Cl (2.15-2.20 Å) [30]. As expected, the average distance for the bridging chlorides is longer (2.397[2] Å) than the terminal chlorides. The Cl-Fe-Cl bond angles fall in the range expected for tetrahedral geometry (108.02(9)

Table 6. Selected Bond Distances (Å) and Angle (deg) for $[H\text{-}TMPP]_2[Fe_2Cl_6]$ (2)

Atom 1	Atom 2	distance
Fe(1)	Fe(1)'	3.350(4)
Fe(1)	Cl(1)	2.235(2)
Fe(1)	Cl(2)	2.385(2)
Fe(1)	Cl(3)	2.227(2)
Fe(1)	Cl(2)'	2.409(2)
P(1)	C(1)	1.773(6)
P(1)	C(10)	1.782(6)
P(1)	C(19)	1.793(6)

Atom 1	Atom 2	Atom 3	angle
Cl(1)	Fe(1)	Cl(2)	108.02(9)
Cl(1)	Fe(1)	Cl(2)'	110.57(8)
Cl(1)	Fe(1)	Cl(3)	120.5(1)
Cl(2)	Fe(1)	Cl(2)'	91.36(8)
Cl(2)	Fe(1)	Cl(3)	110.96(9)
Cl(3)	Fe(1)(	Cl(2)'	111.50(8)
Fe(1)	Cl(2)	Fe(1)'	88.64(8)
C(1)	P(1)	C(10)	115.3(3)
C(1)	P(1)	C(19)	109.2(3)
C(10)	P(1)	C(19)	114.4(3)

Figure 6. ORTEP drawing of $[H\text{-}TMPP]_2[Fe_2Cl_6]$ showing the atom labeling scheme. All phenyl-group atoms are represented as small circles for clarity, whereas all other atoms are represented by their 50% probability ellipsoids.

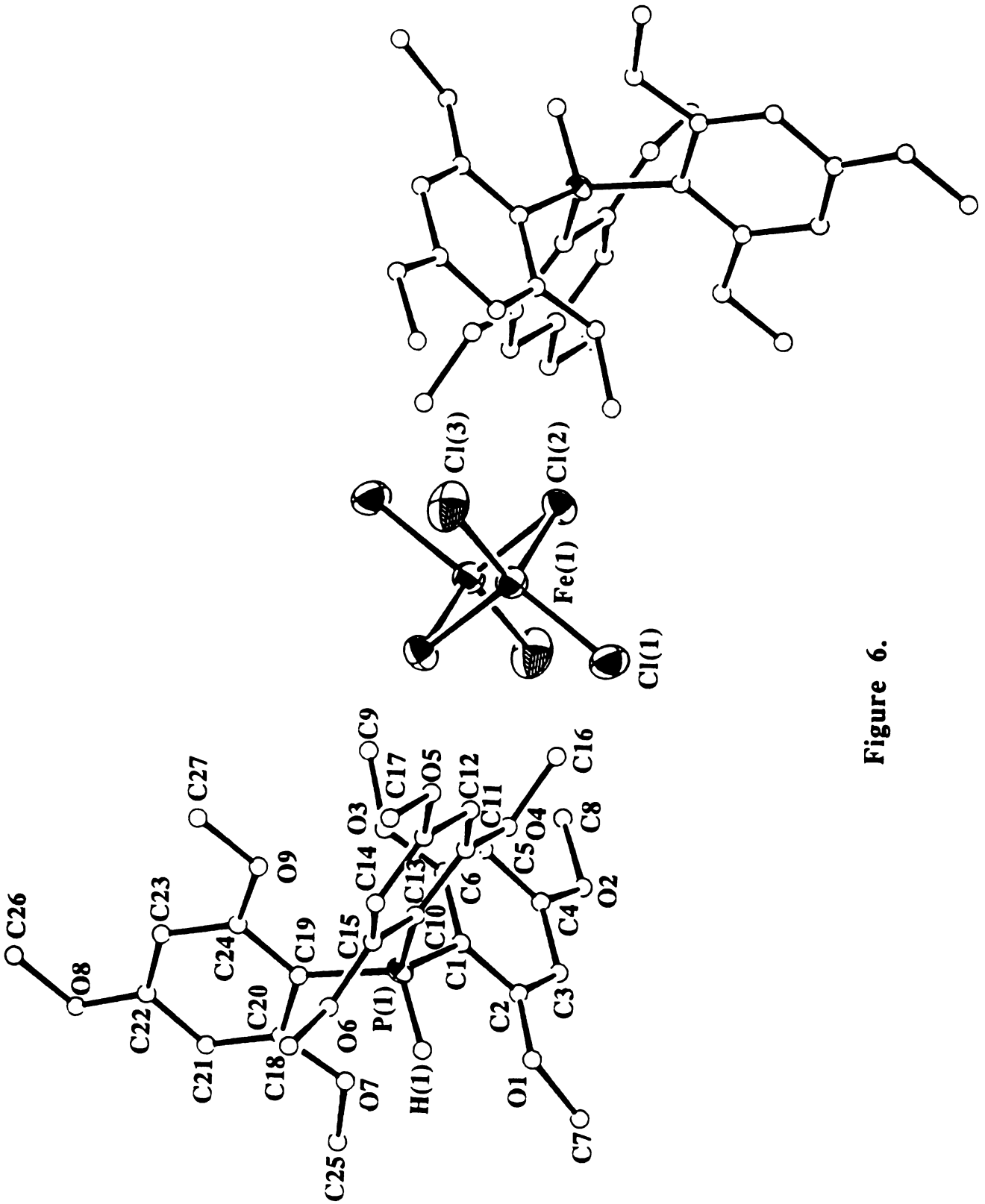
Cl(3)
Cl(2)
Fe(1)
Cl(1)
C9
C17
O5
C12
C11
C16
O3
C14
C13
C10
C6
C5
O4
C8
C27
O9
C23
C24
C19
C15
C1
C4
O2
C26
O8
C22
C20
P(1)
C2
C3
C21
C18
O6
H(1)
O1
O7
C25
C7

Figure 6.

Figure 7. ORTEP diagram of the $[Fe_2Cl_6]^{2-}$ anion.

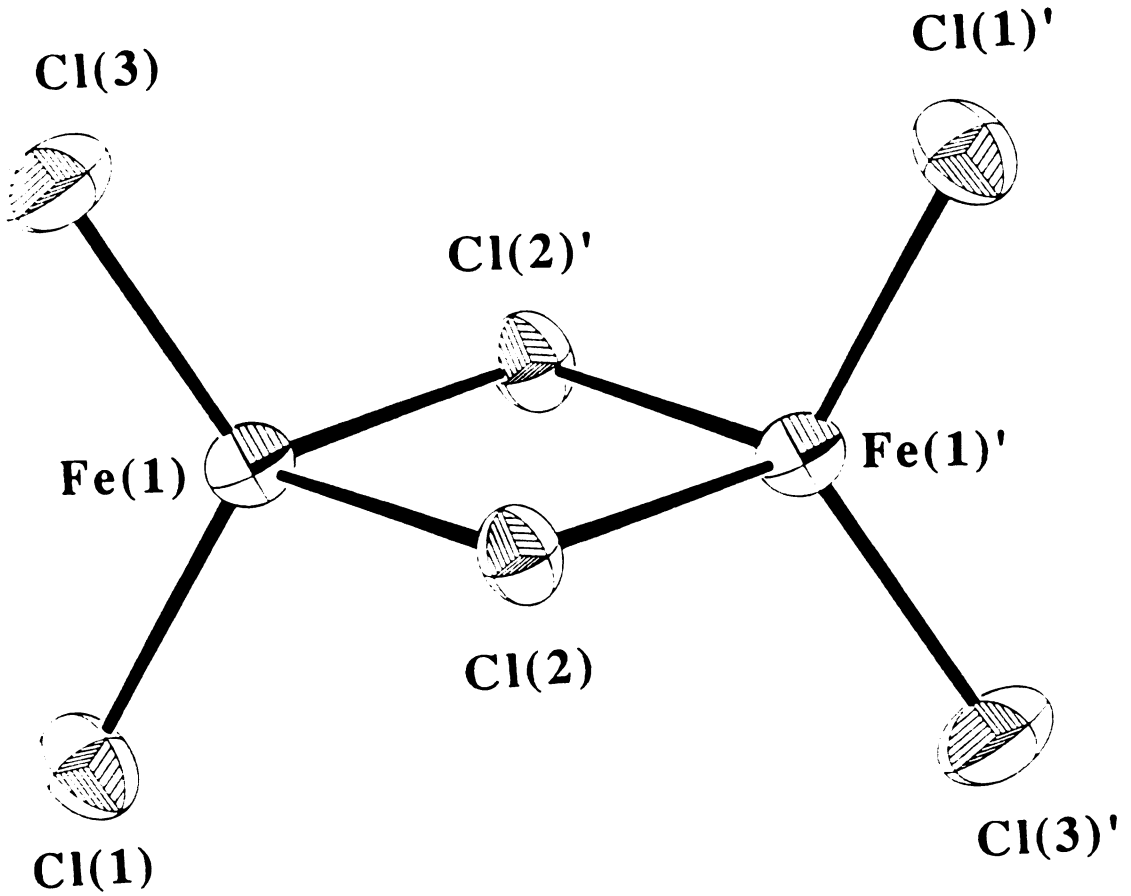

Figure 7.

Figure 8. Three-dimensional packing diagram for $[H\text{-}TMPP]_2[Fe_2Cl_6]$ viewed down the b-axis.

- 120.5(1)°) but the Cl(2)-Fe(1)-Cl(2)' and the Fe(1)-Cl(2)-Fe(1)' angles of 91.36(8) and 88.64(8)°, respectively, are considerably distorted from ideal geometry. A three-dimensional packing diagram of $[H\text{-}TMPP]_2[Fe_2Cl_6]$ is presented in Figure 8 and clearly shows the segregated packing of cations and anions when viewed down the b-axis.

(2) $[H\text{-}TMPP]_2[Fe^{II}Cl_4]$ (4)

An ORTEP drawing of $[H\text{-}TMPP]_2[Fe^{II}Cl_4]$ (**4**) is shown in Figure 9. Pertinent bond distances and angles are summarized in Table 7. The metal atom lies on a crystallographic 2-fold axis and is ligated by four chlorine atoms to form the $[FeCl_4]^{2-}$ anion. Two protonated phosphines, $[H\text{-}TMPP]^+$, serve as countercations in this structure. The Fe-Cl distances (Fe(1)-Cl(1) = 3.304(6) and Fe(1)-Cl(2) = 2.303(6) Å) are typical of Fe^{II}-Cl bond lengths and are in the range of the reported values [29]. The Cl-Fe-Cl angles vary from 106.4(2) to 113.5(3)°, which overall allows for a rather regular tetrahedron. The slight "flattening"of the tetrahedron is obviously a result of packing forces. The structural features of the cation are similar to those of the free phosphine and other phosphonium salts [31]. It is noteworthy that the $[FeCl_4]^{2-}$ anion can only be crystallized using very large countercations such as quaternary ammoniums or phosphoniums [23].

(3) $[H\text{-}TMPP][Fe^{III}Cl_4]$ (5)

An ORTEP diagram of the two ions present in molecule **5** is depicted in Figure 10. Important bond angles and distances are listed in Table 7. The metal atom is surrounded by four chlorine atoms to form the well-known $[FeCl_4]^-$ anion. The Fe-Cl bond distances are in the range 2.161(4)-2.182(5) Å, which is in perfect agreement with the literature [30]. The Cl-Fe-Cl bond angles are comprised between 106.2(2) and 112.6(2)°,

Table 7. Selected Bond Distances (Å) and Angles (deg) for [H-TMPP]$_2$[FeCl$_4$] (4) and [H-TMPP][FeCl$_4$] (5)

Atom 1	Atom 2	Bond Distances (4)	(5)
Fe(1)	Cl(1)	2.304(6)	2.161(4)
Fe(1)	Cl(2)	2.303(6)	2.155(4)
Fe(1)	Cl(3)	---------	2.168(4)
Fe(1)	Cl(4)	---------	2.182(5)
P(1)	C(1)	1.78(2)	1.76(1)
P(1)	C(10)	1.78(2)	1.76(1)
P(1)	C(19)	1.77(2)	1.79(1)

Atom 1	Atom 2	Atom 3	Bond Angles (4)	(5)
Cl(1)	Fe(1)	Cl(1)'/Cl(3)	109.8(3)	106.2(2)
Cl(1)	Fe(1)	Cl(2)	106.4(2)	112.6(2)
Cl(1)	Fe(1)	Cl(2)'/Cl(4)	110.3(2)	109.8(2)
Cl(2)	Fe(1)	Cl(2)'/Cl(4)	113.5(3)	110.0(2)
Cl(2)	Fe(1)	Cl(3)	---------	106.9(2)
Cl(3)	Fe(1)	Cl(4)	---------	111.2(2)
C(1)	P(1)	C(10)	113.9(9)	114.5(7)
C(1)	P(1)	C(19)	108.5(9)	116.0(6)
C(10)	P(1)	C(19)	115.0(8)	112.4(7)

Figure 9. ORTEP drawing of $[H\text{-}TMPP]_2[FeCl_4]$ showing the atom labeling scheme.

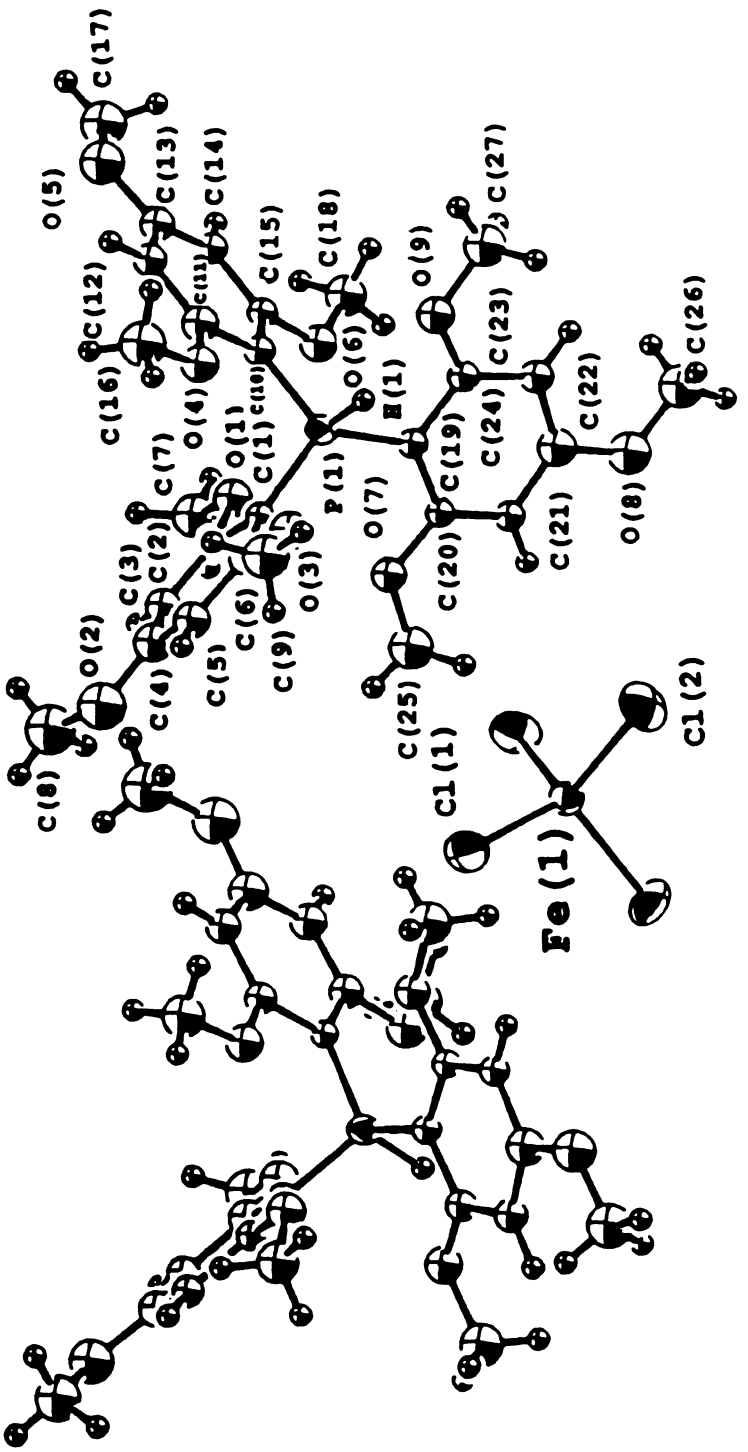
C(17)
O(5)
C(13)
C(14)
C(12)
C(15)
C(18)
C(16)
O(4)
O(6)
O(9)
C(27)
C(7)
O(1)
C(11)
P(1)
H(1)
C(23)
C(3)
C(2)
C(19)
C(24)
C(22)
O(7)
C(6)
O(3)
C(20)
C(21)
O(8)
C(26)
O(2)
C(5)
C(9)
C(4)
C(25)
C(8)
Cl(1)
Cl(2)
Fe(1)

Figure 9.

Figure 10. ORTEP drawing of [H-TMPP][$FeCl_4$] showing the atom labeling scheme. All phenyl group atoms are represented as small circles for clarity, whereas all other atoms are represented as their 50% probability thermal ellipsoids.

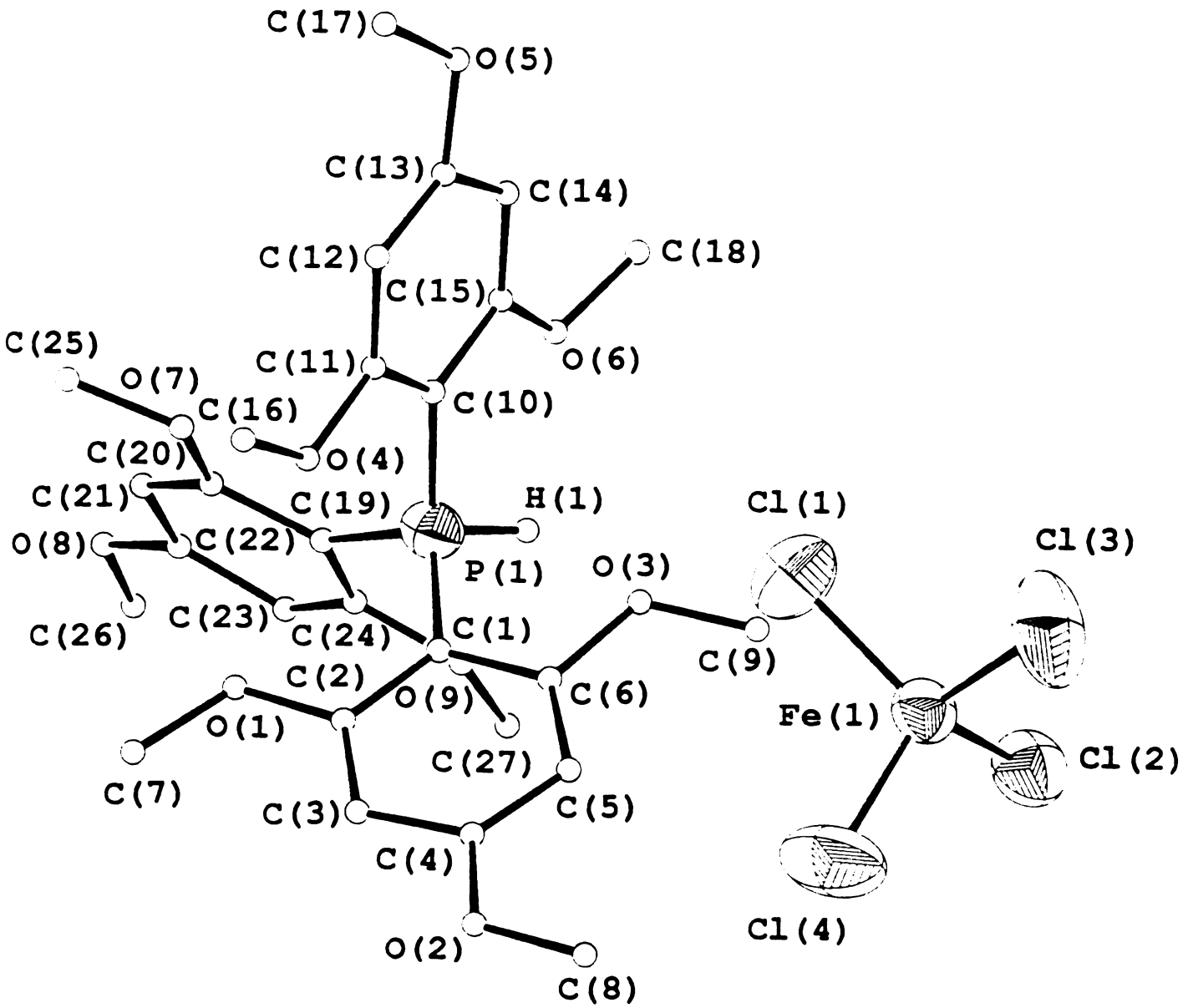
C(17)
O(5)
C(13)
C(14)
C(12)
C(18)
C(15)
O(6)
C(25)
O(7)
C(11)
C(10)
C(16)
O(4)
C(20)
C(21)
C(19)
H(1)
Cl(1)
Cl(3)
O(8)
C(22)
P(1)
O(3)
C(26)
C(23)
C(24)
C(1)
C(9)
C(2)
O(9)
C(6)
Fe(1)
O(1)
C(27)
Cl(2)
C(7)
C(3)
C(5)
C(4)
Cl(4)
O(2)
C(8)

Figure 10.

which deviates very little from the ideal tetrahedral geometry. The phosphonium cation is similar to reported structures [31].

(4) $Fe^{III}Cl_3$(O=TMPP) (6)

Figure 11 presents an ORTEP diagram of molecule **6**, and Table 8 lists important bond distances and angles. The metal center is surrounded by three chlorine atoms and the oxygen atom of a phosphine oxide ligand, resulting in an overall distorted tetrahedral coordination environment. The average Fe-Cl bond distance is 2.179[4] Å, which is typical of the Fe-Cl distances found in salts of the anionic complex $[FeCl_4]^-$ [30]. The O-Fe-Cl angles vary from 108.6 to 110.8°, which is not a large difference, and may be due to a minor steric influence of the phosphine oxide which forms a bent interaction with the metal (Fe-O-P = 163.6(5)°). As a result, the O-Fe-Cl bond angles are considerably distorted from an ideal tetrahedral geometry. The Fe-O bond distance of 1.791(6) Å in **6** is much shorter than the metal-oxygen found in similar tetrahedral phosphine oxide complexes such as $CoCl_2(O{=}PPh_3)_2$ for which the average Co-O distance is 1.999[9] Å [32]. Conversely, the P-O distance of 1.550(7) Å in the $FeCl_3$(O=TMPP) case is much longer than the average corresponding distance in $CoCl_2(O{=}PPh_3)_2$ ($P\text{-}O_{(av)}$ = 1.499[9] Å) [32]. These structural data are not to be interpreted strictly since a comparison of iron(III) and cobalt(II) chemistry must also take into consideration the oxidation state and size of the metal ion. A more relevant comparison would be to the recently reported Lewis acid-triphenylphosphine oxide adducts $MX_3(O{=}PPh_3)$ (M = Al, Ga; X = Cl or Br) [33], in which the P-O distances are 1.519(4) Å for $AlCl_3(O{=}PPh_3)$, 1.513(7) Å for $AlBr_3(O{=}PPh_3)$, and 1.487(11) Å for $GaCl_3(O{=}PPh_3)$. Similarly the metal-oxygen distances are much closer to ours at 1.733(4), 1.736(7) and

Table 8. Selected Bond Distances (Å) and Angles (deg) for $FeCl_3$(O=TMPP) (6)

Atom 1	Atom 2	Bond Distance
Fe(1)	Cl(1)	2.196(4)
Fe(1)	Cl(2)	2.155(4)
Fe(1)	Cl(3)	2.187(4)
Fe(1)	O(10)	1.791(6)
O(10)	P(1)	1.550(7)
P(1)	C(1)	1.76(1)
P(1)	C(10)	1.79(1)
P(1)	C(19)	1.80(1)

Atom 1	Atom 2	Atom 3	Bond Angle
Cl(1)	Fe(1)	Cl(2)	109.4(2)
Cl(1)	Fe(1)	Cl(3)	110.4(2)
Cl(1)	Fe(1)	O(10)	109.9(3)
Cl(2)	Fe(1)	Cl(3)	107.8(2)
Cl(2)	Fe(1)	O(10)	108.6(3)
Cl(3)	Fe(1)	O(10)	110.8(3)
Fe(1)	O(10)	P(1)	163.6(5)
O(10)	P(1)	C(1)	107.3(5)
O(10)	P(1)	C(10)	107.3(5)
O(10)	P(1)	C(19)	108.5(5)

Figure 11. ORTEP drawing of $FeCl_3$(O=TMPP) showing the atom labeling scheme. All phenyl-group atoms are represented as small circles for clarity, whereas all other atoms are represented by their 40% probability thermal ellipsoids.

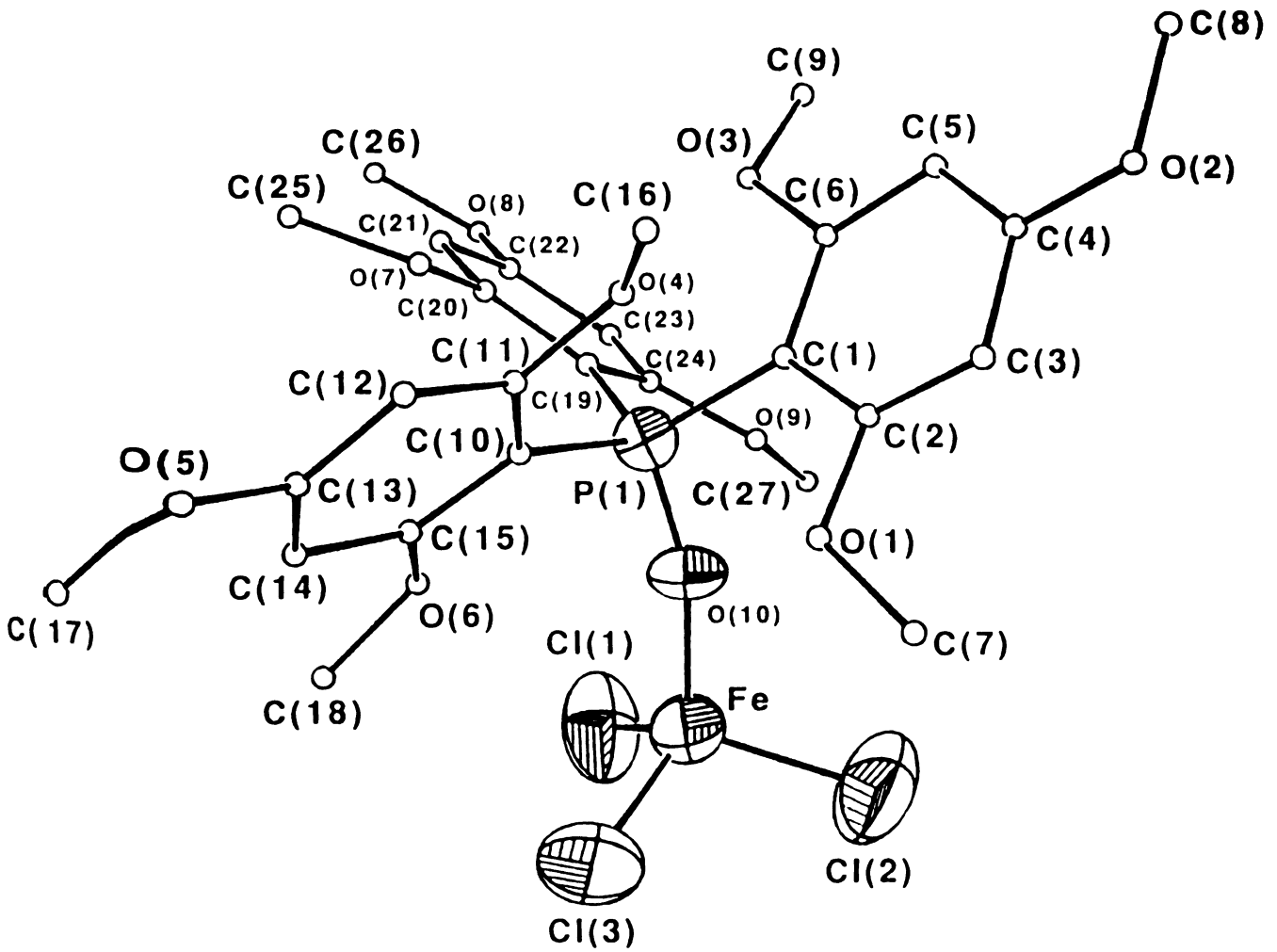
C(8)
C(9)
O(3)
C(5)
O(2)
C(26)
C(25)
O(8)
C(16)
C(6)
C(21)
C(22)
C(4)
O(7)
O(4)
C(20)
C(23)
C(11)
C(24)
C(1)
C(3)
C(12)
C(19)
O(9)
C(10)
C(2)
O(5)
C(13)
P(1)
C(27)
C(15)
O(1)
C(14)
O(6)
O(10)
C(17)
C(7)
Cl(1)
C(18)
Fe
Cl(2)
Cl(3)

Figure 11.

1.818(10) Å, for the $AlCl_3$, $AlBr_3$ and $GaCl_3$ adducts, respectively. Interestingly enough, the M-O-P angles are strictly linear in all three structures, and this was rationalized by the consideration of the strong acceptor capacity of the Lewis acid. Finally the average C-P-C bond angle for the O=TMPP group in **6** is 111.2[5]° which deviates considerably from the ideal tetrahedral geometry due to repulsions between the bulky trisubstituted phenyl rings. This results in a flattening out of the C-P-C angles.

C. Discussion

(1) Chemistry of $FeCl_3$ with TMPP

The salt [H-TMPP]$_2$[Fe_2Cl_6] (**2**) is the first reported example of a compound containing $[Fe_2Cl_6]^{2-}$ unit. The unusual feature of this di-anion is the ferrous oxidation state of both metal centers. Fe_2Cl_6(III,III) is known to be the stable form of gaseous $FeCl_3$, and other di-ferric compounds of the type $[Fe_2Cl_9]^{3-}$ or $[Fe_2Cl_6(\mu\text{-}O)]^{2-}$ or $[Fe_2Cl_6(\mu\text{-}OR)_2]^{2-}$ have been structurally characterized [4b,23]. Compound **2** represents the first all-halide synthetic analogue of the di-ferrous species $[Fe_2(SEt)_6]^{2-}$ and $[Fe_2Cl_4(OPh)_2]^{2-}$ [27,28]. The highly unusual, yet very simple nature of $[Fe_2Cl_6]^{2-}$ prompted us to further investigate its magnetic properties by epr and Mössbauer spectroscopies as well as to re-examine the early magnetic susceptibility data; these will be discussed in Chapter III. The formation of an iron(II) species from the simple stoichiometric reaction of $FeCl_3$ with TMPP casts a serious doubt on the identity of the previously reported other species of this kind, $FeCl_3(PCy_3)$ [3] and $FeCl_3(PPh_3)$ [5a], although the structure of the latter was subsequently confirmed by Mössbauer spectroscopy [5b]. The analytical and infrared properties of the two aforementioned complexes agreed with the $FeCl_3(PR_3)$ formulation,

and both compounds were reported to be yellow in color as is compound **2**. As it turned out, three ν(Fe-Cl) were also observed in the infrared spectrum of **2**, one being split (which accounts for the four bands expected for a D_{2h} symmetry, as illustrated in Figure 12) and the addition of two hydrogen atoms to the molecular weight does not have much effect on the elemental analyses (*ie* $FeCl_3$(TMPP) vs. [$FeCl_3$(H-TMPP)]$_2$). More recently, Poli *et al.* reported the syntheses of $FeCl_3(PCy_3)$ and $FeCl_3(P^tBu_3)$ [4b], along with $FeCl_3(PMe_3)$ and $FeCl_3(PPh_3)$ as elusive species in low-temperature epr experiments [4a]. Neutral, four-coordinate adducts of $FeCl_3$ are quite rare in general; among them only $FeCl_3(S_4N_4)$ [2a] and $FeCl_3$(THF) [2c] have been structurally characterized. Most neutral FeX_3L compounds have actually proven to have the ionic formulation $[FeCl_2L_2][FeCl_4]$ which was ruled out early on in our case because of the absence of any of the characteristic spectroscopic features of the $[FeCl_4]^-$ anion. A more common stoichiometry for this type of complexes is $FeCl_3(PR_3)_2$ (R= Me, Ph) [4a], as in the recent report of $FeBr_3(PMePh_2)_2$ [34]. The synthesis of $[H\text{-TMPP}]_2[Fe_2Cl_6]$ is then quite an unexpected result. It is relevant to point out that Poli *et al.* also detected the formation of Fe(II) species in the 1:1 interaction of $FeCl_3$ and PPh_3 in toluene. The reduction of the metal center was rationalized by the detection of chlorosubstituted toluene, which is the oxidized species. In our case, work-up of the benzene reaction filtrate produced a red-brown solid. The mass-spectrometry, the ^1H and ^{31}P NMR, and the IR data point to a [Cl-TMPP][$FeCl_4$] formulation for this by-product. To verify this, [Cl-TMPP]$^+Cl^-$ was independently prepared by reacting TMPP with Cl_2 gas in benzene, and subsequently reacted with one equivalent of $FeCl_3$, to form

Figure 12. Far-infrared spectrum of $[H\text{-}TMPP]_2[Fe_2Cl_6]$ showing the four ν(Fe-Cl) expected for a D_{2h} symmetry.

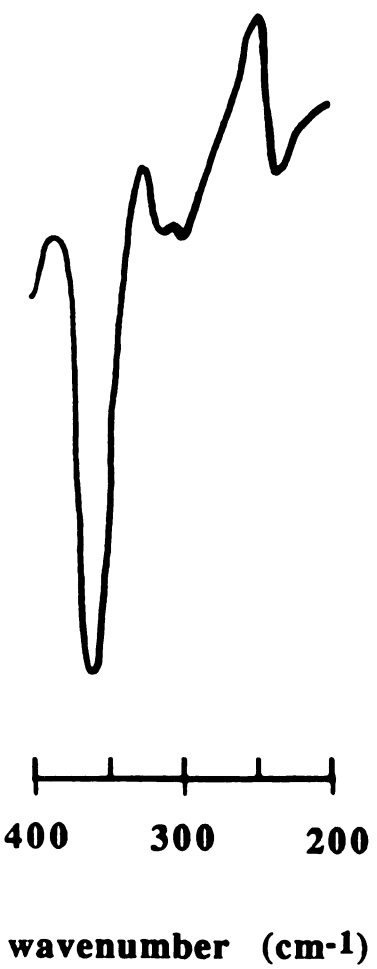

Figure 12.

[Cl-TMPP][$FeCl_4$]. Therefore we propose the following mechanism for the formation of **2**:

$$3\ FeCl_3 + 3\ TMPP \xrightarrow{2\ HCl} [H\text{-}TMPP]_2[Fe_2Cl_6] + [Cl\text{-}TMPP][FeCl_4]$$

Fe(III) P(III) Fe(II), P(III) Fe(III), P(V)

The source of the protons and the extra chloride needed to balance the equation is postulated to be adventitious HCl present in the iron(III) starting material, which is a common feature of metal halides. In order to generalize this result and to compare the results with the previous work on tertiary phosphine chemistry with $FeCl_3$, we set out to investigate the chemistry of PPh_3 and PCy_3 with $FeCl_3$ in benzene. The reactions of $FeCl_3$ with one equivalent of PR_3 (R = Cy, Ph) in benzene produce dark red solutions instantaneously, from which red solids can be isolated. Their spectroscopic properties are in agreement with those of the reported mononuclear $FeCl_3(PR_3)$ complexes. However, if the reaction is allowed to continue, the solutions revert to a yellow color. The far-infrared spectra of the yellow solids isolated from the longer reaction time present the same pattern as that of **2** (ν(Fe-Cl) = 380(s), 360(m), 315(m), 300(w) cm^{-1} for R = Cy and 380(s), 330(m), 320(m), 300(w) cm^{-1} for R = Ph). In addition, the highest peaks in the FAB mass-spectrum of these complexes are m/z = 281 and m/z = 263 corresponding to $[H\text{-}PCy_3]^+$ and $[H\text{-}PPh_3]^+$, respectively, and in the case of the tricyclohexylphosphonium compound, the characteristic P-H stretch at 2400 cm^{-1} can be observed in the infrared spectrum. We take these spectral characteristics as good evidence for the formation of the $[Fe_2Cl_6]^{2-}$ anion with phosphonium cations.

The final oxidized product $FeCl_3(O{=}TMPP)$, **6**, is a very stable compound and unique in itself, since it is not typical for a *mono*-phosphine oxide adduct of $FeCl_3$ to be more stable than the bis-adduct. To date only two analogous compounds have been reported; these are $FeCl_3(O{=}PPh_3)$ by Lindner *et al.* in 1967 [35], and $FeCl_3(O{=}PCy_3)$ by Issleib *et al.* in 1954 [3], but neither has been structurally characterized. A more common stoichiometry is FeX_3L_2 or $[FeL_4]^{n+}$, where L is a phosphine oxide ligand [36].

(2) Oxidation Chemistry of $[Fe_2Cl_6]^{2-}$

We now wish to discuss the reaction pathway that leads to the formation of complex **6** (Scheme 1). In order to understand the present results, we must first take note of previous work in the area, particularly with respect to the solvent dependency of this chemistry. Let us first consider the reactions of $FeCl_3$ and PR_3 ligands that have been carried out in CH_3CN. In the course of studying the oxidation of triphenylphosphine to triphenylphosphine oxide in the presence of iron(III) complexes and molecular oxygen, Ondrejovic and coworkers isolated a series of stable complexes with the empirical formula $FeX_3(O{=}PPh_3)_2$ (X= Cl, NCS, Br) [7a], among which "$FeCl_3(O{=}PPh_3)_2$" was structurally characterized and shown to actually have the formula $[FeCl_2(O{=}PPh_3)_4][FeCl_4]$ [37]. In the 1970's, Sutin *et al.* also investigated the oxidation of PPh_3 in the presence of iron(III) and iron(IV) dithiolate complexes of the type $[Fe(mnt)_2]^-$, where $[mnt]^{2-}$ is maleonitriledithiolate [38]. In this work, only the stable *bis*-phosphine oxide complex $[Fe(mnt)_2(O{=}PPh_3)_2]^-$ was observed, however, with no evidence of other intermediate species such as the previously postulated dioxygen adducts [39,40]. When the identical chemistry was carried out in a protic solvent such as methanol, a different

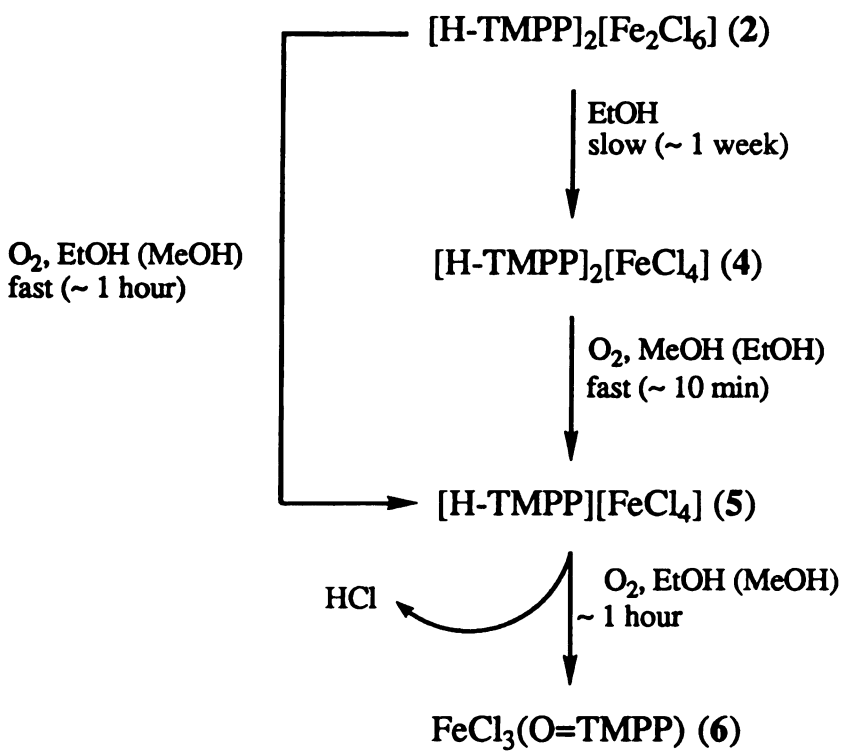

Scheme 1. Successive reactions involved in the formation of **6** in protic solvents

compound, $[CH_3\text{-}PPh_3][FeCl_4]$, was isolated [30a]. Ondrejovic proposes that protic solvents induce the quaternarization of the phosphine, by methylation in this case, which is then oxidized to $Ph_3P{=}O$ [30a]. Recently, McAuliffe and co-workers reported that O_2 assists in the decomposition of $FeBr_3(PMePh_2)_2$ to an orange product that exhibits a strong P=O stretching frequency in the infrared spectrum, but no molecular oxygen species were isolated. This observation also disfavors the hypothesis of stable dioxygen complexes as intermediates in such chemistry [34].

As in previous reports of the phosphine chemistry of ferric chloride, the reaction between $FeCl_3$/TMPP and O_2 is also solvent-dependent. When $[H\text{-}TMPP]_2[Fe_2Cl_6]$ (**2**) is dissolved in acetonitrile, bubbled with oxygen and the solution is layered with a mixture of hexanes/ether, red crystals of $FeCl_3$(O=TMPP) (**6**) are form within hours. No evidence was found to support the existence of detectable phosphonium intermediates. As Scheme 1 clearly indicates, the reaction pathway is quite different in alcohol solvents. In alcohols, the chemistry involves formation of protic phosphonium salts of tetrachloroferrate(II) and (III), respectively. A suspension of $[H\text{-}TMPP]_2[Fe_2Cl_6]$ (**2**) reacts with molecular oxygen in ethanol or methanol to form $[H\text{-}TMPP][FeCl_4]$ (**5**), as determined by infrared spectroscopy and confirmed by X-ray crystallography. One must bear in mind, however, that this reaction is not quantitative, since some of the $[H\text{-}TMPP]_2[Fe_2Cl_6]$ must be sacrificed to yield extra chloride ion for $[FeCl_4]^-$. The salt $[H\text{-}TMPP][FeCl_4]$ further reacts with oxygen in alcohols to form $FeCl_3$(O=TMPP) (**6**) which was fully characterized. The scheme depicted in Scheme 1 also points out that if $[H\text{-}TMPP]_2[Fe_2Cl_6]$ is suspended in ethanol (but without deliberate addition of O_2) for a period of time in excess of 1 week, the compound eventually dissolves with

decomposition to the Fe(II) species $[H\text{-}TMPP]_2[FeCl_4]$ (**4**). Compound **4** can, in turn, be reacted with O_2 in methanol or ethanol to form compound **5**, and subsequently, compound **6**. We have independently prepared complexes **4** and **5** and showed that they indeed behave as indicated in the proposed scheme.

It is worth mentioning at this point that the reaction proceeds quite differently when carried out in dichloromethane. Indeed, upon bubbling dioxygen through a CH_2Cl_2 solution of compound **2**, an instantaneous color change from yellow to dark green is observed. We initially hypothesized that the species was possibly a dioxygen adduct, but subsequent infrared studies of the behavior of **2** in CH_2Cl_2 revealed the appearance of $[FeCl_4]^-$ and $[ClCH_2\text{-}TMPP]^+$ ions over time. Facile decomposition of free TMPP in CH_2Cl_2 to give $[ClCH_2\text{-}TMPP]Cl$ has been documented [41], thus we conclude that the $[H\text{-}TMPP]^+$ cation in $[H\text{-}TMPP]_2[Fe_2Cl_6]$ is fairly unstable in a polar medium such as CH_2Cl_2. Furthermore, photochemically induced reactions of similar $FeCl_3/PR_3$ compounds in chlorinated solvents are known; in fact recently the formation of $[Fe^{III}Cl_2(dmpe)_2][Fe^{III}Cl_4]$ from the photochemical oxidation of $Fe^{II}Cl_2(dmpe)_2$ in chlorinated solvents such as CH_2Cl_2, $CHCl_3$ or CCl_4 was reported [42]. Based on the newly acquired supporting evidence and the literature precedence for such chemistry, we propose that two equivalents of $[ClCH_2\text{-}TMPP][Fe^{III}Cl_4]$ (**7**) are formed by the oxidation of $[H\text{-}TMPP]_2[Fe_2Cl_6]$ in CH_2Cl_2. However, when O_2 was introduced in the system, the reaction proceeded much less cleanly, in that the presence of another iron species can be detected. Indeed, two strong Fe-Cl stretches were observed in the infrared spectrum at 380 and 320 cm^{-1} corresponding to the $[FeCl_4]^-$ unit and to another "Fe-Cl" species, respectively.

Nonetheless, further reaction of this mixture with molecular oxygen eventually leads to $FeCl_3$(O=TMPP) in high yield, demonstrating once again the pivotal role of the $[FeCl_4]^-$ anion in this chemistry.

(3) Catalytic Formation of TMPP=O

Finally, in view of Ondrejovic's work, we were interested to see whether $FeCl_3$(O=TMPP) (**6**) could act as a catalyst for the oxidation of TMPP to TMPP oxide. Indeed, when $FeCl_3$(O=TMPP) is reacted with an excess of the phosphine (from 10 to 100-fold) in acetone or acetonitrile, in the presence of O_2, TMPP=O is formed in high yield with almost total recovery of the catalyst **6**. At this point it is important to mention that TMPP=O cannot be synthesized by the mere reaction of TMPP with oxygen.

3. Summary

In summary, the chemistry of $FeCl_3/PR_3$ compounds with O_2 appears to be dictated by the formation of $[FeCl_4]^{2-}$, $[FeCl_4]^-$ and $[H\text{-}PR_3]^+$ species. In accord with this observation is the demonstrated role of quaternary onium tetrachloroferrate salts in numerous catalyzed reactions such as hydrosilylation [43], polymerization of ε-caprolactone [44], and polymerization of α-oxides [45]. This work supports the conclusion that the formation of the stable and unprecedented mono-phosphine oxide adduct $FeCl_3$(O=TMPP) does not proceed *via* the formation of metal-oxygen adducts, but via quaternarization of the phosphine. Finally, we did not observe the formation of bis-phosphine oxide complexes, a result that is in contrast to previously reported work.

LIST OF REFERENCES

1. Hawker, P. N.; Twigg, M. V. in *Comprehensive Coordination Chemistry*, Wilkinson, G., Ed.; Pergamon Press: Oxford, **1987**; Vol. 4, Ch. 44.1, p. 1179.

2. (a) Thewalt, U. *Z. Naturforsch.* **1980**, *35b*, 855. (b) Thewalt, U. *Z. Anorg. Allg. Chem.* **1981**, *476*, 105. (c) Cotton, F. A.; Luck, R. L.; Son, K.-A. *Acta Cryst.* **1990**, *C46*, 1424.

3. Issleib, K.; Brack, A. *Z. Anorg. Allg. Chem.* **1954**, *277*, 258.

4. (a) Walker, J. D.; Poli, R. *Inorg. Chem.* **1989**, *28*, 1793. (b) Walker, J. D.; Poli, R. *Inorg. Chem.* **1990**, *29*, 756.

5. (a) Singh, P. P.; Rivest, R. *Can. J. Chem.* **1968**, *46*, 1733. (b) Birchall, T. *Can. J. Chem.* **1969**, *47*, 1351.

6. Levason, W. *Comments Inorg. Chem.* **1990**, *9*, 331.

7. (a) Ondrejkovicova, I.; Vancova, V.; Ondrejovic, G. *Coll. Czech. Chem. Commun.* **1983**, *48*, 254. (b) Ondrejkovicova, I.; Vancova, V.; Ondrejovic, G. *Proc. Conf. Coord. Chem.* **1983**, *9th*, 321. (c) Ondrejkovicova, I.; Ondrejovic, G. *Proc. Conf. Coord. Chem.* **1985**, *10th*, 303. (d) Vancova, V.; Ondrejkovicova, I.; Ondrejovic, G. *Chem. Zvesti* **1984**, *38*, 363. (e) Ondrejkovicova, I.; Vancova, V.; Ondrejovic, G. *Proc. Conf. Coord. Chem.* **1989**, *12th*, 263.

8. Hathaway, B. J.; Holah, D. G.; Underhill, A. E. *J. Chem. Soc.* **1962**, 2444.

9. Zuur, A. P.; Groenveld, W. L. *Rec. Trav. Chim. Pays Bas* **1967**, *86*, 1089.

10. Reedijk, J.; Groenveld, W. L. *Rec. Trav. Chim. Pays Bas* **1968**, *87*, 513.

11. (a) Bino, A.; Cotton, F. A.; Fanwick, P. E. *Inorg. Chem.* **1979**, *18*, 3558. (b) Cotton, F. A.; Frenz, B. A.; Deganello, G.; Shaver, A. *J. Organomet. Chem.* **1973**, 227.

12. TEXSAN-TEXRAY Structure Analysis Package, Molecular Corporation (1985).

13. Enraf-Nonius. Structure Determination Package. Enraf-Nonius, Delft, The Netherlands (1979).

14. SHELXS-86: Sheldrick, G. M. in *Crystallographic Computing 3*; Sheldrick, G. M.; Goddard, R. Eds; Oxford University Press, 1984; p.175.

15. DIRDIF: Direct Methods for Difference Structures, An Automatic Procedure for Phase Extension; Refinement of Difference Structure Factors. Technical Report 1984/1. Crystallography Laboratory, Toernooivelt, 6525 Ed Nijmegen, The Netherlands.

16. DIFABS: Walker, N.; Stuart, D. *Acta Cryst.* **1983**, *A39*, 158.

17. CLEGG: Clegg, W. *Acta Cryst.* **1981**, *A37*, 913.

18. MITHRIL: An Integrated Direct Method Computer Program. Gilmore, C. J. *J. Appl. Cryst.* **1984**, *17*, 42.

19. Dunbar, K. R.; Haefner, S. C.; Quillevéré, A. *Polyhedron* **1990**, *9*, 1695.

20. Povey, D. C.; Smith, G. W.; Lobana, T. S.; Bhatia, P. K. *J. Cryst. Spect. Res.* **1991**, *21*, 9.

21. Dunbar, K. R.; Quillevéré, A.; Haefner, S. C. *Acta Cryst.* **1991**, *C47*, 2319.

22. Greenwood, N. N.; Earnshaw, A. *Chemistry of the Elements*; Pergamon Press: Oxford, **1984**; p. 656.

23. Cotton, F. A.; Wilkinson, G. *Advanced Inorganic Chemistry*, 5th Edition; John Wiley, Ed.; New York: **1988**.

24. (a) Hartman, J. R.; Rardin, R. L.; Chaudhuri, P.; Pohl, K.; Wieghardt, K.; Nuber, B.; Weiss, J.; Papaefthymiou, G. C.; Frankel, R. B.; Lippard, S. J. *J. Am. Chem. Soc.* **1987**, *109*, 7387. (b) Chaudhuri, P.; Wieghardt, K. *Angew. Chem. Int. Ed. Engl.* **1985**, *24*, 778.

25. (a) Borovik, A. S.; Que, L. Jr. *J. Am. Chem. Soc.* **1988**, *110*, 2345. (b) Borovik, A. S.; Hendrich, M. P.; Holman, T. R.; Münck, E.; Papaefthymiou, V.; Que, L. Jr. *J. Am. Chem. Soc.* **1990**, *112*, 6031.

26. Tolman, W. B.; Bino, A.; Lippard, S. J. *J. Am. Chem. Soc.* **1989**, *111*, 8523.

27. Hagen, K. S.; Holm, R. H. *Inorg. Chem.* **1984**, *23*, 418.

28. Coucouvanis, D.; Greiwe, K.; Salifoglou, A.; Challen, P.; Simopoulos, A.; Kostikas, A. *Inorg. Chem.* **1988**, *27*, 594.

29. (a) Lauher, J. W.; Ibers, J. A. *Inorg. Chem.* **1975**, *14*, 348. (b) Toan, T.; Dahl, L. F. *J. Am. Chem. Soc.* **1971**, *93*, 2654. (c) Freeman, H. C.; Milburn, G. H. W.; Nockolds, C. E. *Chem. Commun.* **1969**, 55. (d) Mason, R.; McKenzie, E. D.; Robertson, G. B.; Rusholme, G. A. *Chem. Commun.* **1968**, 1673.

30. (a) Glowiak, T.; Durcanska, E.; Ondrejkovicova, I.; Ondrejovic, G. *Acta Cryst.* **1986**, *C42*, 1331. (b) Cotton, F. A.; Murillo, C. A. *Inorg. Chem.* **1975**, *14*, 2467. (c) Constant, G.; Daran, J.-C.; Jeannin, Y. *J. Organomet. Chem.* **1972**, *44*, 353. (d) Walker, J. D.; Poli, R. *Polyhedron* **1989**, *8*, 1293.

31. Dunbar, K. R.; Pence, L. E. *Acta Cryst.* **1991**, *C47*, 23.

32. Mangio, M. M.; Smith, R.; Shore, S. G. *Cryst. Struct. Commun.* **1976**, *5*, 493.

33. Burford, N.; Royan, B. W.; Spence, R. E. H.; Cameron, T. S.; Linden, A.; Rogers, R. D. *J. Chem. Soc., Dalton Trans.* **1990**, 1521.

34. McAuliffe, C. A.; Godfrey, S. M.; Mackie, A. G.; Pritchard, R. G. *J. Chem. Soc., Chem. Commun.* **1992**, 483.

35. Lindner, E.; Lehner, R.; Scheer, H. *Chem. Ber.* **1967**, *100*, 1331.

36. (a) Lobana, T. S.; Cheema, H. S.; Sandhu, S. S. *J. Chem. Soc., Dalton Trans.* **1983**, 2039. (b) Cotton, S. A.; Gibson, J. F. *J. Chem. Soc. (A)* **1971**, 859. (c) Bannister, E.; Cotton, F. A. *J. Chem. Soc.* **1960**, 1878. (d) Povey, D. C.; Lobana, T. S.; Bhatia, P. K. *J. Cryst. Spect. Res.* **1991**, *21*, 13. (e) Beagley, B.; Kelly, D. G.; Mac Rory,

P. P.; McAuliffe, C. A.; Pritchard, R. G. *J. Chem. Soc., Dalton Trans.* **1991**, 2657.

37. Durcanska, E.; Glowiak, T.; Kozisek, J.; Ondrejkovicova, I.; Ondrejovic, G. *Acta Cryst.* **1989**, *C45*, 410.

38. Sutin, N.; Yandell, J. K. *J. Am. Chem. Soc.* **1973**, *95*, 4847.

39. Halpern, J.; Goodall, B. L.; Khare, G. P.; Lim, H. S.; Pluth, J. J. *J. Am. Chem. Soc.* **1975**, *97*, 2301.

40. Balch, A. *Inorg. Chem.* **1971**, *10*, 276.

41. Wada, M. *J. Chem. Res.* **1985**, (S), 38; (M), 0467.

42. Field, L. D.; George, A. V.; Hambley, T. W. *Polyhedron* **1990**, *9*, 2139.

43. Iovel, I.; Goldberg, Y.; Shymanska, M.; Lukevics, E. *Applied Organomet. Chem.* **1987**, *1*, 371.

44. Aliev, Z. G.; Karateev, A. M. *Koord. Khim.* **1988**, *14*, 111.

45. Karateev, A. M.; Kushch, P. P.; Frolov, Ye. N.; Ovanesyan, N. S.; Dzhavadyan, E. A.; Rozenberg, B. A. *Vysokomol. soyed.* **1988**, *A30*, 1075.

46. Dunbar, K. R.; Haefner, S. C. manuscript in preparation.

47. Dunbar, K. R.; Haefner, S. C.; Burzynski, D. J. *Organometallics* **1990**, *9*, 1347.

48. Dunbar, K. R.; Haefner, S. C.; Pence, L. E. *J. Am. Chem. Soc.* **1989**, *111*, 5504.

CHAPTER III

STUDY OF THE MAGNETIC AND ELECTRONIC PROPERTIES OF ANIONIC Fe(II) AND Fe(III) CHLORIDE COMPOUNDS

1. Introduction

The ubiquity of iron in biological and catalytic processes has spurred a considerable amount of research by both bioinorganic and coordination chemists [1]. The demonstrated role of non-heme iron-sulfur proteins as electron transport agents in a variety of fundamental processes such as nitrogen fixation, photosynthesis or hydroxylation to cite a few, generated the need to prepare synthetic analogues of the active sites of these proteins and study their magnetic and redox properties. These model compounds, which have the minimal composition $[Fe_2S_2(SR)_4]^{2-,3-}$ (Fe^{III}, Fe^{III} or Fe^{III}, Fe^{II}) [2] have been studied by a variety of techniques, such as epr, Mössbauer spectroscopies and magnetic susceptibility measurements [3]. Mössbauer spectroscopy is a powerful tool in iron chemistry since it can provide information on the oxidation state as well as the geometry of the metal center [4].

The unexpected synthesis of the unprecedented salt $[H\text{-}TMPP]_2[Fe_2Cl_6]$ (**2**) from the 1:1 reaction of the $FeCl_3$ with TMPP in benzene prompted us to further investigate its magnetic properties by epr, Mössbauer and SQUID experiments for comparison to those of the known di-ferrous systems. In our studies, we took advantage of the fact that we had an homologous series of compounds, *viz.* $[Fe_2Cl_6]^{2-}$ (**2**), $[FeCl_4]^{2-}$ (**4**) and $[FeCl_4]^{-}$ (**5**) with the same phosphonium countercation, which would provide us with a good data base. The compound $FeCl_3$(O=TMPP) (**6**) was also fully studied since its simple magnetic behavior would serve as a useful reference.

This chapter describes the preliminary magnetic study of compounds **2** and **4-6** by SQUID, epr and Mössbauer spectroscopies. Some of these

results have been obtained as part of a collaboration with Dr. W. R. Dunham at the University of Michigan.

2. Experimental

A. Synthesis

Compounds **2, 4-6** were prepared as described in Chapter II of this dissertation. In addition, a more rational synthesis of $[H\text{-}TMPP]_2[Fe_2Cl_6]$ from Fe(II) starting materials was investigated.

(1) Preparation of [H-TMPP]Cl

An amount of TMPP (0.222 g, 0.417 mmol) was dissolved in 10 mL of benzene and stirred at room temperature for 10 minutes. Addition of two drops of hydrochloric acid with a pipet caused the precipitation of a white solid. The resulting suspension was stirred for 15 minutes, after which time the solvent was removed under vacuum to produce a white residue, which was then dissolved in ethanol. Diethyl ether was subsequently added with vigorous stirring, resulting in the precipitation of a white microcrystalline product, which was collected by filtration in air; yield: 0.189 g (80% relative to TMPP).

(2) Reaction of $FeCl_2$ with [H-TMPP]Cl

A suspension of [H-TMPP]Cl (0.081 g, 0.142 mmol) in a 20 mL acetone/benzene mixture (v/v 1:1) was added dropwise to a suspension of $FeCl_2$ (0.018 g, 0.142 mmol) in 10 mL of benzene over the course of 0.5 hour. This resulted in the precipitation of a pale yellow solid. The reaction mixture was stirred at room temperature for *ca.* 24 hours, after which time the supernatant solvent was decanted and the solid dried *in vacuo*; yield: 0.060 g (~ 30% relative to $FeCl_2$). The infrared spectrum was identical to that of an authentic sample of $[H\text{-}TMPP]_2[Fe_2Cl_6]$ (CsI,

Nujol, cm^{-1}): 950, 925, 910, 900 and 880 ([H-TMPP]$^+$ in a 1:2 salt); 360(s), 300(m), 280(m) and 230(w) (ν(Fe-Cl) for $[Fe_2Cl_6]^{2-}$).

B. Spectroscopy

Magnetic susceptibility measurements were carried out in the Physics and Astronomy Department at Michigan State University, while the epr and Mössbauer experiments as well as the fitting of the magnetic data were performed by Dr. W. R. Dunham of the Biophysics Research Division at The University of Michigan.

(1) Magnetic susceptibility

The magnetic susceptibility of compounds **2** and **4-6** was studied over the temperature range 5-300 K under an applied magnetic field of 500 G. The diamagnetic corrections were applied as follows: $[H\text{-}TMPP]_2[Fe_2Cl_6]$: - 843.60 x 10^{-6} cgs/mol (- 2 x 13 x 10^{-6} for 2 Fe^{2+}, - 6 x 26 x 10^{-6} for 6 Cl^-, - 2 x 330.80 x 10^{-6} for 2 TMPP); $[H\text{-}TMPP]_2[FeCl_4]$: - 778.60 x 10^{-6} cgs/mol (- 13 x 10^{-6} for Fe^{2+}, - 4 x 26 x 10^{-6} for 4 Cl^-, and - 2 x 330.8 x 10^{-6} for 2 TMPP's); [H-TMPP][$FeCl_4$]: - 447.73 x 10^{-6} cgs/mol (- 10 x 10^{-6} for Fe^{3+}, - 4 x 26 x 10^{-6} for 4 Cl^-, - 330.80 x 10^{-6} for TMPP and - 2.93 x 10^{-6} for 1 H); $FeCl_3$(O=TMPP): - 430.8 x 10^{-6} cgs/mol (10 x 10^{-6} for Fe^{3+}, 3 x 26 x 10^{-6} for 3 x Cl^-, 330.80 x 10^{-6} for TMPP and 12 x 10^{-6} for O).

(2) epr spectroscopy

The epr experiments were carried out on frozen samples in acetone (**2**, **4** and **5**) and CH_2Cl_2 (**6**), at various temperatures, for known concentrations. The epr tubes were sealed under vacuum for compounds **2** and **4** to ensure complete anaerobic conditions.

(3) Mössbauer spectroscopy

The experiments were performed on the solid samples at 125 and 175 K. All samples were prepared in a dry-box under an argon atmosphere, and subsequently frozen in liquid nitrogen.

3. Results and Discussion

A. Magnetic susceptibility

(1) $[H\text{-}TMPP]_2[Fe_2Cl_6]$ (2)

Initial magnetic susceptibility measurements on powder unrecrystallized samples of $[H\text{-}TMPP]_2[Fe_2Cl_6]$ (**2**) before its identity as a di-ferrous system was established revealed a non-Curie-Weiss behavior with a magnetic moment μ_{eff} corresponding to an iron(II) center at room temperature (see previous Chapter). After the nature of the compound was undoubtedly established as $[H\text{-}TMPP]_2[Fe_2Cl_6]$ by X-ray crystallography, we became very interested in re-investigating its magnetic behavior. Experiments run on the *crystalline* material obtained from the recrystallization in an acetone/hexanes mixture gave very different results. Figure 13 shows a plot of of the molar susceptibility χ_m versus 1/T and clearly indicates that the compound does not follow a simple magnetic behavior, but that it obeys a Curie-Weiss law at high temperature ($T \geq 20K$).

The magnetic moment at room temperature is $\mu_{eff} = 7.22\ \mu_B$ which is very close to the spin-only value of $8.94\ \mu_B$ expected for a $S = 4$ system, once the spin orbit coupling terms are taken into account; this suggests that there is little, if any, interaction between the two ferrous centers, which are actually *ferro*magnetically coupled (see Figure 14). A preliminary fit of the data employing the isotropic spin Hamiltonian $H = -2JS_1 \cdot S_2$ ($S_1 = S_2 = 2$) yields a value of $J \approx 100\ cm^{-1}$ for the exchange constant which is entirely without precedence in di-iron systems. Only a few di-iron systems

Figure 13. Plot of the molar magnetic susceptibility χ_m versus 1/T for $[H\text{-}TMPP]_2[Fe_2Cl_6]$.

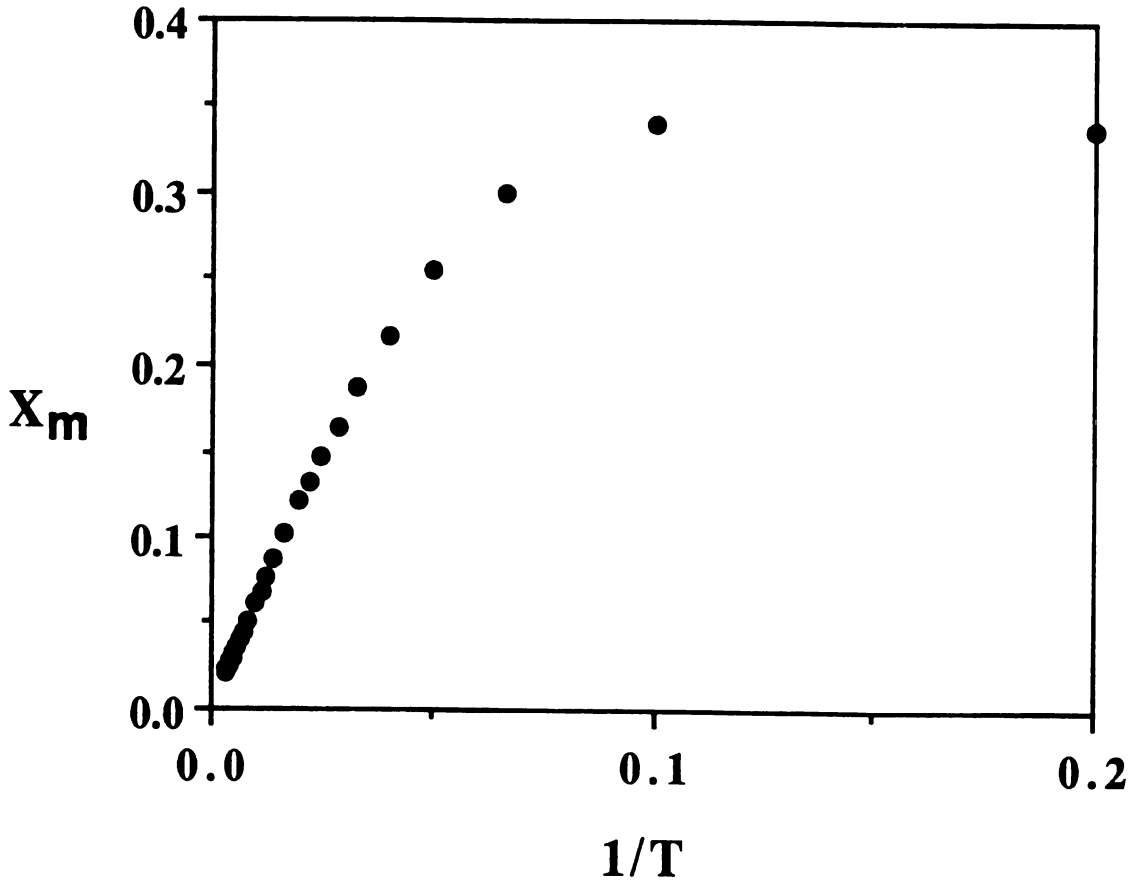

χ_m versus 1/T

Figure 13.

Figure 14. Plot of the effective magnetic moment μ_{eff} versus temperature for $[H\text{-}TMPP]_2[Fe_2Cl_6]$.

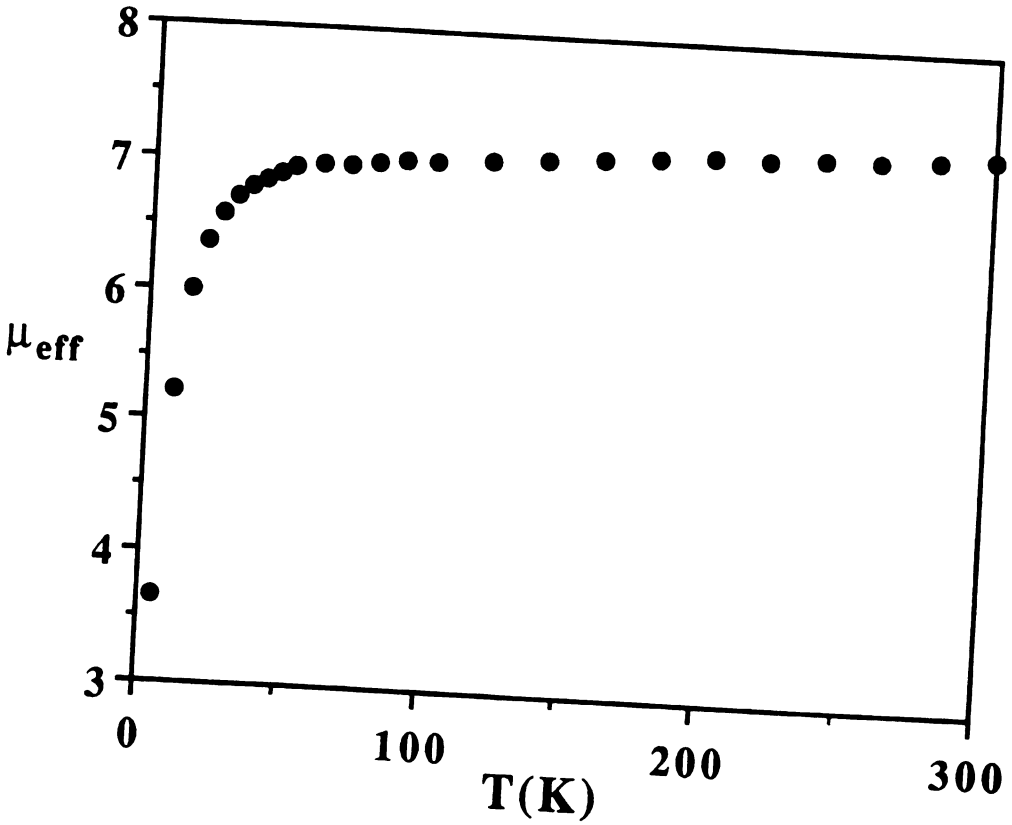

Figure 14.

have been reported to exhibit ferromagnetism and these are weakly coupled [5].

(2) $[H\text{-}TMPP]_2[Fe^{II}Cl_4]$ (4)

The magnetic susceptibility of compound **4** follows a Curie-Weiss behavior in the 5 - 300 K temperature range, with a Weiss temperature of θ = - 1.62 K, as illustrated in Figure 15 (top). The μ_{eff} value of 5.29 μ_B is in the reported range (5.1 - 5.9 μ_B) for S = 2 spin systems [6].

(3) $[H\text{-}TMPP][Fe^{III}Cl_4]$(5)

A plot of the molar susceptibility χ_m versus 1/T for [H-TMPP][$Fe^{III}Cl_4$] is shown in Figure 15 (bottom) and clearly shows that the magnetism of **5** follows a Curie-Weiss behavior with a Weiss temperature of θ = -5.44 K. The value for the magnetic moment is μ_{eff} = 6.11 μ_B which is consistent with a S = 5/2 spin system [6].

(4) $FeCl_3(O{=}PR_3)$ (6)

Figure 16 presents a plot of χ_m versus 1/T for compound **6** and shows that the magnetic behavior obeys a Curie-Weiss law, with a Weiss temperature of -10.08 K. The value of 6.3 μ_B for the magnetic moment is in agreement with a S = 5/2 system [6].

B. epr spectroscopy

Although the chemistry of such simple systems as the $[FeCl_4]^-$ ion has been extensively studied, there are actually no definitive epr studies on tetrachloroferrate salts or any other Fe(II) or Fe(III) chlorides. There are only two reports in the literature from the early 1960's describing the solution epr studies of the decomposition of $FeCl_3$ [7] or $[Cp_2Fe]^+$ [8] in the presence of an external source of Cl^- ions. It then renders any comparison or interpretation of our results very difficult since their is little precedence in the literature.

Figure 15. Plot of the molar magnetic susceptibility χ_m versus 1/T for $[H\text{-}TMPP]_2[FeCl_4]$ (top) and $[H\text{-}TMPP][FeCl_4]$ (bottom).

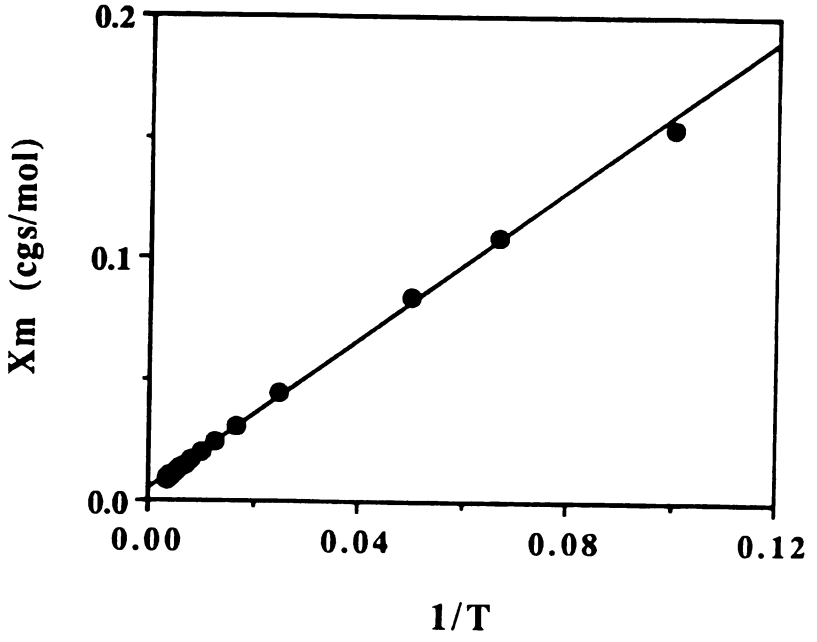
0.2
0.1
0.0
Xm (cgs/mol)
0.00
0.04
0.08
0.12
1/T

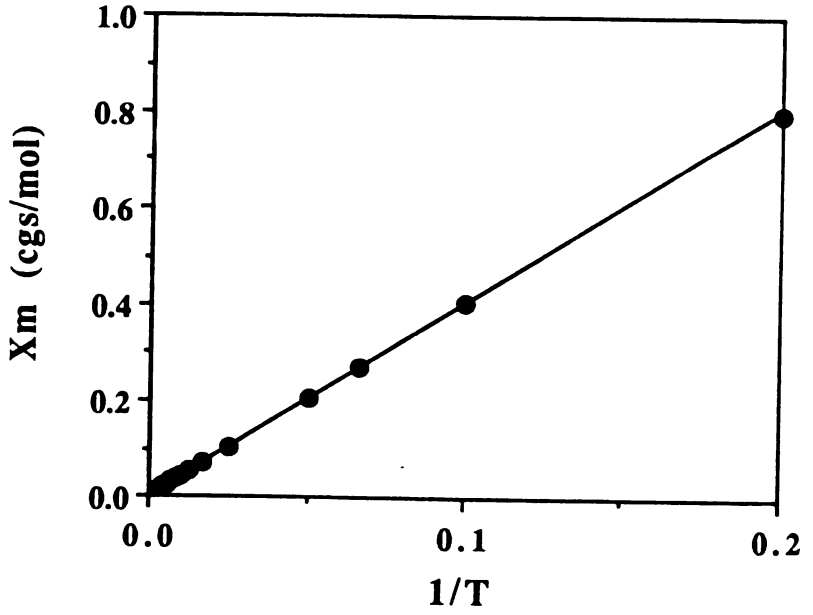
1.0
0.8
0.6
0.4
0.2
0.0
Xm (cgs/mol)
0.0
0.1
0.2
1/T

Figure 15.

Figure 16. Plot of the molar magnetic susceptibility χ_m versus T (top) and versus 1/T (bottom) for $FeCl_3$(O=TMPP).

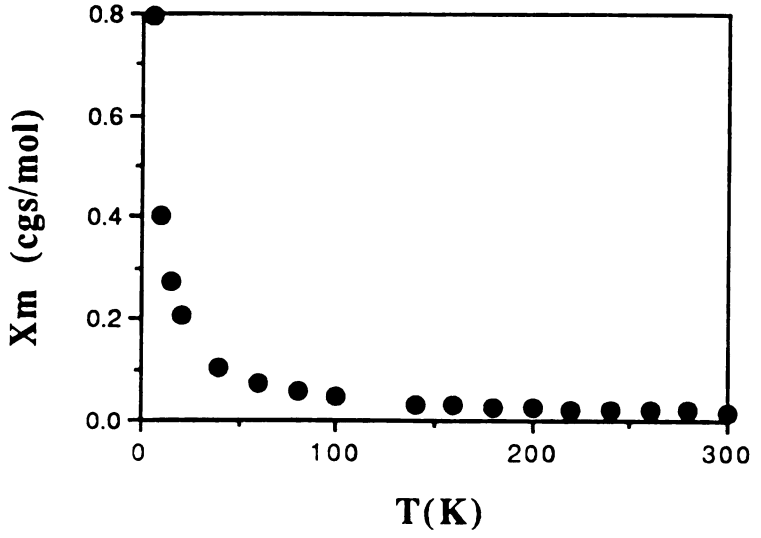
0.8
0.6
0.4
0.2
0.0
Xm (cgs/mol)
0
100
200
300
T(K)

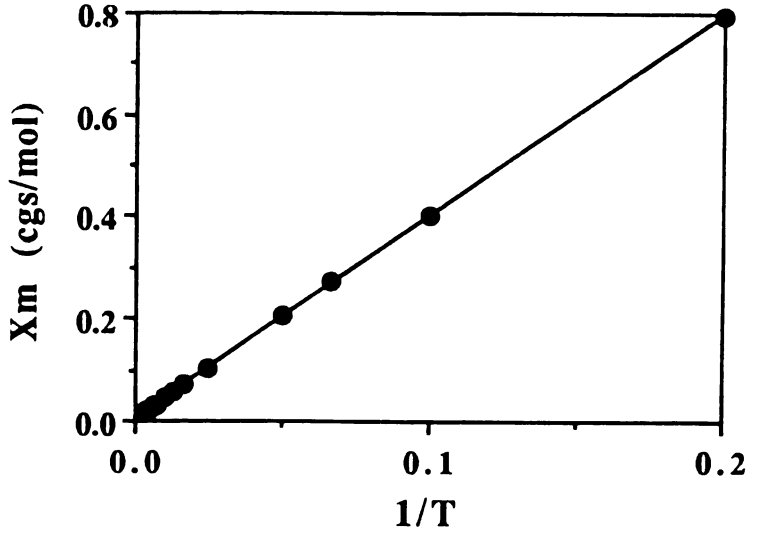
0.8
0.6
0.4
0.2
0.0
Xm (cgs/mol)
0.0
0.1
0.2
1/T

Figure 16.

(1) $[H\text{-}TMPP]_2[Fe_2Cl_6]$ (2)

This compound is expected to be epr-silent because it possesses an integer spin value of S = 4 as its ground state. However, the first experiments that were carried out showed a large signal at *ca.* g = 2.0, which increased in intensity overtime. Being aware of the series of reactions which this compound undergoes in the presence of oxygen, it occurred to us that what we were observing was actually the *in situ* formation of [H-TMPP][$Fe^{III}Cl_4$] (**5**). Indeed we were able to identify this "impurity" as the same signal observed for an authentic sample of compound **5** (*vide infra*). When the epr experiment was performed under anaerobic conditions (sample prepared in the dry-box and tube sealed under vacuum), the spectrum still showed a minor signal at g = 2, but no additional resonances could be detected. Quantitations revealed that this species was a minor component of the sample.

(2) $[H\text{-}TMPP]_2[Fe^{II}Cl_4]$ (4)

We were not able to obtain a spectrum of an authentic sample of compound **4**, since the only detectable signal was that of [H-TMPP][$Fe^{III}Cl_4$], **5**, at g = 2. The quantitative experiments yielded spin density values far larger than those expected, thereby indicating the impure nature of the sample.

(3) [H-TMPP][$Fe^{III}Cl_4$] (5)

The spectrum of **5** at 7 K exhibits a large signal at g = 2, which is in agreement with the reported literature on $[FeCl_4]^-$ [7,8].

(4) $FeCl_3(O{=}PR_3)$ (6)

The epr spectrum for compound **6** at 7 K contains two signals at $g_1 \sim 2$ and $g_2 = 6$, which is typical for a high spin Fe(III) center [3a].

C. Mössbauer spectroscopy

(1) Background

The Mössbauer effect is a nuclear gamma-ray resonance with such high precision that spectral features reflect the chemical state of the corresponding atom. It is a very powerful technique for measuring oxidation state, local symmetry and magnetic ordering [4]. The source of radiation is generally a metastable isotope which decays to the nuclear excited state of the Mössbauer isotope in its ground state (Scheme 2).

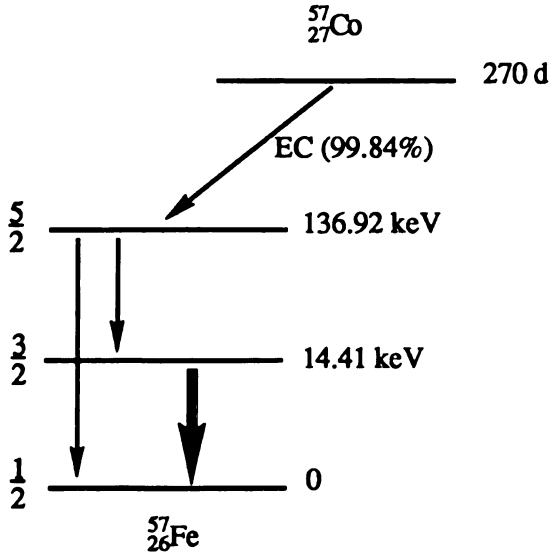

Scheme 2. Nuclear decay scheme for the Mössbauer resonance in ^{57}Fe (adapted from reference 4c)

There are two spectral parameters of particular interest in Mössbauer spectroscopy; these are the isomer shift, δ, measured as the centroid of the spectrum, and the quadrupole splitting, ΔE. The isomer shift (δ) is a measure of the "s" electron density and is influenced by the occupation of d orbitals, d-electrons affecting its value because of shielding. Thus, an increase in the number of 3d electrons from Fe^{3+} to

Figure 17. Mössbauer spectrum of the Fe^{2+} ion in an absorber of $FeSO_4 \cdot 7H_2O$ at nitrogen temperature using a room-temperature stainless steel source.

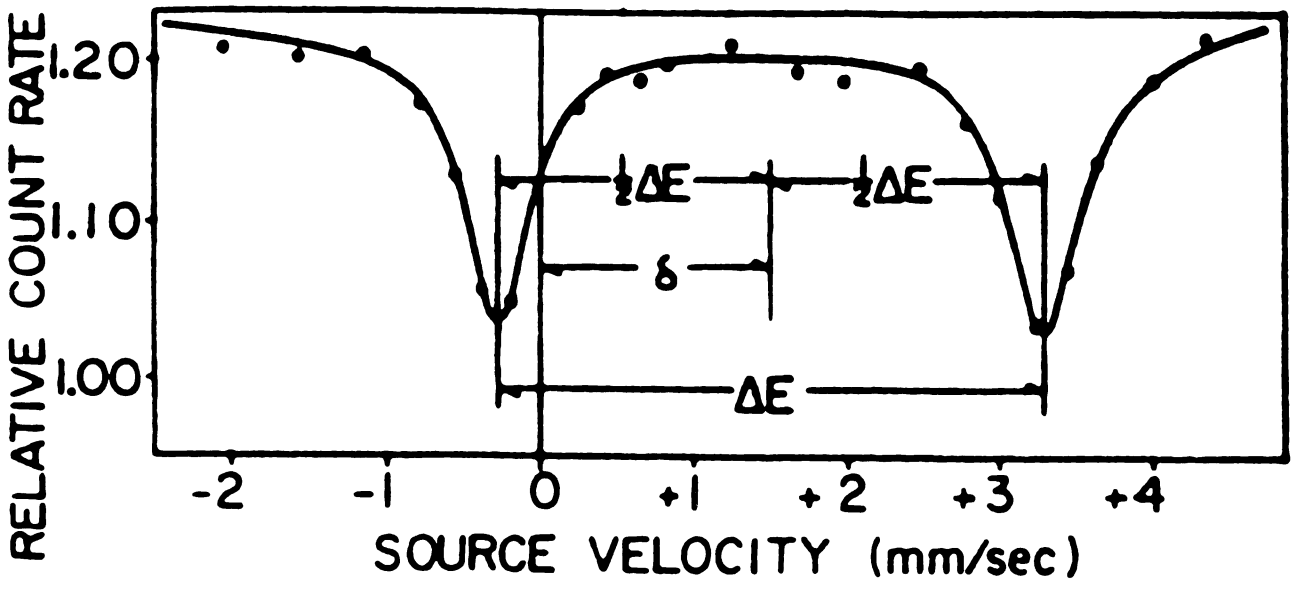
RELATIVE COUNT RATE
1.20
1.10
1.00
½ΔE
½ΔE
δ
ΔE
-2
-1
0
+1
+2
+3
+4
SOURCE VELOCITY (mm/sec)

Figure 17.

Fe^{2+} results in a more efficient screening of the 4s electrons from the nucleus and yields more positive values for δ. The quadrupole splitting values vary considerably and are determined by the 6th electron (d^6 vs. d^5) and which orbital it occupies. Figure 17 presents a schematic Mössbauer spectrum and summarizes the spectral parameters.

(2) $[H\text{-}TMPP]_2[Fe_2Cl_6]$ (2)

Initial studies carried out on a powder sample of compound **2** resulted in the spectrum presented in Figure 18. The isomer shift of δ = 0.31 mms^{-1} is not in the reported range for Fe^{II} species. The quadrupole splitting is $\Delta E = 1.25$ mms^{-1}. Work is in progress to determine whether this value of the isomer shift is a result of the presence of an Fe^{III} impurity in the sample, or of the unprecedented nature of the $[Fe_2Cl_6]^{2-}$ di-ferrous anion.

(3) $[H\text{-}TMPP]_2[Fe^{II}Cl_4]$ (4) and $[H\text{-}TMPP][Fe^{III}Cl_4]$ (5)

The Mössbauer spectra of the $[FeCl_4]^{2-}$ and $[FeCl_4]^{-}$ ions have been known for almost thirty years [9,10]. These tetrachloroferrate salts were studied in the early days because their simple geometry and spin configuration made them the ideal reference compounds. We undertook this study because we wanted to have an homologous series of Fe^{II} and Fe^{III} compounds with the same phosphonium counterion, and indeed our results (Figure 19) are in agreement with the literature.

(4) $FeCl_3$(O=TMPP) (6)

Mössbauer results for compound **6** are in accord with those reported for tetrahedral high-spin Fe^{III} complexes. A high-spin tetrahedrally coordinated Fe^{III} complex has each d orbital singly occupied, thus generating a cubic electric field. The Mössbauer spectrum should then

Figure 18. Mössbauer spectrum at 125 K for $[H\text{-}TMPP]_2[Fe_2Cl_6]$.

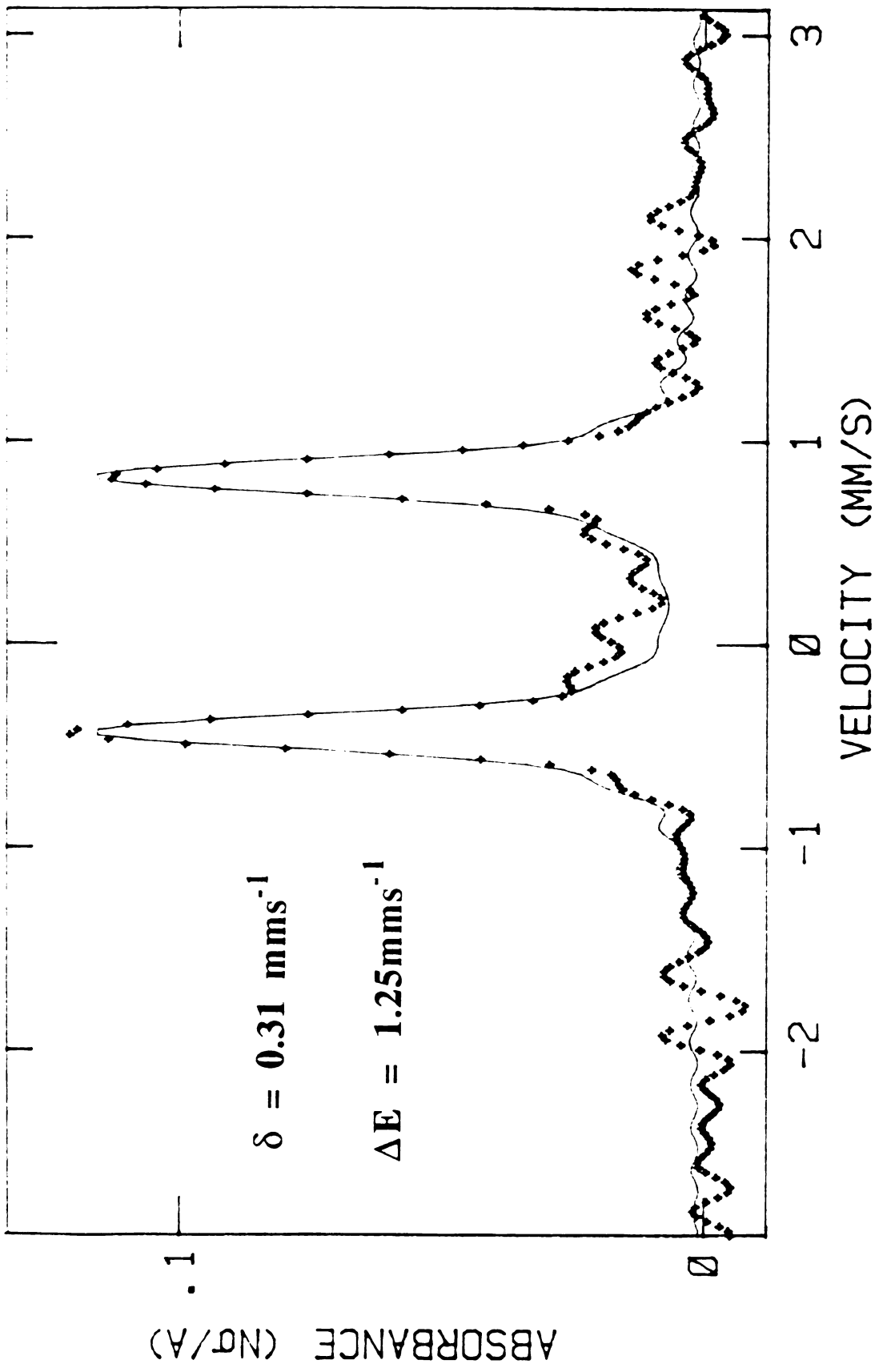

Figure 18.

Figure 19. Mössbauer spectra at 125 K for $[H\text{-}TMPP]_2[FeCl_4]$ (top) and $[H\text{-}TMPP][FeCl_4]$ (bottom).

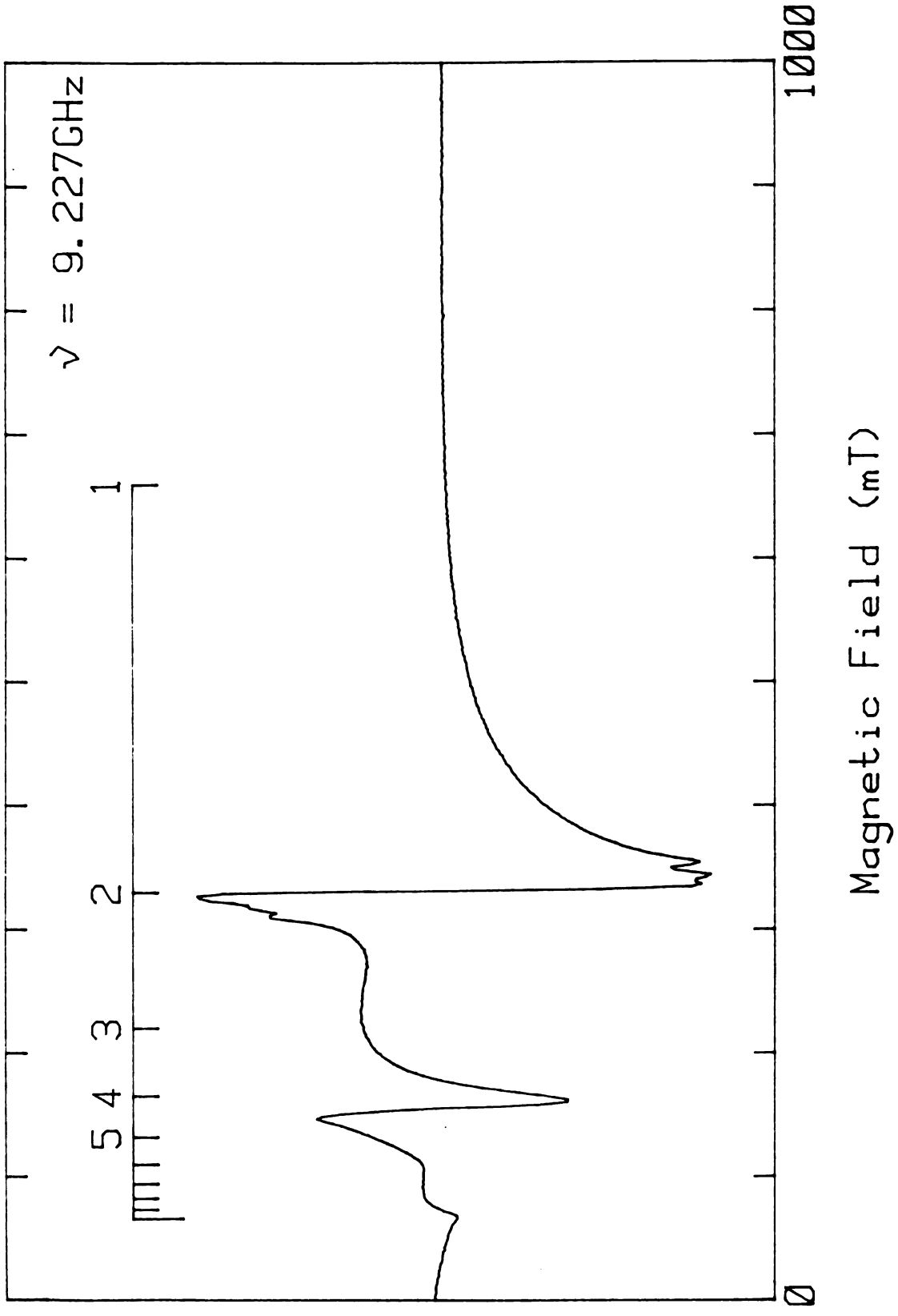

Figure 19.

Figure 20. Mössbauer spectrum at 125 K for $FeCl_3$(O=TMPP).

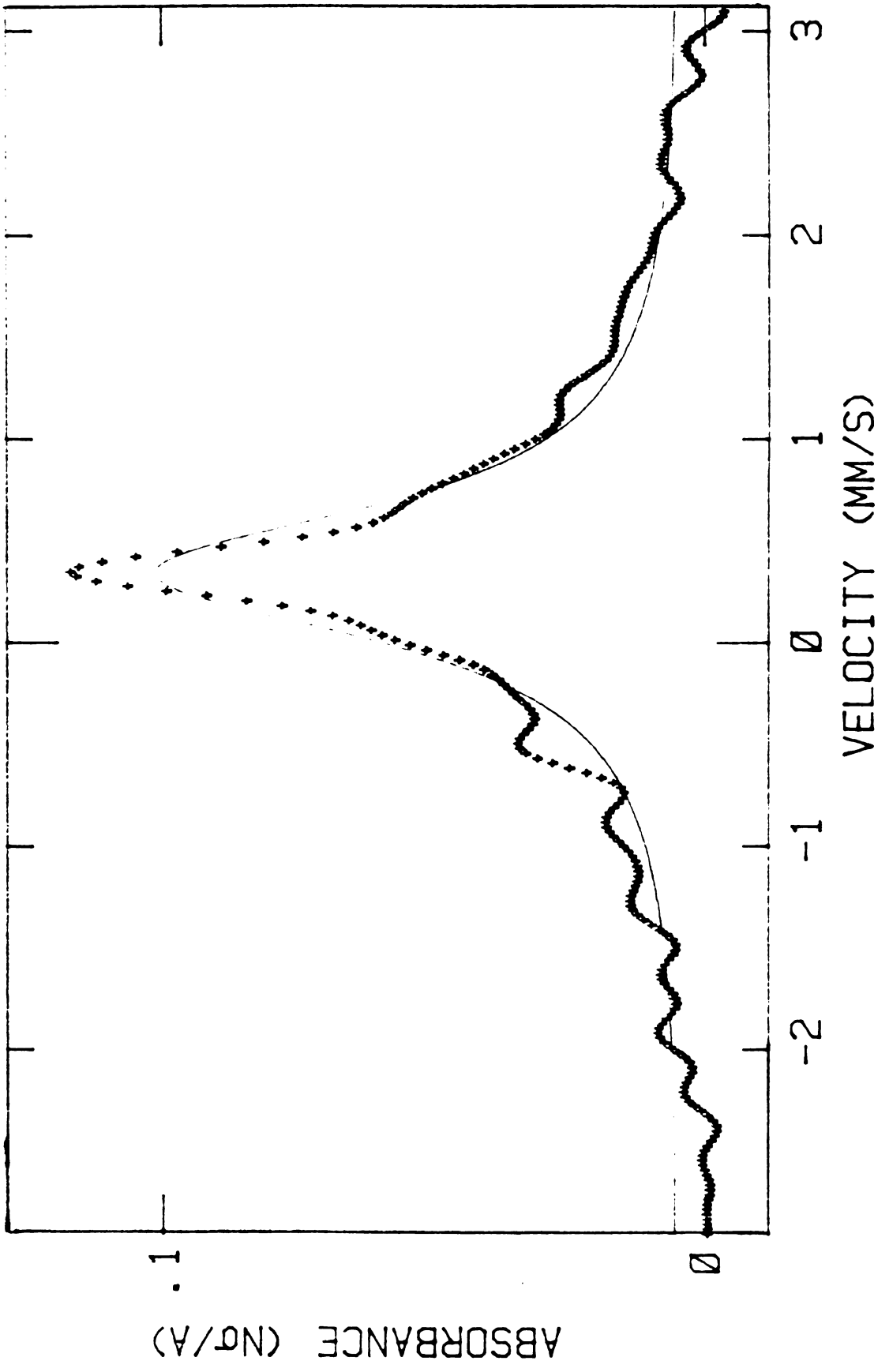

Figure 20.

consist of a single unsplit line, as was observed in the case of the $[FeCl_4]^-$ anion (*vide supra*). Replacement of one chloride ligand, as in $FeCl_3$(O=TMPP), produces an electric field gradient and removes the degeneracy of the I = 3/2 state. A quadrupole split doublet is then observed [11]. These distortions, arising from a non-equivalence of the ligands about a d^5 ion are generally small and result in small ΔE values, sometimes unobserved. Our results for compound **6** (Figure 20) are in good agreement with those reported for the four-coordinate species $FeCl_3(PPh_3)$ and $FeCl_3(AsPh_3)$ (δ = 0.46 mms^{-1} vs 0.46 and 0.57 mms^{-1}, respectively) [11]. We were not, however, able to observe a quadrupole splitting at 125 K because of spin relaxation.

4. Summary

Preliminary studies on the magnetism of compounds **2**, **4-6** have been carried out, the last three compounds serving as references. The magnetic susceptibility data for $[H\text{-}TMPP]_2[Fe_2Cl_6]$ (**2**) revealed that the two Fe^{II} centers are *ferro*magnetically coupled, which is entirely without precedence in di-ferrous systems. More detailed fitting of the magnetism data, along with epr and Mössbauer studies are underway since this compound presents a new opportunity to study a stable di-ferrous system without any sulfur co-ligands, thereby precluding ligand-based chemistry. An energy level diagram for a ferromagnetically coupled di-ferrous system with a S = 4 ground state is depicted in Figure 21. Due to the complicated magnetic behavior of such species, little is known regarding their epr properties. There are only two reports of di-ferrous systems studied by epr spectroscopy in the literature; these are $[Fe_2(BPMP)(OPr)_2](BPh_4)$ [12] and $[Fe_2(BIPhMe)_2(O_2CH)_4]$ [13] for

Figure 21. Energy level diagram for a ferromagnetically coupled di-ferrous system with a S = 4 ground state.

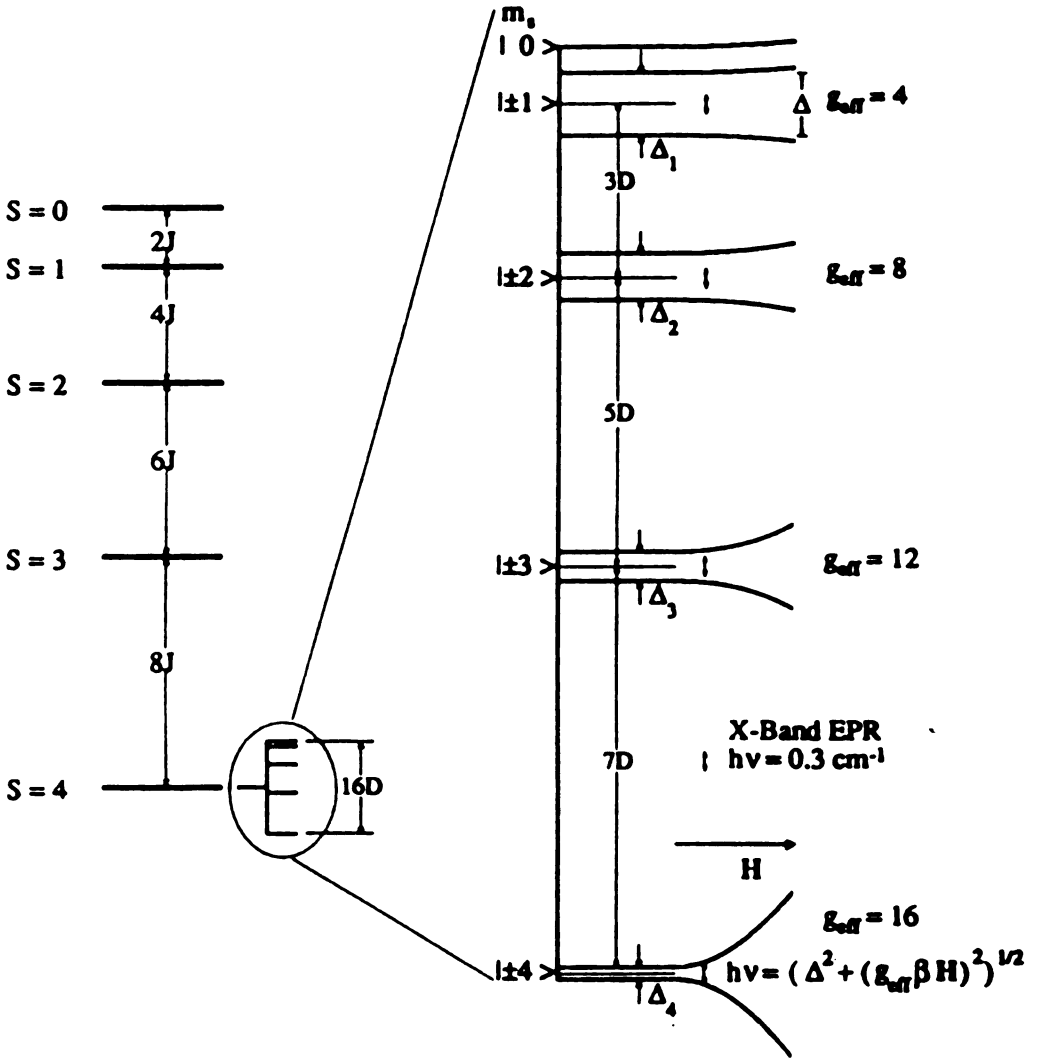
S = 0
2J
S = 1
4J
S = 2
6J
S = 3
8J
S = 4
16D
m_s
| 0 >
| ±1 >
| ±2 >
| ±3 >
| ±4 >
Δ
Δ1
Δ2
Δ3
Δ4
3D
5D
7D
g_eff = 4
g_eff = 8
g_eff = 12
g_eff = 16
X-Band EPR
hν = 0.3 cm⁻¹
H
hν = (Δ² + (g_eff β H)²)^1/2

Figure 21.

which extremely low field epr signals were observed at g = 16, presumably derived from a coupled di-ferrous system [3c].

We are also investigating the possibility of preparing the $[Fe_2Cl_6]^{2-}$ anion by a more rational direct route by using an Fe^{II} starting material such as $FeCl_2$. This approach has recently shown promise in the 1:1 reaction of $FeCl_2$ with the independently prepared [H-TMPP]Cl salt. We are further curious to learn whether this anion can be stabilized by other bulky counterions such as $[PPh_4]^+$, $[H\text{-}PPh_3]^+$ or $[^tBu_4N]^+$, which would render this salt more soluble and therefore more useful to the bioinorganic community.

LIST OF REFERENCES

1. (a) Holm, R. H. *Acc. Chem. Res.* **1977**, *10*, 427. (b) Holm, R. H. *Chem. Soc. Rev.* **1981**, *10*, 455. (c) Averill, B. A. *Fe-S and Mo-S Clusters as Models for the Active Site of Nitrogenase; Struct. Bonding* **1983**, *53*, 59. (d) Holm, R. H.; Ciurli, S.; Weigel, J. A. *Prog. Inorg. Chem.* **1990**, *38*, 1. (e) Vincent, J. B.; Ollivier-Lilley, G. L.; Averill, B. A. *Chem. Rev.* **1990**, *90*, 1447.

2. (a) Mayerle, J. J.; Denmark, S. E.; DePamphilis, B. V.; Ibers, J. A.; Holm, R. H. *J. Am. Chem. Soc.* **1975**, *97*, 1032. (b) Lane, R. W.; Ibers, J. A.; Frankel, R. B.; Papaefthymiou, G. C.; Holm, R. H. *J. Am. Chem. Soc.* **1977**, *99*, 84. (c) Bobrik, M. A.; Hodgson, K. O.; Holm, R. H. *Inorg. Chem.* **1977**, *16*, 1851. (d) Hagen, K. S.; Holm, R. H. *J. Am. Chem. Soc.* **1982**, *104*, 5496. (e) Salifoglou, A.; Simopoulos, A.; Kostikas, A.; Dunham, W. R.; Kanatzidis, M. G.; Coucouvanis, D. *Inorg. Chem.* **1984**, *23*, 418.

3. (a) Sands, R. H.; Dunham, W. R. *Q. Rev. Biophysics* **1975**, *7*, 443. (b) Fee, J. A.; Findling, K. L.; Yoshida, T.; Hille, R.; Tarr, G. E.; Hearshen, D. O.; Dunham, W. R.; Day, E. P.; Kent, T. A.; Münck, E. *J. Biol. Chem.* **1983**, *259*, 124. (c) Que, L. Jr.; True, A. E. *Prog. Inorg. Chem.* **1990**, *38*, 97.

4. (a) Mössbauer, R. L. *Z. Physik* **1958**, *151*, 124. (b) Drago, R. S. *Physical Methods in Chemistry*; W. B. Saunders Co.: Philadelphia, **1977**; Ch. 15, p. 530-551. (c) Gibb, T. C. *Principles of Mössbauer Spectroscopy*; Chapman and Hall: London, **1976**. (d) *Advances in Mössbauer Spectroscopy, Applications to Physics, Chemistry and Biology*; Thosar, B. V.; Srivastava, J. K.; Iyengar, P. K.; Bhargava, S. C.. Eds.; Elsevier Scientific Publishing Company: Amsterdam, **1983**. (e) Delgass, W. N.; Wolf, E. E. *Chem. Ind. (Dekker)* **1987**, *26* (*Chem. React. React. Eng.*), 151-238.

5. (a) Maroney, M. J.; Kurtz, D. M.; Nocek, J. M.; Pearce, L. L.; Que, L. Jr.; *J. Am. Chem. Soc.* **1986**, *108*, 6871. (b) Reem, R. C.; Solomon, E. I. *J. Am. Chem. Soc.* **1987**, *109*, 1216. (c) Dance, J. M.; Mur, J.; Darriet, J.; Hagenmuller, P.; Massa, W.; Kummer, S.; Babel, D. *J. Solid State Chem.* **1986**, *63*, 446. (d) Drüeke, S.; Chaudhuri, P.; Pohl, K.; Wieghard, K.; Ding, X.-Q., Bill, E.; Sawaryn, A.; Trautwein, A. X.; Winkler, H.; Gurman, S. J. *J. Chem.*

Soc., Chem. Commun. **1989**, 59. (e) Snyder, B. S.; Patterson, G. S.; Abramson, A. J.; Holm, R. H. *J. Am. Chem. Soc.* **1989**, *111*, 5223. (f) Mikuriya, M.; Kakuta, Y.; Kawano, K.; Tokii, T. *Chem. Lett.* **1991**, 2031.

6. O'Connor, C. J. *Prog. Inorg. Chem.* **1982**, *29*, 205.

7. Hertel, G. R.; Clark, H. M. *J. Phys. Chem.* **1961**, *65*, 1930.

8. Golding, R. M.; Orgel, L. E. *J. Chem. Soc.* **1962**, 363.

9. (a) Gibb, T. C.; Greenwood, N. N. *J. Chem. Soc.* **1965**, 6989. (b) Edwards, P. R.; Johnson, C. E.; Williams, R. J. P. *J. Chem. Phys.* **1967**, *47*, 2074.

10. DeBenedetti, S.; Lang, G.; Ingalls, R. *Phys. Rev. Letters* **1961**, *6*, 60.

11. Birchall, T. *Can. J. Chem.* **1969**, *47*, 1351.

12. (a) Borovik, A. S.; Que, L. Jr. *J. Am. Chem. Soc.* **1988**, *110*, 2345. (b) Borovik, A. S.; Hendrich, M. P.; Holman, T. R.; Münck, E.; Papaefthymiou, V.; Que, L. Jr. *J. Am. Chem. Soc.* **1990**, *112*, 6031.

13. Tolman, W. B.; Bino, A.; Lippard, S. J. *J. Am. Chem. Soc.* **1989**, *111*, 8523.

CHAPTER IV

CHEMISTRY OF TRIS(2,4,6-TRIMETHOXYPHENYL)PHOSPHINE WITH COBALT(II)

1. Introduction

The chemistry of Co(II) is a vast area of investigation, particularly with respect to O_2 binding and transport [1]. A major advantage of five-coordinate Co(II) is that its complexes typically exhibit a low-spin electronic configuration, with an S = 1/2 ground state, thereby providing the researcher with a convenient epr probe for elucidating small molecule binding and electron distribution. Apart from Co(II) and to a lesser degree Ni(III), little is known regarding the chemistry of d^7 metal ions, primarily since these species are highly reactive, appearing only as short-lived intermediates or impurities in the chemistry of d^6 and d^8 metal complexes. It is of considerable interest to design d^7 complexes and study their reactivity in stoichiometric and catalytic reactions of the late transition elements, especially Rh, in which their presence has been detected but whose potential role in the chemistry is not known [2]. Metalloradicals exhibit the greatest promise for undergoing reversible reactions with important molecules such as CO and O_2 since they bind much less tightly to substrates than their d^8 counterparts.

In order to ascertain whether it was feasible to use a basic tertiary phosphine such as TMPP to stabilize 3d metals, we set out to investigate the chemistry of this ligand with Co(II), in the form of $CoCl_2$, but also $[Co(NCCH_3)_6]^{2+}$, since the use of the solvated dirhodium(II,II) species, $[Rh_2(NCCH_3)_{10}][BF_4]_4$, had proven to be very successful in our earlier work. This chapter reports the chemistry of $CoCl_2$ and of the solvated acetonitrile Co(II) salts of $AlCl_4^-$, $SbCl_6^-$ and BF_4^- with TMPP. The reactions depend on choice of solvent and counterion as well as the Co:PR_3 ratio. Details describing these findings as well as the structures and reactivity of key products are discussed.

2. Experimental

A. Synthesis

(1) Reactions of $CoCl_2$ with TMPP

(i) Preparation of $[CH_3\text{-}TMPP]_2[Co_2Cl_6]$ (8)

Anhydrous $CoCl_2$ (0.112 g, 0.94 mmol) was added to one equivalent of TMPP (0.500 g, 0.94 mmol) in 10 mL of freshly distilled, deoxygenated benzene. The reaction mixture was stirred at room temperature for five days, during which time a bright blue solid formed. This was collected by filtration and washed with copious amounts of benzene. Characterization of this initial product by NMR spectroscopy revealed the presence of [H-TMPP]$^+$ (3.69(s), 3.85(s), 6.33(d) and 8.38(d) ppm in CD_3CN) and [CH_3-TMPP]$^+$ (2.54(d), 3.58(s), 3.84(s) and 6.30(d) ppm in CD_3CN). The crude product was recrystallized from a dichloromethane solution layered with toluene. Blue X-ray quality crystals formed within 24 hours, and their identity was established as $[CH_3\text{-}TMPP]_2[Co_2Cl_6]$ (**8**); ^1H NMR (CD_3CN, δppm): 2.46(d), 3.54(s), 3.84(s) and 6.22(d); Infrared ($\nu_{Co\text{-}Cl}$): 380(s), 300(m), 255(w) and 240(w) cm^{-1}.

(ii) Reaction of $CoCl_2$ with TMPP in $CHCl_3$

A quantity of $CoCl_2$ (0.159 g, 1.335 mmol) was added to one equivalent of TMPP (0.711 g, 1.335 mmol) in 10 mL of $CHCl_3$. The resulting dark blue solution was stirred at room temperature for 3 days, after which time it had turned emerald green with precipitation of a turquoise-blue solid. The reaction mixture was filtered anaerobically through a medium porosity frit to yield a blue solid (yield: 0.023 g) and a dark green solution. This solution was then pumped down to a residue, which was washed with diethyl ether (2 x 10 mL) and dried *in vacuo*; yield: 0.141 g. The blue solid was characterized as $[H\text{-}TMPP]_2[CoCl_4]$ (**9**)

by ^1H NMR and infrared spectroscopies (*vide infra*). The dark green product was identified as $[CH_3\text{-TMPP}]_2[CoCl_4]$ (**10**); ^1H NMR (CD_3CN, δppm): 2.46(d), 3.53(s), 3.84(s) and 6.21(d); Infrared ($\nu_{Co\text{-}Cl}$): 292(s) cm^{-1}; electronic spectrum (CH_3CN, λ_{max} (nm)): 687, 665(sh), 631(sh) and 589.

(2) Reactions of $[Co(NCCH_3)_6][AlCl_4]_2$ with TMPP

A quantity of $[Co(NCCH_3)_6][AlCl_4]_2$ [3] (0.274 g, 0.427 mmol) was reacted with two equivalents of TMPP (0.455 g, 0.854 mmol) in 20 mL of methanol. The resulting solution which changes from blue to pink as the solvent is being added, was stirred at room temperature for *ca.* 30 minutes. Slow evaporation of the solvent, in air, yielded a crop of blue-green crystals of $[H\text{-TMPP}]_2[CoCl_4]$, **9**, that were suitable for an X-ray study; yield: 0.221 g (40% relative to Co^{2+}). Anal. Calc'd for $CoCl_4P_2O_{19}C_{55}H_{72}$: C: 50.82; H: 5.58; Found: C: 50.13; H: 5.58. Infrared (CsI, nujol, cm^{-1}): 295 ($\nu_{Co\text{-}Cl}$); ^1H NMR (CD_3OD, δppm): 3.56(s), 3.74(s), 6.16(d), 8.26(d); UV-visible (CH_2Cl_2, λ_{max} (nm)): 694, 669, 634, 612(sh), 361, 287(sh), 260; CV: $(E_{1/2})_{ox}$ = + 1.16 V; magnetic moment: μ_{eff} = 4.41 μ_B (S = 3/2).

(3) Reactions of $[Co(NCCH_3)_6][SbCl_6]_2$ with TMPP

A quantity of $[Co(NCCH_3)_6][SbCl_6]_2$ [4] (0.276 g, 0.284 mmol) was added to a flask containing 2 equivalents of TMPP (0.302 g, 0.568 mmol). Upon addition of methanol (20 mL), a bright yellow crystalline solid precipitated from a pink solution. Subsequent chilling of the filtrate yielded additional yellow product, formulated as $[H\text{-TMPP}][SbCl_6]$; yield: 0.229 g (47% relative to TMPP). Anal. Calc'd for $SbCl_6PO_9C_{27}H_{34}$: C: 36.69; H: 3.93; Cl: 24.09; Found: C: 37.33; H: 3.92; Cl: 24.51. The pink solution was evaporated to a blue-green residue that was subsequently

dissolved in a mixture acetone/hexanes (v/v 1:1). A crop of navy blue and turquoise crystals grew over the period of 2 days from this solvent mixture. The two crystalline products were separated by taking advantage of the preferential solubility of the turquoise product in THF; yield of the blue crystals, $[H\text{-}TMPP]_2[CoCl_4]$, **9**; 0.033 g (10% relative to Co^{2+}); yield of the turquoise compound, $[ClCH_2\text{-}TMPP]_2[CoCl_4]$, **11**; 0.012 g (4% relative to Co^{2+}).

(4) Reactions of $[Co(NCCH_3)_6][BF_4]_2$ with 2 equivalents of TMPP

The 1:2 reaction between $[Co(NCCH_3)_6][BF_4]_2$ [5] and TMPP was carried out in a variety of solvents (MeOH, CH_3CN, C_6H_6, THF, acetone), and the following procedure describes a typical experiment performed in acetone. A sample of $[Co(NCCH_3)_6][BF_4]_2$ (0.138 g, 0.287 mmol) was reacted with two equivalents of TMPP (0.306 g, 0.575 mmol) in 8 mL of acetone to produce a dark blue-green solution, after stirring at room temperature for 2 hours. After this time, the volume was reduced under dynamic vacuum to *ca.* 4 mL, and 5 mL of diethyl ether were slowly added. A grey solid precipitated from the solution, which was then decanted into another Schlenk tube. The grey by-product was dried, *in vacuo*; yield of $[H\text{-}TMPP][BF_4]$: 0.215 g (60% relative to TMPP). The solution was pumped down to a residue, washed with diethyl ether and dried under vacuum; yield: 0.057 g. The NMR spectrum of this solid showed a mixture of $[H\text{-}TMPP]^+$ and $[CH_3\text{-}TMPP]^+$.

(5) Reactions of $[Co(NCCH_3)_6][BF_4]_2$ with 4 equivalents of TMPP

(i) Preparation of Co(TMPP-*O*)$_2$ (12)

An amount of $[Co(NCCH_3)_6][BF_4]_2$ (0.282 g, 0.590 mmol) was added to 4 equivalents of TMPP (1.256 g, 2.360 mmol) in 10 mL of acetone. The solution, which turned dark purple upon addition of the solvent, was stirred at room temperature for 48 hours until it had turned dark green. The volume was reduced to ~ 5 mL, and diethyl ether was added (~ 10 mL), which caused the precipitation of a white solid. The green solution was decanted from the solid, reduced to a residue by evaporation, and dissolved in 10 mL of THF. Additional precipitation of the white solid, $[CH_3\text{-TMPP}][BF_4]$, ensued; yield: 0.686 g (46% relative to TMPP). The green THF solution was again evaporated to a residue, which was finally washed with diethyl ether (2 x 10 mL) and dried *in vacuo*; yield: 0.499 g (77% relative to Co^{2+}). Slow diffusion of hexanes into an acetone solution produces dark green X-ray quality crystals of Co(TMPP-*O*)$_2$, **12**. ^{1}H NMR ($CDCl_3$, δppm): 1.10(s), 1.55(s), 2.30(s), 2.84(s), 3.33(s), 3.40(s), 3.45(s), 3.78(s), 4.05(s), 4.19(s), 4.60(s), 4.68(s), 5.32(s), 6.18(s), 6.92 (s)), 8.18(s), 8.62(s); electronic spectrum (CH_2Cl_2, λ_{max} (nm); ε, $M^{-1}\,cm^{-1}$): 595(370), 459(310), 379(sh), 312(sh), 287(sh), 257; electrochemistry: $E_{p,a}$ = + 0.50 V; FAB-mass spectrum: m/z = 1093 (corresponding to $[Co(TMPP\text{-}O)_2]^+$), magnetic moment: μ_{eff} = 4.48 μ_B (S = 3/2).

(ii) Preparation of $[ClCH_2\text{-TMPP}]_2[CoCl_4]$ (11)

The salt $[Co(NCCH_3)_6][BF_4]_2$ (0.111 g, 0.231 mmol) was allowed to react with 4 equivalents of TMPP (0.493 g, 0.925 mmol) in the manner specified in method (5)(i) above, with the exception that the reaction was

ceased while the solution was in the intermediate purple stage (< 24 h). By employing the same work-up procedure as described above, the isolated by-product was [H-TMPP][BF_4] (~ 33% relative to TMPP), and the major isolated product was a *purple* solid. Recrystallization of the solid by slow diffusion of diethyl ether into a CH_2Cl_2 solution produced a crop of turquoise-blue crystals of [$ClCH_2$-TMPP]$_2$[$CoCl_4$], **11**, that were suitable for an X-ray study. Anal. Calc'd for $CoCl_6P_2C_{56}H_{70}O_{18}$: C: 49.28: H: 5.17; Found: C: 51.05; H: 5.52. ^{1}H NMR (d_6-acetone, δppm): 3.53(d), 3.80(s), 4.69(d), 6.05(d); Infrared (CsI, nujol): 290 cm^{-1} (ν_{Co-Cl}); UV-visible (CH_2Cl_2, λ_{max} (nm); ε, M^{-1} cm^{-1}): 694(570), 669(490), 634(370), 610(sh), 338(sh).

(iii) Preparation of [Co(TMPP)$_2$][BF_4]$_2$ (13)

An amount of [Co($NCCH_3$)$_6$][BF_4]$_2$ (0.290 g, 0.607 mmol) was added to four equivalents of TMPP (1.292 g, 2.426 mmol) in 10 mL of THF to form an opaque purple solution, which was gently heated until the Co(II) salt had totally dissolved, and finally stirred at room temperature for *ca.* 1 hour. After this time a large quantity of white solid was suspended in the reaction solution, which was removed by filtration of the solution through a medium porosity frit. The resulting dark purple filtrate was layered with 10 mL of hexanes, and the white solid was dried *in vacuo*; yield of [H-TMPP][BF_4]: 0.445 g (30% relative to TMPP). After 48 hours, a mixture of white and purple microcrystals had precipitated out of the acetone/hexanes solvent mixture. This microcrystalline material was then rinsed with diethyl ether, and separated by careful examination under the microscope; yield of purple crystals, [Co(TMPP)$_2$][BF_4]$_2$ (**13**): 0.306 g (~ 40% relative to Co^{2+}); yield of white crystals, free TMPP: 0.156 g (12% relative to TMPP). Characterization of **13**: UV-visible (acetone,

λ_{max} (nm); ε, M^{-1} cm^{-1}): 584(170), 460(sh), 380(sh); electrochemistry: $E_{p,a}$ = + 0.55 V; Infrared (CsI, nujol, cm^{-1}): 1057 and 521 (ν_{B-F}).

(iv) Preparation of $Cl_2Co_2\{\mu$-η^2-(TMPP-*O*)$_2\}$ (14)

Slow diffusion of diethyl ether into a CH_2Cl_2 solution of **12** yielded a crop of blue-green needles of $Cl_2Co_2\{\mu$–η^2-(TMPP-*O*)$_2\}$, **14**, suitable for a single crystal X-ray study. Anal. Calc'd for $Cl_2Co_2P_2C_{52}O_{18}H_{60}$: C: 50.69; H: 4.94; Found: C: 51.04; H: 4.98. ^1H NMR ($CDCl_3$, δppm): 1.19(s), 1.69(s), 2.13(s), 2.83(s), 3.46(s), 4.38(s), 4.54(s), 5.08(s), 5.25(s), 6.05(s), 7.09(s), 7.99(s), 9.80(s); infrared (ν_{Co-Cl}): 330 cm^{-1}; UV-visible (CH_2Cl_2, λ_{max} (nm); ε, M^{-1} cm^{-1}): 654(750), 630(sh), 570(590), 458(495), 380(sh); electrochemistry: $(E_{p,a})_1$ = + 0.50 V, $(E_{p,a})_2$ = + 1.09 V; FAB-mass spectrum: m/z = 1093.

(6) Reaction of $[Co(NCCD_3)_6][BF_4]_2$ with 4 TMPP

The deuterated starting material $[Co(NCCD_3)_6][BF_4]_2$ was prepared by the action of $NOBF_4$ on cobalt pellets in CD_3CN. A quantity of the compound was dissolved (0.168 g, 0.339 mmol) in a 10 mL THF solution containing 4 equivalents of TMPP (0.722 g, 1.356 mmol), resulting in an instantaneous dark red-brown color. The reaction was stirred at room temperature for *ca.* 30 minutes after which time it was filtered through a fritted funnel to yield a white by-product and a dark brown solution. The white solid was characterized as [H-TMPP][BF_4]; yield: 0.377 g (45% relative to TMPP); ^1H NMR (CD_3CN, δppm): 3.67(s, 18 H), 3.86(s, 9 H), 6.25(d, 6 H) and 8.38 (d, 1 H). The brown solution was layered with 10 mL of hexanes, which resulted in the precipitation of a red-brown microcrystalline product. ^1H NMR (CD_3CN, δppm): 2.46(d), 3.54(s), 3.84(s), 6.22(d) ([CH_3-TMPP]$^+$); infrared (CsI, nujol): traces of $[BF_4]^-$.

(7) Conversion of $[Co(TMPP)_2][BF_4]_2$ (13) into Co(TMPP-*O*)$_2$ (12)

A sample of **13** was dissolved in 5 mL of acetone, and an equal volume of hexanes was layered on top of this solution. Within a few days, a crop of dark green crystals of Co(TMPP-*O*)$_2$, **12**, grew from this solvent combination. The transformation from $[Co(TMPP)_2]^{2+}$ to Co(TMPP-*O*)$_2$ can also occur in the solid state over a period of several days.

(8) Oxidation of Co(TMPP-*O*)$_2$ (12) with $[Cp_2Fe][BF_4]$

A sample of **12** (0.044 g, 0.040 mmol) was reacted with one equivalent of $[Cp_2Fe][BF_4]$ (0.011 g, 0.040 mmol) in 10 mL of acetone. An immediate color change from dark green to olive green ensued. The resulting solution was stirred at room temperature for 0.5 h, evaporated to a residue, washed with copious amounts of diethyl ether (3 x 10 mL) and dried *in vacuo*; yield. 0.015 g (32% relative to **12**, based on a [Co(TMPP-*O*)$_2$][BF_4] formulation). ^{1}H NMR ($CDCl_3$): very broad; UV-visible (acetone, λ_{max}): 605 nm.

(9) Reaction of Co(TMPP-*O*)$_2$ with O_2

A solution of Co(TMPP-*O*)$_2$ in CH_2Cl_2 was bubbled with oxygen gas for *ca.* 24 hours. The solvent was replenished regularly, to avoid evaporation. There were no spectroscopic changes to indicate that a reaction had taken place.

(10) Reactions of Co(TMPP-*O*)$_2$ with π-acceptor ligands

(i) with CO

A solution of Co(TMPP-*O*)$_2$ in THF or CH_2Cl_2 was bubbled with carbon monoxide for about 2 hours. Infrared and UV-visible studies of the resulting solution showed that no reaction had occurred.

(ii) with CNPr^i

A quantity of Co(TMPP-*O*)$_2$ (0.024 g, 0.022 mmol) was dissolved in 10 mL of acetone, and 2 equivalents of CNPr^i (4.16 μL, 0.044 mmol) were added with a microsyringe. This resulted in a color change from dark blue-green to olive-green. An infrared spectrum of this solution after 5 minutes exhibited three ν(C≡N) bands at 2162, 2145 (free CNPr^i) and 2120 cm^{-1}. The reaction was stirred at room temperature for one hour until it had turned brown-green. After removal of the solvent under reduced pressure the residue was redissolved in acetone, and the solution was layered with hexanes. Unfortunately, we were unsuccessful at isolating a tractable product from this experiment.

(11) Reactions of Co(TMPP-*O*)$_2$ with metal di-halides: Synthesis of homo- and heterobimetallic compounds

(ii) with $CoCl_2$

A quantity of **12** (0.100 g, 0.091 mmol) was added to 1 equivalent of $CoCl_2$ (0.011 g, 0.091 mmol) in 10 mL of acetone. The solution was heated for 0.5 h to hasten the dissolution of $CoCl_2$, after which time it was stirred at room temperature for 24 hours. The resulting intensely colored blue-green solution was pumped to a residue, washed with diethyl ether (2 x 5 mL) and dried; yield, 0.082 g (74% relative to **12**). Recrystallization from acetone/hexanes (v/v 1:1) produced dark needles of $Cl_2Co_2\{\mu$-η^2-(TMPP-*O*)$_2\}$, **14**.

(iii) with $MnCl_2$

A sample of **12** (0.021 g, 0.020 mmol) was reacted with one equivalent of $MnCl_2$ (0.0024 g, 0.020 mmol) in 10 mL of acetone. The solution was heated under reduced pressure for 24 hours, after which time the resulting bright green solution was layered with hexanes. A crop of green X-ray quality crystals formed within 48 hours; yield of $Cl_2MnCo\{\mu$-

η^2-(TMPP-*O*)$_2$}, **15**: 0.008 g (40% relative to **12**). Anal. Calc'd for $CoMnCl_2P_2C_{58}O_{20}H_{72}$: C: 50.82; H: 4.88; Found: C: 50.50; H: 4.94. IR(ν_{Mn-Cl}): 325 cm^{-1}; UV-visible (acetone, λ_{max} (nm)): 660(sh), 631, 597.

(12) Reactions of Co(TMPP-*O*)$_2$ with metallocene and diene complexes: Attempts to synthesize early-late and late-late heterobimetallic compounds

(i) with Cp_2TiCl_2

Co(TMPP-*O*)$_2$ (0.151 g, 0.138 mmol) and Cp_2TiCl_2 (0.034 g, 0.138 mmol) were dissolved in 10 mL of acetone and the resulting dark red-brown solution was stirred at room temperature for 24 hours, after which time a bright green solid had deposited on the sides of the flask. The solvent was removed under dynamic vacuum to produce a mixture of green and brown residues. Redissolution in 10 mL of acetone followed by slow addition of of diethyl ether caused the precipitation of a bright green solid. A brown filtrate was decanted from the solid, which was dried *in vacuo*; yield: 0.057 g (56% relative to Co^{2+}, based on a [Cp_2TiCo\{μ-η^2-(TMPP-*O*)$_2$][$CoCl_4$] (**16**) formulation). Anal Calc'd for $TiCo_2Cl_4P_2C_{62}O_{18}H_{70}$: C: 50.57; H: 4.79; Found: C: 49.90; H: 5.25. Infrared (CsI, Nujol): ν(Co-Cl) = 295 cm^{-1} ; UV-visible (acetone, λ_{max} (nm)): 692, 667(sh), 635, 592; ^1H NMR: spread out from 1 to 10 ppm, and δ = 6.50 ppm (Cp_2Ti^{2+}).

(ii) with [Rh(COD)Cl]$_2$: Preparation of [(COD)Rh-Co(TMPP-*O*)$_2$]$^{2+}$ (17)

The Rh(I) dinuclear species [Rh(COD)Cl]$_2$ (0.017 g, 0.038 mmol) was reacted with 2 equivalents of $AgBF_4$ (0.013 g, 0.076 mmol) in 8 mL of THF, and stirred at room temperature for 15 minutes. After this time, the yellow solution was filtered into an 8 mL solution of Co(TMPP-*O*)$_2$ (0.037 g, 0.038 mmol) in THF, followed by stirring at room temperature

for 10 minutes and finally removal of the solvent under reduced pressure. The dark brown residue was washed with diethyl ether, redissolved in acetone, and layered with hexanes. This treatment produced dark brown X-ray quality needles within one week; yield: 0.040 g (73% relative to **12**). Anal. Calc'd for $RhCoP_2C_{60}O_{18}H_{72}B_2F_8$: C: 48.71; H: 4.87; Found: C: 48.81; H: 5.24. ^1H NMR (d_6-acetone, δppm): 3.01(s), 3.31(s), 3.49(s), 3.58(s), 3.61(s), 3.84(s), 3.90(s), 4.17(s), 5.43(s), 5.67(s), 5.78(s), 5.94(s), 6.30(s), 6.89(s); ^{31}P NMR (CD_3CN): δ = + 5.6 ppm; UV-visible (λ (nm), acetone): 621(sh), 370.

(13) Reactions of Co(TMPP-*O*)$_2$ with solvated cations: Attempts to synthesize homo- and heterotrimetallic compounds

(i) with $[Co(NCCH_3)_6][BF_4]_2$

The solvated Co(II) salt $[Co(NCCH_3)_6][BF_4]_2$ (0.022 g, 0.046 mmol) was added to a flask containing 2 equivalents of **12** (0.100 g, 0.091 mmol) in 10 mL of acetone. The resulting blue-green solution was stirred at room temperature for 24 hours, after which time the volume was concentrated to *ca.* 5 mL and layered with 5 mL of hexanes. Dark green crystals grew from this solvent mixture within 48 hours; these exhibited the same unit cell as that of **12**. All other spectroscopic data were also in agreement with those of an authentic sample of Co(TMPP-*O*)$_2$.

(ii) with $[Ni(NCCH_3)_6][BF_4]_2$

Co(TMPP-*O*)$_2$ (0.100 g, 0.091 mmol) and $[Ni(NCCH_3)_6][BF_4]_2$ (0.022 g, 0.046 mmol) were charged in a flask, and 10 mL of acetone were added. Upon complete dissolution of the starting materials, a bright green color was observed. A work-up similar to that described in (13)(i) above was employed; yield: 0.020 g. The product exhibited the same spectral characteristics as an authentic sample of Co(TMPP-*O*)$_2$.

B. X-ray Crystal Structures

The structures of complexes **8-12** and **14-17** were determined by applications of general procedures described elsewhere. Geometric and intensity data were collected on a Rigaku AFC6S diffractometer for compounds **9, 12, 14, 15** and on a Nicolet P3/F upgraded to a Siemens P3/V instrument for compounds **8** and **11** and **17**; both are equipped with graphite monochromated MoK_α(λ_α = 0.71069 Å and 0.71071 Å, respectively) radiation. The data were corrected for Lorentz and polarization effects. Calculations were performed on a VAXSTATION 2000 computer using programs from the TEXSAN Crystallographic Package of the Molecular Structure Corporation (**9-17**) and from the Structure Determination Package (SDP) of Enraf-Nonius (**8**).

(1) $[CH_3\text{-}TMPP]_2[Co_2Cl_6]\cdot 2\ CH_2Cl_2$ (8)

A blue crystal of approximate dimensions 0.60 x 0.35 x 0.20 mm^3 was selected and mounted in a glass capillary which was then sealed with epoxy cement. Cell parameters were refined from a least-squares fit of 19 reflections in the range $20 \leq 2\theta \leq 25°$. Intensity data were collected at room temperature by using a θ - 2θ scan mode from 4 - 40° in 2θ. Three intensity standards were monitored at regular intervals and showed no significant decay. An absorption correction was applied by using the program DIFABS. The position of the Co atom was found by the direct methods program in SHELXS-86. The remaining non-hydrogen atoms were located through successive difference Fourier maps and least-squares cycles. All atoms were refined with anisotropic thermal factors with the exception of a C and a Cl atoms of a lattice methylene chloride solvent molecule. The positions of the hydrogen atoms were calculated and then refined using 3204 unique reflections with $F_o^2 \geq 3\sigma(F_o)^2$. The structure

Table 9. Crystallographic data for $[CH_3\text{-}TMPP]_2[Co_2Cl_6]$ (8)

Formula	$Co_2Cl_{10}P_2C_{58}O_{18}H_{76}$
Formula weight	1595.6
Space group	P-1
a, Å	10.889(5)
b, Å	13.54(6)
c, Å	14.005(5)
α, deg	63.45(3)
β, deg	83.87(3)
γ, deg	78.18(4)
V, $Å^3$	1808(2)
Z	1
d_{calc}, g/cm^3	1.465
μ (MoK_α), cm^{-1}	9.35
Data collection range, 2θ, deg	4 - 40
No. unique data	4756
total with $F_o^2 \geq 3\sigma(F_o)^2$	3204
Number of parameters refined	396
R[a]	0.069
R_w[b]	0.090
Quality-of-fit[c]	2.538
Largest shift/esd, final cycle	0.02
Largest peak, $e^-/Å^3$	1.73

[a] $R = \Sigma||F_o|-|F_c||/\Sigma|F_o|$; [b] $R = |\Sigma(w|F_o|-|F_c|)^2/\Sigma w|F_o|^2]^{1/2}$; $w = 1/\sigma^2(|F_o|)$

[c] Quality-of-fit = $[\Sigma(w|F_o|-|F_c|)^2/(N_{obs}-N_{parameters})]^{1/2}$

refinement converged with R = 0.069 and R_w = 0.090 and a goodness-of-fit of 2.538. The ratio of maximum shift to e.s.d. was 0.02. The highest peak from the final difference map was 1.73 $e^-/Å^3$ and was associated with the methylene chloride. The methylene chloride molecule is disordered but attempts to model the disorder in a chemically sensible manner proved unsatisfactory. A summary of crystallographic data is presented in Table 9.

(2) [H-TMPP]$_2$[CoCl$_4$]•MeOH (9)

A blue-green block-shaped crystal of approximate dimensions 0.25 x 0.30 x 0.50 mm^3 was sealed inside a glass capillary. A preliminary monoclinic unit cell was determined by indexing on 20 well-centered reflections. The cell was further refined by least-squares refinement of 24 reflections in the range $20 \leq 2\theta \leq 30°$. Intensity data were collected at room temperature over the range 4 - 50° in 2θ, using the θ - 2θ scan mode. Measurement of three standard reflections at regular intervals during data collection showed no decay in crystal quality. After averaging equivalent reflections, 5740 unique data remained of which 2581 were considered to be observed, *i.e.*, with $F_o^2 \geq 3\sigma(F_o)^2$. The position of the metal atom was obtained from a solution provided by the direct methods program MITHRIL. The positions of the remaining non-hydrogen atoms were located by using the program DIRDIF and were refined anisotropically. The position of the hydrogen atom H(1) bonded to the phosphorus atom, was located from a difference Fourier map, whereas all other hydrogen atom positions were generated by the programs within the TEXSAN package. These were included in the structure factor calculations but not refined. The carbon atom of the interstitial methanol molecule, C(28), was found to be disordered over two sites. After attempts to fix the atom on

the same special position as the oxygen atom O(10), *viz.*, (1/2, y, 3/4), failed, the multiplicity was assigned as 0.5 in each site. An empirical absorption correction was applied using programs in the solution package. The final full-matrix refinement involved 2581 data and 369 parameters. The refinement converged with residuals of R = 0.048 and R_w = 0.049 and a quality-of-fit of 1.93. The final difference Fourier map showed a highest peak of 0.39 $e^-/Å^3$. Table 10 summarizes important crystallographic data.

(3) Co(TMPP-*O*)$_2$ (12)

A dark green triangular platelet of approximate dimensions 0.39 x 0.54 x 0.73 mm^3 was mounted at the end of a fiber with epoxy cement and placed in a N_2 cold stream at - 100° C. A preliminary hexagonal unit cell was determined by centering and indexing 20 reflections. The cell was then refined by least-squares determination of 25 reflections with $20 \leq 2\theta \leq 30$. Intensity data were collected in the 4 - 47° range in 2θ by the ω scan mode. During data collection, three check reflections were collected at regular intervals and showed no decrease in intensity. After averaging equivalent reflections 7607 remained of which 6942 were observed with $F_o^2 \geq 3\sigma(F_o)^2$. Due to the large volume of the unit cell, it was difficult to run any of the programs in the TEXSAN solution package, and no chemically sensible solution was obtained. The extremely high symmetry of this crystal system, combined with such a large volume points to an intimate twinning phenomenon, which could not be detected before data collection. However, the acetone/hexanes mixture from which the crystals were grown is the only solvent combination that has allowed for the growth of large crystals of complex **12**.

(4) [ClCH$_2$-TMPP]$_2$[CoCl$_4$]•3CH$_2$Cl$_2$ (11)

A blue crystal of approximate dimensions 0.35 x 0.20 x 0.83 mm^3 was mounted with epoxy cement on the tip of a glass fiber and placed in a N_2 cold stream at - 120 °C. A preliminary monoclinic unit cell was determined by centering and indexing 20 reflections chosen from a 10 minute rotational photograph. The cell was then refined by least-squares refinement of 25 reflections in the range $20 \leq 2\theta \leq 30°$. Intensity data were collected at room temperature over the range 4 - 47° in 2θ, using the ω-scan mode. Measurement of three standard reflections at regular intervals during data collection showed no decay in crystal quality. After averaging equivalent reflections, 5887 unique data remained of which 2727 were observed with $F_o^2 \geq 3\sigma(F_o)^2$. The position of the metal atom was obtained from a solution provided by the direct methods program MITHRIL. The positions of the remaining non-hydrogen atoms were located by using DIRDIF. An empirical absorption correction was applied with the use of the program DIFABS. All non-hydrogen atoms were refined anisotropically. Hydrogen atoms were generated by the programs within the TEXSAN package; these were included in the structure factor calculations but not refined. The final full-matrix refinement involved 2727 data and 416 parameters. The refinement converged with residuals of R = 0.068 and R_w = 0.074 and a quality-of-fit of 1.68. The final difference Fourier map showed a highest peak of 1.24 $e^-/Å^3$, which is a ghost atom associated with the Cl(5) atom in one of the interstitial CH_2Cl_2 solvent molecules. Table 10 lists important crystallographic data.

(5) $Cl_2Co_2\{\mu\text{-}\eta^2\text{-}(TMPP\text{-}O)_2\}\cdot 2CH_2Cl_2$ (14)

A blue-green crystal of approximate dimensions 0.32 x 0.41 x 0.22 mm^3 was sealed inside a glass capillary. A preliminary monoclinic unit cell was determined by centering and indexing on 20 low-angle reflections.

Table 10. Crystallographic data for [H-TMPP]$_2$[CoCl$_4$] (9) and [ClCH$_2$-TMPP]$_2$[CoCl$_4$] (11).

Formula	$CoCl_4P_2C_{55}O_{19}H_{68}$	$CoCl_{12}P_2C_{59}O_{18}H_{76}$
Formula weight	1295.82	1618.07
Space group	C2/c	C2/c
a, Å	30.011(4)	27.061(6)
b, Å	10.135(3)	12.471(5)
c, Å	23.047(3)	24.201(5)
α, deg	90.00	90.00
β, deg	118.183(7)	116.05(2)
γ, deg	90.00	90.00
V, Å^3	6179(4)	7338(4)
Z	4	4
d_{calc}, g/cm^3	1.393	1.466
μ (MoKα), cm^{-1}	5.679	7.780
Data collection range, 2θ, deg	4 - 50	4 - 47
No. unique data	5740	5887
total with $F_o^2 \geq 3\sigma(F_o)^2$	2581	2727
Number of parameters refined	369	416
R	0.048	0.068
R_w	0.049	0.074
Quality-of-fit	1.93	1.78
Largest shift/esd, final cycle	0.01	0.12
Largest peak, e$^-$/Å^3	0.39	1.24

The cell was further refined by a least-squares fitting of 22 reflections in the range $25 \leq 2\theta \leq 30$ °. Intensity data were collected at room temperature over the range 4 - 47° in 2θ, using the θ - 2θ scan mode. Measurement of three standard reflections at regular intervals during data collection showed a decay in crystal quality of 6% which was corrected for. After averaging equivalent reflections, 4872 unique data remained of which 2946 were observed with $F_o^2 \geq 3\sigma(F_o)^2$. The positions of the two unique cobalt atoms were obtained from a solution provided by the direct methods program in the SHELXS-86 software package. The positions of the remaining non-hydrogen atoms were located using cycles of DIRDIF. After isotropic convergence, an empirical absorption correction was applied using the program DIFABS. All non-hydrogen atoms were subsequently refined anisotropically to convergence. Hydrogen atoms were generated by the program HYDRO within the TEXSAN package and were included in the structure factor calculations but not refined. The final full-matrix refinement involved 2946 data and 371 parameters which led to residuals of R = 0.050 and R_W = 0.058 and a quality-of-fit of 1.94. The final difference Fourier map showed the highest peak to be 0.58 $e^-/Å^3$. A list of crystallographic data can be found in Table 11.

(6) $Cl_2MnCo\{\mu\text{-}\eta^2\text{-}(TMPP\text{-}O)_2\}\cdot 2CH_3COCH_3$ (15)

A green platelet of dimensions 0.36 x 0.18 x 0.08 mm^3 was selected and mounted at the end of a glass fiber with Dow Corning grease and placed in a N_2 cold stream at -90°C. A preliminary monoclinic cell was determined by centering and indexing 20 reflections. The cell was refined by a least-squares fit of 13 reflections with $13 \leq 2\theta \leq 25$ °. Intensity data were collected in the 4 - 47 ° range in 2θ, using the θ - 2θ scan mode. Measurement of three standard reflections at regular intervals during data

Table 11. Crystallographic data for $Cl_2Co_2\{\mu\text{-}\eta^2\text{-}(TMPP\text{-}O)_2\}$ (14) and $Cl_2MnCo\{\mu\text{-}\eta^2\text{-}(TMPP\text{-}O)_2\}$ (15)

Formula	$Co_2Cl_6P_2C_{54}O_{18}H_{60}$	$CoMnCl_2P_2C_{58}O_{19}H_{72}$
Formula weight	1389.59	1335.92
Space group	C2/c	C2/c
a, Å	15.577(5)	15.255(5)
b, Å	21.193(3)	21.322(9)
c, Å	19.544(4)	19.576(6)
α, deg	90.00	90.00
β, deg	118.183(7)	116.05(2)
γ, deg	98.78(2)	99.74(3)
V, $Å^3$	6376(4)	6276(7)
Z	4	4
d_{calc}, g/cm^3	1.447	1.414
μ (MoK_α), cm^{-1}	8.85	6.61
Data collection range, 2θ, deg	4 - 47	4 - 47
No. unique data	4872	4796
total with $F_o^2 \geq 3\sigma(F_o)^2$	2946	1830
Number of parameters refined	371	375
R	0.050	0.078
R_w	0.058	0.096
Quality-of-fit	1.94	2.47
Largest shift/esd, final cycle	0.01	1.45
Largest peak, $e^-/Å^3$	0.58	0.58

collection showed no decay in intensity. After averaging equivalent reflections, 4796 data remained, of which 1935 were observed with $F_o^2 \geq 3\sigma(F_o)^2$. The two metal atoms Co(1) and Mn(1) were located by the direct methods program MITHRIL in the TEXSAN software package. All other non-hydrogen atoms were located by the use of the program DIRDIF and were refined anisotropically with the exception of the oxygen atom of the interstitial acetone molecule O(10). The hydrogen atoms were placed in calculated positions and were included in the structure factor calculation but not refined. The final full-matrix refinement involved 1830 data and 375 parameters and converged with residuals of R = 0.078 and R_w = 0.096 and a quality-of-fit of 2.47. The highest peak in the final difference Fourier map was 0.58 $e^-/Å^3$. Table 11 summarizes crystallographic data for compound **15**.

(7) [(COD)Rh-Co(TMPP-*O*)$_2$][BF_4]$_2$•2CH_3COCH_3 (17)

A red-brown needle of approximate dimensions 0.13 x 0.52 x 0.98 mm^3 was selected and mounted at the end of a glass fiber with Dow Corning silicone grease, and placed in a N_2 cold stream at - 90 ± 2° C. A preliminary monoclinic cell was determined by centering on 20 reflections chosen from a 20 minute rotational photograph. Axial photographs confirmed the choice of a monoclinic cell. The cell was further refined by a least-squares fit of 25 reflections in the range $10 \leq 2\theta \leq 25°$. Intensity data were collected in the 5 - 47° range in 2θ using the ω-scan mode. Three standard reflections were collected at regular intervals during data collection and showed no decay in intensity. After averaging equivalent reflections, 11731 unique data remained of which 5798 were observed with $F_o^2 \geq 3\sigma(F_o)^2$. The two metal atoms Rh(1) and Co(1) were located by the direct methods program SHELXS-86. The position of all other non-

Table 12. Crystal data for [(COD)Rh-Co(TMPP-*O*)$_2$][BF_4]$_2$ (17)

Formula	$RhCoP_2C_{66}O_{20}H_{84}B_2F_8$
Formula weight	1594.82
Space group	$P2_1/n$
a, Å	15.890(4)
b, Å	17.209(5)
c, Å	27.705(9)
α, deg	90.00
β, deg	74.57(2)
γ, deg	90.00
V, Å^3	7303(4)
Z	4
d_{calc}, g/cm^3	1.450
μ (Mo Kα), cm^{-1}	7.976
Data collection range, 2θ, deg	5 - 47
Number of unique data	11731
Total with $F_o^2 \geq 2.2\sigma(F_o)^2$	5798
Number of parameters refined	815
R	0.088
R_w	0.090
Quality-of-fit	1.97
Largest shift/esd, final cycle	1.7
Largest peak, e$^-$/Å^3	1.34

[a] $R = \Sigma||F_o|-|F_c||/\Sigma|F_o|$; [b] $R = |\Sigma(w|F_o|-|F_c|)^2/\Sigma w|F_o|^2]^{1/2}$; $w = 1/\sigma^2(|F_o|)$

[c] Quality-of-fit = $[\Sigma(w|F_o|-|F_c|)^2/(N_{obs}-N_{parameters})]^{1/2}$

hydrogen atoms were found by using the program DIRDIF, and were refined anisotropically. Hydrogen atoms were generated by the program HYDRO in the TEXSAN package and placed in calculated positions. They were included in the structure factor calculation but not refined. An empirical absorption correction was applied using the PSI-Scan program. the final full-matrix refinement involved 5798 data and 815 parameters and converged with residuals of R = 0.088 and R_w = 0.090. The final difference Fourier map showed the highest peak to be 1.34 $e^-/Å^3$ and the final shift/esd was 1.7. A summary of important crystallographic data can be found in Table 12.

3. Results and Discussion

A. Synthetic approaches

The 1:1 reaction of $CoCl_2$ with TMPP in $CHCl_3$ produces salts of the type [R-TMPP]$_2$[$CoCl_4$] (R = H, CH_3), whereas the benzene reaction yields [CH_3-TMPP]$_2$[Co_2Cl_6] (**8**). When the solvated acetonitrile Co(II) cations are used as starting materials in the presence of a chloride source and in protic solvents, the anion $[CoCl_4]^{2-}$ is isolated. While the tetrachlorocobaltate anion is ubiquitous in Co(II) chemistry, there are very few instances of the dinuclear $[Co_2Cl_6]^{2-}$ unit. Its existence has been documented in the decomposition reactions of $CoCl_2$ adducts and in the chemistry of the mononuclear ion $[CoCl_4]^{2-}$ with the chloride salts Et_4NCl, NH_4Cl or MCl (M = Li, K) [6]. The analogous di-ferrous species, $[Fe_2Cl_6]^{2-}$ was also isolated from the 1:1 reaction of $FeCl_3$ with TMPP, as described in Chapter II. If the chemistry of $[Co(NCCH_3)_6]^{2+}$ with TMPP is performed with the $[BF_4]^-$ salt in the presence of an excess of the ligand, one obtains the neutral species Co(TMPP-*O*)$_2$, **12**. Surprisingly, compound **12** is one of the few simple bis(ether-phosphine) complex of

Co(II) to be reported, in spite of the extensive chemistry of such ligands with cobalt [7]. The reactions of $[Co(NCCH_3)_6][X]_2$ ($X = AlCl_4^-$, $SbCl_6^-$) with 2 equivalents of TMPP in methanol yield tetrachlorocobaltate salts of the type $[R\text{-}TMPP]_2[CoCl_4]$ where R is either H or $ClCH_2$. Both $[H\text{-}TMPP]_2[CoCl_4]$, **9**, and $[ClCH_2\text{-}TMPP]_2[CoCl_4]$, **11**, were structurally characterized, the latter also being obtained in a reaction described later in this chapter. Spectroscopic data for compound **9** and **11** are in excellent agreement with the reported literature on various salts of $[CoCl_4]^{2-}$ [8].

The results obtained for $CoCl_2$ reactions with TMPP are in agreement with the general lack of compatibility between first-row transition metals and the soft TMPP ligand that had previously been established in the analogous iron chemistry for which the complexes $[H\text{-}TMPP]_n[FeCl_4]$ ($n = 1, 2$) were isolated. It is apparent that whenever there is a competition between Cl^- anions and the phosphine, the formation of $[CoCl_4]^{2-}$ is favored; furthermore quaternarization of the phosphine is easily effected in a solvent that provides H^+, $ClCH_2^+$ or CH_3^+ groups. Realizing this, we set out to modify the reaction parameters and find the optimal conditions for Co(II)-phosphine binding.

The use of an aprotic, non-chlorinated solvent such as acetone and a chloride-free Co(II) starting material, combined with the use of a two-fold excess of TMPP, constitute the most favorable conditions for this chemistry. The rationale behind this approach is that the presence of a free nucleophile, such as TMPP, promotes demethylation of one of the ortho methoxy groups on the phenyl ring of the ligand, thereby forming a phenoxide moiety. Demethylation or deprotonation of an OR group ($R = CH_3$, H) in the ortho position of a phenyl ring of a phosphine ligand was used by Rauchfuss [9] and also by Shaw [10] to form chelating phosphino-

phenoxide ligands and our group has made use of this synthetic strategy in our work with rhodium [11]. The ligand itself has proven to be the most "innocent" demethylating agent as opposed to CH_3I or KCl that can also act as an oxidizing agent or as a Cl^- source.

B. Characterization

The reaction of $[Co(NCCH_3)_6][BF_4]_2$ with four equivalents of TMPP in acetone formed the neutral complex Co(TMPP-*O*)$_2$, **12**, which was not structurally characterized, the most important feature of this compound being the *cis* configuration of the phosphine ligands, proposed on the basis of its derivative chemistry. The FAB-mass spectrum of **12** exhibits its highest peak at m/z = 1093 which corresponds to the molecular ion $[Co(TMMP\text{-}O)_2]^+$ (Figure 22). The ^1H NMR spectrum was sharp and contact-shifted as expected for a paramagnetic species.

It was discovered quite by accident, that if Co(TMPP-*O*)$_2$ was recrystallized from a mixture of CH_2Cl_2 and diethyl ether, the dinuclear complex $Cl_2Co_2\{\mu\text{–}\eta^2\text{-}(TMPP\text{-}O)_2\}$ (**14**) was obtained in low yield. This transformation was monitored by UV-visible or ^1H NMR spectroscopy. A time-dependent UV-visible study of the conversion of **12** into **14** in CH_2Cl_2 is shown in Figure 23. Complex **12** exhibits a transition at 595 nm and a shoulder at 490 nm while compound **14** exhibits two bands at 654 (shoulder at 630) and 570 nm, corresponding to the tetrahedral and octahedral Co(II) centers, respectively [8]. In order to obtain $Cl_2Co_2\{\mu\text{–}\eta^2\text{-}(TMPP\text{-}O)_2\}$, **14**, in a higher yield, Co(TMPP-*O*)$_2$ was reacted with one equivalent of anhydrous $CoCl_2$ in acetone to give **14** in quantitative yield. In an attempt to generalize the approach, reactions of Co(TMPP-*O*)$_2$ with other metal dihalides were investigated. For example, the equimolar reaction between Co(TMPP-*O*)$_2$ and $MnCl_2$ produces $Cl_2MnCo\{\mu\text{–}\eta^2\text{-}$

Figure 22. Positive ion FAB-Mass spectrum of Co(TMPP-*O*)$_2$.

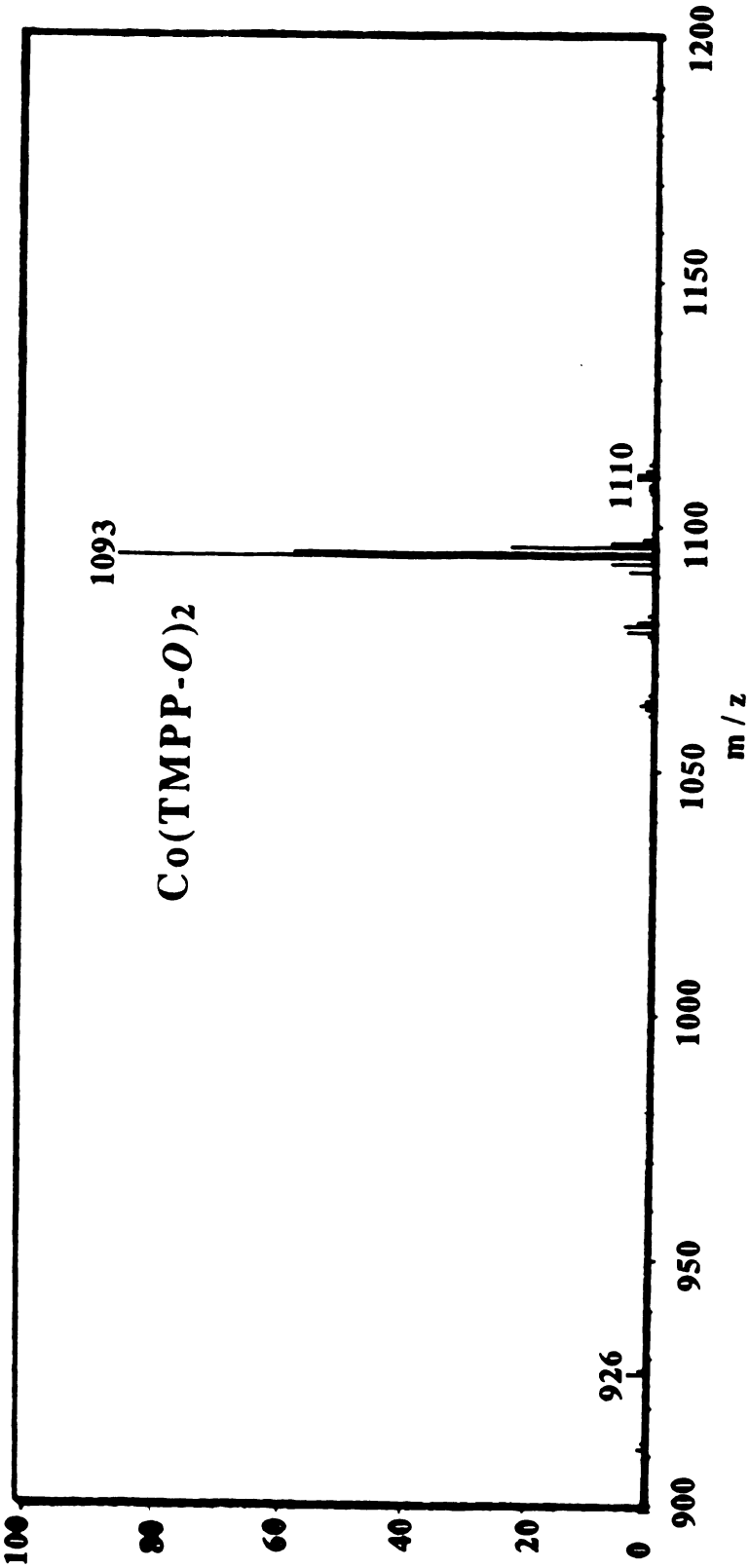
Co(TMPP-O)2
1093
1110
926
100
80
60
40
20
0
900
950
1000
1050
1100
1150
1200
m/z

Figure 22.

Figure 23. Time-dependent UV-visible study of the transformation of Co(TMPP-*O*)$_2$ into $Cl_2Co_2\{\mu\text{-}\eta^2\text{-}(TMPP\text{-}O)_2\}$ in CH_2Cl_2.

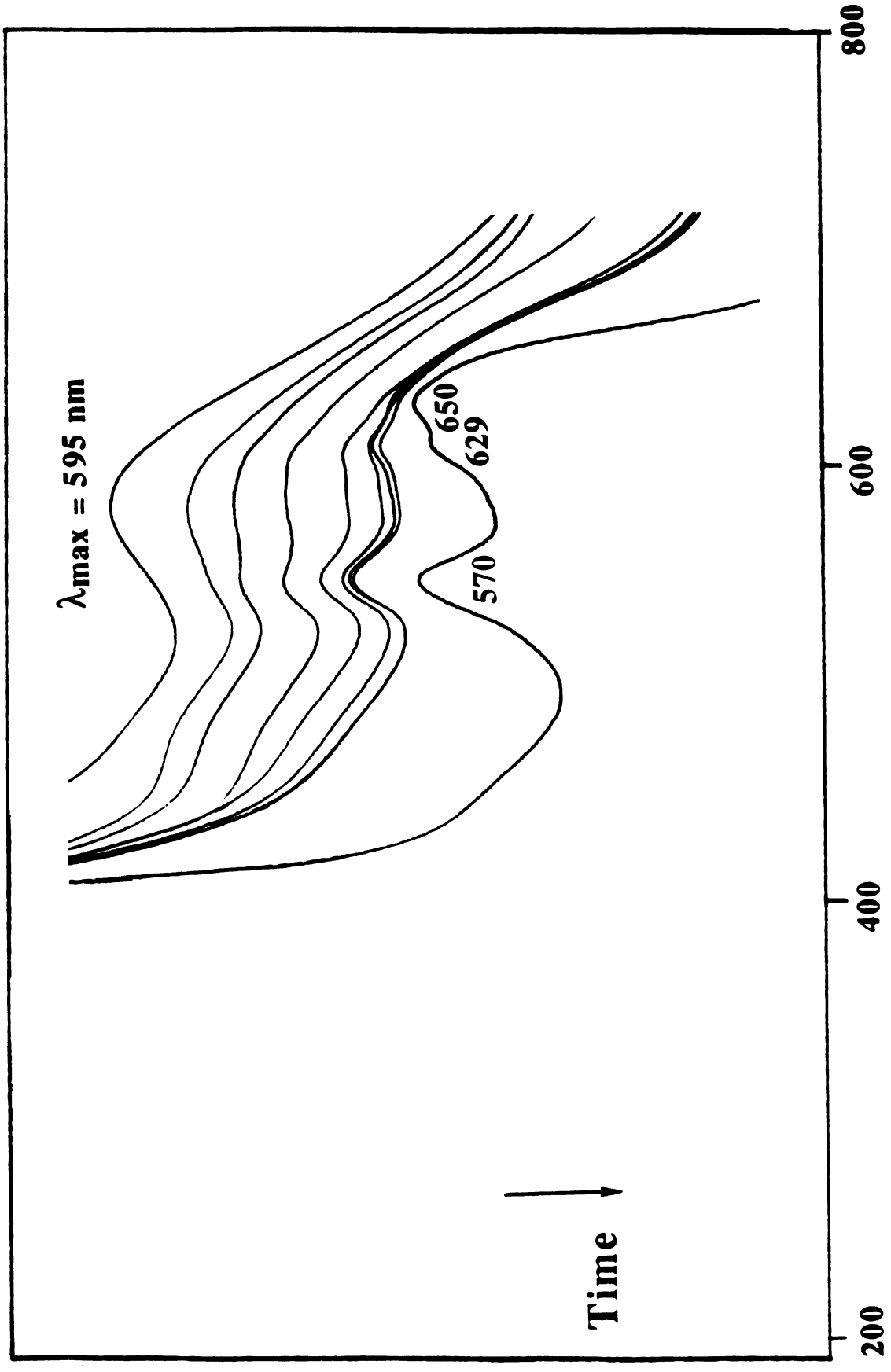

Figure 23.

(TMPP-*O*)$_2$}, **15**, which presents the same general features as complex **14**.

It is worth mentioning at this point that the reaction to give Co(TMPP-*O*)$_2$ is extremely moisture-sensitive. In situations where the acetone solvent is not carefully dried and distilled prior to use, or if the atmosphere of the laboratory is very humid, the reaction solution turns dark purple instantaneously. Subsequent work-up leads to a purple solid and a by-product identified as [H-TMPP][BF_4]. Recrystallization of the purple product from CH_2Cl_2/diethyl ether gives [$ClCH_2$-TMPP]$_2$[$CoCl_4$]. Mild heating of the reaction and longer reaction times promotes a transformation from purple to blue and finally to green. Work-up of the reaction at the green stage revealed that [H-TMPP][BF_4] was only present in small quantities contaminating large quantities of [CH_3-TMPP][BF_4], and that Co(TMPP-*O*)$_2$ was the metal-containing product. In order to ascertain what conditions promote phosphine protonation, we carried out the reaction using the deuterated starting material [Co($NCCD_3$)$_6$][BF_4]$_2$. As before, the by-product of the reaction was [H-TMPP][BF_4], and no trace of [D-TMPP][BF_4] could be detected, by ^{1}H NMR spectroscopy. The identical reaction was performed in acetone that had been treated with NaI and distilled prior to use to rigorously remove any H_2O, with similar results. From these observations we conclude that the nitrile is not responsible for the protonation of the phosphine but that even under extremely careful moisture-free conditions protonation can not be avoided.

We were curious to see if we could isolate a non-demethylated bis-TMPP-Co(II) complex from the purple solid. To this end, the 1:4 reaction between [Co($NCCH_3$)$_6$]$^{2+}$ and TMPP was carried out in THF since [H-

Figure 24. Proposed structure for Co(TMPP-*O*)$_2$.

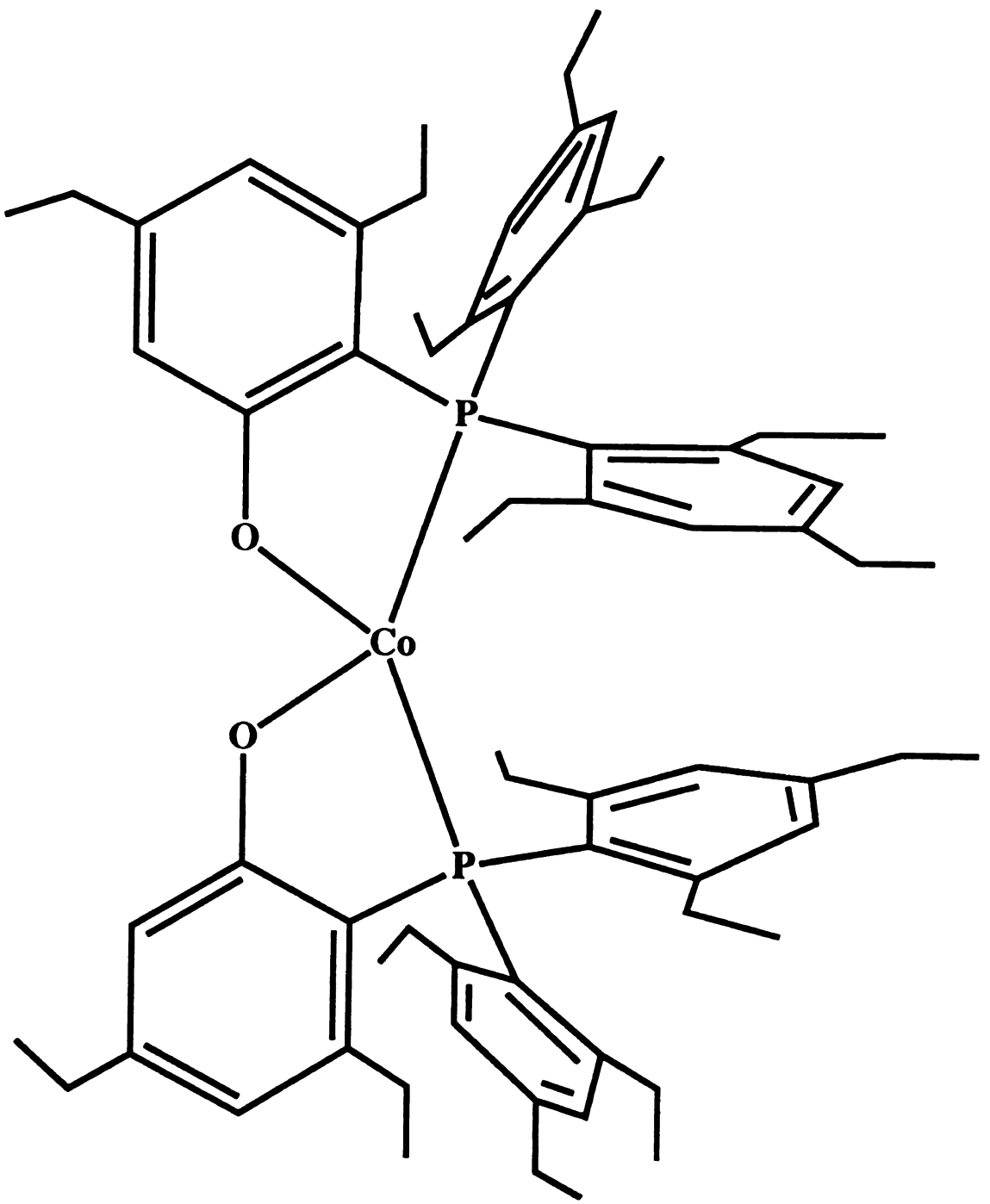

Figure 24.

TMPP]$^+$ and [CH_3-TMPP]$^+$ are only slightly soluble in this solvent. In fact, the interaction of the solvated Co(II) salt with 4 equivalents of TMPP, resulted in the formation of a dark purple solution and a white precipitate. This by-product, confirmed to be [H-TMPP][BF_4], accounted for about a third of the TMPP ligand. The purple solution was layered with hexanes to produce a mixture of white and purple microcrystals. Surprisingly, the white product was identified as free TMPP and calculations revealed that approximately 50% of the ligand had been used to form both [H-TMPP][BF_4] and free TMPP. The purple solid was characterized as [Co(TMPP)$_2$][BF_4]$_2$ (**13**), but could not be structurally characterized since it converts into Co(TMPP-*O*)$_2$ (**12**) very readily, in solution or in the solid state. Similar "spontaneous" demethylation was previously been observed in Rh(III)/TMPP chemistry [11].

Unfortunately, we were not able to structurally characterize compound **12**, as it persistently crystallizes in a hexagonal space group with one very long axis which most likely is due to an intimate twinning problem. On the basis of the successful structural determination of two derivatives of Co(TMPP-*O*)$_2$, complexes **14** and **15**, we propose the structure depicted in Figure 24 for this compound, in which the cobalt center is coordinated to mutually*cis* phosphino-phenoxide ligands.

B. Molecular Structures

(1) [CH_3-TMPP]$_2$[Co_2Cl_6] (8)

Selected bond distances and angles are listed in Table 13 and Figure 25 depicts the molecular structures of the two ions present in **8**. As Figure 25 clearly shows, the dicobalt anion consists of two edge-sharing tetrahedra, with two terminal and two bridging chlorides per metal atom. The methyl phosphonium cation exhibits the characteristic propeller

Table 13. Selected Bond Distances (Å) and Angles (deg) for $[CH_3\text{-}TMPP]_2[Co_2Cl_6]$ (8)

Atom 1	Atom 2	Bond Distance
Co(1)	Co(1)'	3.245(2)
Co(1)	Cl(1)	2.223(2)
Co(1)	Cl(2)	2.218(2)
Co(1)	Cl(3)	2.345(2)
Co(1)	Cl(3)'	2.339(2)
P(1)	C(1)	1.794(5)
P(1)	C(10)	1.805(5)
P(1)	C(19)	1.783(5)
P(1)	C(28)	1.803(5)

Atom 1	Atom 2	Atom 3	Bond Angle
Cl(3)	Co(1)	Cl(3)'	92.32(6)
Co(1)	Cl(3)	Co(1)'	87.68(6)
Cl(1)	Co(1)	Cl(2)	111.08(8)
Cl(1)	Co(1)	Cl(3)	109.42(7)
Cl(2)	Co(1)	Cl(3)	116.99(7)
C(1)	P(1)	C(10)	112.7(2)
C(1)	P(1)	C(19)	115.2(2)
C(1)	P(1)	C(28)	102.4(2)
C(10)	P(1)	C(19)	105.9(2)
C(10)	P(1)	C(28)	108.9(2)

Figure 25. ORTEP diagrams of the two ions present in $[CH_3\text{-}TMPP]_2[Co_2Cl_6]$. All atoms are represented by their 50% probability ellipsoids.

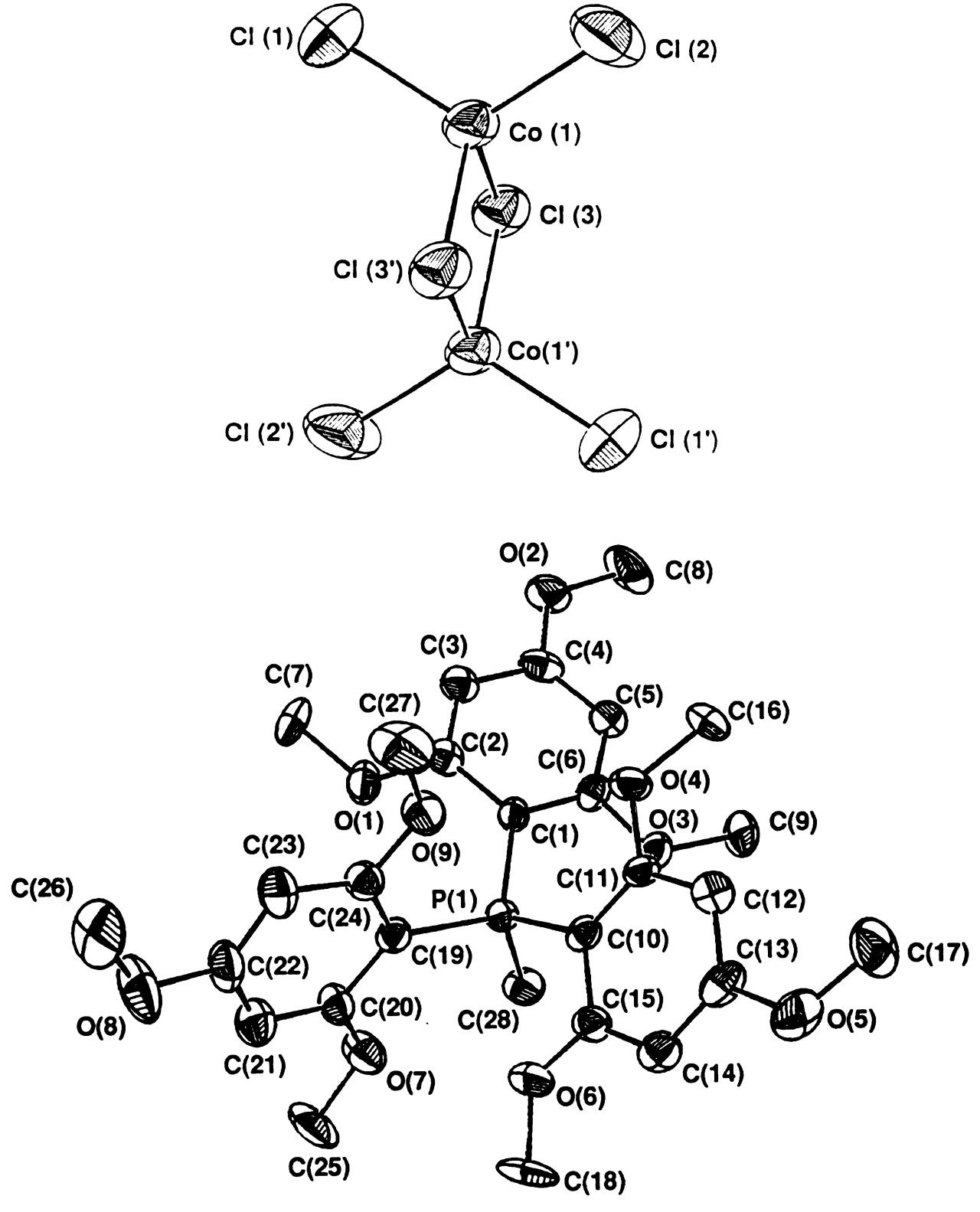
Cl (1)
Cl (2)
Co (1)
Cl (3)
Cl (3')
Co(1')
Cl (2')
Cl (1')
O(2)
C(8)
C(3)
C(4)
C(7)
C(27)
C(5)
C(16)
C(2)
C(6)
O(4)
O(1)
O(9)
C(1)
O(3)
C(9)
C(23)
C(11)
C(26)
P(1)
C(12)
C(24)
C(10)
C(19)
C(13)
C(17)
C(22)
C(28)
C(15)
O(8)
C(20)
O(5)
C(21)
O(7)
C(14)
O(6)
C(25)
C(18)

Figure 25.

arrangement found in aromatic tertiary phosphines. To our knowledge, only two salts of $[Co_2Cl_6]^{2-}$ have been previously structurally characterized; these are $[CoClN_6P_6(NMe_2)_{12}]_2[Co_2Cl_6]\cdot 2CHCl_3$ [12] and $[Co_2(C_5Me_5)(\mu\text{-}Cl)_3]_2\,[Co_2Cl_6]$ [13]. In **8**, the average Co-Cl (bridge) distance (2.342[2] Å) is intermediate between those of the two previous structures found in the literature (2.336 and 2.378 Å). The Co-Cl-Co and the Cl-Co-Cl bond angles (87.68(6) and 92.32(6)°) are more distorted from ideal geometry than in the previous two examples (89.1 and 90.2, 90.1 and 89.9°). Furthermore, the non-bonding Co···Co distance of 3.245(2) Å in the present structure is shorter than the corresponding distances in the other two complexes by 0.03 and 0.12 Å. The considerable distortion from ideal tetrahedral geometry in the present case is attributed to packing influences due to the very large cation.

(2) $[H\text{-}TMPP]_2[CoCl_4]$ (9) and $[ClCH_2\text{-}TMPP]_2[CoCl_4]$ (11)

ORTEP drawings of complexes **9** and **11** are shown in Figures 26 and 27 and pertinent bond distances and angles are listed in Table 14. Both complexes crystallize in the space group $C_{2/c}$ and indeed exhibit the same general features. In both cases the cobalt atom lies on a two-fold axis and is ligated by four chlorine atoms to form the well-known $[CoCl_4]^{2-}$ anion. Two protonated $[H\text{-}TMPP]^+$ or chloromethylated $[ClCH_2\text{-}TMPP]^+$ phosphine ligands serve as counterions in the structures of **9** and **11**, respectively. The Co-Cl distances in various salts of the $[CoCl_4]^{2-}$ anion have been recently reviewed by Rheingold and Burmeister [14]. The bond distances observed in structures **9** and **11** fall in the reported range of 2.23-2.34 Å. The Cl-Co-Cl angles vary from 108.34(6) to 111.8(1)° for **9** and from 107.4(1) to 111.5(2)° for **11**, which overall describes a fairly regular tetrahedron. The structural features of the protic and the

Table 14. Selected Bond Distances (Å) and Angles (deg) for $[H\text{-}TMPP]_2[CoCl_4]$ (9) and $[ClCH_2\text{-}TMPP]_2[CoCl_4]$ (11)

Atom 1	Atom 2	Bond Distances	
		9	11
Co(1)	Cl(1)	2.268(2)	2.300(3)
Co(1)	Cl(2)	2.263(2)	2.276(3)
P(1)	C(1)	1.777(5)	1.796(9)
P(1)	C(10)	1.778(6)	1.810(1)
P(1)	C(19)	1.793(6)	1.805(9)
P(1)	C(28)	---------	1.813(9)

Atom 1	Atom 2	Atom 3	Bond Angles	
			9	11
Cl(1)	Co(1)	Cl(2)	109.33(7)	107.4(1)
Cl(1)	Co(1)	Cl(1)'	111.80(1)	110.7(2)
Cl(2)	Co(1)	Cl(1)'	108.34(7)	109.9(1)
Cl(2)	Co(1)	Cl(2)'	109.60(1)	111.5(2)
C(1)	P(1)	C(10)	115.4(3)	114.4(4)
C(1)	P(1)	C(19)	109.0(3)	113.3(4)
C(10)	P(1)	C(19)	114.8(3)	105.5(4)
C(1)	P(1)	C(28)	---------	104.0(4)
C(10)	P(1)	C(28)	---------	112.7(5)
C(19)	P(1)	C(28)	---------	107.0(4)

Figure 26. ORTEP diagram of $[H\text{-}TMPP]_2[CoCl_4]$. All atoms are represented by their 50% probability ellipsoids.

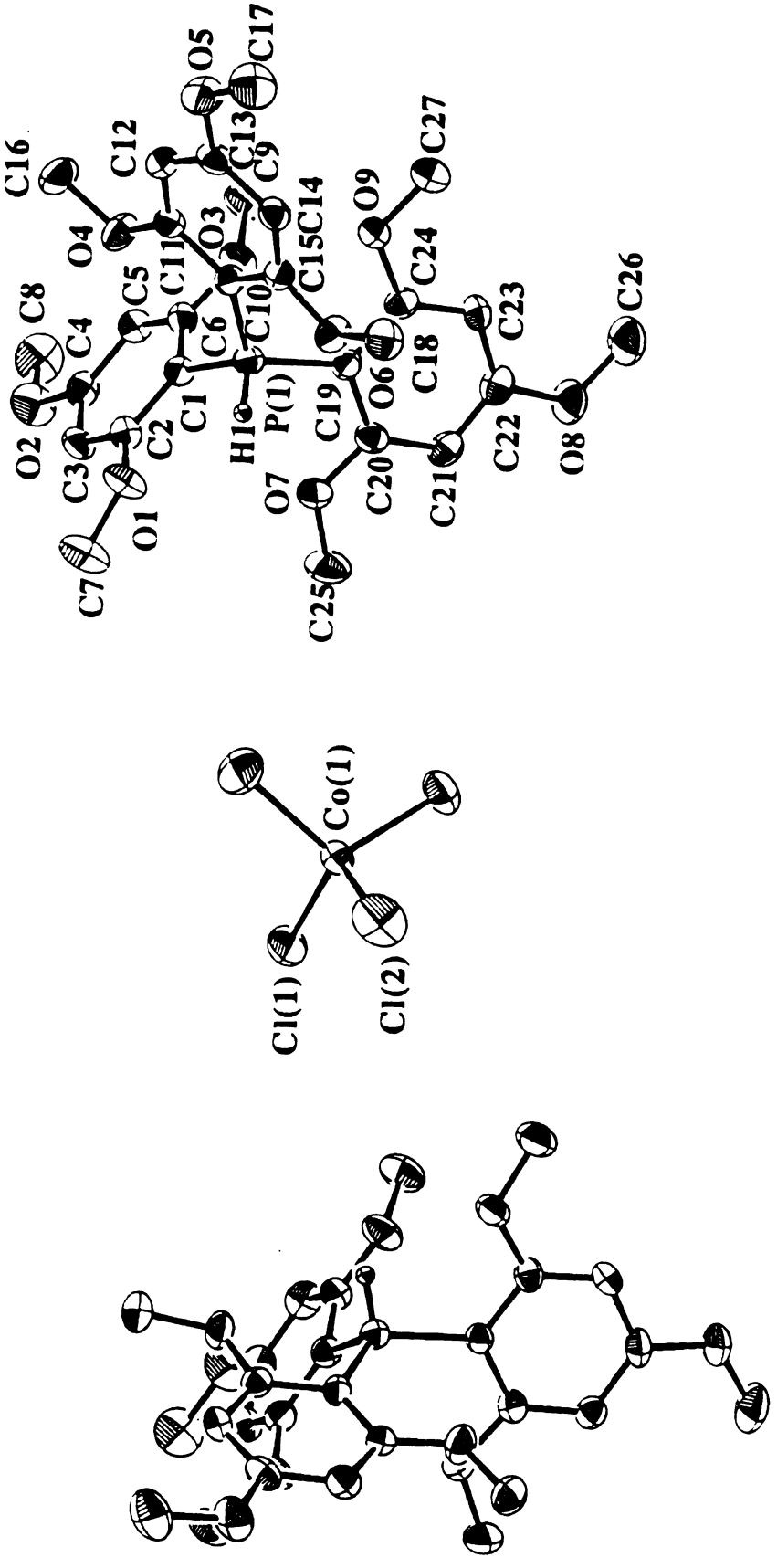
C16
C12
O5
C17
C13
C9
O4
O3
C11
C15C14
O9
C27
C8
C5
C10
C24
C4
C6
C23
C18
O6
C26
O2
C3
C2
C1
H1
P(1)
C19
C22
O8
O1
O7
C20
C21
C7
C25
Co(1)
Cl(1)
Cl(2)

Figure 26.

Figure 27. ORTEP diagram of $[ClCH_2\text{-}TMPP]_2[CoCl_4]$. All atoms are represented by their 50% probability ellipsoids.

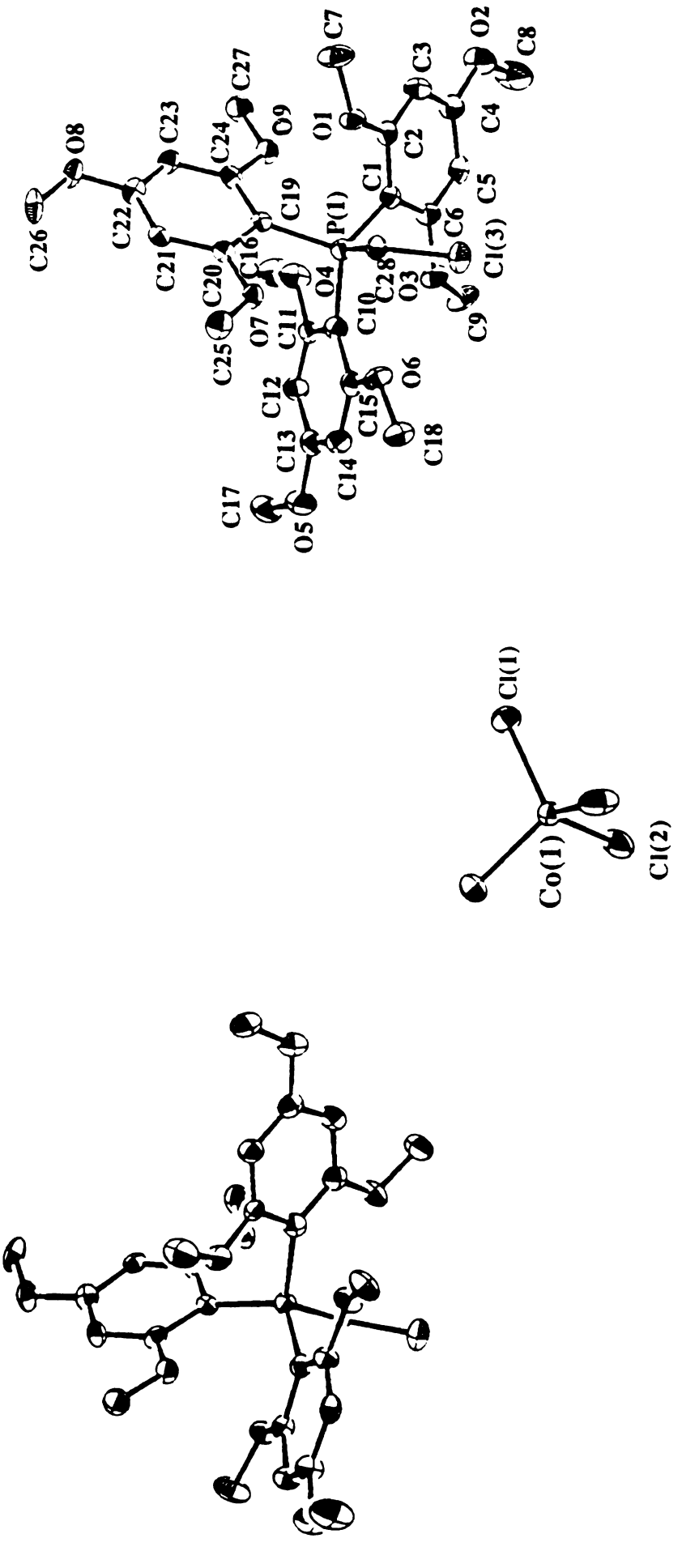
C7
O2
C8
C3
C4
O1
C2
C1
C5
C6
C1(3)
P(1)
C28
O3
C9
C10
O4
C11
O6
C15
C18
C12
C13
C14
C17
O5
C16
C19
C20
C21
C22
C23
C24
C27
O9
O8
C26
C25
O7
Cl(1)
Co(1)
Cl(2)

Figure 27.

chloromethyl phosphonium cations are similar to those of the free phosphine and other phosphonium salts [15,16], and are without exceptional qualities. Unlike previous reports of $[CoCl_4]^{2-}$ salts, we do not observe any hydrogen bonding between any of the chlorine atoms and H(1) [17].

(3) $Cl_2Co_2\{\mu-\eta^2$-(TMPP-*O*)$_2\}$ (14)

Figure 28 depicts an ORTEP representation of **14** and a list of important bond distances and angles is given in Table 15. In this structure, the two Co atoms reside on a two-fold axis. Co(1) is ligated by mutually *cis* phosphorus and oxygen atoms. The two oxygen atoms O(6) and O(6)', derived from demethylated ortho methoxy groups, are further attached via a bridging mode to Co(2). The coordination sphere of Co(2) is completed by two Cl atoms Cl(1) and Cl(2). This structure can be viewed as that of Co(TMPP-*O*)$_2$, described above, with a "$CoCl_2$" fragment attached to it. The Co(1)-P(1) distance of 2.198(2) Å is somewhat shorter than the corresponding distances (2.3-2.5 Å) reported for other Co/(P,O) structures, as is the Co(1)-O(6) bond of 1.927(4) Å [7]. This may be rationalized by considering the very strong σ-donation of the phosphorus lone pair combined with an electron withdrawing effect from the phenoxide ligand in the present case. The two oxygen atoms O(9) and O(9)' form a weak axial interaction at a distance of 2.313(4) Å with the angle O(9)-Co(1)-O(9)' = 172.0(2)°. This long bond distance is in agreement with other reported weak Co(II)-ether interactions [7]. Finally, the distance between the two cobalt centers is 3.034(2) Å, precluding the existence of a metal-metal bond. This coordination mode for TMPP, referred to as (μ-η^2), in which the phosphine is both chelating one metal center through a phosphorus and an oxygen atom (η^2) and bridging two metal centers through an oxygen atom (μ), has been seen only once in our

Table 15. Selected Bond Distances (Å) and Angles (deg) for $Cl_2Co_2\{\mu\text{-}\eta^2\text{-}(TMPP\text{-}O)_2\}$ (14) and $Cl_2MnCo\{\mu\text{-}\eta^2\text{-}(TMPP\text{-}O)_2\}$ (15)

Atom 1	Atom 2	Bond Distances	
		14	15
Co(1)	Co(2)/Mn(1)	3.034(2)	3.046(5)
Co(1)	P(1)	2.198(2)	2.202(5)
Co(1)	O(6)	1.927(4)	1.93(1)
Co(1)	O(9)	2.313(4)	2.30(1)
Cl(1)	Co(2)/Mn(1)	2.215(2)	2.224(6)
O(6)	Co(2)/Mn(1)	1.983(4)	1.99(1)

Atom 1	Atom 2	Atom 3	Bond Angles	
			14	15
P(1)	Co(1)	P(1)'	110.10(9)	109.2(3)
P(1)	Co(1)	O(6)	85.3(1)	85.9(3)
O(6)	Co(1)	O(6)'	79.5(2)	79.2(6)
O(9)	Co(1)	O(9)'	172.0(2)	172.3(7)
P(1)'	Co(1)	O(6)	164.4(1)	164.7(3)
Cl(1)	Co(2)/Mn(1)	Cl(1)'	112.0(1)	114.2(4)
Cl(1)	Co(2)/Mn(1)	O(6)	118.6(1)	117.6(3)
Cl(1)	Co(2)/Mn(1)	O(6)'	113.4(1)	113.0(3)
O(6)	Co(2)/Mn(1)	O(6)'	76.9(2)	76.5(6)

Figure 28. ORTEP drawing of $Cl_2Co_2\{\mu\text{-}\eta^2\text{-}(TMPP\text{-}O)_2\}$. Phenyl- group atoms are represented as small circles for clarity, whereas all other atoms are represented by their 50% probability ellipsoids.

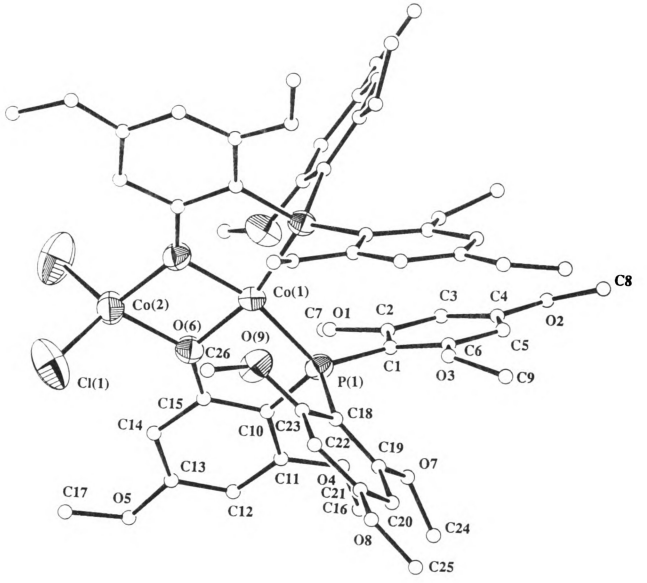
Co(1)
Co(2)
O(6)
O(9)
C26
P(1)
Cl(1)
C1
C2
C3
C4
C5
C6
C7
O1
O2
O3
C8
C9
C10
C11
C12
C13
C14
C15
C16
C17
O5
C18
C19
C20
C21
C22
C23
O4
O7
O8
C24
C25

Figure 28.

Figure 29. ORTEP drawing of $Cl_2MnCo\{\mu\text{-}\eta^2\text{-}(TMPP\text{-}O)_2\}$. Phenyl-group atoms are represented as small circles for clarity, whereas all other atoms are represented by their 50% probability ellipsoids.

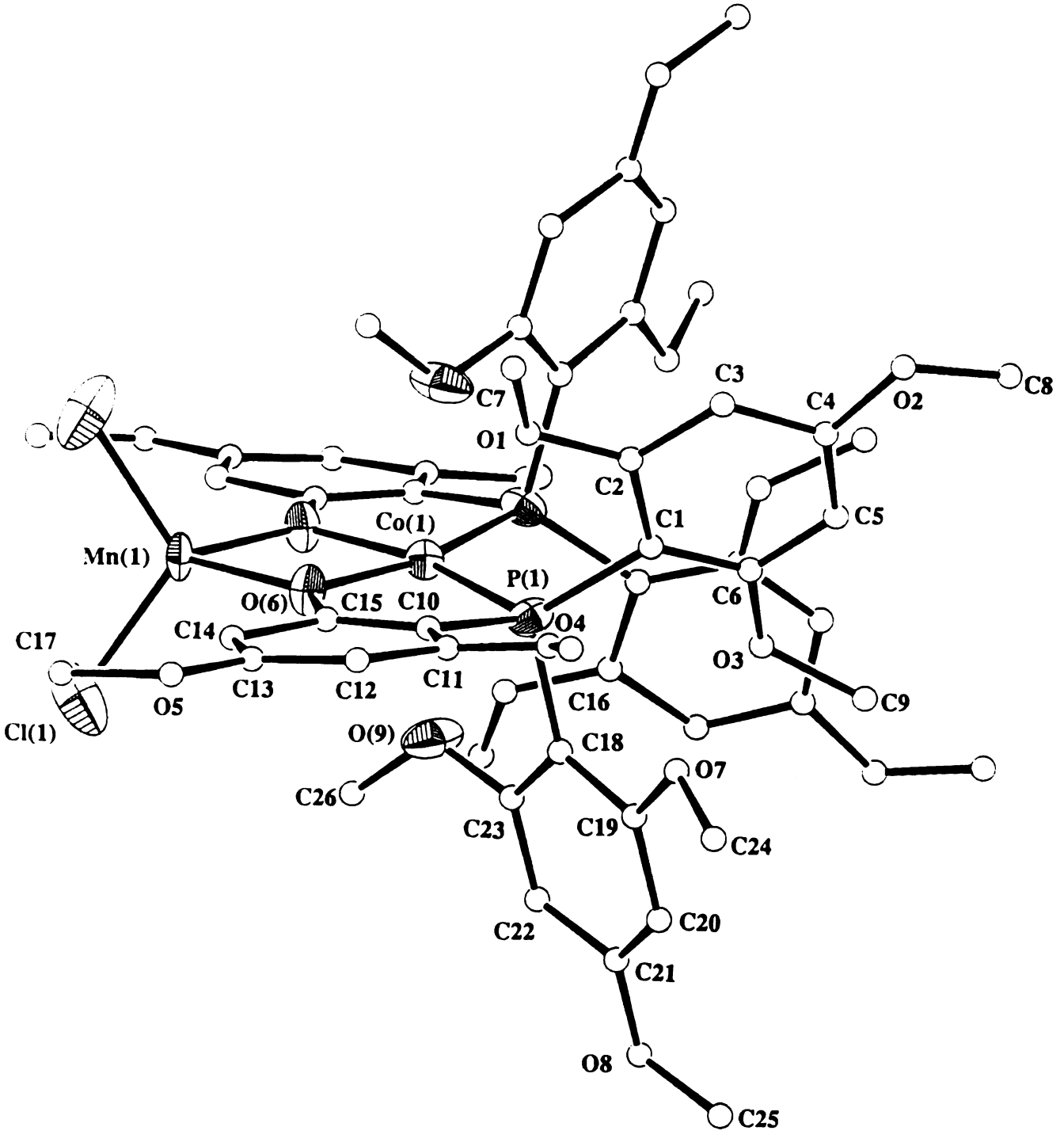
C7
C3
C4
O2
C8
O1
C2
C1
C5
Co(1)
Mn(1)
P(1)
O(6)
C15
C10
C6
O4
C14
C17
O3
C13
C12
C11
C16
C9
O5
Cl(1)
O(9)
C18
O7
C26
C23
C19
C24
C22
C20
C21
O8
C25

Figure 29.

prior chemistry with this phosphine; namely in the trinuclear osmium carbonyl cluster $Os_3(\mu\text{-}OH)(CO)_9\{\mu\text{-}\eta^2\text{-}(TMPP\text{-}O)\}$ [18]. Such a $\mu\text{-}\eta^2$ bridging mode for an oxygen atom, although unusual, has been previously described for keto- or carboxylato- groups [19]. The closest example to the present case is found in a paper by Kraihanzel *et al.* who reported a complex in which two cobalt centers are bridged by the oxygen atom from a carboxylate group of a (P,O) ligand to form the hexanuclear species "$Co_6(P,O)_{12}$" [7a]. To our knowledge, $Cl_2Co_2\{\mu\text{–}\eta^2\text{-}(TMPP\text{-}O)_2\}$ is the sole example of a dinuclear Co(II) species in which the geometries of the two metals are entirely different.

(4) $Cl_2MnCo\{\mu\text{-}\eta^2\text{-}(TMPP\text{-}O)_2\}$ (15)

The molecular structure of compound **15** is presented in the ORTEP diagram in Figure 29 and important bond distances and angles are listed in Table 15. This structure is the analogue of compound **14**, described above, with the "$CoCl_2$" fragment being replaced by a "$MnCl_2$" unit. The Co(1)-P(1) and Co(1)-O(6) distances remain essentially unchanged. The distances between the two metal atoms is slightly longer than in the aforementioned structure.

(5) $[(COD)Rh\text{-}Co(TMPP\text{-}O)_2][BF_4]_2$ (17)

The structure of compound **17** is presented in the ORTEP diagram in Figure 30 and important bond distances and angles are listed in Table 16. As the Figure clearly indicates the Co(III) center is surrounded by four oxygen and two phosphorus atoms to form an overall very regular octahedral environment. The phosphorus and the methoxy-oxygens are mutually *cis*, whereas the phenoxide oxygens are disposed in a *trans* fashion. The average Co-P bond distance of 2.167[5] Å and the metal-ether interactions (2.074[9] versus 2.313(4) Å) are shorter than in the Co(II)

Table 16. Selected Bond Distances (Å) and Angles (deg) for [(COD)Rh-Co(TMPP-*O*)$_2$][BF$_4$]$_2$ (17)

Atom 1	Atom 2	Bond	Atom 1	Atom 2	Bond
Rh(1)	C(20)	2.33(2)	Co(1)	P(1)	2.164(4)
Rh(1)	C(21)	2.35(2)	Co(1)	P(2)	2.170(5)
Rh(1)	C(22)	2.26(2)	Co(1)	O(9)	1.898(9)
Rh(1)	C(23)	2.21(2)	Co(1)	O(18)	1.877(8)
Rh(1)	C(53)	2.16(2)	Co(1)	O(3)	2.05(1)
Rh(1)	C(54)	2.16(2)	Co(1)	O(15)	2.097(9)
Rh(1)	C(57)	2.13(2)			
Rh(1)	C(58)	2.14(2)			

Atom 1	Atom 2	Atom 3	Angle	Atom 1	Atom 2	Atom 3	Angle
C(20)	Rh(1)	C(21)	35.6(6)	P(1)	Co(1)	P(2)	101.4(2)
C(20)	Rh(1)	C(23)	76.4(6)	P(1)	Co(1)	O(3)	83.3(3)
C(21)	Rh(1)	C(22)	37.1(5)	P(1)	Co(1)	O(15)	174.0(3)
C(22)	Rh(1)	C(23)	37.6(6)	P(1)	Co(1)	O(18)	94.7(3)
C(53)	Rh(1)	C(54)	38.7(6)	P(2)	Co(1)	O(3)	174.1(3)
C(53)	Rh(1)	C(57)	96.4(8)	P(2)	Co(1)	O(9)	94.5(4)
C(53)	Rh(1)	C(58)	80.7(7)	P(2)	Co(1)	O(15)	82.6(3)
C(54)	Rh(1)	C(57)	81.6(7)	O(3)	Co(1)	O(9)	89.1(4)
C(54)	Rh(1)	C(58)	92.2(6)	O(3)	Co(1)	O(18)	86.7(4)
C(57)	Rh(1)	C(58)	40.4(6)	O(9)	Co(1)	O(15)	86.4(4)
O(9)	Co(1)	O(18)	174.1(4)	O(15)	Co(1)	O(18)	89.7(4)

Figure 30. ORTEP drawing for the molecular cation [(COD)Rh-Co(TMPP-*O*)$_2$]$^{2+}$. All phenyl-group and COD carbon atoms are represented as small circles for clarity, whereas all other atoms are represented by their 40% probability ellipsoids.

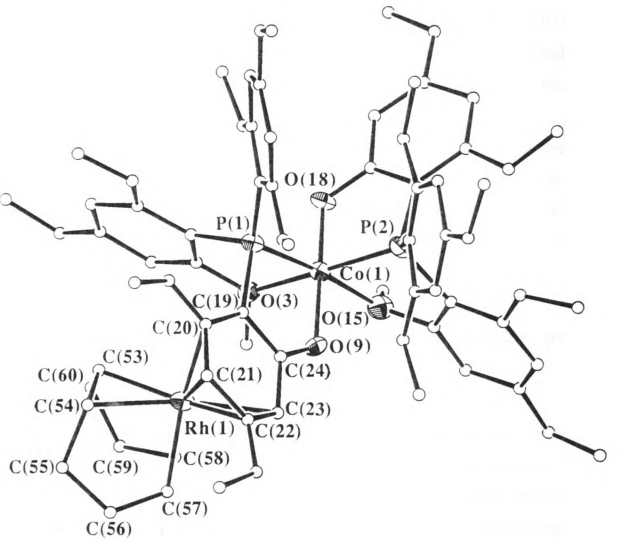
O(18)
P(1)
P(2)
Co(1)
C(19)
O(3)
O(15)
C(20)
O(9)
C(53)
C(60)
C(21)
C(24)
C(54)
C(23)
Rh(1)
C(22)
C(55)
C(59)
C(58)
C(57)
C(56)

Figure 30.

structure $Cl_2Co_2\{\mu\text{-}\eta^2\text{-}(TMPP\text{-}O)_2\}$ (**14**) (2.198(2) Å), as expected for a more electrophilic metal center. The Co-O distances for the oxygen atoms from the phenoxide groups are comparable to those in **14**, being 1.888[9] Å compared to 1.927(4) Å; this value is also in agreement with the Co^{III}-O bond distance of 1.899(2) Å reported for the macrocyclic carboxylato-Co(III) complex $[Co(L^3\text{-}H)][ClO_4]_2$ [20]. The angles about the Co(III) center define a quasi-octahedral geometry with the O(9)-Co(1)-O(18) bond angle being 174.1(4)° and the P(1)-Co(1)-P(2) 101.4(2)°. Such a stable octahedral geometry is expected for a d^6 electronic configuration.

The most interesting feature about this structure however is the mode of binding for the Rh(I) atom to the TMPP ligand. The Rh(I) center is ligated to a COD ligand in the usual manner on one side, and in an η^4 fashion to one of the demethylated phenyl rings of the phosphine on the other side. To date, this constitutes the first example of a TMPP ring participating in such a bonding interaction.

Two $[BF_4]^-$ counterions and two interstitial acetone molecules are also present in the structure.

C. Spectroscopy and Magnetism

The magnetic properties of compounds **9-15** were studied by a variety of techniques, including epr and magnetic susceptibility measurements. The properties of $[H\text{-}TMPP]_2[CoCl_4]$ (**9**) and $[ClCH_2\text{-}TMPP]_2[CoCl_4]$ (**11**) were quite unremarkable and exhibited the properties anticipated for tetrahedral high-spin Co(II) complexes (S = 3/2) [8].

Co(TMPP-*O*)$_2$: The compound $Co(TMPP\text{-}O)_2$ (**12**) was expected to be a S = 1/2 system, based on an analogy to the related species $[Rh(TMPP)_2]^{2+}$ [21], but studies of the magnetic susceptibility of **12** over the 5-300 K temperature range revealed a Curie-Weiss behavior with a $\mu_{eff} = 4.48\ \mu_B$;

this value was in good agreement for a S= 3/2 spin system. High-spin configurations for octahedral or planar Co(II) complexes are actually the general rule, and there are very few instances of octahedral low-spin Co(II) complexes. Only 5-coordinate species favor low-spin (S = 1/2) configurations [22].

$Cl_2Co_2\{\mu-\eta^2$-(TMPP-*O*)$_2\}$: The magnetic behavior of compound **14** was studied over the temperature range 5 - 300 K and showed a Curie-Weiss behavior between 140 and 300 K with a value for the effective moment of 3.65 μ_B which corresponds to a S = 1 spin system for the molecule. The integer spin value for the spin state might be the reason why we were not able to observe an EPR signal for this compound at 110 K.

D. Discussion

Given suitable conditions (*vide supra*), $[Co(NCCH_3)_6]^{2+}$ cations react with the highly basic and bulky ligand tris(2,4,6-trimethoxyphenyl)phosphine (TMPP) to give the two unusual phosphino-phenoxide Co(II) complexes Co(TMPP-*O*)$_2$ (**12**) and $Cl_2MCo\{\mu$-η^2-(TMPP-*O*)$_2\}$ (M = Co (**14**), Mn (**15**)). Although there are numerous Co(II)/ether phosphine complexes in the general literature, few are of the types found in the present work. All previously reported structures are of the types $CoX_2(P,O)_2$ [7i-j] or "$Co(P_4O_2)$ [7b-f], where P_4O_2 is a (P,O) macrocycle, or the hexanuclear complex $Co_6(Ph_2PCH_2CO_2)_{12}$ [7a]. The closest resemblance to **12** and **14-15** are the compounds $Co(OC_6H_4PBu^t_2)_2$ and $Co[(C_6H_5)_2PCH_2C(CF_3)_2O]_2$ [7g,h]. However, in both cases the complexes were assigned a *trans* square-planar geometry by analogy to the structurally characterized Ni(II) species and found to be orange in color, whereas all our compounds are blue or green.

The neutral compound Co(TMPP-*O*)$_2$, which is formally a 15-electron complex if the axial ether interactions are not taken into account, may be predicted to be electron-deficient. Consequently we expected this complex to be very reactive, especially since reversible uptake of dioxygen, high reactivity towards small molecules and enhanced oxidative addition have been noted for many (P,O) ligand complexes [7h]. Since Co(TMPP-*O*)$_2$ contains two weakly bound MeO$^-$ groups in the axial positions, it prompted us to explore its reactivity. We found no reaction between Co(TMPP-*O*)$_2$ and O_2 under ambient conditions of pressure and temperature. This is certainly a result of the electronic configuration of this compound (S = 3/2 instead S = 1/2). We also investigated the reactivity of **12** with π-acceptors such as carbon monoxide (CO) or isopropylisocyanide (^{i}PrNC), but only in the latter case were promising results obtained. After the addition of two equivalents of ^{i}PrNC to a solution of Co(TMPP-*O*)$_2$, two ν(C≡N) stretches were observed, one at higher energy (2162 cm^{-1}) and one at lower energy (2120 cm^{-1}), possibly corresponding to a mono- and a bis-adduct. However, we were not able to isolate any solid from this reaction. The only successful reaction was the rational preparation of $Cl_2MCo\{\mu\text{-}\eta^2\text{-}(TMPP\text{-}O)_2\}$ (M = Co, **14**, M = Mn, **15**) from Co(TMPP-*O*)$_2$ and MCl_2, as shown in the scheme below:

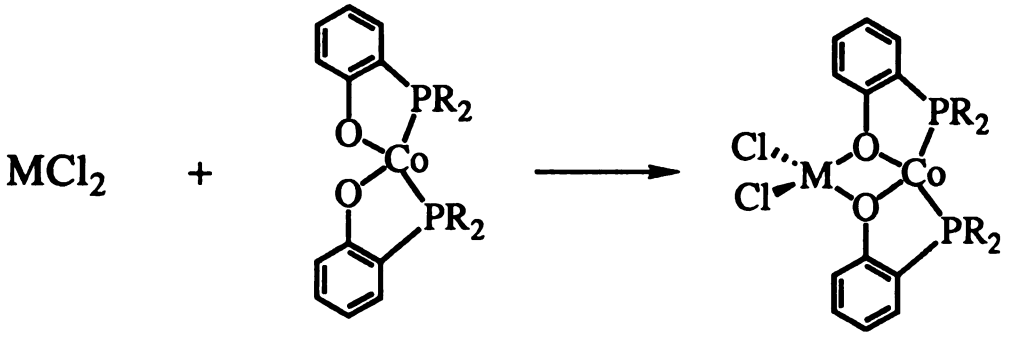

This approach has recently been used by M. Darensbourg *et al.* to form bi- and heterometallic compounds from square-planar Ni(II) complexes possessing a N_2S_2 environment [23]. Other have also used the readily available sulfur donor groups in such complexes to link two units together via coordination of a third metal atom to form either linear or triangular trinuclear complexes [24]. Wieghardt has studied the magnetic properties of asymmetric homo- and heterodinuclear complexes containing the μ-oxo-bis(μ-acetato)dimetal core [25]. In general, this type of chemistry has primarily been investigated with complexes possessing carboxylate ligands [26]. In fact, to our best knowledge there is only one report of an heterobimetallic complex of this type containing a phenoxide ligand [27]. After researching the topic, we became interested in the possibility of preparing other heterobimetallic compounds and study their magnetic and structural properties. As a backdrop for these studies, we note that there are several reports in the literature by Wolczanski *et al.* of early-late heterobimetallic complexes, namely *trans*-$Me_2Ta(\mu\text{-}CH_2)(\mu\text{-}OCMe_2CH_2Ph_2P)_2PtMe$, $(TMEDA)Ta(\mu\text{-}CH_2)(\mu\text{-}OCH_2)(\mu\text{-}Me)(\mu\text{-}OCMe_2CH_2Ph_2P)_2Ni$ [28], and $Cp^*Zr(\mu\text{-}OCH_2Ph_2P)_2RhMe_2$ [29]. To ascertain the possibility of preparing an early-late heterobimetallic compound from the Co(TMPP-*O*)$_2$ "synthon", the 1:1 reaction between **12** and titanocene dichloride, Cp_2TiCl_2, was carried out. The formulation of the product as $[Cp_2TiCo\{\mu\text{-}\eta^2\text{-}(TMPP\text{-}O)_2\}][CoCl_4]$ (**16**) was based on infrared, NMR and UV-visible spectroscopies (equation 2). The presence of the $[CoCl_4]^{2-}$ anion was easily confirmed by the $\nu_{Co\text{-}Cl}$ stretch in the far-IR region at 295 cm^{-1} as well as in the electronic spectrum, while a resonance attributed to the Cp_2Ti^{2+} fragment was observed at δ = 6.50 ppm in the NMR spectrum, along with other resonances due to the TMPP

ligand. In order to improve the yield of this reaction and avoid that half of the cobalt be consumed to form the $CoCl_4^{2-}$ anion, we tried to remove the chlorides from Cp_2TiCl_2 by the use of $AgBF_4$ prior to the reaction with **12**, but this led to decomposition.

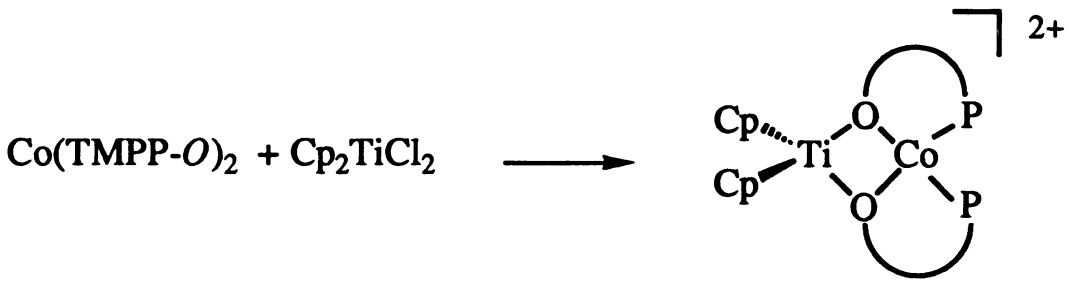

(equation 2)

A similar reaction was carrieed out with $[Rh(COD)(THF)_2]^+$ (COD = 1,5-cyclooctadiene), which was prepared by the action of $AgBF_4$ on the chloro-bridged dimer $[Rh(COD)Cl]_2$ [30]. The rationale behind this reaction was that the Rh(I) center would favor the phenoxide oxygen atoms over the THF molecules as ligands (equation 3).

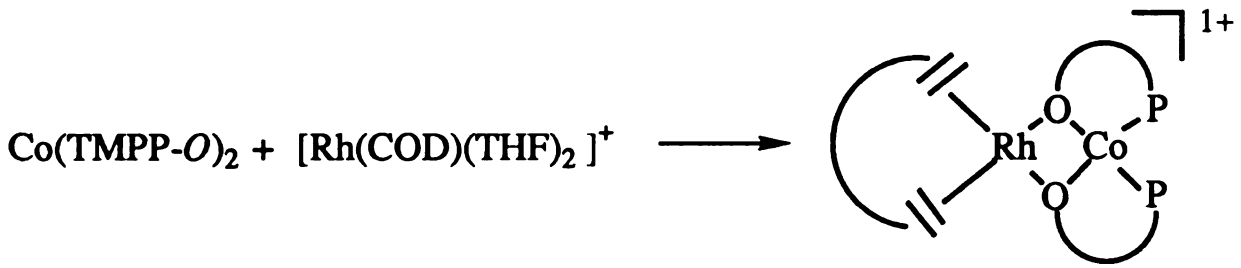

(equation 3)

Surprisingly, the ^1H NMR spectrum of the product of the equimolar reaction between $[Rh(COD)(THF)_2]^+$ and $Co(TMPP\text{-}O)_2$ exhibits the typical pattern of a tridentate TMPP ligand, coordinated to a diamagnetic metal center (see Figure 31). The X-ray structure of this compound

established its identity as $[(COD)Rh^{I}\text{-}Co^{III}(TMPP\text{-}O)_2]^{2+}$ (**17**), in which the Rh(I) atom is bound in an η^4 fashion to one of the demethylated phenyl ring of the TMPP ligand from the $[Co^{III}(TMPP\text{-}O)_2]^{+}$ fragment. The diamagnetic nature of complex **17** arises from the presence of a Rh^{I} and a Co^{III} center in the molecule. The ^1H NMR spectrum shows the presence of 6 *meta* protons and 8 methoxy groups, indicating that the two phosphine ligands are equivalent in solution, the "Rh(COD)$^+$" moiety being labile in a coordinating solvent such as d_6-acetone or d_3-acetonitrile. The ^{31}P NMR result confirmed the equivalence of the phosphines in solution since only one signal was observed at δ = + 5.6 ppm. When the NMR experiment is carried out in a non-coordinating solvent such as CD_2Cl_2, 16 methoxy and 12 *meta* resonances are observed, attributed to 2 inequivalent phosphines, thereby indicating that the Rh(COD)$^+$ fragment remains coordinated. The most surprising aspect of this reaction is undoubtedly the oxidation of the Co^{II} to a Co^{III} center, which may have occurred due to the presence of residual Ag^+ as a contaminant in the Rh(I) starting material. Independent deliberate oxidation of $Co(TMPP\text{-}O)_2$ (**12**) by $AgBF_4$ is then in order. The isomerization from *cis* to *trans* phenoxide ligands that occurred during the oxidation from Co^{II} to Co^{III} explains the irreversibility of the cyclic voltammogram. It is interesting to note that similar results were observed in the chemistry of $Rh^{II}(TMPP\text{-}O)_2$ and $Rh^{III}(TMPP\text{-}O)_2^{+}$ [11].

As a final topic in this research, we were interested in the possibility of preparing linear heterotrimetallic complexes from the $Co(TMPP\text{-}O)_2$ synthon. These complexes are quite rare as evidenced by the fact that there only are two reports in the recent literature of linear trimetallics; these are

Figure 31. ^{1}H NMR spectrum of [(COD)Rh-Co(TMPP-*O*)$_2$][BF_4]$_2$ in CD_3CN.

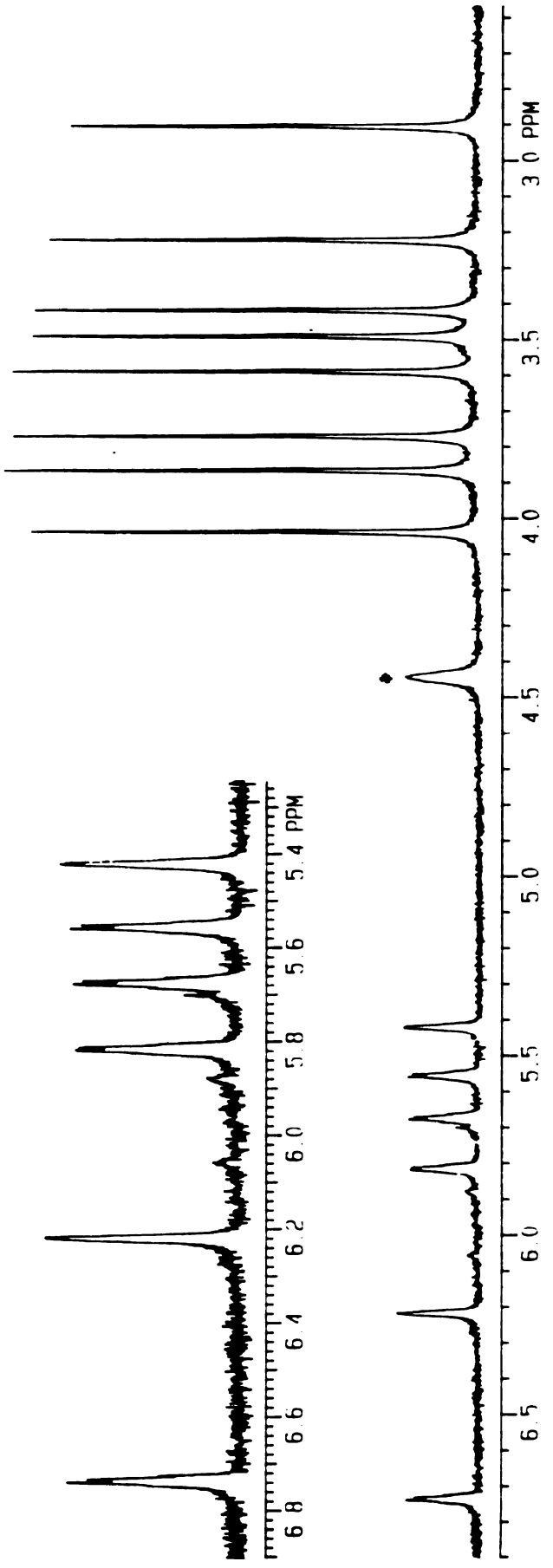

Figure 31.

$[Cu\{ClRu[(MeO)_2PO]_2(C_6Me_6)\}_2]$ [31] and a series of Ni^{II}-Cu^{II}-Ni^{II} complexes with oxamate bridging groups [32].

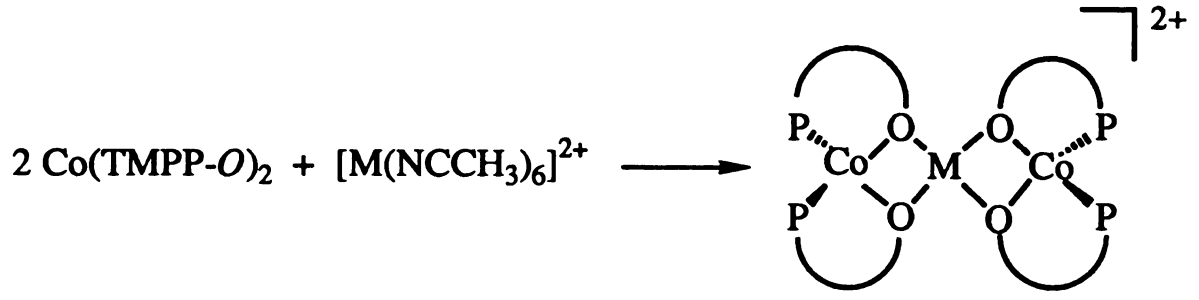

(equation 4)

Equation 4 shows the proposed reaction between Co(TMPP-*O*)$_2$ (**12**) and $[M(NCCH_3)_6]^{2+}$ (M = Co, Ni), but the only isolable product in these reactions was complex **12**.

4. Summary

Although there are many Co(II)/complexes reported in the literature, Co(TMPP-*O*)$_2$ represents one of the very *simple* homoleptic "Co(P,O)$_2$" complexes to be fully characterized. This must certainly be a result of electronic rather than steric effects since the phosphine ligands used in previous studies were also quite bulky. Despite the considerable size of the TMPP ligand, the two phosphines are *cis* to each other, as is the case in the rhodium(II) analogue, $[Rh(TMPP)_2]^{2+}$. This observation is in direct contrast to the two previous reports in the literature in which a *trans* geometry was postulated for Co(II)-ether phosphine complexes [7g,h].

We have been successful in preparing homo- and hetero-bimetallic complexes from the "Co(TMPP-*O*)$_2$" synthon, but our preliminary attempts to synthesize linear trinuclear species did not yield promising results. Another entry into this chemistry would be to use the already

assembled bimetallic compound, and attempt the addition of a third metal complex, as shown in equation 5.

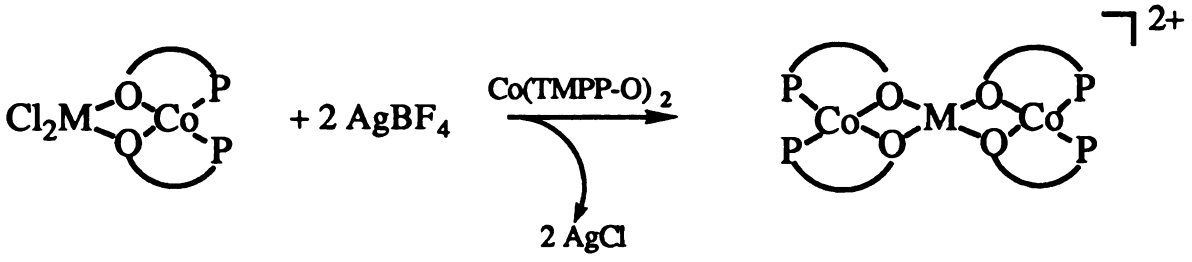

(equation 5)

LIST OF REFERENCES

1. (a) Smith, T. D.; Pilbrow, J. R. *Coord. Chem. Rev.* **1981**, *39*, 295. (b) Drago, R. S. *Comments Inorg. Chem.* **1981**, *1*, 53. (c) Basak, A. K.; Martell, A. E. *Inorg. Chem.* **1988**, *27*, 1948. (d) Taylor, R. J.; Drago, R. S.; George, J. E. *J. Am. Chem. Soc.* **1989**, *111*, 6610. (e) Delgado, R.; Glogowski, M. W.; Busch, D. H. *J. Am. Chem. Soc.* **1987**, *109*, 6855. (f) Cameron, J. H.; Graham, S. *J. Chem. Soc., Dalton Trans.* **1992**, 385. (g) Kurtikyan, T. S.; Gasparyan, A. V.; Martirosyan, G. G.; Zamkochyan, G. A. *Zhur. Prikl. Spektr.* **1990**, *52*, 106.

2. (a) Osborn, J. A.; Jardine, F. H.; Wilkinson, G. *J. Chem. Soc. (A)* **1966**, 1712. (b) Taqui-Khan, M. M.; Samad, S. A.; Siddiqui, M. R. H.; Bajaj, H. C.; Ramachandraiah, G. *Polyhedron* **1991**, *10*, 2729. (c) Howe, J. P.; Lung, R.; Nile, T. A. *J. Organomet. Chem.* **1981**, *208*, 401.

3. Zuur, A. P.; Groenveld, W. L. *Rec. Trav. Chim. Pays Bas* **1967**, *86*, 1089.

4. Reedijk, J.; Groenveld, W. L. *Rec. Trav. Chim. Pays Bas* **1968**, *87*, 513.

5. Hathaway, B. J.; Holah, D. G.; Underhill, A. E. *J. Chem. Soc.* **1962**, 2444.

6. (a) Desai, C. M. *J. Indian Chem. Soc.* **1954**, *31*, 957. (b) Kazi, H. *J. Indian Chem. Soc.* **1956**, *33*, 513. (c) Makarov, L. L.; Malyshev, V. N., Izotov, V. I. *Vestn. Leningr. Univ. Fiz. Khim.* **1968**, *23*, 139. (d) Paul, R. C.; Sharma, R. P.; Verma, R. D. *Indian J. Chem.* **1974**, *12*, 761. (e) Paul, R. C.; Sharma, R. P.; Verma, R. D. *Indian J. Chem.* **1976**, *14A*, 48.

7. (a) Lewis, G. E.; Kraihanzel, C. S. *Inorg. Chem.* **1983**, *22*, 2895. (b) Ciampolini, M.; Dapporto, P.; Dei, A.; Nardi, N.; Zanobini, F. *Inorg. Chem.* **1982**, *21*, 489. (c) Ciampolini, M.; Dapporto, P.; Nardi, N.; Zanobini, F. *Inorg. Chem.* **1983**, *22*, 13. (d) Mealli, C.; Sabat, M.; Zanobini, F.; Ciampolini, M.; Nardi, N. *J. Chem. Soc., Dalton Trans.* **1985**, 479. (e) Ciampolini, M.; Nardi, N.; Orioli, P. L.; Mangani, S.; Zanobini, F. *J. Chem. Soc., Dalton Trans.* **1985**,

1425. (f) Ciampolini, M.; Nardi, N.; Orioli, P. L.; Mangani, S.; Zanobini, F. *J. Chem. Soc., Dalton Trans.* **1985**, 1179. (g) Boeré, R. T.; Montgomery, C. D.; Payne, N. C.; Willis, C. J. *Inorg. Chem.* **1985**, *24*, 3680. (h) Empsall, H. D.; Shaw, B. L.; Turtle, B. L. *J. Chem. Soc., Dalton Trans.* **1976**, 1500. (i) Lindner, E.; Schober, U.; Glaser, E.; Norz, H.; Wegner, P. *Z. Naturforsch.* **1987**, *42b*, 1527. (j) Lindner, E.; Reber, J.-P. *Z. Naturforsch.* **1991**, *46b*, 1581. (k) Kyba, E. P.; Alexander, D. C.; Höhn, A. *Organometallics* **1982**, *1*, 1619.

8. Cotton, F. A.; Wilkinson, G. *Advanced Inorganic Chemistry*, 5th Edition; John Wiley, Ed.; New York: **1988**.

9. (a) Rauchfuss, T. B.; Patino, F. T.; Roundhill, D. M. *Inorg. Chem.* **1975**, *14*, 652. (b) Jeffrey, J. C; Rauchfuss, T. B. *Inorg. Chem.* **1979**, *18*, 2658.

10. (a) Mason, R.; Thomas, K. M.; Empsall, H. D.; Fletcher, S. R.; Heys, P. N.; Hyde, E. M.; Jones, C. E.; Shaw, B. L. *J. Chem. Soc., Chem. Commun.* **1974**, 612. (b) Jones, C. E.; Shaw, B. L.; Turtle, B. L. *J. Chem. Soc., Dalton Trans.* **1974**, 992. (c) Empsall, H. D.; Heys, P. N.; Shaw, B. L. *J. Chem. Soc., Dalton Trans.* **1978**, 257.

11. Haefner, S. C. Ph. D. dissertation, Michigan State University, **1992**.

12. Harrison, W.; Trotter, J. *J. Chem. Soc., Dalton Trans.* **1973**, 61.

13. Olson, W. L.; Dahl, L. F. *Acta Cryst.* **1986**, *C42*, 541.

14. (a) Albanese, J. A.; Staley, D. L.; Rheingold, A.; Burmeister, J. L. *Acta Cryst.* **1989**, *C45*, 1128. (b) Willett, R. D. *Acta Cryst.* **1991**, *C47*, 1083. (c) Lindroos, S.; Lumme, P. *Acta Cryst.* **1991**, *C47*, 872.

15. Dunbar, K. R.; Haefner, S. C. manuscript in preparation.

16. Dunbar, K. R.; Pence, L. E. *Acta Cryst.* **1991**, *C47*, 23.

17. (a) Williams, I. D.; Brown, P. W.; Taylor, N. J. *Acta Cryst.* **1992**, *C48*, 263. (b) Guo, N.; Lin, Y.-H.; Zeng, G.-F.; Xi, S.-Q. *Acta Cryst.* **1992**, *C48*, 542.

18. Chen, S. - J. Ph. D. dissertation, Michigan State University, **1991**.

19. (a) Cotton, F. A.; Elder, R. C. *Inorg. Chem.* **1966**, *5*, 423. (b) Bertrand, J. A.; Kalyanaraman, A. R. *Inorg. Chim. Acta* **1971**, *5*, 167. (c) Sumner, C. E.; Steinmetz, G. R. *Inorg. Chem.* **1989**, *28*, 4290.

20. Hambley, T. W.; Lawrance, G. A.; Maeder, M.; Wilkes, E. N. *J. Chem. Soc., Dalton Trans.* **1992**, 1283.

21. Dunbar, K. R.; Haefner, S. C.; Pence, L. E. *J. Am. Chem. Soc.* **1989**, *111*, 5504.

22. Backes, G.; Reinen, D. *Z. Anorg. Allg. Chem.* **1975**, *418*, 217.

23. Mills, D. K.; Hsiao, M. H.; Farmer, P. J.; Atnip, E. V.; Reibenspies, J. H.; Darensbourg, M. Y. *J. Am. Chem. Soc.* **1991**, *113*, 1421.

24. (a) Jicha, D. C.; Busch, D. H. *Inorg. Chem.* **1962**, *1*, 872. (b) Wei, C. H.; Dahl, L. F. *Inorg. Chem.* **1970**, *9*, 1878. (c) Turner, M. A.; Driesen, W. L.; Reedijk, J. *Inorg. Chem.* **1990**, *29*, 3331. (d) Ciriano, M. A.; Perez-Torrente, J. J.; Viguri, F.; Lahoz, F. J.; Oro, L. A.; Tiripicchio, F.; Tiripicchio-Camellini, M. *J. Chem. Soc., Dalton Trans.* **1990**, 1493.

25. (a) Hotzelmann, R.; Wieghardt, K.; Flörke, U.; Haupt, H.-J.; Weatherburn, D. C.; Bonvoisin, J.; Blondin, G.; Girerd, J.-J. *J. Am. Chem. Soc.* ***1992***, *114*, 1681. (b) Martin, L. L.; Wieghardt, K.; Blondin, G.; Girerd, J.-J.; Nuber, B.; Weiss, J. *J. Chem. Soc., Chem. Commun.* **1990**, 1767. (c) Nieman, A.; Bossek, U.; Wieghardt, K.; Butzlaff, C.; Trautwein, A. X.; Nuber, B. *Angew. Chem. Int. Ed. Engl.* **1992**, *31*, 311.

26. (a) Tupeinen, U.; Hämäläinen, R.; Reedijk, J. *Polyhedron* **1987**, *6*, 1603. (b) Morgenstern-Baradau, I.; Laroque, D.; Bill, E.; Winkler, H.; Trautwein, A. X.; Robert, F.; Jeannin, Y. *Inorg. Chem.* **1991**, *30*, 3180. (c) Knopp, P.; Wieghardt, K.; Nuber, B.; Weiss, J.; Sheldrick, W. S. *Inorg. Chem.* **1990**, *29*, 363. (d) Batsanov, A. S.; Timko, G. A.; Struchkov, Yu. T.; Gérbéléu, N. V.; Manole, O. S. *Koord. Khim.* **1991**, *17*, 922.

27. Laroque, D.; Morgenstern-Baradau, I.; Winkler, H.; Bill, E.; Trautwein, A. X. *Inorg. Chim. Acta* **1992**, *192*, 107.

28. Baxter, S. M.; Wolczanski, P. T. *Organometallics* **1990**, *9*, 2498.

29. Ferguso, G. S.; Wolczanski, P. T.; Párkányi, L.; Zonnevylle, M. C. *Organometallics* **1988**, *7*, 1967.

30. Green, M.; Kuc, T. A.; Taylor, S. H. *J. Chem. Soc. (A)* **1971**, 2334.

31. Van Albada, G. A.; De Graaf, R. A. G.; Hage, R.; Reedijk, J.; Buchholz, E.; Kläui, W. *Polyhedron* **1991**, *10*, 1091.

32. Vicente, R.; Escuer, A.; Ribas, J. *Polyhedron* **1992**, *11*, 857.

CHAPTER V

CHEMISTRY OF TRIS(2,4,6-TRIMETHOXYPHENYL)PHOSPHINE WITH NICKEL(II) AND NICKEL(III)

1. Introduction

Following the successful chemistry of TMPP with Rh(II) and Co(II), we were interested in extending this work to other catalytically relevant metals of the first-row series, particularly nickel, since Ni(III) would provide us with another d^7 system. Interestingly, (P,O) ligands have demonstrated a selectivity enhancing effect in the nickel-catalyzed oligomerization of ethylene [1]. Although many (P,O) ligand/Ni(II) complexes have been reported, the only structurally characterized ones are of general formula $NiX_2(P,O)_2$ (X = Cl, Br, I, SCN) [2]. The use of macrocyclic polyphosphine ligands of the crown-ether or crown thio-ether type afforded the stabilization of several 6-coordinate Ni(II) complexes [3]. In the late 70's, Shaw reported compounds of the type *trans*-$Ni(P,O)_2$ whose structure was assigned by analogy to the platinum and palladium analogues [4], and the use of a fluoro-alcohol diarylphosphino ligand afforded the stabilization of an homoleptic *trans* 4-coordinate *bis*-(P,O) ligand Ni(II) complex, namely $Ni[Ph_2PCH_2C(CF_3)_2O]_2$, which was structurally characterized [5].

This chapter describes the successful use of the solvated cation $[Ni(NCCH_3)_6]^{2+}$ in preparing a bis-TMPP/Ni(II) complex and its oxidation to a stable Ni(III) species.

2. Experimental

A. Synthesis

(1) Reaction of $[Ni(H_2O)_6][BF_4]_2$ with TMPP

(i) Reactions with 2 equivalents of TMPP

A quantity of $[Ni(H_2O)_6][BF_4]_2$ (0.164 g, 0.481 mmol) was reacted with 2 equivalents of TMPP (0.512 g, 0.962 mmol) in 20 mL of methanol.

The limpid, pale green solution was stirred at room temperature for 1 hour, after which time its volume was reduced to *ca.* 5 mL. Slow addition of diethyl ether resulted in the precipitation of a pale green solid which was dried *in vacuo*. ^{1}H NMR and IR spectroscopic measurements established its identity as [H-TMPP][BF_4]. Similar results were obtained when the reaction was carried out in acetonitrile.

(ii) Reaction with 4 equivalents of TMPP

The solvated Ni(II) salt (0.129 g, 0.377 mmol) and 4 equivalents of TMPP (0.809 g, 1.519 g) were dissolved in 10 mL of acetone to produce a green solution that was stirred at r.t. for 2 hours. After this time the solvent was removed under reduced pressure to yield a pale green residue, which was washed with diethyl ether and dried under vacuum. Dissolution of this solid in 10 mL of THF resulted in the separation of a white solid from a yellow solution; yield of the white solid, [H-TMPP][BF_4]: 0.422 g (45% relative to TMPP). The yellow solution was pumped to a residue and its identity was established as free TMPP by NMR and IR spectroscopies; yield: 0.340 g (42% relative to TMPP).

(2) Reaction of [Ni(NCCH$_3$)$_6$][BF$_4$]$_2$ with 4 TMPP: Preparation of Ni(TMPP-*O*)$_2$ (18)

A quantity of [Ni(NCCH$_3$)$_6$][BF$_4$]$_2$ [6] (0.099 g, 0.207 mmol) was reacted with four equivalents of TMPP (0.441 g, 0.828 mmol) in 8 mL of acetone. The resulting green-brown solution was stirred at r.t. for 24 h, after which time its color had turned red-brown, and the volume was reduced under dynamic vacuum to ~ 4 mL. Addition of diethyl ether (10 mL) induced precipitation of [CH$_3$-TMPP][BF_4] as a dingy white solid. The brown filtrate was decanted from this solid, and subsequently pumped to a residue which was redissolved in THF to give additional [CH$_3$-

TMPP][BF_4] and a brown solution; total yield of [CH_3-TMPP][BF_4]: 0.226 g (43% relative to TMPP). The remaining solution was decanted from the solid, evaporated to a residue and finally dissolved in acetone. After careful layering of hexanes over the acetone solution, red-brown crystals of **18** formed at the bottom of the Schlenk tube within 1 week; yield: 0.121 g (53% relative to Ni^{2+}). Anal. Calc'd for $NiP_2O_{18}C_{52}H_{60}$: C: 57.11; H: 5.53; Found: C: 56.92; H: 5.68; electronic spectrum (acetone, λ_{max} (nm); ε, $M^{-1}cm^{-1}$): 598(sh), 470(1050), 377(sh); FAB-mass spectrum: m/z = 1093 (corresponding to [Ni(TMPP-*O*)$_2$]$^+$); cyclic voltammetry: $(E_{1/2})_{ox}$ = - 0.07 V (vs. Ag/AgCl).

(3) Chemical oxidation of Ni(TMPP-*O*)$_2$ (18) with [Cp_2Fe][BF_4]

An amount of **18** (0.031 g, 0.029 mmol) was reacted with one equivalent of ferrocenium (0.008 g, 0.029 mmol) in 10 mL of acetone. A color change from red-brown to dark green immediately ensued. The solution was stirred at r.t. for 30 min., after which time it was evaporated to a residue, washed with a copious amount of diethyl ether (3 x 10 mL) and dried *in vacuo*; yield: 0.026 g (78% relative to **18**). Anal. Calc'd for $NiP_2O_{18}C_{52}H_{60}BF_4$: C: 52.91; H: 5.12: Found: C: 52.54; H: 5.20. X-ray quality crystals were grown by slow evaporation of a Me-THF/CH_2Cl_2 solution of **19**. UV-visible (CH_2Cl_2, λ_{max} (nm); ε, $M^{-1}cm^{-1}$): 704(sh), 620(sh), 444(6500), 370(sh); cyclic voltammetry: $(E_{1/2})_{red}$ = - 0.07 V; FAB-mass spectrum: m/z = 1093; IR: ν(B-F) = 1057(br, s) and 520(m) cm^{-1}; magnetic moment: μ_{eff} = 2.13 μ_B.

(4) Reaction of Ni(TMPP-*O*)$_2$ (18) with O_2

A sample of **18** (0.062 g, 0.056 mmol) was dissolved in 20 mL of acetone and a stream of dry O_2 was passed through this solution for *ca.* 24 h after which time its color had turned from red-brown to dark green.

Slow diffusion of hexanes into this solution produced a crop of dark green crystals; yield: 0.013 g (21% relative to **18**). This compound was identified as $[Ni^{III}(TMPP\text{-}O)_2][BF_4]$ (**19**) by infrared and UV-visible spectroscopies, electrochemistry and preliminary crystal data.

(5) Reactivity of Ni(TMPP-*O*)$_2$ (18) with CO_2

A stream of CO_2 was passed through a solution of **18** (0.021 g, 0.019 mmol) in acetone for *ca.* 2 hours. The solution was allowed to stand under a CO_2 atmosphere at r.t. for another hour. An aliquot of the solution was used to perform an infrared experiment, which revealed only the presence of free carbon dioxide (ν_{CO} at 2330 and 650 cm^{-1}).

B. X-ray Crystal Structures

The structure of complex **18** was determined by applications of general procedures described elsewhere. Geometric and intensity data were collected on a Rigaku AFC6S diffractometer, equipped with graphite monochromated MoK_α(λ_α = 0.71069 Å) radiation. The data were corrected for Lorentz and polarization effects. Calculations were performed on a VAXSTATION 2000 computer using programs from the TEXSAN Crystallographic Package of the Molecular Structure Corporation.

(1) Ni(TMPP-*O*)$_2$ (18)

A red-brown platelet of approximate dimensions 0.15 x 0.44 x 0.59 mm^3 was mounted at the end of a glass fiber with the use of epoxy cement and placed in a cold N_2(g) stream at - 90 ± 2° C. A preliminary triclinic unit cell was determined by centering and indexing on 20 intense reflections. The cell was then further refined by a least-squares determination of 24 reflections in the range $19 \leq 2\theta \leq 30°$. Intensity data

were collected over the range 4 - 47° in 2θ by the θ - 2θ scan mode. Three standard reflections were measured at regular intervals during data collection and showed no decay. After averaging equivalent reflections, 4605 unique data remained, of which 2875 were observed with $F_o^2 \geq 3\sigma(F_o)^2$. The position of the metal atom was determined from a solution provided by the direct methods program in SHELXS-86. The positions of the remaining non-hydrogen atoms were located by the program DIRDIF. An empirical absorption correction was applied using the program DIFABS. After isotropic convergence had been achieved, all of the non-hydrogen atoms were refined anisotropically. The hydrogen atoms were generated by programs in the solution package and were included in the structure factor calculations but not refined. The final full-matrix refinement involved 2875 data and 367 parameters. The refinement converged with residuals R and R_w of 0.062 and 0.108, respectively, and a quality-of-fit indicator of 2.77. The final difference Fourier map showed the highest peak to be 0.51 $e^-/Å^3$ and the final shift/esd was 0.01. Important crystallographic data are listed in Table 17.

(2) [Ni(TMPP-*O*)$_2$][BF$_4$] (19)

A dark green parallelepiped was carefully selected and mounted at the end of a glass fiber with Dow Corning silicone grease and placed in a N_2 cold stream at -100 ± 2°C. A preliminary triclinic cell was determined by centering and indexing 20 reflections and this cell was further refined by a least-squares fit of 10 reflections with $20 \leq 2\theta \leq 25°$. Unfortunately we were not able to continue with a full data collection due to the poor quality of the crystals. The final refined cell parameters were as follows: a = 14.591(6) Å, b = 18.458(6) Å, c = 12.468(5) Å, α = 97.66(3)°, β = 108.58(3)°, γ = 73.36(3)° and V = 3046(3) Å^3 and Z = 2.

Table 17. Crystallographic data for Ni(TMPP-*O*)$_2$ (18)

Formula	$NiP_2C_{58}O_{20}H_{72}$
Formula weight	1209.84
Space group	P-1
a, Å	12.218(4)
b, Å	12.829(3)
c, Å	11.940(4)
α, deg	114.84(2)
β, deg	114.85(2)
γ, deg	93.71(3)
V, Å^3	1473(1)
Z	1
d_{calc}, g/cm^3	1.363
μ (MoK$_\alpha$), cm^{-1}	7.976
Data collection range, 2θ, deg	4 - 47
Number of unique data	4605
total with $F_o^2 \geq 3\sigma(F_o)^2$	2875
Number of parameters refined	367
R[a]	0.062
R_w[b]	0.108
Quality-of-fit	2.77
Largest shift/esd, final cycle	0.01
Largest peak, e$^-$/Å^3	0.51

[a] $R = \Sigma||F_o|-|F_c||/\Sigma|F_o|$; [b] $R = [\Sigma(w|F_o|-|F_c|)^2/\Sigma w|Fo|^2]^{1/2}$; $w = 1/\sigma^2(|Fo|)$

[c] Quality-of-fit = $[\Sigma(w|F_o|-|F_c|)^2/(N_{obs}-N_{parameters})]^{1/2}$

3. Results and Discussion

A. Synthetic Approach

The reactions of the Ni(II) aqua cation $[Ni(H_2O)_6]^{2+}$ with 2 or 4 equivalents of TMPP yield [H-TMPP][BF_4] as the major phosphine-containing product; we were not able to isolate any metal-containing species. These results are perhaps not unexpected in view of our previous work with the Co(II) solvated cations, in which we showed that any source of H^+ would promote the formation of the protonated phosphine [H-TMPP]$^+$ (see Chapter IV). However, if one uses the same synthetic approach that was successful in the preparation of Co(TMPP-*O*)$_2$, a stable bis-phosphino-phenoxide complex of Ni(II) is obtained. Indeed, the reaction of $[Ni(NCCH_3)_6][BF_4]_2$ with 4 equivalents of TMPP in acetone yields the neutral compound Ni(TMPP-*O*)$_2$ (**18**), along with the anticipated quantity of [CH_3-TMPP][BF_4] as the by-product.

B. Molecular Structure of Ni(TMPP-*O*)$_2$ (18)

The ORTEP drawing of Ni(TMPP-*O*)$_2$ (**18**) depicted in Figure 32 clearly shows that the Ni(II) center, which lies on a crystallographic inversion center, is ligated by two phosphorus atoms in a *trans* disposition and two oxygen atoms from the demethylated ortho-methoxy groups, engendering an overall square-planar geometry. The Ni(1)-P(1) distance of 2.232(3) Å is somewhat shorter than those values normally observed for *trans*-$NiX_2(PR_3)_2$ complexes, which range from 2.23 to 2.32 Å [7], but is longer than the corresponding value in $Ni[Ph_2PCH_2C(CF_3)_2O]_2$ (2.193(3) Å) [5]. The short Ni-P bond in the latter structure was rationalized on the basis of a strong σ-donation from the phosphorus lone pair combined with electron withdrawal from the nickel atom to the two fluorine-containing alkoxide ligands; this is likely to be occurring in the present case but to a

Figure 32. ORTEP drawing for Ni(TMPP-*O*)$_2$. All phenyl-group atoms are represented as small circles for clarity, whereas all other atoms are represented by their 50% probability ellipsoids.

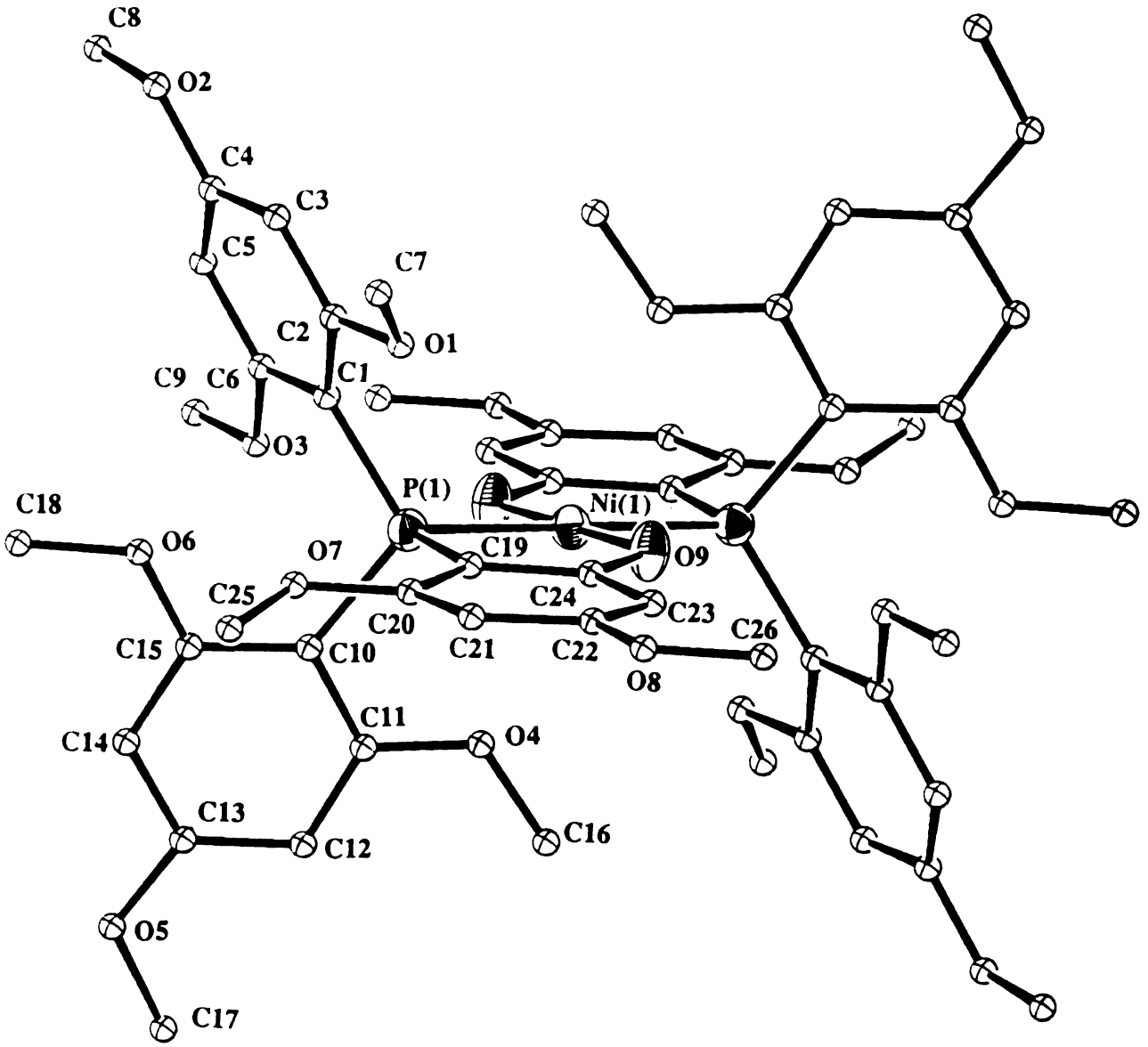
C8
O2
C4
C3
C5
C7
C2
O1
C9
C6
C1
O3
P(1)
Ni(1)
C18
O6
O7
C19
O9
C25
C24
C23
C26
C20
C15
C10
C21
C22
O8
C11
C14
O4
C13
C16
C12
O5
C17

Figure 32.

lesser extent. The Ni-O bond length of 1.856(5) Å also falls short of the reported range for square planar nickel(II) compounds (1.85 - 1.93 Å) [8], but is similar to that found in the aforementioned structure of $Ni[Ph_2PCH_2C(CF_3)_2O]_2$ (1.839(2) Å). There is essentially no axial interaction between the nickel center in the present structure and pendent methoxy groups. The closest contact is between Ni(1) and O(4) at 2.78 Å which is outside any expected range for covalent radii bonding. The P(1)-Ni(1)-O(9) and P(1)-Ni(1)-O(9)' angles are 87.6(2)° and 92.4(2)°, respectively, allowing for an almost perfect square planar geometry about the metal center. The O(9)-Ni-P(1) angle of 78.6(2)° demonstrates the extreme flexibility of the TMPP ligand, which has also been shown to adopt chelating O-M-P angles ranging from 71.6(2)° [9] to 107.1(1)° [10]. Interestingly comparison with the recently reported *cis*-bis(diphenylphosphino-enolate) $[Ni(Ph_2PCH{=}COR)_2]$ suggests that the trans disposition of the ligands dramatically affects the Ni-P bond distance in the present structure, with the Ni-P being considerably shorter in the aforementioned compound (2.185(1) versus 2.232(3) Å) [11].

Another interesting feature of this structure can be seen in the three-dimensional packing diagram presented in Figure 33. As it is often the case for d^8 square-planar structures, a stacking of the molecules is observed, but it does not consist of a stacking along the z axis via overlap of the d_{z^2} orbitals, but of the phenyl rings of the TMPP ligand, and this in all three directions. The perfect ordering of the crystal structure certainly explains the great stability of this compound in the solid state, even after loss of the solvent of crystallization.

A selection of bond distances and angles is listed in Table 18.

Table 18. Selected Bond Distances (Å) and Angles (deg) for Ni(TMPP-*O*)$_2$ (18)

Atom 1	Atom 2	Bond Distance
Ni(1)	P(1)	2.232(3)
Ni(1)	O(9)	1.856(5)
P(1)	C(1)	1.841(8)
P(1)	C(10)	1.834(8)
P(1)	C(19)	1.807(8)

Atom 1	Atom 2	Atom 3	Bond Angle
P(1)	Ni(1)	P(1)'	180.00
P(1)	Ni(1)	O(9)	87.6(2)
P(1)	Ni(1)	O(9)'	92.4(2)
O(9)	Ni(1)	O(9)'	180.00
Ni(1)	P(1)	C(1)	115.8(3)
Ni(1)	P(1)	C(10)	115.5(3)
Ni(1)	P(1)	C(19)	97.7(3)
C(1)	P(1)	C(10)	109.9(4)
C(1)	P(1)	C(19)	111.9(4)
C(10)	P(1)	C(19)	105.0(4)

Figure 33. Three-dimensional packing diagram for Ni(TMPP-*O*)$_2$.

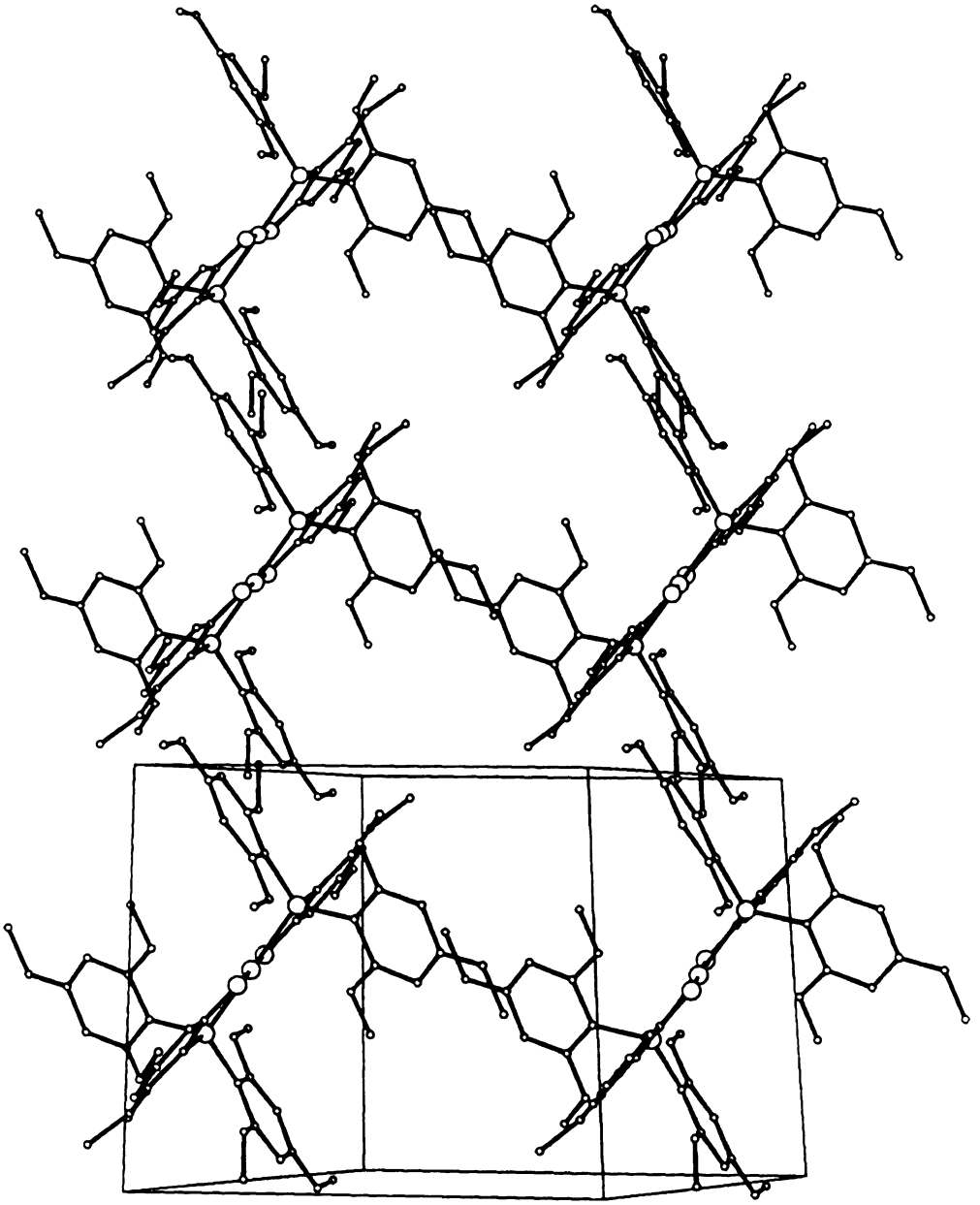

Figure 33.

C. Magnetic properties of Ni(TMPP-*O*)$_2$ (18)

The ^{1}H NMR spectrum of a pure crystalline sample of Ni(TMPP-*O*)$_2$ (**18**) reveals a mixture of diamagnetic and paramagnetic complexes in solution, leading us to conclude that an equilibrium exists between square-planar and tetrahedral solution structures. This phenomenon has been noted in the literature for Ni(II) complexes both in the solid state and in solution [2f,4,11,12,17]. A solid state magnetic susceptibility study of **18** in the 5 - 300 K temperature range revealed diamagnetism at low temperature (5 - 80 K, $\mu \leq 0.80\ \mu_B$) and paramagnetism from 80 to 300 K. We were not completely satisfied with this result, thus we carried out an epr study of this compound. The solid-state spectrum at room temperature is featureless as expected for a diamagnetic compound.

D. Electrochemical and Chemical Oxidation of the Ni(II) to the Ni(III) Complex

Of utmost importance in this work is the discovery that Ni(TMPP-*O*)$_2$ (**18**) exhibits a very accessible and reversible oxidation at - 0.07 V as first demonstrated by cyclic voltammetry (Figure 34). Chemical oxidation was carried out in acetone with one equivalent of ferrocenium to produce [Ni^{III}(TMPP-*O*)$_2$][BF$_4$] (**19**) in high yield. Compound **19** is a remarkably stable Ni(III) complex in striking contrast to most previously reported examples [13]. As expected in the case of an authentic reversible redox couple, compound **19** exhibits a reversible reduction at - 0.07 V under the same experimental conditions. The Ni(III) species can also be obtained by the reaction of Ni^{II}(TMPP-*O*)$_2$ (**18**) with molecular oxygen. We had noted quite accidentally that solutions of **18** left in contact with air would turn from a brown to a dark green color, characteristic of the Ni(III) complex, and that their electronic spectrum was identical to that of **19**. The

Figure 34. Cyclic voltammogram of Ni(TMPP-*O*)$_2$ in 0.1M $TBABF_4$ in CH_2Cl_2.

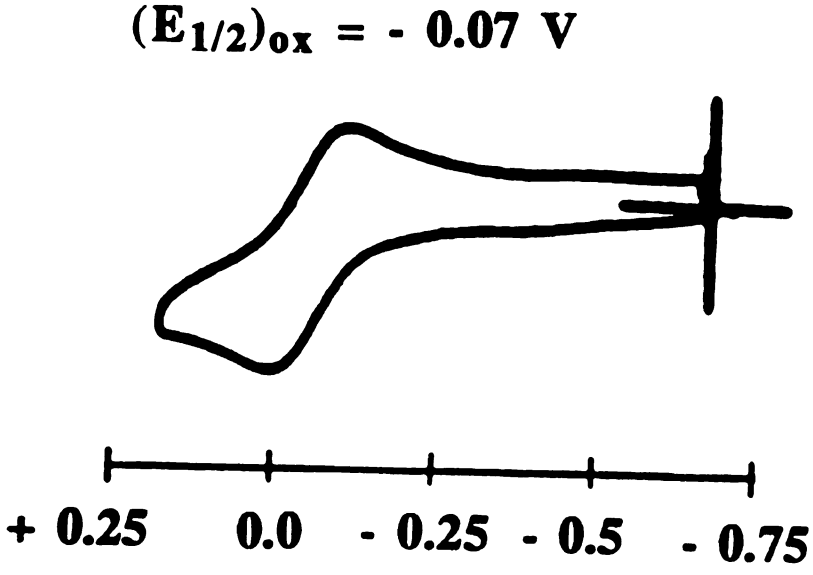

Figure 34.

deliberate purging of an acetone solution of **18** with dry oxygen for about 1 day, followed by the layering of hexanes atop resulted in the formation of dark green crystals of the Ni(III) compound. The identity of the product was confirmed by UV-visible spectroscopy, cyclic voltammetry, elemental analysis as well as by the determination of the preliminary unit cell. The source of the $[BF_4]^-$ anion is likely to be the presence of $[CH_3$-TMPP$][BF_4]$ as a contaminant in the starting material and this explains the rather low yield of the species (~20%). Deliberate addition of a counterion, in the form of $NaPF_6$ for example, during the oxygen reaction definitively ought to be tested.

E. Magnetic Properties of $[Ni^{III}$(TMPP-*O*)$_2][BF_4]$ (19)

The ^1H NMR spectrum of $[Ni^{III}$(TMPP-*O*)$_2][BF_4]$ is broad and featureless as expected for a d^7, odd-electron complex. The paramagnetism of compound **19** is supported by variable temperature magnetic susceptibility measurements, carried out in the range 5 - 300 K. The magnetism follows a Curie-Weiss behavior, with $\mu_{eff} = 2.13\ \mu_B$, which is consistent with a S = 1/2 (d^7, low-spin) system and Figure 35 shows a plot of the molar susceptibility χ_m versus 1/T. The epr spectrum is shown in Figure 36 and is typical of a d_z^2 ground state for an axially elongated octahedral d^7 complex [14], with g values of $g_\perp = 2.28$ and $g_{//} = 2.04$ and an hyperfine coupling to the phosphorus center (I = 1/2) of $A_{//} = 8$ G. These results are in agreement with a participation of the axial ether groups in a bonding interaction with the Ni(III) metal center, since a purely square planar geometry would require $g_{//} > g_\perp$ [14].

4. Summary

The use of the unusual tris(2,4,6-trimethoxyphenyl)phosphine (TMPP) has allowed for the stabilization of Ni(II) and Ni(III) centers with

Figure 35. Plot of the molar magnetic susceptibility χ_m versus 1/T for [Ni(TMPP-*O*)$_2$][BF_4].

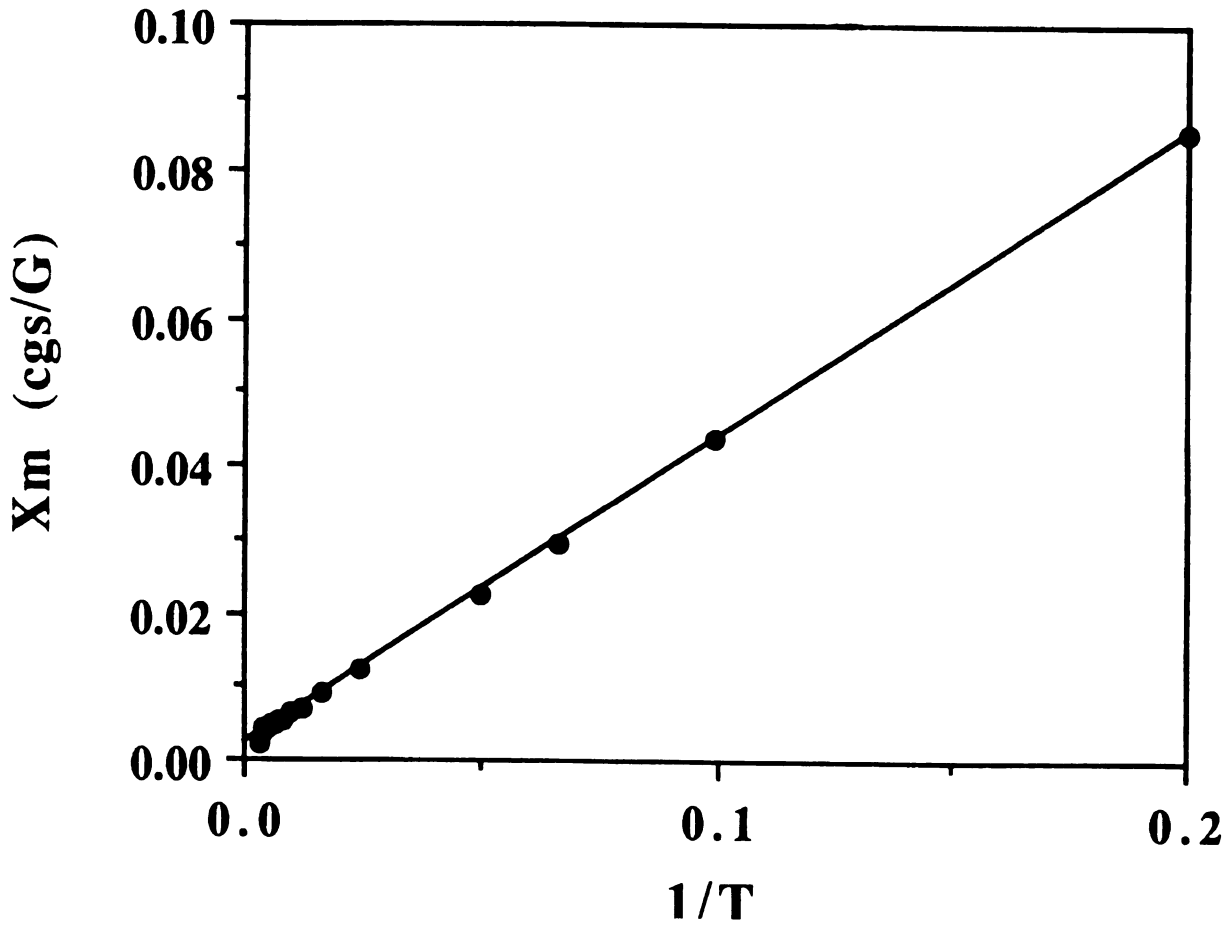

Figure 35.

Figure 36. EPR spectrum of [Ni(TMPP-*O*)$_2$][BF_4] at 110 K in a Me-THF/CH_2Cl_2 glass.

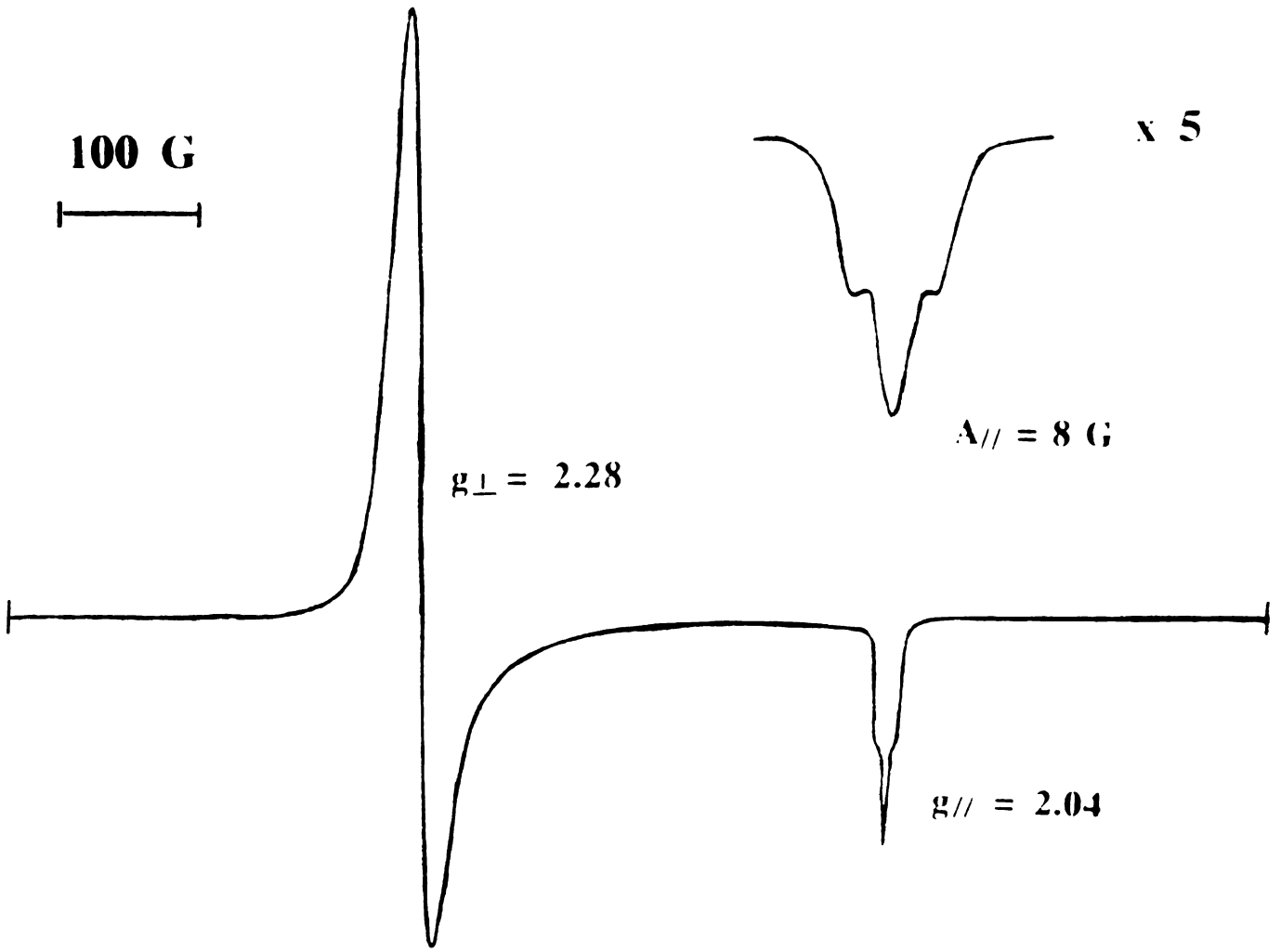

Figure 36.

an identical ligand set. The chemistry of low-valent nickel (0 to +2) with phosphines, especially (P,O) ligands, is quite rich due to the use of nickel phosphine complexes in homogeneous catalysis [1,2f], but the chemistry of higher valent nickel (+3 and higher) with soft donor ligands has not been extensively developed [15]. In fact, the domain of investigation has been primarily that of the bioinorganic chemists who employ biologically relevant ligands with sulfur or nitrogen donors [16]. The present work is a unique example of how the use of a bulky phosphino-phenoxide ligand can link two distinct areas of inorganic chemistry that are not ordinarily associated, thereby opening new avenues into the chemistry of Ni(III).

LIST OF REFERENCES

1. (a) Keim, W. *Chem. Ing. Techn.* **1984**, *56*, 850. (b) Klabunde, U.; Ittel, S. D. *J. Molec. Catal.* **1987**, *41*, 123. (c) Keim, W.; Behr, A.; Gruber, B.; Hoffmann, B.; Kowaldt, F. H.; Kürschner, U.; Limbäcker, B.; Sistig, F. *Organometallics* **1986**, *5*, 2356. (d) Huang, Q.; Xu, M.; Qian, Y.; Xu, W.; Shao, M.; Tang, Y. *J. Organomet. Chem.* **1985**, *287*, 419.

2. (a) Braunstein, P.; Matt, D.; Nobel, D.; Balegroune, F.; Bouaoud, S.-E.; Grandjean, D.; Fisher, J. *J. Chem. Soc., Dalton Trans.* **1988**, 353. (b) Hill, W. E.; Taylor, J. G.; Muir, K. W.; Manojlovic-Muir, L. *J. Chem. Soc., Dalton Trans.* **1982**, 833. (c) Greene, P. T.; Sacconi, L. *J. Chem. Soc. (A)* **1970**, 866. (d) Sacconi, L.; Dapporto, P. *J. Am. Chem. Soc.* **1970**, *92*, 4133. (e) Jarolim, T.; Podlahova, J. *J. Inorg. Nucl. Chem.* **1976**, *38*, 125. (f) Lindner, E.; Dettinger, J. *Z. Naturforsch.* **1991**, *46b*, 432.

3. (a) Ciampolini, M.; Dapporto, P.; Dei, A.; Nardi, N.; Zanobini, F. *Inorg. Chem.* **1982**, *21*, 489. (b) Ciampolini, M. Dapporto, P.; Nardi, N.; Zanobini, F. *Inorg. Chem.* **1983**, *22*, 13. (c) Mealli, C.; Sabat, M.; Zanobini, F.; Ciampolini, M.; Nardi, N. *J. Chem. Soc., Dalton Trans.* **1985**, 479. (d) Ciampolini, M.; Nardi, N.; Orioli, P. L.; Mangani, S.; Zanobini, F. *J. Chem. Soc., Dalton Trans.* **1985**, 1425. (e) Lewis, G. E.; Kraihanzel, C. S. *Inorg. Chem.* **1983**, *22*, 2895.

4. (a) Empsall, H. D.; Shaw, B. L.; Turtle, B. L. *J. Chem. Soc., Dalton Trans.* **1976**, 1500. (b) Moulton, C. J.; Shaw, B. L. *J. Chem. Soc., Dalton Trans.* **1980**, 299.

5. Boeré, R. T.; Montgomery, C. D.; Payne, N. C.; Willis, C. J. *Inorg. Chem.* **1985**, *24*, 3680.

6. Hathaway, B. J.; Holah, D. G.; Underhill, A. E. *J. Chem. Soc.* **1962**, 2444.

7. (a) Stalick, J. K.; Ibers, J. A. *Inorg. Chem.* **1970**, *9*, 453. (b) Scatteron, V.; Turzo, A. *J. Inorg. Nucl. Chem.* **1958**, *8*, 447. (c) Watkin, D. J. *J. Chem. Soc., Dalton Trans.* **1976**, 1803. (d) McPhail, A. T.; Steele, J. C. M. *J. Chem. Soc. (A)* **1972**, 2680. (e)

Jiang, F.; Wei, G.; Lei, X.; Huang, Z.; Hong, M.; Liu, H. *J. Chem. Res. (S)* **1991**, 238; *(M)* **1991**, 2356.

8. Fox, M. R.; Lingafelter, E. C.; Sacconi, L. *Acta Cryst.* **1964**, *17*, 1159.

9. Dunbar, K. R.; Haefner, S. C.; Burzynski, D. J. *Organometallics* **1990**, *9*, 1347.

10. Dunbar, K. R.; Haefner, S. C.; Pence, L. E. *J. Am. Chem. Soc.* **1989**, *111*, 5504.

11. Georgiev, E. M.; Dieck, H. T.; Fendesak, G.; Hahn, G.; Petrov, G.; Kirilov, M. *J. Chem. Soc., Dalton Trans.* **1992**, 1311.

12. Van Hecke, G. R.; Horrocks, W. DeW. *Inorg. Chem.* **1966**, *5*, 1968.

13. Escuer, A.; Ribas, J.; Vicente, R.; Faulmann, C.; de Montauzon, D.; Cassoux, P. *Polyhedron* **1991**, *10*, 2025.

14. (a) Haines, J.; McAuley, A. *Coord. Chem. Rev.* **1981**, *39*, 94. (b) Lappin, A. G.; McAuley, A. *Adv. Inorg. Chem.* **1988**, *32*, 241.

15. (a) Gray, L. R.; Higgins, S. J.; Levason, W.; Webster, M. *J. Chem. Soc., Dalton Trans.* **1984**, 459. (b) Hanton, L. R.; Evans, J.; Levason, W.; Perry, R. J.; Webster, M. *J. Chem. Soc., Dalton Trans.* **1991**, 2039.

16. (a) Holm, R. H.; Krüger, H.-J. *Inorg. Chem.* **1987**, *26*, 3647. (b) Castro, B.; Freire, C. *Inorg. Chem.* **1990**, *29*, 5113. (c) Choudhury, S. B.; Ray, D.; Chakravorky, A. *Inorg. Chem.* **1990**, *29*, 4603. (d) Krüger, H.-J.; Peng, G.; Holm, R. H. *Inorg. Chem.* **1991**, *30*, 734.

17. Frömmel, T.; Peters, W.; Wunderlich, H.; Kuchen, W. *Angew. Chem. Int. Ed. Engl.* **1992**, *31*, 612.

CHAPTER VI

REACTIONS OF TRIS(2,4,6-TRIMETHOXYPHENYL)PHOSPHINE WITH VANADIUM, CHROMIUM AND MANGANESE HALIDES

1. Introduction

Phosphine chemistry has been heavily investigated by inorganic and organometallic chemists for more than twenty years, primarily because of their ability to stabilize metal centers in low oxidation states [1]. The synergistic σ-donor and π-acceptor properties, as well as steric effects, play a major role in the coordination of phosphines to transition elements. The complexes thus formed exhibit an enhanced reactivity toward small molecules such as N_2, O_2, CO or C_2H_4 and therefore can be of great interest for homogeneous catalysis [2]. Our contribution in this domain has been centered on the study of the coordination chemistry of tris(2,4,6-trimethoxyphenyl)phosphine (TMPP) with 3d metals such as vanadium, chromium and manganese. In general, the large atomic radii and the relatively electropositive nature of low-valent transition metals suggest that electron-donating phosphines would be good ligands. First-row metal cations however, are much smaller hard acids than their second and third row conjugers, therefore are not as compatible with the soft tertiary phosphines. Our goal was to synthesize highly coordinatively unsaturated complexes with TMPP, and we rationalized that this could be achieved due to the chelating ability of this phosphine, and that loose oxygen-metal interactions could easily be cleaved in solution, leaving vacant coordination sites.

Despite their insolubility in common solvents, the commercial availability of first-row transition metal halides, MX_2 or MX_3, as well as the easy access to partially solvated compounds such as $MX_3(THF)_3$, prompted us to use them in our study of the coordination chemistry of TMPP, along with the fact that compounds of the type $MX_n(PR_3)_x$

constitute excellent starting materials for the investigation of low-valent organometallic complexes of 3d metals [3].

2. Experimental

(1) Reaction of VCl_3 with TMPP

A sample of anhydrous vanadium trichloride (0.156 g, 0.931 mmol) was reacted with one equivalent of TMPP (0.496 g, 0.931 mmol) in *ca.* 20 mL of benzene. The resulting purple solution was stirred at room temperature for 10 days, after which time the solvent was removed under dynamic vacuum to yield a pale grey residue. The solids were washed with 10 mL of THF and dried *in vacuo*, yield: 0.072 g. ^{1}H NMR (CD_3CN, δppm): 3.67 (s, 18 H, *o*-O$\underline{CH_3}$), 3.86 (s, 9 H, *p*-O$\underline{CH_3}$), 6.25 (d, 6 H, *m*-$\underline{H}$, $^{P,H}J$ = 6.25 Hz) and 8.38 (d, 1 H, P-$\underline{H}$, $^{P,H}J$ = 543 Hz) corresponding to [H-TMPP]$^+$ and 3.50 (s, 18 H, *o*-O$\underline{CH_3}$), 3.80 (s, 9 H, *p*-O$\underline{CH_3}$), 4.88 (d, 2 H, -$\underline{CH_2}$Cl, $^{P,H}J$ = 9 Hz) and 6.22 (d, 6 H, *m*-$\underline{H}$, $^{P,H}J$ ~ 6 Hz) corresponding to [$ClCH_2$-TMPP]$^+$ in approximately a 6:1 ratio.

(2) Reaction of $CrCl_3$ with TMPP

A quantity of $CrCl_3$ (0.150 g, 0.950 mmol) was added to one equivalent of TMPP (0.5062 g, 0.950 mmol) in 10 mL of carefully deoxygenated benzene to give a purple solution which was stirred at room temperature for about 6 days. Evaporation of the solvent yielded a pink-purple solid which was washed with benzene (10 mL) followed by THF (10 mL) and dried *in vacuo*, yield: 0.040 g. ^{1}H NMR (CD_3CN, δppm): 3.67 (s, 18 H, *o*-O$\underline{CH_3}$), 3.86 (s, 9 H, *p*-O$\underline{CH_3}$), 6.25 (d, 6 H, *m*-$\underline{H}$, $^{P,H}J$ = 5 Hz) and 8.38 (d, 1 H, P-$\underline{H}$, $^{P,H}J$ = 542 Hz) corresponding to [H-TMPP]$^+$ and 2.47 (d, 3 H, P-$\underline{CH_3}$, $^{P,H}J$ = 15 Hz), 3.54 (s, 18 H, *o*-O$\underline{CH_3}$), 3.86 (s, 9 H, *p*-O$\underline{CH_3}$) and 6.22 (d, 6 H, *m*-$\underline{H}$, $^{P,H}J$ ~ 6 Hz) corresponding to [CH_3-

TMPP]$^+$ in approximately a 4:1 ratio. Infrared (CsI, nujol; cm-1): 320 (s) (ν Cr-Cl).

(3) Reaction of $CrCl_3(THF)_3$ with TMPP

$CrCl_3(THF)_3$ was prepared as reported in the literature [4]. A sample of this partially solvated compound (0.279 g, 0.746 mmol) was added to one equivalent of TMPP (0.397 g, 0.746 mmol) in 20 mL of THF. The resulting purple solution was stirred at room temperature for *ca.* 24 hours during which time a pale purple solid precipitated from solution. The solvent was decanted from the solid, which was washed with THF (3 x 10 mL) and benzene (3 x 10 mL) and dried *in vacuo*, yield: 0.175 g. The ^{1}H NMR spectrum is identical to the one described for the previous reaction and the infrared spectrum exhibits two Cr-Cl stretching modes at 345 (s) and 290 (w) cm^{-1}.

(4) Reaction of CrI_2 with TMPP

Anhydrous CrI_2 (0.230 g, 0.752 mmol) was added to one equivalent of TMPP (0.400 g, 0.752 mmol) in 10 mL of ethanol to produce a dark green solution. After *ca.* two hours a grey solid had deposited at the bottom of the flask (yield: 22 mg). The solution was filtered through a sintered glass filter under argon and dried to give a green residue, which was subsequently washed with copious amounts of ethanol (3 x 10 mL) and dried under vacuum, yield: 0.389 g. ^{1}H NMR (CD_3CN, δ ppm): 3.67 (s, 18 H, *o*-O$\underline{CH_3}$), 3.85 (s, 9 H, *p*-O$\underline{CH_3}$), 6.25 (d, 6 H, *m*-$\underline{H}$, $^{P,H}J$ = 5 Hz) and 8.37 (d, 1 H, P-$\underline{H}$, $^{P,H}J$ = 537 Hz) corresponding to [H-TMPP]$^+$. The infrared spectrum of this product does not contain a band due to a Cr-I stretch.

(5) Reaction of $MnCl_2$ with one equivalent of TMPP

An amount of anhydrous $MnCl_2$ (0.119 g, 0.948 mmol) was reacted with one equivalent of TMPP (0.505 g, 0.948 mmol) in 15 mL of THF. The resulting pale pink suspension was stirred at room temperature for *ca.* 24 hours after which time the solution was decanted and the solid washed with several aliquots of THF and dried under vacuum; yield, 0.311 g. The product is insoluble in THF, toluene and benzene and slightly soluble in CH_3CN. ^1H NMR (CD_3CN, δppm): 3.43 (broad), 3.75 (broad), 6.05 (broad); infrared (CsI, nujol; cm^{-1}): 288(s), 275(m) (ν_{Mn-Cl}); electronic spectrum (CH_3CN; λ, nm): 288(sh), 260, 198; cyclic voltammetry: $E_{p,a}$ = + 0.49 V; magnetic data: μ_{eff} = 5.5 μ_B; FAB-mass spectrum: m/z 533 ([TMPP]$^+$).

(6) Reaction of $MnCl_2$ with two equivalents of TMPP

$MnCl_2$ (0.072 g, 0.572 mmol) was reacted with two equivalents of TMPP (0.610 g, 1.145 mmol) in 20 mL of diethyl ether to produce a thick white suspension during a 24 hours period. After this time, the solvent was decanted from the white solid, which was washed with diethyl ether and dried under vacuum, yield: 0.559 g. ^1H NMR (CD_3CN, δppm): 3.44 (s, 18 H, *o*-O<u>CH</u>$_3$), 3.75 (s, 9 H, p-O<u>CH</u>$_3$), 6.05 (d, 6 H, *m*-<u>H</u>, $^{P,H}J$ ~ 5 Hz) corresponding to free TMPP and small resonances corresponding to [H-TMPP]$^+$.

3. Results and Discussion

The reactions of MX_n (M = V, Cr; n = 3 and X = Cl; M = Cr, n = 2, X = I) or $MCl_3(THF)_3$ (M = Cr) with one equivalent of TMPP in aprotic solvents such as benzene produce phosphonium salts of general formula [H-TMPP][MX_4] as established by infrared and ^1H NMR

spectroscopies. In some cases, the presence of the methyl- and chloromethylphosphonium cations can also be detected, revealing that redistribution of chloride and/or demethylation of the phosphine is occurring. Tetrachlorometallate salts of first-row transition elements are ubiquitous [5], and the very nature of the phosphine ligand, in particular its extreme basicity, renders the stabilization of the metal center by such a soft ligand very difficult. It was our rationale that the presence of methoxy substituents on the phenyl rings of the phosphine would increase its compatibility with (hard) early transition metals such as chromium and vanadium. Several years ago, Girolami had shown that the use of bidentate diphosphines such as dippe or dmpe, allowed for the stabilization of complexes of general formula $MX_2(P\sim P)_n$ (X = Cl, Br; n = 1, 2) with a variety of 3d elements [6c], thus the demonstrated chelating ability of TMPP prompted us to investigate its reactivity with Cr and V.

The chemistry of low-valent vanadium is still very little characterized, due in part to the lack of suitable starting materials [6a], and $VCl_2(dmpe)_2$ and $VBr_2(dippe)$ are the only two structurally characterized V(II)-phosphine complexes [6a]. Vanadium(II) complexes are of interest as potential catalysts for the polymerization of ethylene [6] as well as for the study of their reactivity with small molecules (O_2, N_2, CO) [7]. Recently, Gambarotta reported the first dinitrogen-V(II) adduct [8] and earlier this year, the structure of *trans*-$[V(N_2)(dppe)_2]^-$ was published [9]. We investigated the chemistry of TMPP with V(II) starting materials such as VBr_2 and $[V(NCCH_3)_6]^{2+}$ but could not isolate any tractable products from these reactions. The chemistry of vanadium(III) with phosphines has been widely investigated, but only two monodentate phosphine complexes, $VCl_3(PMePh_2)_2$ and $VCl_3(PEt_3)_2$, were reported [10,11]. It was therefore

our contention that the bulk of TMPP would allow for the stabilization of a V(III)-TMPP adduct. Nevertheless the only isolable products in this chemistry were [H-TMPP]$^+$ and [$ClCH_2$-TMPP]$^+$ and it was not possible to identify the metal-containing anion (probably [VCl_4]$^-$).

Many phosphine adducts of Cr(III) are known, with either monodentate phosphines as in $CrCl_3(PHEt_2)_3$ [12], $[CrCl_3(PR_3)]_n$ (R = Ph, *n*-Bu) [13], bidentate as in $CrCl_3(dppe)(H_2O)$ [14], $CrCl_3$(dippe) [6c], or tridentate as in $CrCl_3$(tripod) [15]. The latter compound is an example of the tridentate capping mode that we expected to observe for a "$CrCl_3$(TMPP)" complex, this particular coordination mode having been previously observed in our earlier work with (η^3-TMPP)$Mo(CO)_3$ [16]. As in the V(III) chemistry we were not able to isolate anything other than salts of general formulae [H-TMPP][$CrCl_4$] or [CH_3-TMPP][$CrCl_4$]. Although Cr(II) seems to be more compatible with TMPP than Cr(III), similar results were obtained.

The equimolar reaction of $MnCl_2$ with TMPP yields a product formulated as "$MnCl_2$(TMPP)" on the basis of infrared spectroscopy and magnetic measurements. Two ν(Mn-Cl) stretching modes are observed in the far-infrared spectrum of "$MnCl_2$(TMPP)" at 288 and 275 cm^{-1}, which can be attributed to the A' and A" vibration modes in the C_s point group. A proposed structure of this compound is shown below:

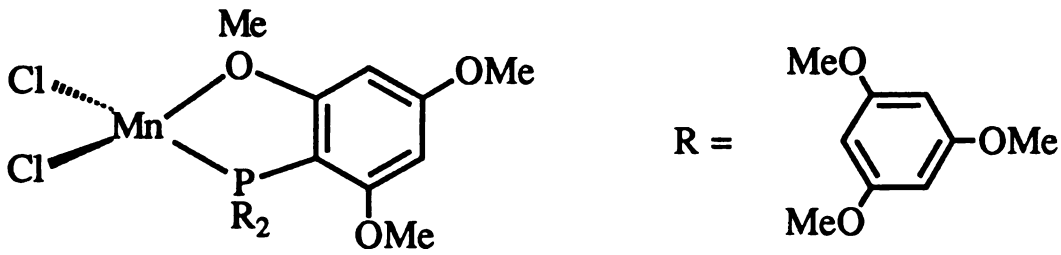

The magnetic susceptibility of $MnCl_2(TMPP)$ was studied over the 5-400 K temperature range and follows a Curie-Weiss behavior with a μ_{eff} = 5.5 μ_B corresponding to a S = 5/2 system (Mn^{2+}, d^5, high-spin). A study of the electrochemistry of a series of Mn(II) complexes with tertiary arylphosphines (including TMPP), namely, $[\{Mn[P(aryl)_3]X_2\}_n]$, was recently published by McAuliffe [17], wherein an irreversible oxidation at + 1.70 V (in CH_2Cl_2 vs. Ag/AgCl) is reported for $[MnCl_2(TMPP)]_n$; this does not agree however, with our results (+ 0.48 V vs. Ag/AgCl in CH_3CN). The interest in the chemistry of Mn(II) halides with tertiary phosphines was sparked by the contention that such complexes could reversibly bind dioxygen and other small molecules [18]. Ten years ago, McAuliffe and coworkers reported a series of complexes of general formula MnX_2L (L = tertiary phosphine), which they claim react *reversibly* with dioxygen. It was then proven that this reversible reaction was actually accompanied by an irreversible ligand oxidation, producing a phosphine oxide complex [19]. It was not until 1989 that a reversible interaction of dioxygen with a MnX_2L complex was identified in an unequivocal manner, by Worley *et al.* The other unsettled aspect of this chemistry was the actual identity of the "Mn(II)-O_2" species, namely was it a superoxo or a peroxo species. Once again, Worley showed that at low temperature a side-on peroxo species was formed, whereas ambient or higher temperature reactions yielded a superoxo species which subsequently decomposed to form a phosphine oxide complex [20]. In view of this interesting and, for the most part, unresolved chemistry, we set out to investigate the reactivity of $MnCl_2(TMPP)$ with molecular oxygen. We found that no reaction occurred under ambient conditions of temperature

and pressure. In addition, the solubility problems encountered hampered all attempts at any further investigations.

4. Summary

The chemistry of TMPP with di- and trihalides of early first-row transition elements such as vanadium and chromium was investigated and resulted primarily in the formation of phosphonium salts. In the case of manganese dichloride, a product, formulated as "$MnCl_2$(TMPP)" was obtained. These data did not agree with those reported by McAuliffe and coworkers [21] and, in our case, no reactivity with molecular oxygen was observed.

From these results, it is apparent that our approach with these metal dihalides is not promising and that, especially in the case of early transition metals, the extreme basicity, and not the bulk, of TMPP is a major drawback. In addition, the readily available Cl^- ions compete with the phosphine ligand for coordination to the metal center. Recently, a new approach to the preparation of $MX_n(L)_m$ (L = tertiary phosphine) complexes was advanced by McAuliffe for a variety of metals [49] that involves the use of coarse-grain metal powder and phosphoranes, $R_3P\text{-}X_2$, according to the following reaction:

$$M + 2\,R_3P\text{-}X_2 \longrightarrow MX_2(PR_3)_2 + X_{2\,(g)}$$

This is a clean route to mononuclear phosphine complexes and should definitively be used in the chemistry of TMPP with early transition elements. Alternatively, the phosphine could be modified so that its

basicity would be decreased, and this could be achieved by changing the number of methoxy substituents on the phenyl ring.

LIST OF REFERENCES

1. McAuliffe, C. A.; Levason, W. *Phosphine, Arsine and Stibine Complexes of the Transition Elements*; Elsevier: New York, **1979**.

2. (a) Alyea, E. C.; Meek, D. W. *Catalytic Aspects of Metal Phosphine Complexes*.; Adv. in Chemistry Series 196; American Chemical Society: Washington, DC, **1982**. (b) Pignolet, L. H. *Homogeneous Catalysis with Metal Phosphine Complexes*; Plenum: New York, **1983**. (c) Kagan, H. B. *Comprehensive Organometallic Chemistry*; Pergamon Press: Oxford, **1982**, vol. 8, p. 464. (d) Parshall, G. W. *Homogeneous Catalysis: Applications and Chemistry of Catalysis by Soluble Transition Metal Complexes*; Wiley: New York, **1980**. (e) Stelzer, O. *Top. Phosphorus Chem.* **1977**, *9*, 1. (f) McAuliffe, C. A. *Comprehensive Coordination Chemistry*; Pergamon Press: Oxford, **1987**, Vol. 2, Ch. 14, p. 989. (g) Lukehart, C. M. *Fundamental Transition Metal Organometallic Chemistry*; Brooks/Cole Publishing Company: Monterey, CA, **1985**, Ch. 13, p. 389.

3. (a) Hermes, A. R.; Girolami, G. S. *Organometallics* **1987**, *6*, 763. (b) Hermes, A. R.; Girolami, G. S. *Organometallics* **1988**, 7, 394. (c) Hermes, A. R.; Moris, R. J.; Girolami, G. S. *Organometallics* **1988**, 7, 2372.

4. Herwig, W.; Zeiss, H. H. *J. Org. Chem.* **1958**, *23*, 1404.

5. Cotton, F. A.; Wilkinson, G. *Advanced Inorganic Chemistry*, 5th Edition; John Wiley, Ed.: New York, **1988**.

6. (a) Girolami, G. S.; Wilkinson, G.; Galas, A. M. R.; Thornton-Pett, M.; Hursthouse, M. B. *J. Chem. Soc., Dalton Trans.* **1985**, 1339. (b) Hermes, A. R.; Girolami, G. S. *Inorg. Chem.* **1988**, *27*, 1775. (c) Hermes, A. R.; Girolami, G. S. *Inorg. Chem.* **1990**, *29*, 313.

7. Hall, V. W.; Schmulbach, C. D.; Soby, W. N. *J. Organomet. Chem.* **1981**, *209*, 69.

8. Edema, J. J. H.; Meetsma, A.; Gambarotta, S. *J. Am. Chem. Soc.* **1989**, *111*, 6878.

9. Rehder, D.; Woitha, C.; Priebsch, W.; Gailus, H. *J. Chem. Soc., Chem. Commun.* **1992**, 364.

10. Bansemer, R. L.; Huffman, J. C.; Caulton, K. G. *Inorg. Chem.* **1985**, *24*, 3003.

11. Issleib, K.; Fröhlich, H. O. *Z. Anorg. Allg. Chem.* **1959**, *298*, 84.

12. Issleib, K.; Döll, G. *Z. Anorg. Allg. Chem.* **1960**, *305*, 1.

13. Bennett, M. A.; Clark, R. J. H.; Goodwin, A. D. *J. Chem. Soc. (A)* **1970**, 541.

14. Gray, L. R.; Hale, A. L.; Levason, W.; McCullough, F. P.; Webster, M. *J. Chem. Soc., Dalton Trans.* **1984**, 47.

15. Arif, A. M.; Hefner, J. G.; Jones, R. A.; Whittlesey, B. R. *Inorg. Chem.* **1986**, *25*, 1080.

16. Dunbar, K. R.; Haefner, S. C.; Burzynski, D. J. *Organometallics* **1990**, *9*, 1347.

17. Li, G. Q.; McAuliffe, C. A.; Mackie, A. G., Mac Rory, P. P.; Ndifon, P. T. *J. Chem. Soc., Dalton Trans.* **1992**, 1297.

18. (a) Levason, W.; McAuliffe, C. A. *J. Chem. Soc., Dalton Trans.* **1973**, 455. (b) Casey, S.; Levason, W.; McAuliffe, C. A. *J. Chem. Soc., Dalton Trans.* **1974**, 886. (c) Levason, W.; McAuliffe, C. A. *J. Inorg. Nucl. Chem.* **1975**, *37*, 340. (d) Jones, M. H.; Levason, W.; McAuliffe, C. A.; Parrott, M. J. *J. Chem. Soc., Dalton Trans.* **1976**, 1642. (d) Hosseiny, A.; McAuliffe, C. A.; Minten, K.; Parrott, M. J.; Pritchard, R.; Tames, J. *Inorg. Chim. Acta* **1980**, *39*, 227. (e) Hosseiny, A.; Mackie, A. G.; McAuliffe, C. A.; Minten, K. *Inorg. Chim. Acta* **1981**, *49*, 99. (f) Howard, C. G.; Wilkinson, G.; Thornton-Pett, M.; Hursthouse, M. B. *J. Chem. Soc., Dalton Trans.* **1983**, 2025. (g) Howard, C. G.; Girolami, G. S.; Wilkinson, G.; Thornton-Pett, M.; Hursthouse, M. B. *J. Chem. Soc., Dalton Trans.* **1983**, 2631. (h) Wickens, D. A.; Abrams, G. *J. Chem. Soc., Dalton Trans.* **1985**, 2203. (i) Hebendanz, N.; Köhler, F. H.; Müller, G. *Inorg. Chem.* **1984**, *23*, 3043. (j) Beagley, B.; Briggs, J. C.; Hosseiny, A.; Hill, W. E.; King, T. J.; McAuliffe, C. A.; Minten, K. *J. Chem. Soc., Dalton Trans.* **1984**, 305. (k) Beagley, B.; Benson, C. G.; Gott, G. A.; McAuliffe, C. A.; Pritchard, R.; Tanner, S. P. *J.*

Chem. Soc., Dalton Trans. **1988**, 2261. (l) Barratt, D. S.; Gott, G. A.; McAuliffe, C. A. *Inorg. Chim. Acta* **1988**, *145*, 289. (m) Al-Farhan, K.; Beagley, B.; El-Sayrafi, O.; Gott, G. A.; McAuliffe, C. A.; Mac Rory, P. P.; Pritchard, R. G. *J. Chem. Soc., Dalton Trans.* **1990**, 1243. (n) Beagley, B.; Mackie, A. G.; Matear, P. P.; McAuliffe, C. A.; Ndifon, P. T.; Pritchard, R. G. *J. Chem. Soc., Dalton Trans.* **1992**, 1301. (o) Godfrey, S. M.; Kelly, D. G.; McAuliffe; C. A. *J. Chem. Soc., Dalton Trans.* **1992**, 1305.

19. (a) McAuliffe, C. A.; Al-Khateeb, H.; Jones, M. H.; Levason, W.; Minten, K.; McCullough, F. P. *J. Chem. Soc., Dalton Trans.* **1979**, 736. (b) McAuliffe, C. A. *J. Organomet. Chem.* **1982**, *228*, 255. (c) Barber, M.; Bordoli, R. S.; Hosseiny, A.; Minten, K.; Perkin, C. R.; Sedgwick, R. D.; McAuliffe, C. A. *Inorg. Chim. Acta* **1980**, *45*, L89. (d) Burkett, H. D.; Newberry, V. F.; Hill, W. E.; Worley, S. D. *J. Am. Chem. Soc.* **1983**, *105*, 4097. (e) Newberry, V. F.; Burkett, H. D.; Worley, S. D.; Hill, W. E. *Inorg. Chem.* **1984**, *23*, 3911. (f) McAuliffe, C. A.; Al-Khateeb, H. *Inorg. Chim. Acta* **1980**, *45*, L195. (g) Beagley, B.; McAuliffe, C. A.; Mac Rory, P. P.; Ndifon, P. T.; Pritchard, R. G. *J. Chem. Soc., Dalton Trans.* **1990**, 309.

20. Burkett, H. D.; Worley, S. D. *J. Am. Chem. Soc.* **1989**, *111*, 5992.

21. (a) Godfrey, S. M.; Kelly, D. G.; Mackie, A. G.; Matear, P. P.; McAuliffe, C. A.; Pritchard, R. G.; Watson, S. M. *J. Chem. Soc., Chem. Commun.* **1991**, 1447. (b) McAuliffe, C. A.; Godfrey, S. M.; Mackie, A. G.; Pritchard, R. G. *J. Chem. Soc., Chem. Commun.* **1992**, 483.

CHAPTER VII

CONCLUDING REMARKS AND FUTURE DIRECTIONS

The results presented in this dissertation have demonstrated the extreme versatility of the ligand tris(2,4,6-trimethoxyphenyl)phosphine (TMPP), which can act as a large counterion (in its protonated form) to stabilize small cations, as an anionic phosphino-phenoxide ligand or as a neutral, multidentate ligand. Figure 37 summarizes the different bonding modes that we have discovered in our laboratories, some of which have been presented throughout this work. In addition to those depicted, we have recently unearthed a new mode in the compound [(COD)Rh-Co(TMPP-*O*)$_2$]$^{2+}$ (**17**), namely an η^4 coordination of one of the phenyl rings of the ligand to the metal center.

The unusual properties of the TMPP ligand, in particular its bulk, have allowed for the isolation of unprecedented compounds such as the di-ferrous, ferromagnetic anion $[Fe_2Cl_6]^{2-}$. The subsequent reactivity with molecular oxygen in which this salt is involved, eventually leads to the formation of the stable mono-phosphine oxide adduct $FeCl_3$(O=TMPP) (**6**), chemistry that lends new insight into how the $FeCl_3$-catalyzed oxidation of triphenylphosphine to triphenylphosphine oxide might proceed. Future directions include the preparation of the $[Fe_2Cl_6]^{2-}$ unit by more rational routes, as well as the generalization of this chemistry to other tertiary phosphines such as PCy_3 and PPh_3. Stabilization of the $[Fe_2Cl_6]^{2-}$ with other cations should be investigated, in order to study the effect of the size of the counterion on the stability and reactivity of the resulting salt. We are also interested in preparing other $[M_2X_6]^{2-}$ anions with 3d elements in order to study their magnetism.

The chemistry of TMPP with solvated cations of Co(II) and Ni(II) has revealed that, given suitable reaction conditions, *bis*-phosphino-phenoxide complexes of general formula M^{II}(TMPP-*O*)$_2$ (M = Co, Ni) may

Figure 37. Different binding modes for TMPP.

TMPP (neutral)

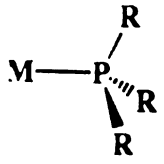

η^1

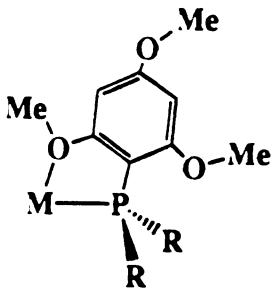

η^2

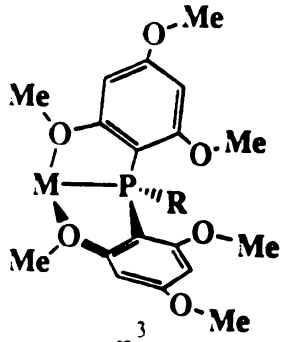

η^3

TMPP-O (anionic)

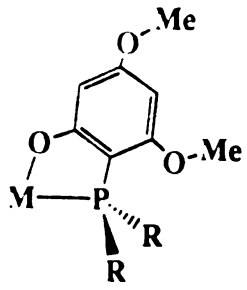

η^2

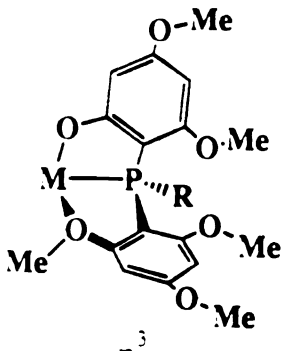

η^3

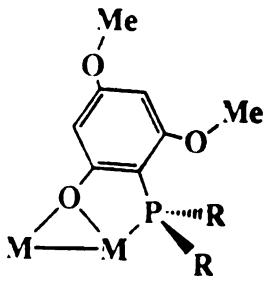

μ_2-O, η^2

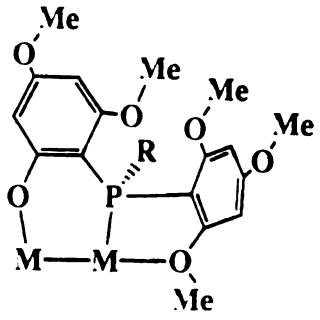

μ_2, η^3

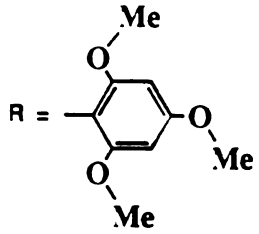

R =

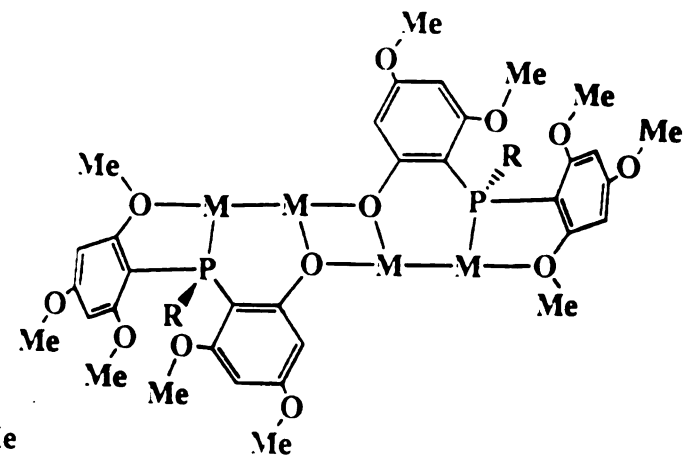

$\{\mu_2, \eta^3\}$-μ_2, O

Figure 37.

be isolated. In both cases it was possible to prepare the oxidation product, namely $[M^{III}(TMPP\text{-}O)_2]^+$, either chemically or electrochemically. The Co^{II}/Co^{III} redox reaction involves an isomerization of the phenoxide groups from a *cis* to a *trans* disposition, whereas the Ni^{III} complex retains its *trans* configuration. Further studies of this redox chemistry, along with additional structural characterization, are in order. The compound $Co(TMPP\text{-}O)_2$ represents a very suitable "synthon" for the preparation of homo- and heterometallic complexes, due to the presence of nucleophilic phenoxide groups in a *cis*-position which can be used to bridge to a second metal center. This has been achieved by the equimolar reaction of $Co(TMPP\text{-}O)_2$ with MCl_2 (M = Co, Mn) to produce the dinuclear species $Cl_2MCo\{\mu\text{-}\eta^2\text{-}(TMPP\text{-}O)_2\}$. Preliminary magnetic studies on the di-cobalt system have shown coupling of the two metal centers and further investigations are in order. Synthesis of linear trinuclear compound was briefly mentioned in Chapter IV and is certainly one of the directions in which this chemistry should be taken.

Finally, one of the greatest challenges in this chemistry will be to investigate how minor modifications of the TMPP phosphine ligand affect its chemistry with transition metals and then subsequent reactivity. As mentioned in Chapter VI of this dissertation, decreasing the number of substituents on the phenyl rings will reduce the basicity of the ligand, thereby rendering it more compatible with early 3d metals. A phosphine possessing di-substituted phenyl rings in the ortho position will have a much lower basicity [1], while maintaining the considerable bulk required for stabilizing purposes.

Although there is a considerable interest in continuing our research with ether-phosphines [2], we are also interested in preparing a sulfur

analogue of TMPP, *viz.* $P\{C_6H_2(SMe)_3\}_3$, and study its reactivity with transition elements. In view of the successful chemistry of TMPP with Ni^{II} and Ni^{III}, it is even more relevant because of the inherent compatibility of Ni^{III} with sulfur. A recent paper by Hursthouse and co-workers highlights the use of mixed sulfur-phosphine ligands with Pd^{II} and Pt^{II} complexes, which possess ortho-substituted methyl-thio phenyl rings [3] and serves as a useful back-drop for this chemistry.

LIST OF REFERENCES

1. Wada, M. *J. Chem. Res.* **1985**, (S), 38; (M), 0467.

2. (a) Lindner, E.; Rothfuß, H.; Fawzi, R.; Hiller, W. *Chem. Ber.* **1992**, *125*, 541. (b)Lindner, E.; Dettinger, J.; Möckel, A. *Z. Naturforsch.* **1991**, *46b*, 1519. (c) Lindner, E.; Bader, A.; Mayer, H. A. *Z. Anorg. Allg. Chem.* **1991**, *598/599*, 235. (d) Werner, H.; Stark, A.; Schulz, M.; Wolf, J. *Organometallics* **1992**, *11*, 1126. (e) Mason, M. R.; Su, Y.; Jacobson, R. A.; Verkade, J. G. *Organometallics* **1991**, *10*, 2335. (d) Mason, M. R.; Verkade, J. G. *Organometallics* **1992**, *11*, 1514.

3. Abel, E. W.; Dormer, J. C.; Ellis, D.; Orrell, K. G.; Sik, V.; Hursthouse, M. B.; Mazid, M. A. *J. Chem. Soc., Dalton Trans.* **1992**, 1073.

APPENDICES

APPENDIX A

GENERAL EXPERIMENTAL PROCEDURES

1. Synthesis

All reactions were carried out under an inert atmosphere using standard Schlenk and dry-box techniques, unless otherwise specified. All solvents were predried over 4Å molecular sieves for 3 months prior to use. Diethyl ether, THF, benzene, toluene, hexanes were distilled from sodium/potassium benzophenone ketyl radical, whereas acetone, methylene chloride, acetonitrile and alcohols were distilled under a nitrogen atmosphere from $Mg(OCH_3)_2$ or P_2O_5.

All metal halides, metal pellets, $NOBF_4$ and $AgBF_4$ were purchased from Strem Chemicals whereas triphenylphosphite, (1,3,5-trimethoxy)benzene and *n*-butyllithium from Aldrich; all were used without further purification.

Elemental analyses were performed by Galbraith Laboratories, Inc. or Desert Analytics.

2. Spectroscopy

Infrared spectra were recorded on a Perkin-Elmer 599 or a Nicolet FT-IR/42 spectrophotometer. ^1H NMR spectra were measured on a VARIAN VXR-300 MHz or on a VARIAN Gemini 300 MHz instrument and referenced to the residual proton impurity of deuterated solvents (1.93, 2.05, 3.30 and 4.78, 5.32, 7.24 ppm with respect to TMS for d_3-acetonitrile, d_6-acetone, d_4-methanol, d_2-dichloromethane and d-chloroform, respectively). Electronic spectra were recorded on a Hitachi U-2000 UV spectrometer. Electrochemical measurements were performed by using an EG&G Princeton Applied Research Model 362 scanning potentiostat in conjunction with a BAS Model RXY recorder. Cyclic voltammetry experiments were carried out at 22 ± 2°C in methylene chloride containing 0.1 M tetra-*n*-butylammonium tetrafluoroborate

($TBABF_4$) as the supporting electrolyte. $E_{1/2}$ values, determined as ($E_{p,a}$ + $E_{p,c}$)/2 were referenced to the Ag/AgCl electrode and are uncorrected for junction potentials. The Cp_2Fe/Cp_2Fe^+ couple occurs at $E_{1/2}$ = + 0.52 V and shows a $E_{p,a}$ to $E_{p,c}$ separation of 30 mV under the same experimental conditions. X-band EPR spectra were obtained by using a Brucker ER200D spectrometer. Variable temperature magnetic susceptibility measurements were carried out on a Quantum Design MPMS susceptometer housed in the Physics and Astronomy Department at Michigan State University and provided by The Center for Fundamental Materials Research, Michigan State University. Data points were collected over the 5 to 300 K temperature range at 20 degree intervals. Mössbauer spectra and the epr spectra presented in Chapter III were recorded by Dr. W. R. Dunham at the Institute of Science and Technology, The University of Michigan. FAB-mass spectrometry experiments were performed at the Mass Spectrometry Facility in the Department of Biochemistry, Michigan State University.

APPENDIX B

SYNTHESIS AND CHARACTERIZATION OF $[Re_2(NCCH_3)_{10}][BF_4]_4$

1. Experimental: Synthesis of $[Re_2(NCCH_3)_{10}][BF_4]_4$ (20)

An amount of $Re_2(O_2CC_3H_7)_4Cl_2$ (0.118 g, 0.149 mmol) was reacted with 2 equivalents of $AgBF_4$ (0.058 g, 0.298 mmol) in 10 mL of acetonitrile. The resulting green solution was stirred for *ca.* 0.5 hour, after which time the AgCl was removed by filtration and the filtrate transferred to a clean vessel. An aliquot of liquid Et_3OBF_4 (8 mL) was added, resulting in a color change from green to orange. This solution was refluxed for 20 days, after which time the volume was reduced to about 5 mL with addition of *ca.* 5 mL of CH_2Cl_2. After about 12 hours at - 10°C, a crop of blue microcrystals deposited, along with some white by-product, from a dark brown solution. The solution was filtered from the solid which was washed with diethyl ether (2 x 10 mL) and hexanes (2 x 10 mL) and dried *in vacuo*. The sample was recrystallized from a mixture of CH_3CN/CH_2Cl_2 (v/v 1:1); yield: ~ 0.075 g (~ 45% relative to $Re_2(O_2CC_3H_7)_4Cl_2$).

2. Characterization of $[Re_2(NCCH_3)_{10}][BF_4]_4$ (20)

The presence of coordinated acetonitrile was confirmed by infrared spectroscopy (ν(CN) = 2320(w), 2280(m) cm^{-1}) and the BF_4^- counteranion was evident by the prominent stretches at ν(B-F) = 1030(s) and 520(m) cm^{-1}.

The electronic spectrum (in CH_3CN) consists of a very broad absorption at 561 nm (ε = 425 $M^{-1}cm^{-1}$) with a shoulder at 650 nm and three bands at 450 nm (ε = 507 $M^{-1}cm^{-1}$), 351 nm (ε = 2.3 x 10^4 $M^{-1}cm^{-1}$) and 246 nm (ε = 3.0 x 10^4 $M^{-1}cm^{-1}$). In dimethylacetamide (DMAA), the spectrum exhibits the same general features (572(414), 356(1.19 x 10^4)) with the exception that the shoulder at 650 nm is much diminished.

The ^1H NMR spectrum of **20** exhibits a singlet at δ = + 3.38 ppm along with a large signal at δ = + 1.95 ppm attributed to the equatorially bound CH_3CN and free CH_3CN, respectively.

The cyclic voltammogram of **20** in CH_3CN exhibits two quasi-reversible reductions at $E_{1/2}$ = + 0.25 V and $E_{1/2}$ = + 0.08 V as well as an irreversible reduction at $E_{p,c}$ = - 0.82 V versus Ag/AgCl (in 0.05 M $TBABF_4$).

3. X-ray Crystallography

Data Collection and Reduction:

A blue cubic crystal was mounted on the tip of a glass fiber with Dow Corning silicone grease and placed in a N_2 cold stream at - 100 ± 2°C. A preliminary cubic cell was determined by centering and indexing on 20 reflections. The cell was then refined by a least-squares fit of 14 reflections in the range $20 \leq 2\theta \leq 30$. Intensity data were collected over the range 4 - 50 in 2θ , using the ω-scan mode. Measurements of three standard reflections at regular intervals during data collection showed no decay in crystal quality. After averaging equivalent reflections, 2149 unique data remained, of which 1002 were observed with $F_o^2 \geq 3\sigma(F_o)^2$.

Structure Determination

There are three possible space groups corresponding to the systematic absences of the data set, these are I_{432} (# 211), I_{43m} (# 217) and I_{m3m} (# 229), but according to the statistics, only an acentric space group is possible, which rules out space group # 229. In the two other space groups one needs only to solve for one rhenium atom (or rather 1/4 of a rhenium atom) which generates 5 other metal atoms to form a regular octahedron, as illustrated in Fig. 38. The Re-Re distance is approximately 2.26 Å and there seems to be one axial nitrogen at 2.2-2.3 Å and one

Table 19. Preliminary crystal data for $[Re_2(NCCH_3)_{10}][BF_4]_4$ (20)

Formula	$Re_2C_{20}N_{10}H_{30}B_4F_{16}$
Formula Weight	1146.15
Space group	I_{432}
a, Å	29.310(5)
b, Å	29.310(5)
c, Å	29.310(5)
α, deg	90.00
β, deg	90.00
γ, deg	90.00
V, Å^3	25181(12)
Z	24
d_{calc}, g/cm^3	1.788
Data collection instrument	Rigaku AFC6S
Radiation (monochromated in incident beam)	graphite monochromated (MoKα, λ_α = 0.71069 Å)
Orientation reflections number, range (2θ)	14, 20 - 30
Temperature	- 100 ± 2°C
Scan method	ω
Data collection range, 2θ, deg	4 - 50
Number of unique data	2149
Total with $F_o^2 \geq 3\sigma(F_o)^2$	1002
Trans. factors max., min.	1.00 - 0.83

equatorial nitrogen at 2.0 Å. Preliminary crystal data are summarized in Table 19.

Figure 38. Schematic representation of the 3-fold disorder of the Re≡Re unit in the crystal structure of $[Re_2(NCCH_3)_{10}][BF_4]_4$.

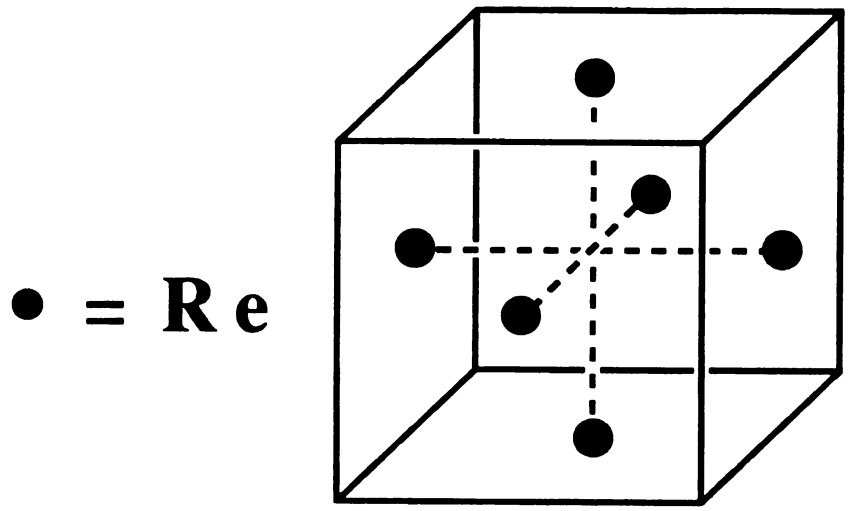

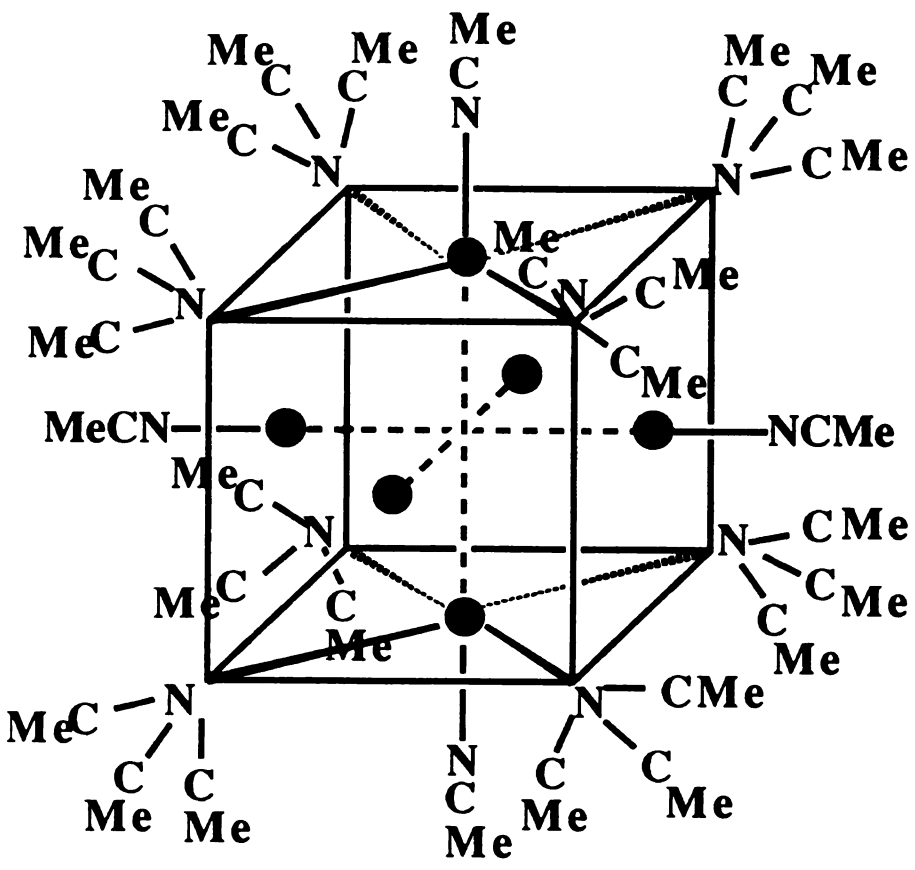

Figure 38.

APPENDIX C

TABLES OF ATOMIC POSITIONAL PARAMETERS AND EQUIVALENT ISOTROPIC DISPLACEMENT PARAMETERS.

Table 20. **Atomic Positional Parameters and Equivalent Isotropic Displacement Parameters ($Å^2$) and their Estimated Standard Deviations for $[H\text{-}TMPP]_2[Fe_2Cl_6]$ (1).**

atom	x	y	z	B(eq)
Fe(1)	0.52799(6)	0.3397(1)	0.51003(4)	2.40(4)
Cl(1)	0.4063(1)	0.1942(2)	0.49538(9)	3.42(8)
Cl(2)	0.4944(1)	0.4843(2)	0.42336(8)	2.66(7)
Cl(3)	0.6819(1)	0.2714(2)	0.5343(1)	4.6(1)
P(1)	0.4210(1)	0.0253(2)	0.79519(7)	1.44(6)
O(1)	0.2082(3)	0.0202(4)	0.7388(2)	2.3(2)
O(2)	0.1959(3)	0.3389(5)	0.5839(2)	3.2(2)
O(3)	0.5013(3)	0.1950(4)	0.7230(2)	2.0(2)
O(4)	0.4611(3)	-0.0721(4)	0.6750(2)	2.2(2)
O(5)	0.6813(3)	-0.4090(5)	0.7664(2)	3.3(2)
O(6)	0.5194(3)	-0.1409(4)	0.8858(2)	2.2(2)
O(7)	0.3267(3)	0.2002(4)	0.8530(2)	2.4(2)
O(8)	0.5950(3)	0.4393(4)	0.9770(2)	2.8(2)
O(9)	0.6379(3)	0.0847(4)	0.8439(2)	2.2(2)
C(1)	0.3530(4)	0.1095(6)	0.7284(3)	1.4(2)
C(2)	0.2506(4)	0.1055(6)	0.7083(3)	1.8(2)
C(3)	0.2007(4)	0.1834(6)	0.6598(3)	2.1(3)
C(4)	0.2516(4)	0.2670(6)	0.6308(3)	2.1(3)
C(5)	0.3538(4)	0.2749(6)	0.6489(3)	1.8(2)
C(6)	0.4027(4)	0.1954(6)	0.6983(3)	1.6(2)
C(7)	0.1047(4)	0.0306(7)	0.7280(3)	2.9(3)
C(8)	0.2428(5)	0.4372(7)	0.5553(3)	3.0(3)
C(9)	0.5612(5)	0.2627(8)	0.6920(3)	3.4(3)
C(10)	0.4950(4)	-0.1064(6)	0.7815(3)	1.5(2)
C(11)	0.5100(4)	-0.1412(6)	0.7245(3)	1.6(2)
C(12)	0.5723(4)	-0.2448(6)	0.7214(3)	2.0(3)
C(13)	0.6201(4)	-0.3114(6)	0.7749(3)	2.2(3)
C(14)	0.6056(4)	-0.2831(6)	0.8318(3)	1.9(2)
C(15)	0.5421(4)	-0.1803(6)	0.8338(3)	1.7(2)
C(16)	0.4780(5)	-0.0986(7)	0.6160(3)	2.7(3)
C(17)	0.7293(6)	-0.4870(8)	0.8179(4)	4.3(4)
C(18)	0.5528(5)	-0.2152(7)	0.9410(3)	2.8(3)
C(19)	0.4841(4)	0.1434(6)	0.8510(3)	1.5(2)
C(20)	0.4240(4)	0.2269(6)	0.8753(3)	1.8(2)
C(21)	0.4624(4)	0.3250(6)	0.9173(3)	1.9(3)
C(22)	0.5639(4)	0.3402(6)	0.9362(3)	1.9(3)
C(23)	0.6244(4)	0.2610(6)	0.9134(3)	1.7(2)
C(24)	0.5846(4)	0.1638(6)	0.8702(3)	1.7(2)
C(25)	0.2575(5)	0.2788(7)	0.8717(3)	2.7(3)
C(26)	0.6967(5)	0.4606(8)	0.9978(3)	3.4(3)
C(27)	0.7414(4)	0.0880(7)	0.8666(3)	2.8(3)
H(1)	0.3501	-0.0354	0.8211	1.3
H(2)	0.1295	0.1799	0.6464	2.2
H(3)	0.3906	0.3378	0.6298	1.8
H(4)	0.0905	0.1144	0.7430	2.8
H(5)	0.0733	0.0174	0.6879	2.8
H(6)	0.0853	-0.0362	0.7540	2.8
H(7)	0.2923	0.3993	0.5380	3.2
H(8)	0.1975	0.4821	0.5217	3.2
H(9)	0.2753	0.5048	0.5838	3.2

Table 20. (continued)

atom	x	y	z	B(eq)
H(10)	0.6272	0.2500	0.7100	3.6
H(11)	0.5493	0.2190	0.6488	3.6
H(12)	0.5438	0.3496	0.6836	3.6
H(13)	0.5806	-0.2692	0.6801	2.3
H(14)	0.6405	-0.3293	0.8696	1.8
H(15)	0.4666	-0.1886	0.6049	3.0
H(16)	0.4419	-0.0434	0.5851	3.0
H(17)	0.5479	-0.0826	0.6189	3.0
H(18)	0.6930	-0.5291	0.8401	5.2
H(19)	0.7771	-0.5496	0.8096	5.2
H(20)	0.7771	-0.4275	0.8511	5.2
H(21)	0.5333	-0.1783	0.9745	3.0
H(22)	0.5289	-0.3050	0.9353	3.0
H(23)	0.6236	-0.2221	0.9538	3.0
H(24)	0.4215	0.3844	0.9348	2.1
H(25)	0.6961	0.2724	0.9279	1.7
H(26)	0.2683	0.2706	0.9146	2.9
H(27)	0.2623	0.3670	0.8603	2.9
H(28)	0.1932	0.2463	0.8515	2.9
H(29)	0.7259	0.3842	1.0165	3.8
H(30)	0.7183	0.4801	0.9618	3.8
H(31)	0.7085	0.5335	1.0243	3.8
H(32)	0.7593	0.0616	0.9107	3.0
H(33)	0.7709	0.0275	0.8460	3.0
H(34)	0.7657	0.1737	0.8651	3.0

Table 21. Atomic Positional Parameters and Equivalent Isotropic Displacement Parameters ($Å^2$) and their Estimated Standard Deviations for $[H\text{-}TMPP]_2[FeCl_4]$ (3).

atom	x	y	z	B(eq)
Fe(1)	3/4	0.1074(4)	1/2	2.1(2)
Cl(1)	0.6691(3)	0.2392(6)	0.4562(2)	4.8(3)
Cl(2)	0.7174(2)	-0.0180(6)	0.5549(2)	4.0(3)
P(1)	1.0442(2)	-0.2686(6)	0.6848(2)	2.2(3)
O(1)	1.1034(5)	-0.440(1)	0.7612(5)	3.1(3)
O(2)	1.2281(6)	-0.680(1)	0.6885(5)	3.7(3)
O(3)	1.0893(5)	-0.337(1)	0.5983(5)	2.7(3)
O(4)	1.1336(6)	-0.107(1)	0.6744(5)	2.8(3)
O(5)	1.0122(6)	0.166(1)	0.5358(5)	3.8(3)
O(6)	0.9259(6)	-0.171(1)	0.6095(4)	2.6(3)
O(7)	0.9740(6)	-0.443(1)	0.6121(5)	3.5(3)
O(8)	0.8318(7)	-0.575(2)	0.6966(5)	4.9(4)
O(9)	0.9874(5)	-0.260(1)	0.7652(5)	2.8(3)
C(1)	1.0979(8)	-0.389(2)	0.6795(7)	1.7(4)
C(2)	1.1237(8)	-0.470(2)	0.7217(7)	2.3(5)
C(3)	1.1682(9)	-0.566(2)	0.7240(7)	2.7(5)
C(4)	1.1834(9)	-0.581(2)	0.6813(8)	2.4(5)
C(5)	1.1600(8)	-0.506(2)	0.6384(7)	1.6(4)
C(6)	1.1167(8)	-0.413(2)	0.6402(7)	1.1(4)
C(7)	1.126(1)	-0.512(2)	0.8091(8)	3.9(5)
C(8)	1.246(1)	-0.706(2)	0.6470(8)	3.8(6)
C(9)	1.1158(9)	-0.322(2)	0.5597(8)	3.4(5)
C(10)	1.0296(8)	-0.140(2)	0.6386(6)	1.0(4)
C(11)	1.0800(9)	-0.069(2)	0.6379(7)	1.9(5)
C(12)	1.0779(8)	0.034(2)	0.6041(7)	1.7(4)
C(13)	1.023(1)	0.067(2)	0.5732(8)	2.9(5)
C(14)	0.9689(8)	-0.001(2)	0.5723(7)	2.7(5)
C(15)	0.9757(8)	-0.102(2)	0.6063(7)	1.3(4)
C(16)	1.193(1)	-0.035(2)	0.6842(7)	3.6(5)
C(17)	1.063(1)	0.238(2)	0.5333(8)	4.6(6)
C(18)	0.868(1)	-0.137(2)	0.5760(8)	4.1(6)
C(19)	0.9790(7)	-0.352(2)	0.6884(7)	1.0(4)
C(20)	0.9507(9)	-0.440(2)	0.6517(7)	2.0(5)
C(21)	0.8993(9)	-0.517(2)	0.6489(7)	2.9(5)
C(22)	0.883(1)	-0.502(2)	0.6920(8)	3.4(5)
C(23)	0.9097(9)	-0.420(2)	0.7315(7)	2.5(5)
C(24)	0.9574(8)	-0.347(2)	0.7284(7)	1.7(4)
C(25)	0.946(1)	-0.528(2)	0.5654(8)	3.7(5)
C(26)	0.805(1)	-0.674(3)	0.6614(9)	5.9(7)
C(27)	0.977(1)	-0.268(2)	0.8131(8)	4.1(6)
H(1)	1.1864	-0.6210	0.7528	4.1
H(2)	1.1755	-0.5233	0.6093	2.3
H(3)	1.1073	-0.4762	0.8367	3.4
H(4)	1.1171	-0.6057	0.8102	3.4
H(5)	1.1692	-0.5026	0.8286	3.4
H(6)	1.2115	-0.7415	0.6156	4.0
H(7)	1.2761	-0.7754	0.6515	4.0
H(8)	1.2606	-0.6312	0.6319	4.0
H(9)	1.1162	-0.4151	0.5443	3.0
H(10)	1.0885	-0.2740	0.5315	3.0

Table 21. (continued)

atom	x	y	z	B(eq)
H(11)	1.1531	-0.2915	0.5701	3.0
H(12)	1.1138	0.0861	0.6044	3.3
H(13)	0.9303	0.0125	0.5522	2.2
H(14)	1.2246	-0.0727	0.7073	2.1
H(15)	1.2007	-0.0364	0.6505	2.1
H(16)	1.1875	0.0568	0.6897	2.1
H(17)	1.0956	0.1957	0.5271	3.4
H(18)	1.0527	0.3170	0.5092	3.4
H(19)	1.0861	0.2949	0.5662	3.4
H(20)	0.8561	-0.0484	0.5781	3.5
H(21)	0.8657	-0.1561	0.5418	3.5
H(22)	0.8373	-0.1945	0.5828	3.5
H(23)	0.8805	-0.5801	0.6258	3.0
H(24)	0.8958	-0.4211	0.7660	4.4
H(25)	0.9089	-0.4989	0.5494	3.2
H(26)	0.9731	-0.5098	0.5442	3.2
H(27)	0.9518	-0.6144	0.5755	3.2
H(28)	0.7741	-0.7236	0.6704	6.0
H(29)	0.7897	-0.6424	0.6292	6.0
H(30)	0.8359	-0.7449	0.6616	6.0
H(31)	0.9987	-0.2085	0.8386	2.1
H(32)	0.9327	-0.2521	0.8094	2.1
H(33)	0.9836	-0.3581	0.8281	2.1
H(34)	1.0680	-0.1982	0.7376	2.4

Table 22. Atomic Positional Parameters and Equivalent Isotropic Displacement Parameters ($Å^2$) and their Estimated Standard Deviations for [H-TMPP][$FeCl_4$] (4).

atom	x	y	z	B(eq)
Fe(1)	1.0049(1)	0.0399(1)	0.2320(1)	5.7(1)
Cl(1)	0.9063(2)	0.0846(2)	0.2448(3)	9.7(3)
Cl(2)	1.0477(2)	0.0063(2)	0.3384(2)	7.7(2)
Cl(3)	0.9921(3)	-0.0517(2)	0.1635(3)	11.7(3)
Cl(4)	1.0716(2)	0.1141(3)	0.1779(3)	11.4(3)
P(1)	0.8230(2)	0.2539(2)	0.0683(2)	5.1(2)
O(1)	0.8728(4)	0.3860(5)	-0.0003(5)	5.6(5)
O(2)	1.0585(5)	0.2904(5)	-0.1283(5)	5.8(6)
O(3)	0.9074(4)	0.1501(5)	0.0213(5)	6.7(6)
O(4)	0.7723(4)	0.2903(5)	-0.0849(6)	6.4(6)
O(5)	0.5890(6)	0.1272(5)	-0.0781(6)	7.7(7)
O(6)	0.7368(4)	0.1517(5)	0.1255(6)	5.5(6)
O(7)	0.7187(5)	0.3669(5)	0.0513(6)	6.1(6)
O(8)	0.7450(5)	0.4602(6)	0.2954(8)	8.7(7)
O(9)	0.8883(5)	0.2798(5)	0.2013(5)	6.2(6)
C(1)	0.8935(6)	0.2686(9)	0.0110(6)	3.6(8)
C(2)	0.9138(7)	0.3319(8)	-0.0189(7)	4.0(9)
C(3)	0.9691(7)	0.3381(7)	-0.0644(8)	4.3(8)
C(4)	1.0059(7)	0.279(1)	-0.0798(8)	4.6(8)
C(5)	0.9884(7)	0.2154(7)	-0.0503(8)	4.5(8)
C(6)	0.9325(8)	0.2120(8)	-0.0073(8)	5(1)
C(7)	0.8893(7)	0.4517(9)	-0.0288(8)	7(1)
C(8)	1.0988(7)	0.2344(8)	-0.1464(8)	7(1)
C(9)	0.946(1)	0.0913(9)	0.021(1)	10(1)
C(10)	0.7533(6)	0.2197(7)	0.021(1)	4.4(8)
C(11)	0.7339(7)	0.2391(8)	-0.051(1)	5.1(9)
C(12)	0.6789(8)	0.2102(7)	-0.0888(7)	4.5(8)
C(13)	0.6450(7)	0.1608(8)	-0.0513(9)	4.5(9)
C(14)	0.6618(8)	0.1383(6)	0.0195(8)	4.7(8)
C(15)	0.7145(8)	0.1673(8)	0.0544(9)	4.7(9)
C(16)	0.7556(7)	0.3133(8)	-0.157(1)	8(1)
C(17)	0.561(1)	0.152(1)	-0.146(1)	12(1)
C(18)	0.7078(8)	0.0942(9)	0.1614(9)	8(1)
C(19)	0.8007(7)	0.3225(7)	0.1307(8)	3.8(8)
C(20)	0.7490(8)	0.3699(8)	0.119(1)	5(1)
C(21)	0.7317(7)	0.4136(9)	0.175(1)	6(1)
C(22)	0.7655(9)	0.4138(8)	0.243(1)	6(1)
C(23)	0.8195(9)	0.370(1)	0.2549(8)	6(1)
C(24)	0.8345(7)	0.3250(7)	0.198(1)	4.4(9)
C(26)	0.778(1)	0.464(1)	0.365(1)	11(1)
C(27)	0.9252(7)	0.2749(8)	0.2693(8)	7(1)
C(25)	0.6716(8)	0.418(1)	0.0350(9)	8(1)
H(1)	0.8384	0.2070	0.1126	5.9
H(2)	0.9834	0.3817	-0.0891	4.4
H(3)	1.0186	0.1742	-0.0615	5.3
H(4)	0.9341	0.4656	-0.0102	8.6
H(5)	0.8924	0.4523	-0.0822	8.6
H(6)	0.8592	0.4869	-0.0130	8.6
H(7)	1.0753	0.1971	-0.1681	8.0
H(8)	1.1346	0.2477	-0.1800	8.0

Table 22. (continued)

atom	x	y	z	B(eq)
H(9)	1.1211	0.2168	-0.1011	8.0
H(10)	0.9255	0.0489	0.0417	11.2
H(11)	0.9605	0.0756	-0.0304	11.2
H(12)	0.9892	0.0946	0.0478	11.2
H(13)	0.6645	0.2255	-0.1404	5.3
H(14)	0.6366	0.0996	0.0458	5.8
H(15)	0.7875	0.3487	-0.1736	8.0
H(16)	0.7588	0.2764	-0.1931	8.0
H(17)	0.7124	0.3328	-0.1593	8.0
H(18)	0.5483	0.2021	-0.1438	11.5
H(19)	0.5940	0.1515	-0.1879	11.5
H(20)	0.5223	0.1290	-0.1645	11.5
H(21)	0.6594	0.0956	0.1702	9.5
H(22)	0.7145	0.0483	0.1365	9.5
H(23)	0.7261	0.0842	0.2132	9.5
H(24)	0.6913	0.4432	0.1741	5.9
H(25)	0.8461	0.3694	0.3029	6.4
H(26)	0.7800	0.4202	0.3913	11.2
H(27)	0.8255	0.4769	0.3567	11.2
H(28)	0.7601	0.4974	0.3983	11.2
H(29)	0.8957	0.2615	0.3144	8.1
H(30)	0.9598	0.2406	0.2709	8.1
H(31)	0.9450	0.3179	0.2867	8.1
H(32)	0.6884	0.4648	0.0379	8.9
H(33)	0.6495	0.4131	-0.0124	8.9
H(34)	0.6337	0.4178	0.0727	8.9

Table 23. Atomic Positional Parameters and Equivalent Isotropic Displacement Parameters (Å^2) and their Estimated Standard Deviations for $FeCl_3$(O=TMPP)(6).

Atom	x	y	z	B(Å^2)
Fe	0.3058(2)	0.8347(2)	0.0933(2)	5.49(7)
Cl(1)	0.2656(4)	1.0026(3)	0.1189(5)	8.6(2)
Cl(2)	0.1663(4)	0.7941(4)	0.1308(5)	10.4(2)
Cl(3)	0.4721(5)	0.7911(5)	0.2359(5)	11.9(2)
O(10)	0.3139(7)	0.7651(6)	-0.0740(7)	4.2(3)
P(1)	0.3454(3)	0.7256(3)	-0.2093(3)	3.2(1)
C(1)	0.271(1)	0.6232(9)	-0.310(1)	3.0(4)
C(2)	0.283(1)	0.5380(8)	-0.259(1)	3.5(4)
C(3)	0.234(1)	0.4533(9)	-0.328(1)	4.5(4)
C(4)	0.169(1)	0.4469(8)	-0.462(1)	4.5(4)
C(5)	0.152(1)	0.5240(9)	-0.523(1)	3.6(3)*
C(6)	0.2050(9)	0.6080(8)	-0.442(1)	3.1(3)
O(1)	0.3549(8)	0.5503(6)	-0.1313(8)	5.5(3)
O(2)	0.1231(7)	0.3591(6)	-0.533(1)	5.9(3)
O(3)	0.1963(8)	0.6847(6)	-0.4998(8)	5.2(3)
C(7)	0.347(1)	0.490(1)	-0.054(1)	7.8(5)
C(8)	0.062(1)	0.342(1)	-0.676(1)	7.3(6)
C(9)	0.093(1)	0.707(1)	-0.608(1)	6.2(5)
C(10)	0.503(1)	0.6817(8)	-0.176(1)	3.1(4)
C(11)	0.561(1)	0.5853(9)	-0.241(1)	3.8(4)
C(12)	0.685(1)	0.550(1)	-0.214(1)	5.0(4)

Table 23. (continued)

Atom	x	y	z	B(A2)
C(13)	0.750(1)	0.620(1)	-0.116(1)	4.9(4)
C(14)	0.704(1)	0.720(1)	-0.047(1)	5.4(4)
C(15)	0.577(1)	0.7485(8)	-0.081(1)	3.9(4)
O(4)	0.4916(7)	0.5201(7)	-0.3403(8)	4.9(3)
O(5)	0.8709(8)	0.5847(8)	-0.086(1)	7.7(4)
O(6)	0.5177(8)	0.8441(6)	-0.0258(9)	5.3(3)
C(16)	0.543(1)	0.411(1)	-0.392(2)	7.3(6)
C(17)	0.946(1)	0.654(2)	0.017(2)	11.3(8)
C(18)	0.586(1)	0.912(1)	0.089(1)	6.4(5)
C(19)	0.297(1)	0.8312(8)	-0.283(1)	3.4(4)
C(20)	0.361(1)	0.8528(9)	-0.347(1)	3.7(4)
C(21)	0.327(1)	0.9387(9)	-0.401(1)	5.2(5)
C(22)	0.216(1)	1.001(1)	-0.388(1)	6.0(5)
C(23)	0.144(1)	0.9826(9)	-0.329(1)	5.9(5)
C(24)	0.186(1)	0.8960(9)	-0.278(1)	4.5(4)
O(7)	0.4671(7)	0.7856(6)	-0.3587(8)	4.7(3)
O(8)	0.172(1)	1.0880(6)	-0.435(1)	8.5(4)
O(9)	0.1168(7)	0.8663(7)	-0.230(1)	6.4(3)
C(25)	0.555(1)	0.816(1)	-0.391(1)	5.7(5)
C(26)	0.246(2)	1.113(1)	-0.490(2)	10.0(6)
C(27)	0.015(1)	0.938(1)	-0.191(2)	7.4(6)

Starred atoms were refined isotropically.
Anistropically refined atoms are given in the form of the equivalent isotropic displacement parameter defined as $4/3[a^2\beta_{11} + b^2\beta_{22} + c^2\beta_{33} + ab(\cos\gamma)\beta_{12} + ac(\cos\beta)\beta_{13} + bc(\cos\alpha)\beta_{23}]$.

Table 24. Atomic Positional Parameters and Equivalent Isotropic Displacement Parameters (Å^2) and their Estimated Standard Deviations for $[CH_3\text{-}TMPP]_2[Co_2Cl_6]$ (8).

Atom	x	y	z	B(A2)
Co(1)	0.3618(1)	-0.92560(9)	-0.53779(9)	4.40(3)
Cl(1)	0.2884(2)	-0.8800(2)	-0.6970(2)	5.92(7)
Cl(2)	0.2306(3)	-0.8543(3)	-0.4429(2)	9.06(9)
Cl(3)	0.4396(2)	-1.1188(2)	-0.4544(2)	4.91(6)
P(1)	0.2831(2)	-0.2919(1)	-0.8806(1)	2.82(5)
C(28)	0.1863(8)	-0.3438(6)	-0.9384(6)	3.9(2)
C(1)	0.2285(7)	-0.1434(5)	-0.9452(5)	2.7(2)
C(2)	0.1599(7)	-0.0792(6)	-0.8941(5)	3.0(2)
C(3)	0.1203(7)	0.0348(6)	-0.9497(6)	3.6(2)
C(4)	0.1466(7)	0.0875(6)	-1.0583(6)	3.5(2)
C(5)	0.2082(7)	0.0278(6)	-1.1131(6)	3.3(2)
C(6)	0.2454(7)	-0.0868(6)	-1.0556(5)	3.3(2)
O(1)	0.1328(5)	-0.1370(4)	-0.7883(4)	4.2(1)
O(2)	0.1055(6)	0.2001(4)	-1.1049(5)	4.9(2)
O(3)	0.3038(5)	-0.1531(4)	-1.1021(4)	4.0(1)
C(7)	0.081(1)	-0.0756(7)	-0.7283(6)	5.6(3)
C(8)	0.135(1)	0.2618(7)	-1.2158(8)	6.6(3)
C(9)	0.336(1)	-0.1032(7)	-1.2135(6)	5.0(3)
C(10)	0.4455(7)	-0.3310(5)	-0.9117(5)	2.8(2)
C(11)	0.5320(7)	-0.2599(5)	-0.9622(5)	2.9(2)
C(12)	0.6537(7)	-0.2982(6)	-0.9868(6)	3.6(2)
C(13)	0.6902(7)	-0.4117(6)	-0.9610(6)	3.6(2)
C(14)	0.6098(8)	-0.4871(6)	-0.9082(6)	3.7(2)
C(15)	0.4894(8)	-0.4474(6)	-0.8827(5)	3.4(2)

Table 24. (continued)

Atom	x	y	z	B(A2)
O(4)	0.4946(5)	-0.1499(4)	-0.9843(4)	3.8(1)
O(5)	0.8063(5)	-0.4550(4)	-0.9857(4)	4.9(2)
O(6)	0.4029(5)	-0.5140(4)	-0.8296(4)	4.2(1)
C(16)	0.5622(9)	-0.0708(6)	-1.0661(6)	4.6(2)
C(17)	0.8844(9)	-0.3780(8)	-1.0564(8)	6.2(3)
C(18)	0.439(1)	-0.6311(6)	-0.7910(8)	5.6(3)
C(19)	0.2701(7)	-0.3545(5)	-0.7385(5)	2.9(2)
C(20)	0.2029(7)	-0.4418(6)	-0.6754(5)	3.6(2)
C(21)	0.2075(9)	-0.4947(7)	-0.5650(6)	4.8(2)
C(22)	0.2774(9)	-0.4555(7)	-0.5161(6)	4.8(2)
C(23)	0.3446(8)	-0.3705(7)	-0.5711(6)	4.3(2)
C(24)	0.3390(7)	-0.3217(6)	-0.6818(5)	3.3(2)
O(7)	0.1331(5)	-0.4739(4)	-0.7281(4)	4.5(1)
O(8)	0.2745(7)	-0.5131(6)	-0.4056(4)	7.1(2)
O(9)	0.4053(5)	-0.2386(4)	-0.7456(4)	4.0(1)
C(25)	0.069(1)	-0.5669(7)	-0.6699(8)	6.7(3)
C(26)	0.348(1)	-0.4837(9)	-0.3467(7)	7.9(3)
C(27)	0.482(1)	-0.2008(8)	-0.6983(7)	6.9(3)
C(29)	0.051(1)	0.864(1)	0.634(1)	10.8(4)*
Cl(4)	0.1016(4)	0.7539(4)	0.7660(3)	13.3(2)
Cl(5)	0.1207(6)	0.7988(5)	0.5536(4)	15.8(2)*

---

* refined isotropically.

Anisotropically refined atoms are given in the form of the equivalent isotropic displacement parameter defined as $B_{eq} = \frac{1}{3} \sum_i \sum_j B_{ij} a_i^* a_j^* a_i \cdot a_j$

Table 25. **Atomic Positional Parameters and Equivalent Isotropic Displacement Parameters (Å^2) and their Estimated Standard Deviations for [H-TMPP]$_2$[CoCl$_4$] (9).**

atom	x	y	z	B(eq)
Co(1)	1.0000	0.1074(1)	3/4	3.37(5)
Cl(1)	1.05211(7)	-0.0179(2)	0.83743(8)	5.29(8)
Cl(2)	1.04689(8)	0.2361(2)	0.7193(1)	7.3(1)
P(1)	0.68401(6)	0.2268(2)	0.63832(7)	2.75(6)
O(1)	0.6103(1)	0.0546(4)	0.6375(2)	3.8(2)
O(2)	0.7008(2)	-0.0778(5)	0.8657(2)	5.0(2)
O(3)	0.7668(1)	0.2369(4)	0.7750(2)	4.1(2)
O(4)	0.6089(1)	0.3247(4)	0.6835(2)	4.0(2)
O(5)	0.5369(2)	0.6630(4)	0.5257(2)	4.9(2)
O(6)	0.6740(1)	0.3924(4)	0.5390(2)	3.7(2)
O(7)	0.7599(2)	0.0547(4)	0.6540(2)	4.2(2)
O(8)	0.6812(2)	-0.1813(4)	0.4529(2)	5.2(2)
O(9)	0.5948(1)	0.1659(4)	0.5038(2)	4.0(2)
C(1)	0.6881(2)	0.1427(5)	0.7083(3)	2.5(2)
C(2)	0.6494(2)	0.0576(6)	0.7003(3)	2.9(3)
C(3)	0.6511(2)	-0.0187(6)	0.7508(3)	3.1(3)
C(4)	0.6938(2)	-0.0084(6)	0.8118(3)	3.4(3)
C(5)	0.7337(2)	0.0754(6)	0.8214(3)	3.4(3)
C(6)	0.7304(2)	0.1515(6)	0.7702(3)	2.9(3)
C(7)	0.8146(2)	0.2290(7)	0.8322(3)	5.4(3)
C(8)	0.6654(3)	-0.1747(7)	0.8590(3)	6.0(4)
C(9)	0.5674(2)	-0.0226(7)	0.6217(3)	4.9(3)
C(10)	0.6395(2)	0.3581(5)	0.6083(3)	2.7(2)
C(11)	0.6056(2)	0.3949(6)	0.6314(3)	2.8(2)
C(12)	0.5725(2)	0.4982(6)	0.6027(3)	3.4(3)
C(13)	0.5723(2)	0.5657(6)	0.5506(3)	3.5(3)
C(14)	0.6050(2)	0.5337(6)	0.5264(3)	3.1(3)
C(15)	0.6388(2)	0.4319(6)	0.5569(3)	2.8(3)
C(16)	0.5752(2)	0.3533(7)	0.7091(3)	5.1(3)
C(17)	0.5335(3)	0.7380(7)	0.4721(3)	6.2(4)
C(18)	0.6800(2)	0.4639(7)	0.4901(3)	4.5(3)
C(19)	0.6780(2)	0.1076(6)	0.5775(3)	2.8(2)
C(20)	0.7205(2)	0.0276(6)	0.5934(3)	3.1(3)
C(21)	0.7208(2)	-0.0685(6)	0.5517(3)	3.6(3)
C(22)	0.6776(3)	-0.0837(6)	0.4913(3)	3.7(3)
C(23)	0.6352(2)	-0.0066(6)	0.4728(3)	3.2(3)
C(24)	0.6356(2)	0.0888(6)	0.5164(3)	3.0(3)
C(25)	0.8034(2)	-0.0235(7)	0.6789(3)	5.2(3)
C(26)	0.6390(3)	-0.2031(7)	0.3897(4)	6.0(4)
C(27)	0.5569(2)	0.1837(7)	0.4376(3)	5.2(3)
H(1)	0.7204	0.2627	0.6555	2.5
H(2)	0.6224	-0.0759	0.7437	3.5
H(3)	0.7636	0.0778	0.8639	3.9
H(4)	0.8300	0.1467	0.8382	5.3
H(5)	0.8376	0.2963	0.8315	5.3
H(6)	0.8114	0.2494	0.8719	5.3
H(7)	0.6306	-0.1426	0.8316	6.5
H(8)	0.6682	-0.2100	0.8971	6.5
H(9)	0.6673	-0.2505	0.8316	6.5
H(10)	0.5420	-0.0190	0.5764	5.0

Table 25. (continued)

atom	x	y	z	B(eq)
H(11)	0.5754	-0.1181	0.6310	5.0
H(12)	0.5502	-0.0008	0.6476	5.0
H(13)	0.5490	0.5215	0.6202	3.9
H(14)	0.6035	0.5816	0.4884	3.4
H(15)	0.5405	0.3434	0.6775	5.1
H(16)	0.5817	0.2996	0.7467	5.1
H(17)	0.5793	0.4452	0.7247	5.1
H(18)	0.5251	0.6792	0.4341	6.7
H(19)	0.5079	0.8035	0.4574	6.7
H(20)	0.5649	0.7791	0.4812	6.7
H(21)	0.7069	0.4258	0.4821	4.7
H(22)	0.6506	0.4685	0.4487	4.7
H(23)	0.6913	0.5546	0.5040	4.7
H(24)	0.7504	-0.1249	0.5639	4.0
H(25)	0.6050	-0.0187	0.4297	3.7
H(26)	0.8202	-0.0157	0.6501	5.7
H(27)	0.8293	0.0069	0.7214	5.7
H(28)	0.7978	-0.1134	0.6813	5.7
H(29)	0.6446	-0.2750	0.3664	6.2
H(30)	0.6089	-0.2275	0.3936	6.2
H(31)	0.6302	-0.1269	0.3623	6.2
H(32)	0.5698	0.2255	0.4100	5.1
H(33)	0.5416	0.1018	0.4156	5.1
H(34)	0.5298	0.2397	0.4342	5.1
C(28)	0.5332(7)	0.010(2)	0.796(1)	11(1)
O(10)	1/2	0.085(1)	3/4	18(1)

Table 26. **Atomic Positional Parameters and Equivalent Isotropic Displacement Parameters (Å^2) and their Estimated Standard Deviations for [ClCH$_2$-TMPP]$_2$[CoCl$_4$] (11).**

atom	x	y	z	B(eq)
Co(1)	1.0000	0.0259(2)	3/4	2.90(8)
Cl(1)	0.9239(1)	0.1307(2)	0.6961(1)	3.8(1)
Cl(2)	0.9813(1)	-0.0768(3)	0.8163(1)	5.8(2)
P(1)	0.7308(1)	0.4391(2)	0.1261(1)	2.1(1)
O(1)	0.6377(2)	0.4492(5)	0.0102(3)	2.6(3)
O(2)	0.5033(3)	0.2952(6)	0.0602(3)	4.1(3)
O(3)	0.6949(3)	0.3037(5)	0.2062(3)	2.9(3)
O(4)	0.7142(3)	0.5379(5)	0.2178(3)	3.1(3)
O(5)	0.8886(3)	0.4675(6)	0.3903(3)	3.7(3)
O(6)	0.8450(3)	0.3304(5)	0.1915(3)	3.1(3)
O(7)	0.8169(2)	0.5520(5)	0.1139(3)	2.6(3)
O(8)	0.7311(3)	0.9000(5)	0.0601(3)	3.2(3)
O(9)	0.6393(2)	0.6075(5)	0.0974(3)	2.6(3)
C(1)	0.6647(4)	0.3834(7)	0.1102(4)	2.2(4)
C(2)	0.6223(4)	0.4019(8)	0.0506(4)	2.2(4)
C(3)	0.5686(4)	0.3717(8)	0.0354(4)	2.6(4)
C(4)	0.5568(4)	0.3223(8)	0.0794(5)	2.9(4)
C(5)	0.5982(4)	0.2978(8)	0.1378(5)	2.7(4)
C(6)	0.6518(4)	0.3287(8)	0.1524(4)	2.4(4)
C(7)	0.5957(4)	0.491(1)	-0.0461(5)	4.2(5)
C(8)	0.4870(5)	0.248(1)	0.1035(6)	6.0(7)
C(9)	0.6843(4)	0.2649(9)	0.2559(5)	3.6(5)
C(10)	0.7797(4)	0.4358(8)	0.2063(4)	2.5(4)
C(11)	0.7645(4)	0.4944(8)	0.2456(4)	2.3(4)
C(12)	0.7986(4)	0.5082(8)	0.3070(4)	2.9(4)
C(13)	0.8501(4)	0.4602(8)	0.3297(5)	2.7(4)
C(14)	0.8670(4)	0.4005(9)	0.2927(5)	2.8(4)
C(15)	0.8315(4)	0.3878(8)	0.2307(5)	2.7(4)
C(16)	0.6901(5)	0.586(1)	0.2530(5)	4.8(6)
C(17)	0.8778(4)	0.538(1)	0.4306(5)	4.1(5)
C(18)	0.8960(4)	0.2732(9)	0.2168(5)	3.8(5)
C(19)	0.7277(4)	0.5776(7)	0.1031(4)	1.9(4)
C(20)	0.7743(4)	0.6208(8)	0.1001(4)	2.2(4)
C(21)	0.7776(4)	0.7297(8)	0.0858(4)	2.0(4)
C(22)	0.7323(4)	0.7941(8)	0.0743(4)	2.5(4)
C(23)	0.6860(4)	0.7554(8)	0.0772(5)	2.5(4)
C(24)	0.6836(4)	0.6484(8)	0.0919(4)	2.3(4)
C(25)	0.8642(4)	0.5876(9)	0.1077(5)	3.5(5)
C(26)	0.7801(5)	0.9450(8)	0.0620(5)	3.6(5)
C(27)	0.5949(4)	0.6760(9)	0.0900(5)	3.4(5)
C(28)	0.7534(4)	0.3621(7)	0.0778(4)	2.3(4)
Cl(3)	0.7446(1)	0.2207(2)	0.0845(1)	3.6(1)
H(1)	0.5393	0.3840	-0.0058	2.4
H(2)	0.5894	0.2565	0.1677	2.5
H(3)	0.5731	0.5459	-0.0380	4.2
H(4)	0.6096	0.5244	-0.0715	4.2
H(5)	0.5696	0.4366	-0.0701	4.2
H(6)	0.4957	0.2930	0.1392	5.6
H(7)	0.4487	0.2322	0.0862	5.6
H(8)	0.5065	0.1803	0.1196	5.6

Table 26. (continued)

atom	x	y	z	B(eq)
H(9)	0.6629	0.3163	0.2671	2.9
H(10)	0.6608	0.1998	0.2438	2.9
H(11)	0.7160	0.2475	0.2915	2.9
H(12)	0.7874	0.5509	0.3341	3.3
H(13)	0.9023	0.3631	0.3102	2.7
H(14)	0.7117	0.6452	0.2792	4.4
H(15)	0.6536	0.6151	0.2291	4.4
H(16)	0.6857	0.5358	0.2823	4.4
H(17)	0.9069	0.5376	0.4707	3.3
H(18)	0.8735	0.6113	0.4150	3.3
H(19)	0.8443	0.5188	0.4320	3.3
H(20)	0.8991	0.2252	0.2491	4.4
H(21)	0.9018	0.2347	0.1866	4.4
H(22)	0.9271	0.3239	0.2358	4.4
H(23)	0.8111	0.7598	0.0830	2.5
H(24)	0.6547	0.8024	0.0689	2.3
H(25)	0.8914	0.5336	0.1168	3.5
H(26)	0.8560	0.6169	0.0679	3.5
H(27)	0.8823	0.6470	0.1371	3.5
H(28)	0.8111	0.9401	0.1050	4.1
H(29)	0.7947	0.9090	0.0371	4.1
H(30)	0.7782	1.0202	0.0526	4.1
H(31)	0.6064	0.7351	0.1187	3.0
H(32)	0.5783	0.7089	0.0490	3.0
H(33)	0.5661	0.6390	0.0946	3.0
H(34)	0.7924	0.3751	0.0892	2.4
H(35)	0.7340	0.3827	0.0350	2.4
C(29)	0.4508(6)	0.181(1)	0.6097(8)	9(1)
Cl(4)	0.3802(1)	0.1921(3)	0.5558(2)	5.5(2)
Cl(5)	0.4917(2)	0.1264(4)	0.5843(2)	10.7(3)
H(36)	0.4656	0.2448	0.6328	8.9
H(37)	0.4526	0.1292	0.6462	8.9
C(30)	0	0.365(1)	3/4	4.6(8)
Cl(6)	0.0442(2)	0.4438(3)	0.7310(2)	8.6(2)
H(38)	0.0248	0.3008	0.7778	5.2

Table 27. **Atomic Positional Parameters and Equivalent Isotropic Displacement Parameters (Å^2) and their Estimated Standard Deviations for $Cl_2Co_2\{\mu\text{-}\eta^2\text{-}(TMPP\text{-}O)_2\}$ (14)**

atom	x	y	z	B(eq)
Co(1)	1/2	0.44225(5)	1/4	2.63(5)
Co(2)	1/2	0.58543(5)	1/4	3.89(6)
Cl(1)	0.5871(2)	0.6439(1)	0.1964(1)	7.7(1)
P(1)	0.5925(1)	0.38283(7)	0.31776(7)	2.67(6)
O(1)	0.5148(3)	0.3824(2)	0.4442(2)	5.0(2)
O(2)	0.4846(4)	0.1648(3)	0.4784(3)	8.6(4)
O(3)	0.5954(3)	0.2471(2)	0.2775(2)	4.7(2)
O(4)	0.7108(3)	0.3764(2)	0.4659(2)	4.7(2)
O(5)	0.7612(3)	0.5962(2)	0.4867(2)	5.5(2)
O(6)	0.5591(2)	0.5121(2)	0.2997(2)	3.2(2)
O(7)	0.7525(3)	0.3002(2)	0.3552(2)	4.6(2)
O(8)	0.8524(3)	0.3179(3)	0.1344(2)	6.6(3)
O(9)	0.6105(3)	0.4347(2)	0.1837(2)	4.0(2)
C(1)	0.5616(4)	0.3141(3)	0.3632(3)	3.1(3)
C(2)	0.5250(4)	0.3219(3)	0.4243(3)	4.1(3)
C(3)	0.5017(5)	0.2705(4)	0.4616(4)	5.3(4)
C(4)	0.5112(5)	0.2113(4)	0.4374(4)	5.5(4)
C(5)	0.5435(5)	0.2006(3)	0.3772(4)	5.2(4)
C(6)	0.5674(4)	0.2526(3)	0.3396(3)	4.0(3)
C(7)	0.5019(7)	0.3947(5)	0.5129(4)	8.9(6)
C(8)	0.4774(7)	0.1050(5)	0.4540(6)	11.2(7)
C(9)	0.6339(6)	0.1887(4)	0.2600(5)	7.7(5)
C(10)	0.6411(3)	0.4429(3)	0.3784(3)	2.8(2)
C(11)	0.6984(4)	0.4362(3)	0.4412(3)	3.5(3)
C(12)	0.7359(4)	0.4888(3)	0.4756(3)	4.1(3)
C(13)	0.7185(4)	0.5485(3)	0.4487(3)	3.9(3)
C(14)	0.6604(4)	0.5573(3)	0.3883(3)	3.4(3)
C(15)	0.6207(3)	0.5041(3)	0.3553(3)	3.0(3)
C(16)	0.7615(6)	0.3667(4)	0.5317(4)	7.5(5)
C(17)	0.7523(6)	0.6585(4)	0.4594(4)	7.0(4)
C(18)	0.6788(3)	0.3632(3)	0.2678(3)	2.9(3)
C(19)	0.7472(4)	0.3230(3)	0.2900(3)	3.4(3)
C(20)	0.8082(4)	0.3068(3)	0.2476(3)	4.3(3)
C(21)	0.7993(4)	0.3325(3)	0.1819(3)	4.4(3)
C(22)	0.7345(4)	0.3753(3)	0.1591(3)	4.3(3)
C(23)	0.6756(4)	0.3908(3)	0.2027(3)	3.3(3)
C(24)	0.8328(5)	0.2789(4)	0.3907(3)	6.0(4)
C(25)	0.9221(5)	0.2764(5)	0.1539(4)	8.1(5)
C(26)	0.6225(5)	0.4789(3)	0.1316(4)	5.5(4)
H(1)	0.4792	0.2767	0.5035	6.4
H(2)	0.5497	0.1589	0.3612	6.2
H(3)	0.5500	0.3793	0.5443	10.7
H(4)	0.4964	0.4389	0.5192	10.7
H(5)	0.4503	0.3743	0.5218	10.7
H(6)	0.4591	0.0782	0.4880	13.5
H(7)	0.4360	0.1037	0.4130	13.5
H(8)	0.5322	0.0912	0.4441	13.5
H(9)	0.5929	0.1555	0.2600	9.3
H(10)	0.6505	0.1921	0.2154	9.3
H(11)	0.6837	0.1799	0.2932	9.3

Table 27. (continued)

atom	x	y	z	B(eq)
H(12)	0.7737	0.4841	0.5180	4.9
H(13)	0.7641	0.3227	0.5418	9.0
H(14)	0.8183	0.3824	0.5315	9.0
H(15)	0.7353	0.3880	0.5661	9.0
H(16)	0.7841	0.6870	0.4909	8.4
H(17)	0.7739	0.6599	0.4164	8.4
H(18)	0.6926	0.6701	0.4521	8.4
H(19)	0.8546	0.2788	0.2636	5.1
H(20)	0.7307	0.3939	0.1146	5.1
H(21)	0.8249	0.2633	0.4348	7.1
H(22)	0.8542	0.2460	0.3648	7.1
H(23)	0.8730	0.3128	0.3960	7.1
H(24)	0.9005	0.2371	0.1676	9.8
H(25)	0.9521	0.2697	0.1156	9.8
H(26)	0.9607	0.2939	0.1913	9.8
H(27)	0.6733	0.5032	0.1464	6.6
H(28)	0.5736	0.5060	0.1232	6.6
H(29)	0.6291	0.4571	0.0902	6.6
Cl(2)	0.5484(5)	0.0480(3)	0.6433(4)	26.9(6)
Cl(3)	0.6514(5)	-0.0299(3)	0.7358(4)	30.1(6)
C(27)	0.645(1)	0.0276(8)	0.690(1)	16(1)
H(30)	0.6475	0.5998	0.3692	4.1

Table 28. **Atomic Positional Parameters and Equivalent Isotropic Displacement Parameters (Å^2) and their Estimated Standard Deviations for $Cl_2MnCo\{\mu\text{-}\eta^2\text{-}(TMPP\text{-}O)_2\}$ (15)**

atom	x	y	z	B(eq)
Co(1)	1/2	0.0573(2)	1/4	1.9(2)
Mn(1)	1/2	-0.0855(2)	1/4	1.9(2)
Cl(1)	0.4110(4)	-0.1422(3)	0.3047(3)	6.0(3)
P(1)	0.4058(3)	0.1172(2)	0.1813(2)	2.2(2)
O(1)	0.4844(9)	0.1111(6)	0.0555(6)	4.3(7)
O(2)	0.523(1)	0.3288(9)	0.0170(8)	7(1)
O(3)	0.4093(8)	0.2538(5)	0.2173(6)	3.4(6)
O(4)	0.2828(8)	0.1234(6)	0.0338(6)	3.9(7)
O(5)	0.2362(8)	-0.0981(7)	0.0092(6)	4.7(7)
O(6)	0.4390(7)	-0.0124(5)	0.2001(5)	2.1(5)
O(7)	0.2475(8)	0.2021(6)	0.1421(6)	3.8(7)
O(8)	0.1454(9)	0.1888(7)	0.3632(6)	5.3(8)
O(9)	0.3854(8)	0.0646(6)	0.3126(6)	3.5(6)
C(1)	0.439(1)	0.1861(8)	0.1356(8)	2.5(9)
C(2)	0.476(1)	0.172(1)	0.076(1)	4(1)
C(3)	0.500(1)	0.224(1)	0.0371(9)	4(1)
C(4)	0.493(2)	0.285(1)	0.062(1)	5(1)
C(5)	0.461(1)	0.294(1)	0.122(1)	4(1)
C(6)	0.435(1)	0.2448(9)	0.157(1)	3(1)
C(7)	0.495(2)	0.100(1)	-0.014(1)	8(2)
C(8)	0.531(2)	0.391(1)	0.037(2)	10(2)
C(9)	0.374(2)	0.314(1)	0.231(1)	6(1)
C(10)	0.354(1)	0.0555(8)	0.1206(8)	2.0(8)
C(11)	0.295(1)	0.064(1)	0.0572(8)	3(1)
C(12)	0.259(1)	0.011(1)	0.0208(8)	3.1(9)
C(13)	0.277(1)	-0.050(1)	0.0478(8)	3(1)
C(14)	0.336(1)	-0.0590(9)	0.1100(8)	2.3(8)
C(15)	0.375(1)	-0.0035(8)	0.1422(8)	2.3(9)
C(16)	0.236(1)	0.134(1)	-0.034(1)	6(1)
C(17)	0.252(2)	-0.161(1)	0.034(1)	6(1)
C(18)	0.321(1)	0.1369(8)	0.2303(8)	2.7(9)
C(19)	0.252(1)	0.1797(8)	0.2093(9)	3(1)
C(20)	0.190(1)	0.196(1)	0.252(1)	4(1)
C(21)	0.198(1)	0.173(1)	0.318(1)	4(1)
C(22)	0.263(1)	0.127(1)	0.3371(9)	4(1)
C(23)	0.323(1)	0.1107(9)	0.2953(9)	3(1)
C(24)	0.165(1)	0.223(1)	0.107(1)	6(1)
C(25)	0.081(1)	0.236(1)	0.345(1)	5(1)
C(26)	0.371(1)	0.020(1)	0.366(1)	5(1)
H(1)	0.5220	0.2160	-0.0053	5.3
H(2)	0.4550	0.3343	0.1391	5.0
H(3)	0.5037	0.0556	-0.0191	9.0
H(4)	0.4451	0.1133	-0.0443	9.0
H(5)	0.5471	0.1211	-0.0224	9.0
H(6)	0.5744	0.3939	0.0801	12.5
H(7)	0.5542	0.4148	0.0031	12.5
H(8)	0.4771	0.4069	0.0450	12.5
H(9)	0.4163	0.3460	0.2277	7.0
H(10)	0.3213	0.3225	0.1979	7.0
H(11)	0.3585	0.3148	0.2762	7.0

Table 28. (continued)

atom	x	y	z	B(eq)
H(12)	0.2205	0.0151	-0.0234	3.6
H(13)	0.3497	-0.0992	0.1289	2.9
H(14)	0.2349	0.1779	-0.0435	7.0
H(15)	0.2641	0.1126	-0.0664	7.0
H(16)	0.1763	0.1195	-0.0370	7.0
H(17)	0.2314	-0.1661	0.0775	7.5
H(18)	0.2190	-0.1901	0.0017	7.5
H(19)	0.3127	-0.1711	0.0398	7.5
H(20)	0.1408	0.2225	0.2340	4.6
H(21)	0.2627	0.1056	0.3795	5.6
H(22)	0.1436	0.2551	0.1328	6.8
H(23)	0.1735	0.2394	0.0628	6.8
H(24)	0.1251	0.1891	0.1001	6.8
H(25)	0.1083	0.2736	0.3356	6.4
H(26)	0.0406	0.2224	0.3050	6.4
H(27)	0.0488	0.2416	0.3823	6.4
H(28)	0.3668	0.0404	0.4066	6.3
H(29)	0.3166	-0.0028	0.3492	6.3
H(30)	0.4186	-0.0097	0.3720	6.3
O(10)	0.270(9)	0.008(6)	0.273(7)	69(1)
C(27)	0.153(4)	-0.007(3)	0.215(3)	18(4)
C(28)	0.028(4)	-0.020(2)	0.176(2)	20(4)
C(29)	0.087(8)	0.024(5)	0.158(4)	47(1)
H(31)	-0.0256	0.0117	0.1782	17.8
H(32)	0.0020	-0.0324	0.1225	17.8
H(33)	-0.0004	-0.0575	0.1965	17.8
H(34)	0.1260	0.0739	0.1335	41.9
H(35)	0.0605	0.0235	0.0977	41.9
H(36)	0.0324	0.0670	0.1537	41.9

Table 29. Atomic Positional Parameters and Equivalent Isotropic Displacement Parameters ($Å^2$) and their Estimated Standard Deviations for [(COD)Rh-Co(TMPP-*O*)$_2$][BF_4]$_2$ (17)

atom	x	y	z	B(eq)
Rh(1)	0.36565(6)	0.63264(5)	0.16607(4)	3.00(5)
Co(1)	0.1159(1)	0.78442(8)	0.17025(5)	2.40(9)
P(1)	0.2419(2)	0.8070(2)	0.1186(1)	2.4(2)
P(2)	0.0360(2)	0.7615(2)	0.1194(1)	2.7(2)
O(1)	0.4065(5)	0.9111(4)	0.0920(3)	3.7(5)
O(2)	0.3867(5)	0.9798(4)	0.2641(3)	3.9(5)
O(3)	0.1803(5)	0.8125(4)	0.2226(2)	2.8(4)
O(4)	0.2218(5)	0.9671(4)	0.1010(3)	3.6(5)
O(5)	0.3057(5)	0.9726(5)	-0.0753(3)	4.8(6)
O(6)	0.2829(5)	0.7312(4)	0.0160(3)	3.7(5)
O(7)	0.4199(5)	0.7381(4)	0.0634(3)	3.7(5)
O(8)	0.3342(5)	0.4711(4)	0.1113(3)	4.6(6)
O(9)	0.1491(5)	0.6788(4)	0.1735(3)	3.0(5)
O(10)	0.0693(5)	0.8471(5)	0.0216(3)	4.0(5)
O(11)	0.1031(7)	0.6135(6)	-0.0799(4)	7.5(8)
O(12)	0.0936(5)	0.6059(4)	0.0913(3)	3.9(5)
O(13)	-0.0886(5)	0.6401(5)	0.0916(3)	4.3(5)
O(14)	-0.2137(6)	0.5580(5)	0.2624(3)	5.6(6)
O(15)	0.0013(5)	0.7540(4)	0.2235(3)	3.1(5)
O(16)	-0.1133(5)	0.8169(4)	0.0795(3)	4.1(5)
O(17)	-0.1154(5)	1.0763(5)	0.1375(3)	4.2(5)
O(18)	0.0793(4)	0.8883(4)	0.1742(2)	2.5(4)
C(1)	0.2922(7)	0.8632(6)	0.1573(4)	2.6(6)
C(2)	0.3692(7)	0.9105(6)	0.1421(4)	2.6(7)
C(3)	0.4014(7)	0.9489(6)	0.1772(4)	3.0(7)
C(4)	0.3599(8)	0.9427(6)	0.2268(5)	3.2(7)
C(5)	0.2857(7)	0.8977(6)	0.2438(4)	2.6(6)
C(6)	0.2544(6)	0.8607(6)	0.2087(4)	2.4(6)
C(7)	0.4859(9)	0.9510(8)	0.0728(5)	5.2(9)
C(8)	0.4580(9)	1.0321(7)	0.2508(5)	5(1)
C(9)	0.1643(8)	0.7749(8)	0.2709(4)	4.7(8)
C(10)	0.2576(7)	0.8506(6)	0.0575(4)	2.6(7)
C(11)	0.2478(7)	0.9322(6)	0.0552(4)	3.1(7)
C(12)	0.2661(7)	0.9703(6)	0.0106(4)	3.0(7)
C(13)	0.2910(7)	0.9281(8)	-0.0327(4)	3.4(8)
C(14)	0.2984(8)	0.8475(6)	-0.0323(4)	3.4(8)
C(15)	0.2796(7)	0.8091(7)	0.0118(4)	2.8(7)
C(16)	0.225(1)	1.0495(7)	0.1036(5)	6(1)
C(17)	0.330(1)	0.934(1)	-0.1226(5)	6(1)
C(18)	0.315(1)	0.6895(8)	-0.0292(5)	6(1)
C(19)	0.2855(7)	0.7092(6)	0.1165(4)	2.5(6)
C(20)	0.3666(7)	0.6817(7)	0.0876(4)	3.1(7)
C(21)	0.3900(7)	0.6010(7)	0.0809(4)	3.2(7)
C(22)	0.3258(8)	0.5498(7)	0.1122(5)	3.5(8)
C(23)	0.2506(7)	0.5781(6)	0.1496(4)	3.4(7)
C(24)	0.2255(7)	0.6563(6)	0.1470(4)	2.8(7)
C(25)	0.4985(8)	0.7177(8)	0.0261(5)	5(1)
C(26)	0.415(1)	0.4397(7)	0.0840(5)	6(1)
C(27)	0.0723(7)	0.7260(7)	0.0568(4)	3.1(7)
C(28)	0.0754(7)	0.7693(7)	0.0145(4)	3.4(8)

Table 29. (continued)

atom	x	y	z	B(eq)
C(29)	0.0847(8)	0.7351(8)	-0.0325(4)	4.4(9)
C(30)	0.096(1)	0.6550(8)	-0.0358(5)	5(1)
C(31)	0.1011(9)	0.6096(7)	0.0032(5)	5(1)
C(32)	0.0907(8)	0.6447(7)	0.0496(5)	3.8(8)
C(33)	0.065(1)	0.8971(8)	-0.0187(5)	6(1)
C(34)	0.097(1)	0.653(1)	-0.1223(6)	9(1)
C(35)	0.094(1)	0.5234(7)	0.0890(5)	6(1)
C(36)	-0.0430(7)	0.6951(6)	0.1573(4)	2.9(7)
C(37)	-0.0958(7)	0.6416(7)	0.1418(5)	3.3(7)
C(38)	-0.1535(8)	0.5959(7)	0.1772(6)	4(1)
C(39)	-0.1600(8)	0.6021(7)	0.2264(5)	3.6(8)
C(40)	-0.1097(7)	0.6552(6)	0.2434(4)	3.4(7)
C(41)	-0.0526(7)	0.7000(6)	0.2079(4)	2.7(7)
C(42)	-0.147(1)	0.5942(8)	0.0729(5)	6(1)
C(43)	-0.262(1)	0.4986(9)	0.2475(5)	6(1)
C(44)	-0.0418(8)	0.8054(8)	0.2647(5)	4.8(9)
C(45)	-0.0152(7)	0.8540(6)	0.1239(4)	2.4(6)
C(46)	-0.0832(7)	0.8756(7)	0.1033(4)	3.1(7)
C(47)	-0.1154(7)	0.9493(7)	0.1081(4)	3.2(7)
C(48)	-0.0773(8)	1.0047(6)	0.1343(4)	3.2(7)
C(49)	-0.0131(7)	0.9850(6)	0.1560(4)	3.0(7)
C(50)	0.0184(7)	0.9090(6)	0.1517(4)	2.6(6)
C(51)	-0.170(1)	0.8351(8)	0.0490(5)	6(1)
C(52)	-0.084(1)	1.1344(7)	0.1651(5)	6(1)
C(53)	0.4517(8)	0.7154(7)	0.1855(5)	3.9(8)
C(54)	0.5015(7)	0.6510(7)	0.1636(4)	3.8(8)
C(55)	0.534(1)	0.592(1)	0.1948(5)	6(1)
C(56)	0.473(1)	0.5258(9)	0.2107(6)	7(1)
C(57)	0.379(1)	0.5449(7)	0.2170(5)	5(1)
C(58)	0.3340(8)	0.6086(7)	0.2443(4)	4.1(8)
C(59)	0.3785(9)	0.6640(8)	0.2729(5)	4.9(9)
C(60)	0.4254(8)	0.7309(7)	0.2408(6)	5(1)
O(19)	0.1190(8)	0.2234(7)	0.0844(5)	9(1)
C(61)	0.173(2)	0.325(1)	0.1230(8)	11(2)
C(62)	0.178(1)	0.266(1)	0.0840(7)	7(1)
C(63)	0.262(1)	0.259(1)	0.0471(8)	12(2)
O(20)	0.380(2)	0.171(2)	0.745(1)	23(3)
C(64)	0.278(2)	0.231(2)	0.802(2)	28(4)
C(65)	0.372(2)	0.142(2)	0.820(1)	20(3)
C(66)	0.341(2)	0.182(2)	0.786(1)	11(2)
F(6)	0.9101(6)	0.0244(7)	0.4703(4)	11.2(9)
F(7)	0.834(1)	-0.0012(6)	0.4163(5)	12(1)
F(8)	0.7663(6)	0.0283(7)	0.4915(4)	11.0(9)
B(2)	0.837(1)	0.041(1)	0.457(1)	6(2)
B(3)	0.4368(6)	0.1840(5)	0.1197(3)	7.0(2)
F(9)	0.4910(8)	0.1665(8)	0.1488(5)	7.0(2)
F(10)	0.3532(6)	0.1661(8)	0.1448(5)	7.0(2)
F(11)	0.461(1)	0.1423(8)	0.0765(4)	7.0(2)
F(12)	0.442(1)	0.2612(5)	0.1088(5)	7.0(2)
B(1)	0.4448(7)	0.1925(6)	0.1177(4)	8.5(3)
F(1)	0.3602(7)	0.216(1)	0.1286(6)	8.5(3)
F(2)	0.497(1)	0.2549(7)	0.1177(6)	8.5(3)
F(3)	0.467(1)	0.159(1)	0.0717(5)	8.5(3)
F(4)	0.455(1)	0.1404(8)	0.1526(6)	8.5(3)

Table 30. **Atomic Positional Parameters and Equivalent Isotropic Displacement Parameters ($Å^2$) and their Estimated Standard Deviations for Ni(TMPP-*O*)$_2$ (18)**

atom	x	y	z	B(eq)
Ni(1)	0	1/2	1/2	1.96(5)
P(1)	0.1692(2)	0.6601(2)	0.6289(2)	1.96(7)
O(1)	0.1001(7)	0.8962(5)	0.6678(6)	3.8(2)
O(2)	0.175(1)	1.0540(6)	1.1359(8)	6.5(3)
O(3)	0.2484(6)	0.6748(5)	0.9024(6)	2.8(2)
O(4)	0.2039(6)	0.4493(5)	0.4616(6)	3.9(2)
O(5)	0.6464(7)	0.5209(7)	0.7642(8)	5.1(3)
O(6)	0.4398(5)	0.8124(5)	0.8885(6)	2.7(2)
O(7)	0.3329(6)	0.8534(5)	0.6272(6)	3.3(2)
O(8)	0.0554(6)	0.7534(6)	0.1538(6)	3.9(2)
O(9)	-0.0467(6)	0.5348(5)	0.3533(6)	2.7(2)
C(1)	0.1762(7)	0.7847(7)	0.7853(8)	1.9(2)
C(2)	0.1391(8)	0.8874(7)	0.7877(8)	2.2(3)
C(3)	0.1399(9)	0.9736(8)	0.904(1)	3.0(3)
C(4)	0.176(1)	0.9608(8)	1.023(1)	3.3(3)
C(5)	0.2124(8)	0.8619(8)	1.0272(9)	2.8(3)
C(6)	0.2125(8)	0.7741(7)	0.9051(9)	2.2(3)
C(7)	0.106(1)	1.0093(9)	0.679(1)	4.0(4)
C(8)	0.201(2)	1.040(1)	1.256(1)	8.0(7)
C(9)	0.278(1)	0.657(1)	1.021(1)	4.1(4)
C(10)	0.3215(8)	0.6280(7)	0.6780(8)	1.9(3)
C(11)	0.3184(9)	0.5160(8)	0.5811(9)	2.7(3)
C(12)	0.424(1)	0.4755(8)	0.602(1)	3.2(3)
C(13)	0.536(1)	0.5496(9)	0.726(1)	3.3(3)
C(14)	0.5443(9)	0.6645(8)	0.824(1)	3.4(3)
C(15)	0.4372(8)	0.7017(8)	0.7996(9)	2.5(3)
C(16)	0.190(1)	0.342(1)	0.348(1)	5.1(4)
C(17)	0.646(1)	0.404(1)	0.672(1)	5.2(4)
C(18)	0.551(1)	0.8820(9)	1.023(1)	4.2(3)
C(19)	0.1436(8)	0.6986(7)	0.4925(8)	2.1(3)
C(20)	0.2258(8)	0.7880(7)	0.4995(9)	2.3(3)
C(21)	0.1920(9)	0.8050(8)	0.386(1)	2.8(3)
C(22)	0.0776(9)	0.7290(8)	0.2594(9)	2.8(3)
C(23)	0.0009(9)	0.6383(8)	0.2466(8)	2.7(3)
C(24)	0.0319(8)	0.6213(7)	0.3649(8)	2.0(3)
C(25)	0.428(1)	0.930(1)	0.635(1)	4.8(4)
C(26)	-0.054(1)	0.686(1)	0.023(1)	5.7(4)
H(1)	0.1141	1.0425	0.9031	3.8
H(2)	0.2367	0.8529	1.1087	3.7
H(3)	0.1910	1.0593	0.7393	5.0
H(4)	0.0757	1.0019	0.5876	5.0
H(5)	0.0555	1.0451	0.7180	5.0
H(6)	0.1385	0.9700	1.2260	10.6
H(7)	0.2813	1.0314	1.2960	10.6
H(8)	0.1932	1.1082	1.3245	10.6
H(9)	0.2078	0.6514	1.0337	5.2
H(10)	0.3038	0.5865	1.0053	5.2
H(11)	0.3467	0.7247	1.1033	5.2
H(12)	0.4165	0.3981	0.5338	4.0
H(13)	0.6219	0.7168	0.9068	4.2

Table 30. (continued)

atom	x	y	z	B(eq)
H(14)	0.1014	0.3085	0.2759	6.1
H(15)	0.2379	0.3566	0.3106	6.1
H(16)	0.2127	0.2859	0.3797	6.1
H(17)	0.5898	0.3423	0.6620	6.3
H(18)	0.6226	0.3942	0.5799	6.3
H(19)	0.7297	0.3945	0.7099	6.3
H(20)	0.5662	0.8404	1.0739	4.9
H(21)	0.6199	0.8969	1.0085	4.9
H(22)	0.5391	0.9568	1.0734	4.9
H(23)	0.2453	0.8661	0.3894	3.3
H(24)	-0.0755	0.5855	0.1560	3.5
H(25)	0.4985	0.9714	0.7279	5.7
H(26)	0.4578	0.8804	0.5716	5.7
H(27)	0.3971	0.9839	0.6051	5.7
H(28)	-0.1249	0.6959	0.0370	7.0
H(29)	-0.0549	0.7141	-0.0388	7.0
H(30)	-0.0562	0.6046	-0.0144	7.0
O(10)	0.3928(9)	0.2153(8)	0.659(1)	7.0(4)
C(27)	0.189(1)	0.232(1)	0.595(1)	6.0(5)
C(28)	0.324(1)	0.271(1)	0.693(1)	4.1(4)
C(29)	0.372(2)	0.389(1)	0.825(1)	8.3(6)
H(31)	0.1490	0.2853	0.6387	7.3
H(32)	0.1727	0.2337	0.5107	7.3
H(33)	0.1524	0.1533	0.5717	7.3
H(34)	0.4189	0.3801	0.9061	9.9
H(35)	0.4235	0.4476	0.8259	9.9
H(36)	0.3015	0.4151	0.8305	9.9